

**COLLECTION AND PHYSICAL CHARACTERIZATION  
OF AIRBORNE PARTICULATES**

Thesis submitted for the degree of Doctor of Philosophy

By

**SHAMZANI AFFENDY BIN MOHD.DIN**

JANUARY 2007

INSTITUTE OF SUSTAINABILITY, ENERGY AND  
ENVIRONMENTAL MANAGEMENT  
CARDIFF SCHOOL OF ENGINEERING  
CARDIFF UNIVERSITY

UMI Number: U584901

All rights reserved

INFORMATION TO ALL USERS

The quality of this reproduction is dependent upon the quality of the copy submitted.

In the unlikely event that the author did not send a complete manuscript and there are missing pages, these will be noted. Also, if material had to be removed, a note will indicate the deletion.



UMI U584901

Published by ProQuest LLC 2013. Copyright in the Dissertation held by the Author.  
Microform Edition © ProQuest LLC.

All rights reserved. This work is protected against  
unauthorized copying under Title 17, United States Code.




ProQuest LLC  
789 East Eisenhower Parkway  
P.O. Box 1346  
Ann Arbor, MI 48106-1346

## DECLARATION / STATEMENTS


### Declaration

This work has not previously been accepted in substance for any degrees and is not concurrently submitted in candidature for any degree.

Signed : .....  ..... (candidate)  
Date : ..... 30/01/2007 .....


### Statement 1

This thesis is being submitted in partial fulfilment of the requirements for the degree of PhD.

Signed : .....  ..... (candidate)  
Date : ..... 30/01/2007 .....

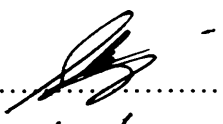
### Statement 2

This is the result of my own independent work/investigation, except where otherwise stated. Other sources are acknowledged by explicit references.

Signed : .....  ..... (candidate)  
Date : ..... 30/01/2007 .....

### Statement 3

I hereby give consent for my thesis, if accepted, to be available for photocopying and for inter-library loan, and for the title and summary to be made available to outside organisations.

Signed : .....  ..... (candidate)  
Date : ..... 30/01/2007 .....

## ABSTRACT

Airborne particulates are one of the most complex air pollutants and considerable concern surrounds their environmental impact especially with regards to human health. An investigation of the efficiency of various total inhalable and respirable dust samplers has been conducted to identify the most convenient way of collecting dust particles to examine their physical characteristics. The efficiency of a variety of dust samplers were investigated using limestone dust clouds generated inside an environmental dust chamber. Various sampling periods were employed to establish dust concentrations in the environmental dust chamber. The experimental dust cloud was found to contain on average 55.74 % of respirable dust as defined by different instruments while a consistent dust concentration of approx  $200 \text{ mg/m}^3$  was repeatedly produced.

The methods for collecting and estimating airborne asbestos fibre concentrations were studied and found to be extremely limited. Standard optical techniques grossly underestimated both airborne fibre concentrations and respirable dimensions of fibres. The size and dimensions of respirable asbestos fibres are defined by their ability to gain access to the lungs and there is no instrument or technique available at present, which will allow collection and estimation of respirable fibrous dust clouds. A comparison of coal dust particles with similar particles retained in the lungs has shown a difference from the predicted respirable fractions as proposed by the British Medical Research Council (BMRC) and other conventions. Respirable dust sampling instruments may therefore be under sampling larger particles.

The difficulty in estimating the characteristics of airborne particulate material has been demonstrated by illustrating urban particulate collection and analysis. The extremely large differences in terms of physical size, and aerodynamic properties of dust particles formed by different materials have been demonstrated.



## ACKNOWLEDGEMENT

Alhamdulillah, I am so grateful to Allah swt for giving me this opportunity, strength, and great health to complete my PhD studies. I extend my greatest thanks and appreciation to my supervisor, Professor Fred. D. Pooley for his knowledge, dedication, guidance and motivation in the airborne particulate research area over the past three years. My thanks also to my technician, Mel Griffiths and Jeff Rowland, Chris Lee, Research Office staff, Finance Division and Cardiff School of Engineering.

I would like to express my sincere appreciations to my dearest friends in Cardiff, Fieka, Bean, Chibob, Dee, Farid, Farah, Yanti, Ahmad, Taufiq, Aisha, Owain, Dr.Devin, and Andy, whom I would like to thank very much for giving me strong support during my most difficult time, especially the last three months during the period of writing my thesis and throughout my invaluable time in Cardiff. I would also like to thank my friends in Malaysia, who have supported me from the very beginning: Syah and family, Assoc. Prof. Zainudin and family, Ahmad Nazri and Family, Eddy and Family, Ahmad Yusry, Rizal and family, Hakimi and family, Akmalina and family, Hani, Adlin, and Aslinda.

Most of all I would like to extend special thanks to my beloved family, Dr.Sadiyah, Mohd.Din, Shaiful Affendy and Nurul Aini. I wish to thank you all for giving me continuous motivations and moral support while I have been in Cardiff, working towards my PhD. There has been a great deal of sacrifice in contribution to this great achievement, and I am therefore dedicated to you all.

Lastly, I would like thank greatly Professor Mansor Ibrahim, Dean of Kulliyyah of Architecture and Environmental Design, Management Services Division, International Islamic University Malaysia, General Services Department and Ministry of Higher Education for all moral and financial support during my study leave at Cardiff University, Wales.

# CONTENTS

	<b>Page</b>
<b>DECLARATION / STATEMENTS</b>	i
<b>ABSTRACT</b>	ii
<b>ACKNOWLEDGMENT</b>	iii
<b>CONTENTS</b>	iv
<b>LIST OF FIGURES</b>	x
<b>LIST OF TABLES</b>	xx
<b>NOMENCLATURE</b>	xxii
<b>CHAPTER 1      ATMOSPHERE &amp; AIRBORNE PARTICULATES</b>	
1.1              Introduction	1
1.2              The Atmosphere	2
1.3              Composition and Structure of the Atmosphere	5
1.4              Dynamics of the Atmosphere	6
1.5              Airborne Particulate Matter	11
1.5.1        Morphology of Particulates	14
1.5.2        Sources of Particulate Pollution	15
1.5.3        Primary Particulates	18
1.5.4        Sources of Primary Particulates	18
1.5.5        Secondary Particulates	20
1.5.6        Sources of Secondary Particulates	20
1.5.7        Fine & Ultrafine Particulates	22
1.6              General Chemical Characteristics of Airborne Particulates	23
1.6.1        Organic Chemistry of Airborne Material	26
1.6.2        Inorganic Chemistry of Airborne Particulates	26
1.7              Conclusion	28
<b>CHAPTER 2      THE IMPACTS OF AIRBORNE PARTICULATES</b>	
2.1              Introduction	29

2.2	The Impact of Gaseous Atmospheric Pollution on Human Health	29
2.3	The Impact of Particulate Atmospheric Pollution on Human Health	33
2.3.1	Particulates Deposition in Human Lungs	35
2.3.2	Lung Diseases and Affected Groups	37
2.3.3	Occupational Pollution	40
2.3.4	Effects of Particulate Environmental Exposure	50
2.3.5	Effects Particulate Indoor Air Pollution Exposures	52
2.4	Atmospheric Particulate Pollution Impact on Flora and Fauna	53
2.5	Impact of Air Pollution on Buildings and Materials	55
2.6	Impact of Air Pollution on the Global Environment	56
2.7	Conclusion	60
<b>CHAPTER 3</b>	<b>INSTRUMENTS FOR INHALABLE AND RESPIRABLE AIRBORNE PARTICULATE SAMPLING</b>	
3.1	Introduction	61
3.2	Review on Design of Sampling Instruments	61
3.2.1	Environmental Size Classification of Airborne Particulates	66
3.2.1.1	The Inhalable Fraction	67
3.2.1.2	The Thoracic Fraction	68
3.2.1.3	The Respirable Fraction	71
3.2.2	Particle Deposition Mechanisms	74
3.2.2.1	Inertial Impaction	77
3.2.2.2	Settling	78
3.2.2.3	Diffusion	78
3.2.2.4	Interception	79
3.2.2.5	Electrostatic Deposition	79
3.2.3	Lung Structure and Airflow in the Lungs	80
3.2.4	Particle Types and Sizes Deposited in the Lungs	81
3.2.5	Human Respiratory Patterns	83
3.2.6	Regional Fractional Deposition of Inhaled Particles	84
3.2.7	ISO Health-related Particle Sampling Conventions	85
3.3	Conclusion	89
<b>CHAPTER 4</b>	<b>METHODS, MATERIALS, AND APPARATUS</b>	
4.1	Introduction	90

4.2	Description and Operation of Airborne Sampling Instruments	93
4.2.1	The Casella MRE Sampler	93
4.2.2	The Cyclone Sampler	95
4.2.3	The Seven Hole Sampler	97
4.2.4	The IOM Sampler	99
4.2.5	The Casella CIS Sampler	100
4.2.6	The RespiCon Sampler	103
4.2.7	The Thermal Precipitator	110
4.2.8	The Marple Personal Cascade Impactor (Series 290)	112
4.2.9	The Anderson Cascade Impactor (Mark II)	115
4.3	Materials used in this study experimental	118
4.3.1	Types of Dust	118
4.3.2	Types of Filter	119
4.3.3	Environmental Dust Chamber Design	121
4.3.4	The Mechanical Dust Dispenser	122
4.3.5	Dust Pump Flow	125
4.3.6	Flow Measurement	126
4.3.7	Measurement of Sample Weight	126
4.3.8	Other Ancilliary Equipment Employed	127
4.4	Description and Operation of Instruments for Measurement of Particle Size and Concentration	127
4.4.1	The Phase Contrast Optical Microscope (PCOM)	128
4.4.2	The Transmission Electron Microscope (TEM)	128
4.4.3	Asbestos Fibres Sampling, Counting, and Sizing	129
4.4.4	Mass Concentration Sampling	132
4.4.5	Size Distribution Samples Preparation	133
4.5	Conclusion	136
<b>CHAPTER 5</b>	<b>RESULTS OF MASS CONCENTRATION ANALYSIS</b>	
5.1	Dust Dispersion	137
5.2	Comparison of Mass Concentration Results Obtained Using Several Total Inhalable Dust Samplers	139
5.3	Comparison of Mass Concentration Results Obtained Using Several Respirable Dust Samplers	145
5.4	Comparison of the Particulate Size Distributions of Inhalable, Thoracic, and Respirable Dust Samplers	154
5.4.1	Calibration of the Transmission Electron Microscope System and Sizing Software	156

5.4.2	Sizing of the Airborne Limestone Dust Sampling Using Thermal Precipitator Dust Samples	159
5.4.3	A Comparison of Size Distributions from Dust Samples Collected with Total and Respirable Dust Sampling Instruments	163
5.5	Conclusion	171
<b>CHAPTER 6</b>	<b>THE PHYSICAL CHARACTERISTICS OF ASBESTOS AND COAL DUST FROM AIRBORNE AND BIOLOGICAL SOURCES TOGETHER WITH URBAN ATMOSPHERIC POLLUTION</b>	
6.1	Introduction	173
6.2	Size Characteristics of Asbestos Fibres from Airborne and Biological Sources	174
6.2.1	Characteristics of Airborne Amosite Asbestos Fibres	175
6.2.2	Characteristics of Airborne Crocidolite Asbestos Fibres	180
6.2.3	Characteristics of Airborne Chrysotile Asbestos Fibres	189
6.2.4	Physical Characteristics of Airborne Asbestos Fibres	192
6.3	Comparison of the Physical Characteristics of Airborne and Inhaled Coal Dust Samples	196
6.4	Physical Characterization of Urban Air Pollution Particulates	204
6.5	Conclusion	210
<b>CHAPTER 7</b>	<b>GENERAL CONCLUSIONS</b>	213
<b>REFERENCES</b>		216
<b>Appendix A-1</b>	A Convenient Algorithm for $F(x)$	223
<b>Appendix B-1</b>	Apparatus of Method for the Determination of Asbestos using Transmission Electron Microscopy	224
<b>Appendix C</b>	Mass Concentration and Size Distribution of Limestone Dust Particles	225
<b>Appendix C-1a</b>	Comparison of total inhalable sampler (5 minutes limestone dust sampling)	226
<b>Appendix C-1b</b>	Comparison of total inhalable sampler (5 minutes limestone dust sampling)	227

<b>Appendix C-2a</b>	Comparison of total inhalable sampler (10 minutes limestone dust sampling)	228
<b>Appendix C-2b</b>	Comparison of total inhalable sampler (10 minutes limestone dust sampling)	229
<b>Appendix C-3</b>	Comparison of respirable sampler (5 minutes limestone dust sampling)	230
<b>Appendix C-4</b>	Comparison of respirable sampler (10 minutes limestone dust sampling)	231
<b>Appendix C-5</b>	Comparison of cyclone sampler at different flow rates 1.6 to 2.4 LPM	232
<b>Appendix C-6</b>	Raw data : Latex standard	233
<b>Appendix C-7a</b>	Comparison of number of frequency limestone dust particles obtained using TEM for 7 hole, CIS, RespiCon sampler with thermal precipitator	234
<b>Appendix C-7b</b>	Comparison of limestone dust particles size distribution obtained using TEM for 7 hole, CIS, RespiCon sampler with thermal precipitator	235
<b>Appendix C-7c</b>	Comparison of limestone dust particles mass distribution obtained using TEM for 7 hole, CIS, RespiCon sampler with thermal precipitator	236
<b>Appendix C-8a</b>	Comparison of number of frequency limestone dust particles obtained using TEM for cyclone 2.2, MRE, RespiCon and IOM sampler	237
<b>Appendix C-8b</b>	Comparison of limestone dust particles size distribution obtained using TEM for cyclone 2.2, MRE, RespiCon and IOM sampler	238
<b>Appendix C-8c</b>	Comparison of limestone dust particles mass distribution obtained using TEM for cyclone 2.2, MRE, RespiCon and IOM sampler	239
<b>Appendix D</b>	Size Distribution of Asbestos Fibres, Coal Dust Particles, and Urban Airborne Pollution.	240
<b>Appendix D-1a</b>	Particle number frequency of amosite respirable fibres using optical microscope (OM)	241
<b>Appendix D-1b</b>	Particle number frequency of amosite fibres from lung (10%) and crocidolite fibres from lung (20%) using optical microscope (OM)	242

<b>Appendix D-1c</b>	Particle number frequency of Koegas and Australia crocidolite respirable fibres using optical microscope (OM)	243
<b>Appendix D-1d</b>	Particle number frequency of airborne chrysotile fibres using optical microscope (OM)	244
<b>Appendix D-2a</b>	Comparison of amosite fibres length and diameter distribution TEM results i). Airborne Penge amosite fibres ii). Amosite fibres from lung tissue	245
<b>Appendix D-2b</b>	Comparison of crocidolite fibres length and diameter TEM results i). Airborne Koegas crocidolite fibres ii). Airborne Australian crocidolite fibres iii). Crocidolite fibres from lung tissue	246
<b>Appendix D-2c</b>	Comparison of chrysotile fibres length and diameter TEM results i). Airborne chrysotile fibres	247
<b>Appendix D-3a</b>	Comparison of number of frequency coal dust particles obtained using EM for 7 hole sampler, cyclone sampler, and from lung tissue	248
<b>Appendix D-3b</b>	Comparison of coal dust particles size distribution obtained using EM for 7 hole sampler, cyclone sampler, and from lung tissue	249
<b>Appendix D-3c</b>	Comparison of coal dust particles mass distribution obtained using EM for 7 hole sampler, cyclone sampler, and from lung tissue	250
<b>Appendix D-3d</b>	Coal particles shadowing $45^\circ$ length	251
<b>Appendix D-4a</b>	Comparison of sizing data obtained using TEM at different magnification of 2006 airborne dust sample	252
<b>Appendix D-4b</b>	Comparison of particle size distribution using TEM at different magnification between 1961 and 2006 airborne dust sample	253
<b>Appendix D-4c</b>	Comparison of particle mass distribution using TEM at different magnification between 1961 and 2006 airborne dust sample	254

## LIST OF FIGURES

<b>Figure</b>	<b>Figure Title</b>	<b>Page</b>
1.1	The five spheres.	3
1.2	The nitrogen cycle.	4
1.3	The patterns of carbon cycling through the great spheres.	5
1.4	Layers of the atmosphere.	7
1.5	The % frequency of winds direction of Beaufort force in Ireland.	8
1.6	The change of ambient temperature at ground level.	9
1.7	The general circulation of air in the atmosphere.	10
1.8	Profiles of wind speed in the United Kingdom.	11
1.9	Typical size distribution for atmospheric particles, indicating some formation pathways.	14
1.10	Electron micrograph of various particles : a). combustion particles, b). coal dust particles, c). limestone dust particles, and d). amosite fibres.	15
1.11	Fractional Semiquantitative Chemical Composition of an Urban (Cardiff) PM <sub>10</sub> sample. (a). Major Fractional Components of an Urban PM <sub>10</sub> sample; (b). Composition of Water-Soluble Fraction; (c). Composition of Inorganic Material Associated with Carbon-Based Fraction; (d). Composition of Inorganic Fraction After Removal of other Components from the sample.	24
2.1	The physiological dose-effect relationship for toxic agents.	30
2.2	Respirable sampling curve defined at the International pneumoconiosis conference in Johannesburg, 1959.	34
2.3	Thin section of a normal human lung.	41
2.4	Thin section of a coal worker's pneumoconiosis lung.	42
2.5	Thin section of lung of an individual heavily exposed to kaolin dust.	44
2.6	Thin section of a lung affected by cigarette smoking.	47



2.7	Thin section of lung of an individual exposed to asbestos dust.	49
3.1	The summary of methods used in sampling of airborne particulates.	62
3.2	The respiratory system. Adapted from the International Commission on Radiological Protection [43].	68
3.3	General scheme for deposition, clearance, translocation and retention of particles, derived from the ICRP lung model. (Heavy arrows – deposition; light dotted arrows – clearance pathways; light arrows – translocation pathways).	76
3.4	Diagram illustrating the mechanisms of particle deposition in the lung.	77
3.5	Average deposition model normally distributed (log) aerosols with given mass median aerodynamic diameters (MMAD). The results are calculated for tidal volumes of 750 mL at 15 breath/min. The deposition fraction is relative to the aerosol inhaled at nose. .... : inhalable; — : extrathoracic; ----- : respirable; - - - : trancheobronchial. Modified from the Task Group on Lung Dynamics, 1966.	82
3.6	Fractional deposition of inhaled spherical particles in various compartments of the lung predicted by the <i>International Commission on Radiological Protection Task Group on Lung Dynamics</i> . (A) Total deposition in the respiratory tract; (B) Nasal deposition; (C) Pulmonary deposition; (D) Trancheobronchial deposition.	85
3.7	Curves defining inhalable, thoracic and respirable particle fraction.	86
3.8	Fraction of airborne dust collected by sampling device vs. particle aerodynamic diameter based on (A) <i>British Medical Research Council</i> recommendations, (B) <i>American Conference Governmental Industry Hygienists</i> recommendations, (C) Predicted efficiency of pulmonary deposition based on the <i>International Radiological Protection Task Group on Lung Dynamics</i> .	88
4.1	Range of aerosol concentrations.	92
4.2a	The Casella MRE sampler.	94
4.2b	Schematic diagram of MRE sampler.	94
4.3a	The cyclone sampler.	96
4.3b	Schematic diagram of cyclone sampler.	96

4.4a	The seven hole sampler.	98
4.4b	Schematic diagram of seven hole sampler.	98
4.5a	The IOM sampler.	99
4.5b	Schematic diagram of IOM dual-fraction dust sampler and the components of the foam cassette.	100
4.6a	The Casella CIS sampler.	101
4.6b	Cassette holding a foam for PM <sub>10</sub> / thoracic (left) and cassette holding a twin foam of thoracic for thoracic (foam 1) and respirable (foam 2)(right).	102
4.7a	The RespiCon sampler.	104
4.7b	The RespiCon multistage virtual impactor.	105
4.7c	Place body unit on removal cylinder. Cover with removal disk.	108
4.7d	Press down to remove filter stage.	108
4.7e	Filter stage #1 with filter holder.	108
4.7f	Tap side of filter stage to center filter over nozzle.	108
4.7g	Place body unit over removal cylinder. Place stacked filter stages into body unit.	109
4.7h	Lift body unit to cover filter stages.	109
4.7i	Press down to seat filter stages into body unit.	109
4.8a	Cutaway view.	111
4.8b	Cross-sectional view.	111
4.9a	Marple personal cascade impactor (series 290)	113
4.9b	Pressure drop across the series 290 impactors with clean 34 mm 5-micron PVC back-up filter.	114
4.10a	Anderson cascade impactor (Mark II) with personal pump and L-shape tube.	116
4.10b	Anderson cascade impactor simulates human respiratory system.	116
4.11a	High-efficiency glass fibre filter at 4,150 X.	119

4.11b	Cellulose ester porous membrane filter with a pore size of 0.8 $\mu\text{m}$ at 4,150 X.	119
4.11c	Capillary pore membrane filter with a pore size of 0.8 $\mu\text{m}$ at 4,150 X.	120
4.12	Environmental dust chamber.	122
4.13a	Mechanical dust dispenser.	123
4.13b	Components of the dispenser.	125
4.13c	(a) Metal plate to form the rotor, and (b) dispensing chamber.	125
4.14	Personal pump and charger.	126
4.15	Respirable asbestos fibres sampling process.	130
4.16	Walton-Bracket graticulate for optical microscope counting of fibres.	131
5.1	Variation of mass concentration values determined using 5 total inhalable dust sampling devices each result obtained over a 5 minutes sampling period.	140
5.2	Variation of mass concentration values determined using 5 total inhalable dust sampling devices each result obtained over a 10 minutes sampling period.	141
5.3	Average mean and standard deviation values of mass concentration of 6 total inhalable dust sampling devices over 5 minutes sampling period.	143
5.4	Average mean and standard deviation values of mass concentration of 6 total inhalable dust sampling devices over 10 minutes sampling period.	144
5.5	Variation of mass concentration values determined using 5 respirable dust sampling devices each result obtained over a 5 minutes sampling period.	146
5.6	Variation of mass concentration values determined using 5 respirable dust sampling devices each result obtained over a 10 minutes sampling period.	146
5.7	Average mean and standard deviation values of 5 respirable dust sampling devices each result obtained over a 5 minutes sampling period.	149

5.8	Average mean and standard deviation values of 5 respirable dust sampling devices each result obtained over a 10 minutes sampling period.	150
5.9	Variation of mass concentration values of 5 cyclone dust sampling devices obtained over a 5 minutes sampling period between 1.6 to 2.4 L/min flow rates.	151
5.10	Average mean and standard deviation values of mass concentration values of 5 cyclone dust sampling devices at different flow rates between 1.6 to 2.4 L/min.	152
5.11a	Limestone aggregates images sampled using thermal precipitator at 2,050 X.	153
5.11b	Limestone aggregates images sampled using thermal precipitator at 4,400 X.	154
5.12a	Standard latex spheres image taken using TEM at 2,100 X magnification before analyse using the AnalySIS software.	157
5.12b	Standard latex spheres image taken using TEM at 2,100 X magnification after analyse using the AnalySIS software.	157
5.13	Latex sphere standard particle number frequency distribution.	158
5.14	Latex sphere standard particle number distribution cumulative %.	158
5.15a	Magnesium oxide particles end of thermal precipitator deposit taken using PCOM.	160
5.15b	Magnesium oxide particles middle of thermal precipitator deposit taken using PCOM.	161
5.16a	Magnesium oxide particles sampled using thermal precipitator at 4,400 X taken using TEM.	161
5.16b	Magnesium oxide particles sampled using thermal precipitator at 26,000 X taken using TEM.	162
5.17	Comparisons of number of particles frequency collected by the total inhalable samplers with thermal precipitator unmodified results.	162
5.18	Comparisons of number of particles frequency collected by the total inhalable samplers with thermal precipitator modified results.	163
5.19	Comparisons of cumulative % particle size distributions of the total inhalable samples and thermal precipitator result expressed in terms of equivalent circular diameter and calculated aerodynamic	164

	diameter.	
5.20	Comparisons of cumulative % particle size distributions of the respirable samples result expressed in terms of equivalent circular diameter and calculated aerodynamic diameter.	165
5.21	Comparisons of cumulative % particle size distributions between total inhalable and respirable samples result expressed in terms of equivalent circular diameter and calculated aerodynamic diameter.	166
5.22	Comparisons of particle mass distributions of the total inhalable samplers result.	166
5.23	Comparisons of particle mass distributions of the respirable samplers result.	167
5.24	Comparisons of cumulative % particle mass distributions of the average inhalable and respirable samples on the basis of ECD and AED values.	167
5.25	Comparisons of cumulative % particle mass distributions of the RespiCon sampler.	170
5.26	Comparisons of cumulative % particle mass distributions of the Marple impactor.	170
6.1	Filter with airborne amosite fibres preparation at 2,650 X.	175
6.2	Comparison of the length distributions frequency % of airborne amosite fibres obtained using PCOM and TEM analysis techniques.	177
6.3	Comparison of the length distributions frequency % of airborne amosite fibres and amosite fibres from lung obtained using TEM analysis techniques.	177
6.4	Comparison of the length distributions frequency % of amosite fibres from lung tissue obtained using PCOM and TEM analysis techniques.	178
6.5	Comparisons of diameter distributions frequency % of airborne amosite fibres and amosite fibres from lung tissue obtained using TEM analysis techniques.	178
6.6	Comparisons of aerodynamic diameter distributions frequency % of airborne amosite fibres and amosite fibres from lung tissue obtained using TEM analysis techniques.	179
6.7	Filter with airborne Koegas crocidolite fibres preparation at 2,650 X.	181

6.8	Comparisons of length distributions frequency % of airborne Koegas crocidolite fibres obtained using PCOM and TEM analysis techniques.	182
6.9	Comparisons of length distributions frequency % of crocidolite fibres from lung tissue obtained using PCOM and TEM analysis techniques.	182
6.10	Comparisons of length distributions frequency % of airborne Koegas crocidolite fibres and crocidolite fibres from lung tissue obtained using TEM analysis techniques.	183
6.11	Comparisons of diameter distributions frequency % of airborne Koegas crocidolite fibres and crocidolite fibres from lung tissue obtained using TEM analysis techniques.	184
6.12	Comparisons of aerodynamic diameter distributions frequency % of airborne Koegas crocidolite fibres and crocidolite fibres from lung tissue obtained using TEM analysis techniques.	185
6.13	Filter with airborne Australian crocidolite fibres preparation at 2,650 X.	185
6.14	Comparisons of length distributions frequency % of airborne Australian crocidolite fibres obtained using PCOM and TEM analysis techniques.	187
6.15	Comparisons of length distributions frequency % of airborne Koegas and airborne Australian crocidolite fibres obtained using TEM analysis techniques.	187
6.16	Comparisons of diameter distributions frequency % of airborne Koegas and airborne Australian crocidolite fibres obtained using TEM analysis techniques.	188
6.17	Comparisons of aerodynamic diameter distributions frequency % of airborne Koegas and airborne Australian crocidolite fibres obtained using TEM analysis techniques.	188
6.18	Filter with airborne Chrysotile fibres preparation at 2,650 X.	189
6.19	Comparisons of length distributions frequency % of airborne Australian crocidolite fibres obtained using PCOM and TEM analysis techniques.	190
6.20	Comparisons of length distributions frequency % of airborne Chrysotile fibre, airborne Koegas crocidolite fibre and airborne Penge amosite fibre obtained using TEM analysis techniques.	191

6.21	Comparisons of diameter distributions frequency % of airborne Chrysotile fibre, airborne Koegas crocidolite fibre and airborne Penge amosite fibre obtained using TEM analysis techniques.	191
6.22	Comparisons of aerodynamic diameter distributions frequency % of airborne Chrysotile fibre, airborne Koegas crocidolite fibre and airborne Penge amosite fibre obtained using TEM analysis techniques.	192
6.23	Variation of average fibre length of airborne amosite fibre and amosite fibre from lung tissue with diameter of fibre.	194
6.24	Variation of average fibre length of airborne crocidolite fibre and crocidolite fibre from lung tissue with diameter of fibre.	194
6.25	Variation of average fibre length of airborne Penge amosite fibre, airborne Koegas crocidolite fibre, airborne Australian crocidolite fibre, and airborne Chrysotile fibre with diameter of fibre.	195
6.26	Thin section of a coal mine worker lung.	197
6.27	Coal dust particles from the lung tissue at 2,100 X.	198
6.28	Coal dust particles sampled using 7 hole sampler at 2,100 X.	198
6.29	Coal dust particles sampled using cyclone sampler at 2,100 X.	199
6.30a	Coal particle shadowing concept.	200
6.30b	Coal dust particles 45 <sup>0</sup> shadows at 3,400 X.	200
6.31	Particle size (ECD) vs thickness (length) of Coal Dust Particles shadow.	202
6.32	Average Particle size (ECD) vs thickness (length) of Coal Dust Particles shadow.	202
6.33	Comparisons of the cumulative mass distribution of coal particles collected with the 7 hole sampler, cyclone sampler, and coal particles from lung tissue on the basis of calculated aerodynamic diameter values.	203
6.34	Comparisons of the cumulative mass distribution of coal particles collected with the 7 hole sampler, cyclone sampler, and coal particles from lung tissue on the basis of ECD diameter values.	203
6.35	Cumulative mass distribution of coal particles which have been size selected by a cyclone sampler and retained in the lung tissue in comparison with the ACGIH and the BMRC convention of predicted respirable dust.	204

6.36	Comparison of 2006 airborne particulates at different magnifications : a). 2,100 X, b). 4,400 X, c). 11,000 X, and d). 13,000 X.	206
6.37	Comparison of 2006 airborne particulates distribution % at different magnification obtained using the TEM analysis techniques.	206
6.38	Comparison of particle distributions number % of 1961 and 2006 airborne particulates on the basis of ECD diameter values.	207
6.39	Comparison of particle distributions number % of 1961 and 2006 airborne particulates on the basis of aerodynamic diameter values.	208
6.40	Comparison of mass distributions number % of 1961 and 2006 airborne particulates on the basis of ECD values.	208
6.41	Comparison of mass distributions number % of 1961 and 2006 airborne particulates on the basis of aerodynamic diameter values.	209
6.42	Comparison of 1961 and 2006 airborne particulates.	210
7.1	Comparison of mass distribution % of coal dust particle from lung tissue, crocidolite fibres from lung tissue, and airborne limestone dust particles on the basis of aerodynamic diameter.	215



## LIST OF TABLES

<b>Table</b>	<b>Table Title</b>	<b>Page</b>
1.1	Mass of different gases in the world's atmosphere	6
1.2	Characteristics of gaseous, aerosol particles, and hydrometeor particles	12
1.3	Summary sources of man-made airborne particulates	16
1.4	Summary of primary and secondary sources of natural airborne particulates	16
1.5	Sources of air pollutants in the United States in 1980*	17
1.6	Pollution emissions in the United States in 1977*	17
1.7	Semiquantitative composition of an airborne particulate Sample collected from the Cardiff Area (Expressed As Parts Per Thousand on a Mass Basis)	25
2.1	Classification of health hazards associated with gases and vapours	31
2.2	Classification of health hazards associated with airborne particulates	35
2.3	Main known human carcinogens linked to cancers	50
3.1	Proposed values of inspirable fraction, thoracic fraction and thoracic fraction as a subdivision of inspirable	71
3.2	Proposed values of respirable fraction collected and the respirable fraction as a subdivision of inspirable and thoracic fraction	73
3.3	Inhalable, thoracic, and respirable fractions.	74
3.4	Mass deposition fractions according to the <i>International Standards Organizations (ISO)</i> .	86
4.1	Relationship between size/number and mass concentration.	92
4.2	Series 290 impactor cut-points at 2 L/min.	113
4.3	Anderson cascade impactor cut-points at 28.3 L/min.	117
4.4	Summary of airborne sampling equipments descriptions.	121

4.5	Fibres and health-related diseases.	130
5.1a	Mean and standard deviation average fro total inhalable samplers obtained over a 5 minutes sampling.	141
5.1b	Mean and standard deviation average fro total inhalable samplers obtained over a 10 minutes sampling.	142
5.2a	Mean and standard deviation average for respirable samplers obtained over a 5 minutes sampling.	148
5.2b	Mean and standard deviation average for respirable samplers obtained over a 10 minutes sampling.	148
5.3	Mean and standard deviation average for cyclone samplers sampling at different flow rates between 1.6 to 2.4 L/min.	152
5.4	Comparisons of the fractional % and mass content of the experimental respirable limestone dust cloud produced by gravimetric and arithmetic methods.	168
5.5	Comparison of results for size slective sampler i.e. the RespiCon and CIS sampler for respirable, thoracic, and inhalable dust fractions.	169
6.1	Summary of physical characteristics of asbestos fibres from airborne and lung dust samples.	193

## NOMENCLATURE

### Symbol

aq	Aqueous (dissolved in water)
g	Gaseous
s	Solids
TM	Trade mark
<sup>0</sup> C	Degree celcius
a.m.	Ante meridien
p.m	Post meridien
mb	Pressure
pH	A measure of the acidity of a solution in terms of activity of hydrogen (H <sup>+</sup> )
R	Respirable concentrations
T	Particle thickness

### Mathematical Symbol

$d$	Particle diameter
$d_l$	Spherical particle density
$d_F$	Fibre diameter
$d_{AE}$	Particle aerodynamic diameter
$d_{AEF}$	Fibre aerodynamic diameter
$x$	$\ln(d_{AE}/\Gamma)/\ln(\Sigma)$ , dummy argument used in calculating $ST(d_{AE})$ and $SI(d_{AE})$
$F(x)$	Cumulative probability function of a standardized normal random variable [see Appendix A]
$SI(d_{AE})$	Sampling efficiency of an ideal collector of the inspirable fraction (also called inhalable fraction) which is proposed by Soderholm [40].
$SI\{ACGIH\}$	Sampling efficiency of an ideal collector of the inspirable fraction which was given by ACGIH [43].
$SI\{ISO\}$	Sampling efficiency of an ideal collector of the inspirable fraction which was given by ISO [42].
$SR(d_{AE})$	Sampling efficiency of an ideal collector of the respirable fraction

which was given by Soderholm [40].

*SR{ACGIH}* Sampling efficiency of an ideal collector of the respirable fraction which was given by ACGIH [43].

*SR{BMRC}* Sampling efficiency of an ideal collector of the respirable fraction which was given by Orenstein [48].

*ST(d<sub>AE</sub>)* Sampling efficiency of an ideal collector of the thoracic fraction which was given by Soderholm [40].

*ST{ACGIH}* Sampling efficiency of an ideal collector of the thoracic fraction which was given by ACGIH [43].

*ST{ISO}* Sampling efficiency of an ideal collector of the thoracic fraction which was given by ISO [42].

$\rho_0$  Unit density

$\rho_1$  Spherical density

$\sigma_g$  Geometric standard deviation

$e_F$  Fibre density

$e_0$  Unit density

# Number

% Percent

< Less than

\$ Dollar sign

D<sub>20</sub> 20 % Distribution

### Greek Letter

$\Gamma$  Parameter with units length which is sometimes used when calculating the thoracic or respirable fraction

$\Sigma$  Unitless parameter which is sometimes used when calculating the thoracic or respirable fraction

$\pi$  Pi

### SI Unit

ml Millilitres

nm Nanometres

mg Milligrams

$\mu\text{m}$	Micrometres
$\mu\text{m}^2$	Square micrometres
gm	Grams
kg	Kilograms
$\text{cm}^3$	Cubic centimetres
$\text{dm}^3$	Cubic decimetres
$\text{m}^3$	Cubic metres
mm	Millimetres
m	Metres
s	Second
$\mu\text{g}$	Micrograms
$\text{gm}/\text{cm}^3$	Unit density
ng	Nanograms
L/min	Litre per minutes
mppcf	Million of particles per cubic foot
kV	Kilovolts

#### Abbreviation

TEQ	Toxic equivalent
PCB	Polychlorinated biphenyls
PAH	Polynuclear aromatic hydrocarbons
TOMPs	Toxic organic micropollutants
QUARG	Quality of Urban Air Review Group
PEC	Particulate elemental carbon
NOA	Naturally occurring asbestos
CWP	Coal Worker's Pneumoconiosis
COPD	Chronic obstructive pulmonary disease
EPA	Environmental Protection Agency
ICRP	International Commission of Radiological Protection
MDHS	Methods for determination of hazardous substances
EDXA	Energy-dispersive X-ray analysis
ACGIH	American Conference of Governmental Industrial Hygienists
PVC	Polyvinyl chloride

PUF	Poly urethane foam
MPC	Magnetic particle clutch
TWA	Time Weighted Average
D.D.T	Dichloro-diphenyl-trichloroethane
SPM	Suspended particulates measurements
TSP	Total suspended particulate
PM	Particulate matter
PM <sub>10</sub>	Coarse particulate
PM <sub>2.5</sub>	Fine particulate
PM <sub>1.0</sub> & PM <sub>0.1</sub>	Ultrafine particulate
CIS	Conical inhalable sampler
MRE	Mining Research Establishment
IOM	Institute of Medicine
LPM	Liter per minutes
BMRC	British Medical Research Council
UK	United Kingdom
USA	United State of America
NAAQS	National Ambient Air Quality Standard
CEN	European Committee for Standardization
OSHA	Occupational Safety and Health Administration
ACFM	Actual Cubic Feet per Minute
C.C.D.	Charge-Couple-Device
IARC	International Agency for Research on Cancer
WHO	World Health Organization
ISO	International Standards Organization
O.M.	Optical microscopy
E.M.	Electron microscopy
TEM	Transmission electron microscope
PCOM	Phase contrast optical microscope
DGP	Dust generating period
SP	Sampling period
IAP	Indoor air pollution
TP	Thermal Precipitator

MMAD	Mass median aerodynamic diameters
TLV	Threshold limit value
SD	Standard Deviation
ECD	Equivalent circular diameter
AED	Aerodynamic diameter

Chemical  
Symbol

Zn	Zinc
Pb	Lead
Cu	Copper
Hg	Mercury
Cd	Cadmium
As	Arsenic
P	Phosphorus
Se	Selenium
S	Sulphur
O <sub>2</sub>	Oxygen
SO <sub>x</sub>	Sulphur oxides
CO	Carbon monoxide
HC	Hydrocarbon vapour
NO <sub>x</sub>	Nitrogen oxides
N <sub>2</sub>	Atmosphere nitrogen
NO <sub>2</sub>	Nitrogen dioxide
NH <sub>3</sub>	Ammonia
NO <sub>3</sub>	Soil nitrates
CO <sub>2</sub>	Carbon dioxide
CO <sub>3</sub> <sup>2-</sup>	Carbonate
HCO <sub>3</sub>	Bicarbonate
Ar	Argon
H <sub>2</sub> O	Water vapour
Ne	Neon
Kr	Krypton

CH <sub>4</sub>	Methane
He	Helium
O <sub>3</sub>	Ozone
Xe	Xeon
N <sub>2</sub> O	Dinitrogen oxide
H <sub>2</sub>	Hydrogen
NO	Nitric oxide
SO <sub>2</sub>	Sulphur dioxide
H <sub>2</sub> S	Hydrogen sulfide
C	Carbon / Carbon black
H	Hydrogen
N	Nitrogen
O	Oxygen
Na <sup>+</sup>	Sodium
Ca <sub>2</sub> <sup>+</sup>	Calcium
Mg <sup>2+</sup>	Magnesium
K <sup>+</sup>	Potassium
SO <sub>4</sub> <sup>2-</sup>	Sulfate
Cl <sup>-</sup>	Chloride
NH <sub>4</sub> <sup>+</sup>	Ammonium
NO <sub>3</sub> <sup>-</sup>	Nitrate
OH	Hydroxyl free
H <sub>2</sub> SO <sub>4</sub>	Sulphuric acid
HCL	Hidrochloric acid
Ti	Titanium
Ni	Nickel
Co	Cobalt
Mn	Manganese
Si	Silicon
Fe	Iron
Al	Aluminium
Cr	Chromium



# CHAPTER 1 : **THE ATMOSPHERE AND AIRBORNE PARTICULATES**

## **1.1 Introduction**

In our modern society, many countries are rapidly developing in an attempt to become industrial powers in the world and in the process becoming more urbanized. Some of this development has managed to improve the quality of human life on a daily basis, but at a cost to the environment which has become more polluted even though the policies adopted highlight the need for sustainable development. This progress has been dependant upon integrating many aspects of life to produce a better world for human beings in terms of political, economical and social welfare. However, there are still aspects of the environment today which have been neglected. The world where we live has shown a steady anthropogenic increase in the pollution of soil, water supplies and also a reduction in the quality of the air we breathe.

In this chapter a review of air pollution, its history, sources and classification of air pollutants are discussed. The focus will be on airborne particulates; covering their definition, terminology, sources (natural and anthropogenic) of particulates both primary and secondary in origin. The characterization of suspended particulate matter and its environmental effects are the matter of a significant amount of research especially with the respect to human health.

Air quality has been changing steadily as a result of the increase in world population. Many more human activities such as rapid development of rural and urban areas, with development of transportation, increased number of factories, greater consumption of fossil fuel are the main sources of anthropogenic pollution. Many sources of natural pollution such as wind erosion, and natural forest fires have also been exacerbated by human activity. These natural sources, create air pollution which consist of additional gases, particulates, and also vapours. Some of the major gaseous pollutants include sulphur oxides ( $\text{SO}_x$ ), carbon monoxide (CO), hydrocarbon vapours (HC), nitrogen oxides ( $\text{NO}_x$ ). All of which create problems in our atmosphere producing effects such as acid rain, ozone depletion in the upper atmosphere and global warming, haze, and interference with the quality of the air we breathe

everyday. Fortunately, most of these gaseous pollutants have short half-lives but are a major contributor to secondary particulate pollution in the atmosphere. There are many published definitions of air pollution some examples of which are listed as follows :

- ‘Undesirable material in air, in quantities large enough to produce harmful effects [1].’
- ‘The presence in the atmosphere of one or more contaminants (i.e. dust, fumes, gas, mist, odour, smoke, or vapour) in sufficient quantities, of such characteristics and of such duration as to be or threaten to be injurious to human, plant, or animal life or to property, or which reasonably interferes with the comfortable enjoyment of life or property [2].’

The simple dictionary definition of this term refers to the process of making air, water, soil, etc. contaminated by substances that make air, water, soil, etc. polluted [3].

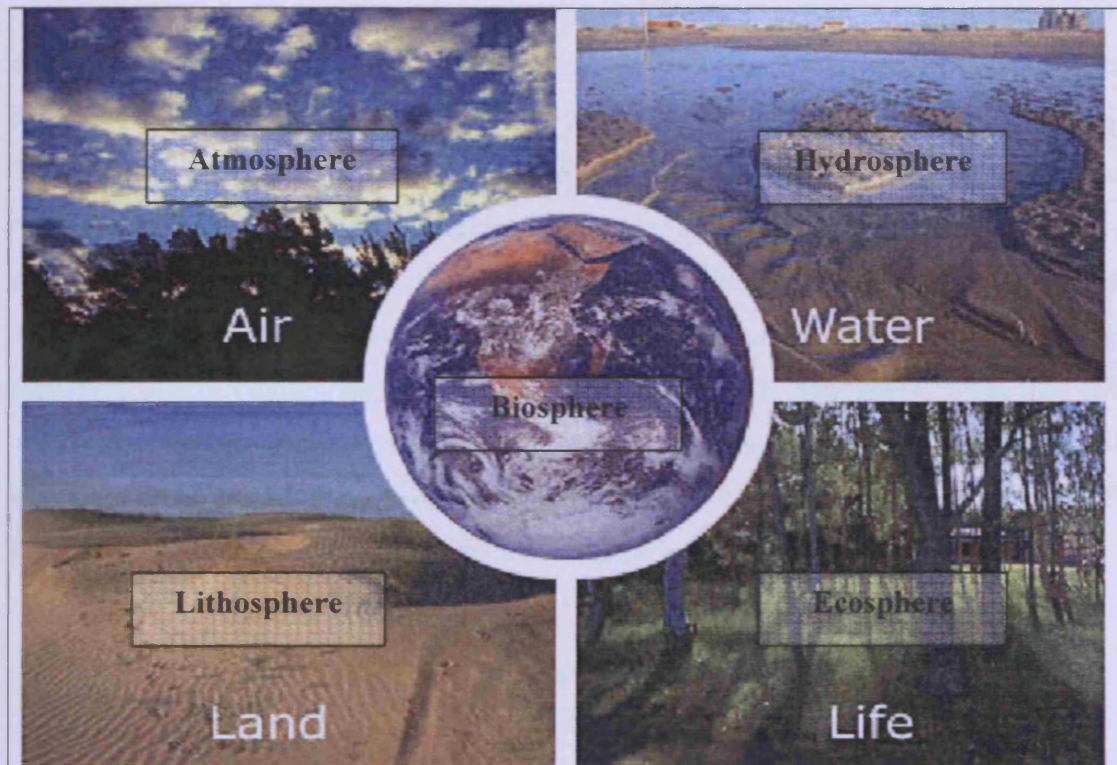
An increase in airborne particulate material of an unnatural nature is one of the major atmospheric pollution problems facing the world. It has been the subject of many studies conducted in the UK since the smog tragedy of London in 1952. Researchers have developed a great interests in particulates with an emphasis being directed towards total suspended particulates (TSP), coarse particulate (PM<sub>10</sub>) and now is concentrated on fine particulates (PM<sub>2.5</sub>) and ultra-fine particulates (PM<sub>1.0</sub> & PM<sub>0.1</sub>). This study has focused on the collection and characterization of the particulates found in the atmosphere, and most importantly upon those characteristics of particulates which affect human health.

## 1.2 The Atmosphere

The atmosphere is an integral part of our environment which itself can be described in terms of five major spheres encompassing all material things on our planet earth as illustrated by **Figure 1.1**. The environment consists of the atmosphere, the lithosphere, the hydrosphere, the biosphere, and also the ecosphere. The lithosphere, comprises all the solid rock of the planet’s crust (surface), and all the rock

that lies beneath the crust. The hydrosphere consists of the total liquid water of the planet. The biosphere is that part of the planet comprising of all living things. While the atmosphere, defines all of the gaseous component of our planet.

**Figure 1.1 : The Five Spheres.**



\* Source : [82].

Early humans used natural resources such as water, air, food and shelter to live with little impact on the environment. However, with an increase of the human population and an increase in the requirement to satisfy their needs, an impact on our environment became apparent. As humans we are aware that changes in our environment are occurring but we are not motivated to reduce or reverse the impact we create because of our insatiable desire to improve our standard of living. China is a good example of the new developing countries neglecting their environment and as a result their rivers are polluted and the risk to human health from the air they breathe has increased.

As illustrated in **Figure 1.1**, the spheres are closely interconnected and the area of common overlap is often referred to as the ecosphere. If there are any changes



in one of the spheres, it will create changes in one or more of the other spheres. These changes within an ecosystem are often referred to as events. There is a continual cycling between the spheres of our environment and this is illustrated by the nitrogen cycle in **Figure 1.2**. These cycles are natural features of our environment and there is a continuous interaction between the major spheres, which is illustrated by the cycling of the elements and compounds between them. Another example is that of the carbon cycle as illustrated in **Figure 1.3** in which it can be seen that carbon can transfer steadily between the atmosphere, the hydrosphere, the lithosphere, and the biosphere. It is to be expected that any pollution of a carbonaceous nature can transfer and distribute itself readily around the planet as shown by the world wide spread of D.D.T. Pesticide D.D.T was used widely for the elimination of malaria in many parts of the world and was used extensively to control insect pests on food and fiber plants [4]. However, many studies have shown that the D.D.T is a cumulative toxin that has adversely affected many non-target species and thus, it can be found in almost all living things throughout the world including humans. D.D.T has been banned in U.S but still it is being produced for used in several developing countries.

**Figure 1.2 : The Nitrogen Cycle.**

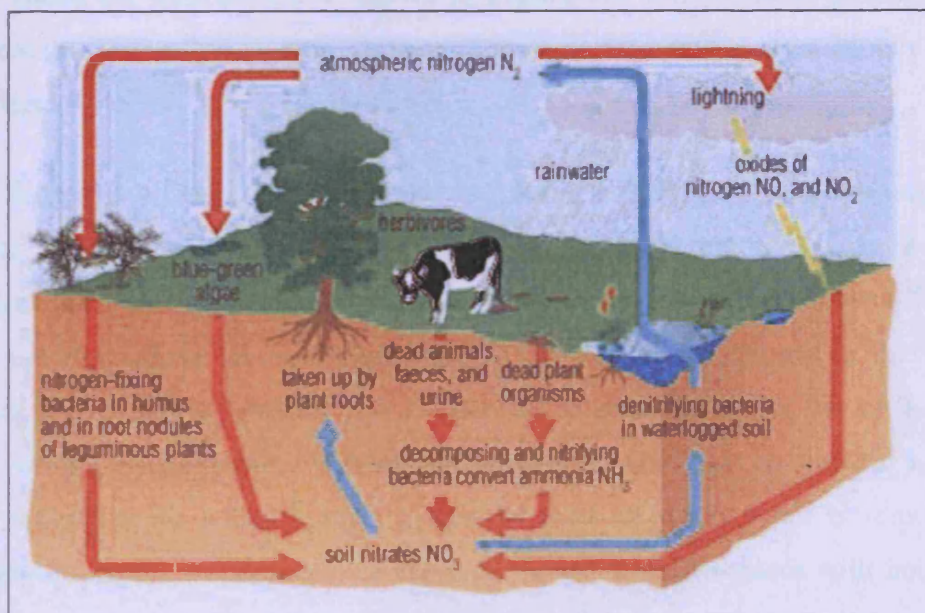
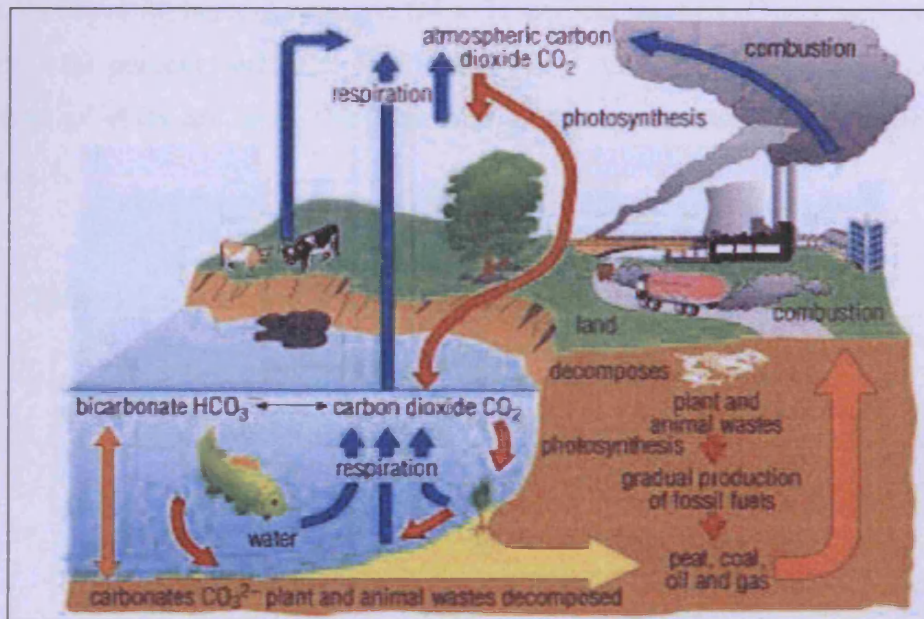


Figure 1.3 : The Patterns of Carbon Cycling through the Great Spheres.



### 1.3 Composition and Structure of the Atmosphere

The atmosphere can be divided into four layers and these are the thermosphere, mesosphere, stratosphere, and the most important layer at the planet surface called the troposphere as shown in **Figure 1.4**. Air pollution produced from either natural or anthropogenic (human-made) sources and occurs mostly in the troposphere.

*Tropos* is a Greek word meaning as turning or changing. The Troposphere is the layer in which we live. This layer begins at sea level and is between 8 and 15 kilometres thick [5]. It contains 50 % of all the air in the entire atmosphere. It is that part of the atmosphere where we can see all the clouds and changes in the weather occurring and it is in a constant rate of flux due to solar heating at the surface. This heating warms the air masses, which rise to release latent heat as sensible heat that further buoys the air mass. It then, continues until all water vapor is removed by condensation. In the troposphere, on average, temperature decreases with height due to expansive cooling. The average temperature of the atmosphere at the surface of earth is 14 °C and temperature of air normally reduces by 1 °C per 100 metres in height. The variation of temperature with height and air pressure is illustrated by **Figure 1.4**.



The air in the troposphere is the air, which we breathe and it consists, by volume, of about 78 percent nitrogen (N<sub>2</sub>), 21 percent oxygen (O<sub>2</sub>), 1 percent argon (Ar), and 0.03 percent carbon dioxide (CO<sub>2</sub>) [4,5]. Also present are traces of other gases, most of which are inert. The total mass of each gas in the atmosphere are given in Table 1.1.

**Table 1.1 : Mass of Different Gases in the World's Atmosphere.**

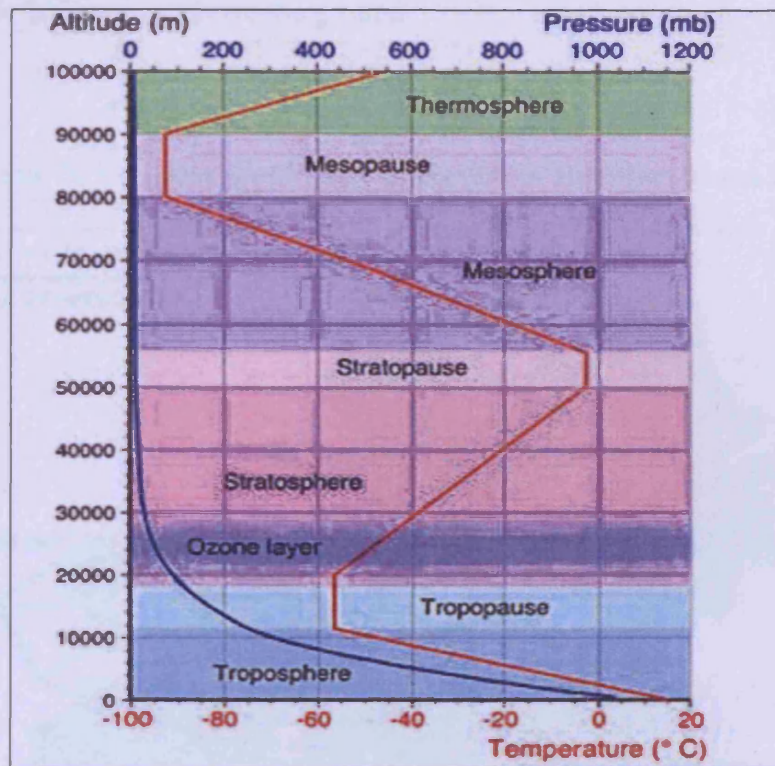
Gas of vapour	Trillions of tonnes
Nitrogen (N <sub>2</sub> )	3900
Oxygen (O <sub>2</sub> )	1200
Argon (Ar)	67
Water vapour (H <sub>2</sub> O)	14
Carbon dioxide (CO <sub>2</sub> )	2.5
Neon (Ne)	0.065
Krypton (Kr)	0.017
Methane (CH <sub>4</sub> )	0.004
Helium (He)	0.004
Ozone (O <sub>3</sub> )	0.003
Zenon (Xe)	0.002
Dinitrogen oxide (N <sub>2</sub> O)	0.002
Carbon monoxide (CO)	0.0006
Hydrogen (H <sub>2</sub> )	0.0002
Ammonia (NH <sub>3</sub> )	0.00002
Nitrogen dioxide (NO <sub>2</sub> )	0.000013
Nitric oxide (NO)	0.000005
Sulphur dioxide (SO <sub>2</sub> )	0.000002
Hydrogen sulfide (H <sub>2</sub> S)	0.000001

\* Source : Giddings[6].

#### 1.4 Dynamics of the Atmosphere

The dramatic and rapid changes that can occur in the atmosphere are referred to as the weather, which has great influence upon our immediate atmosphere. The dynamics of the atmosphere are controlled by temperature, humidity, and planetary motion [7]. The weather has a dramatic effect upon pollution levels [8]. Pollutants can be dispersed and diluted by the wind, turbulence, and mixing depth. **Figure 1.5**, is an example of Ireland frequency of winds of different Beaufort Force where the predominant wind direction is from the south west for the majority of the year. Sometimes in the summer months, the wind will blow from the south east. During these periods, the polluted air arrives from Europe directly increasing the pollution levels in the UK.

Figure 1.4 : Layers of the Atmosphere.



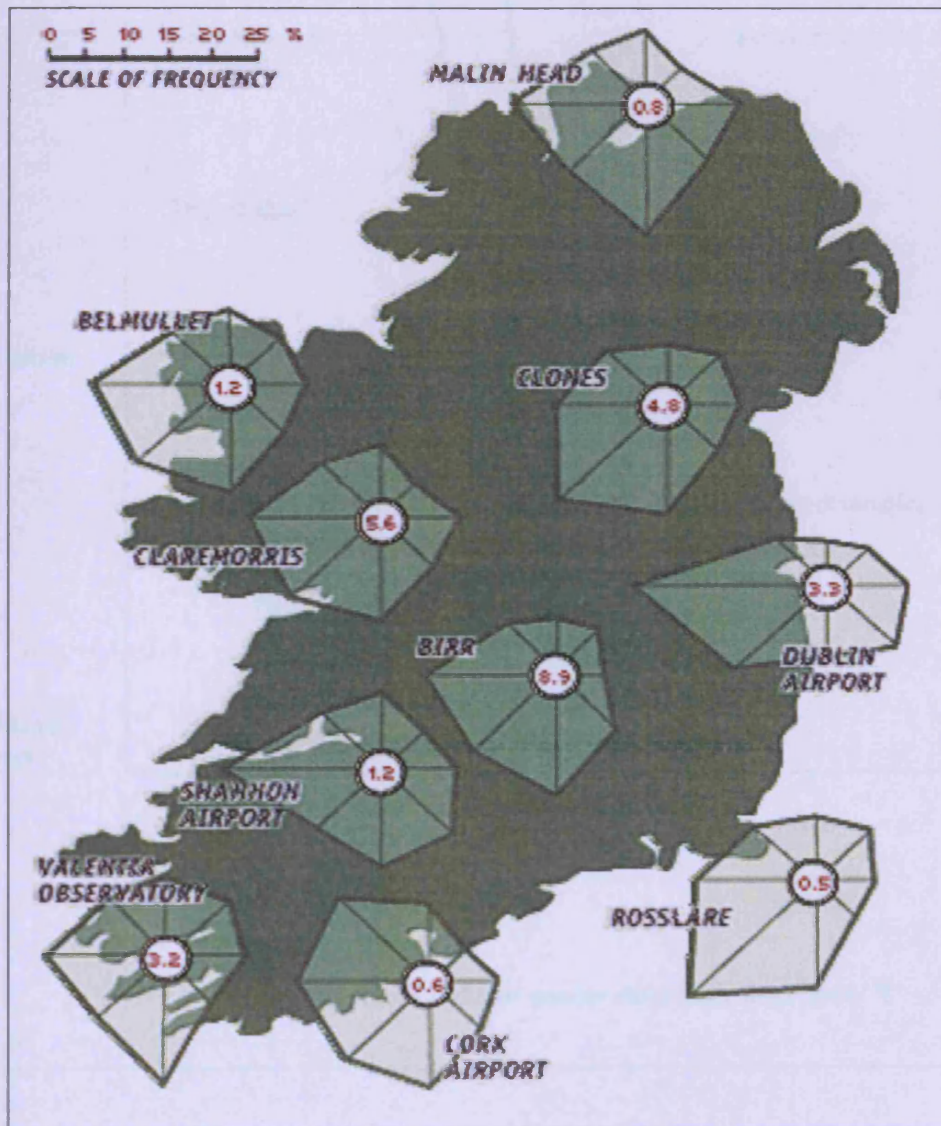
\* Source : [83].

Atmospheric turbulence determines how rapidly a parcel of polluted air is dispersed as it moves away from the source [8]. While dispersion on the other hand, is less under stable atmospheric conditions, which occur largely at night-time, than under unstable conditions, which can occur during the middle of the day when heating of the ground by the sun causes thermal turbulence. In between atmospheric turbulence and thermal turbulence, there is neutral stability, which is the most frequent condition between the two extremes. **Figure 1.6** and **Figure 1.7** show the change of ambient temperature at ground level and the general circulation of low and high pressure air in the atmosphere.

The mixing depth is the depth of the atmosphere into which the pollutants readily mix. Temperature inversions can restrict the depth of this mixed layer, and act as a lid to the atmosphere, allowing pollutants to build up underneath. Temperature inversions normally occur at night-time when there is a rapid cooling of the ground, and also when warm air moves in over cold ground. In rural areas the inversions may occur only a few tens of metres above the ground. But contrary to large urban areas,

the heat islands effect created by additional heat sources produce inversions more typically 100 to 200 metres above the ground.

**Figure 1.5 : The % Frequency of Winds Direction of Beaufort Force in Ireland.**



\* Note : Circled Number = % Calm.  
\* Source : The Irish Meteorological Service Online [9].



**Figure 1.6 : The Change of Ambient Temperature at Ground Level.**

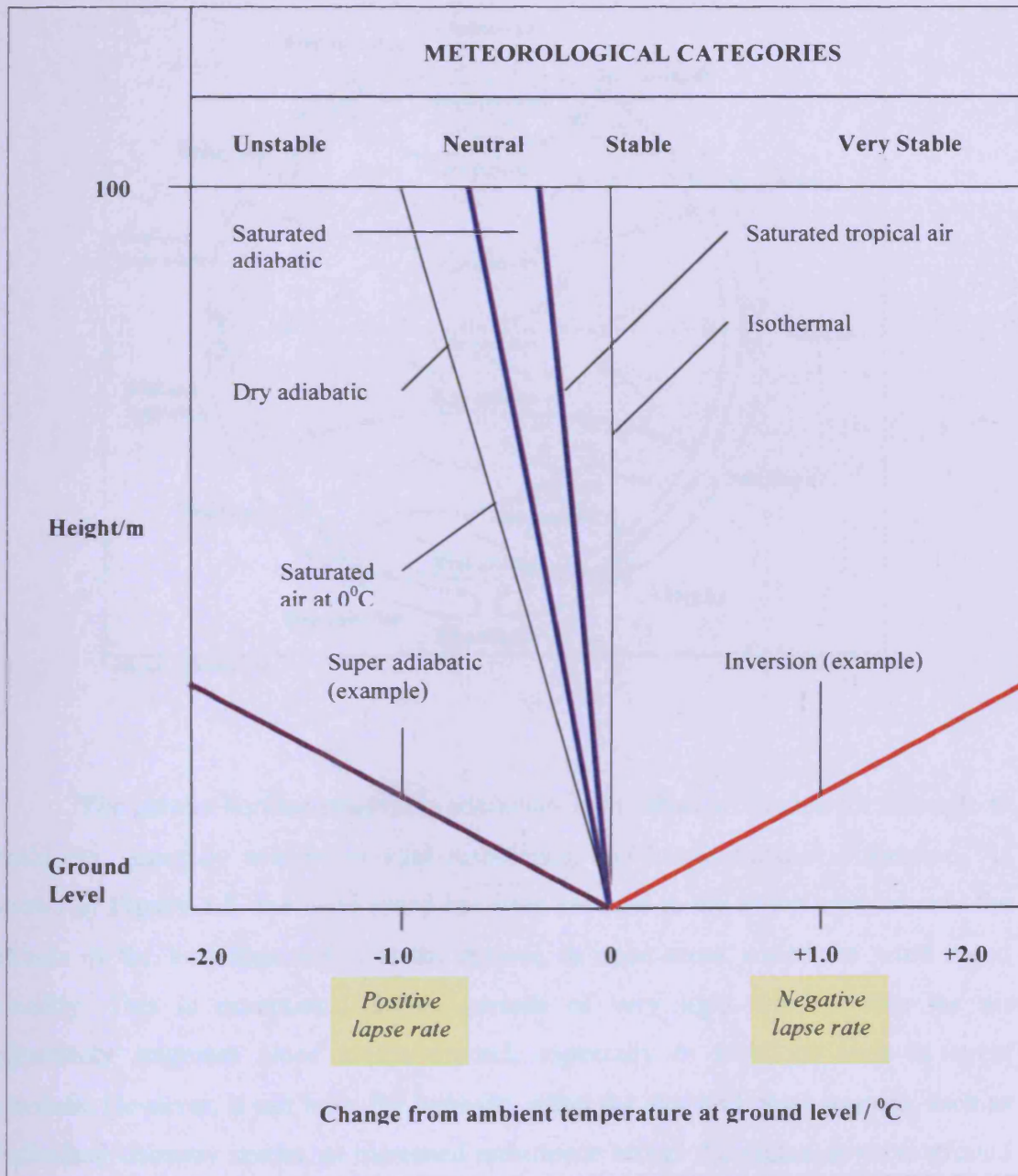
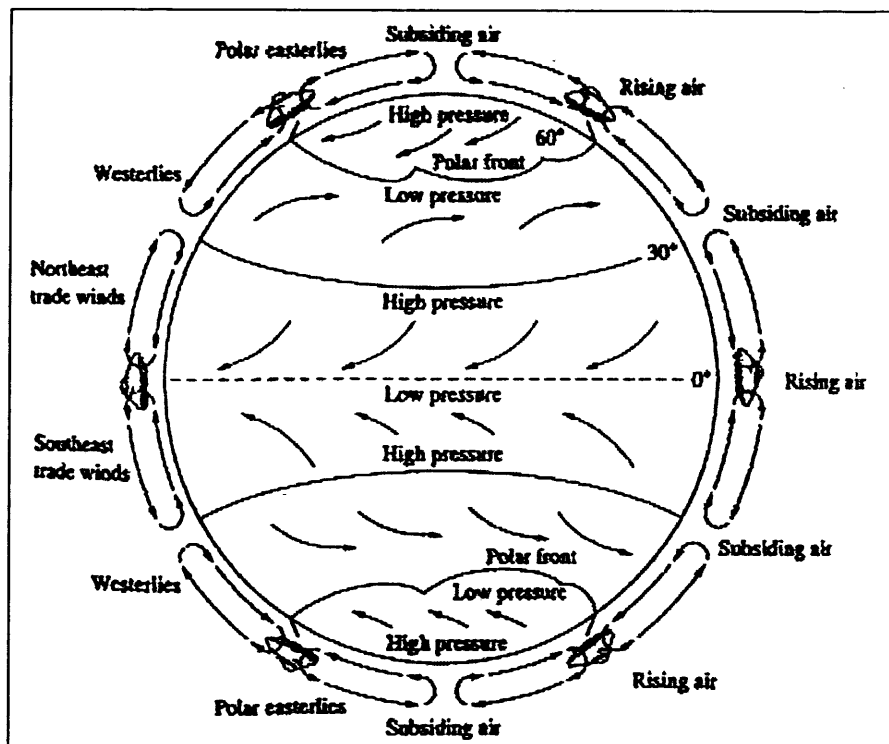


**Figure 1.7 : The General Circulation of Air in the Atmosphere.**



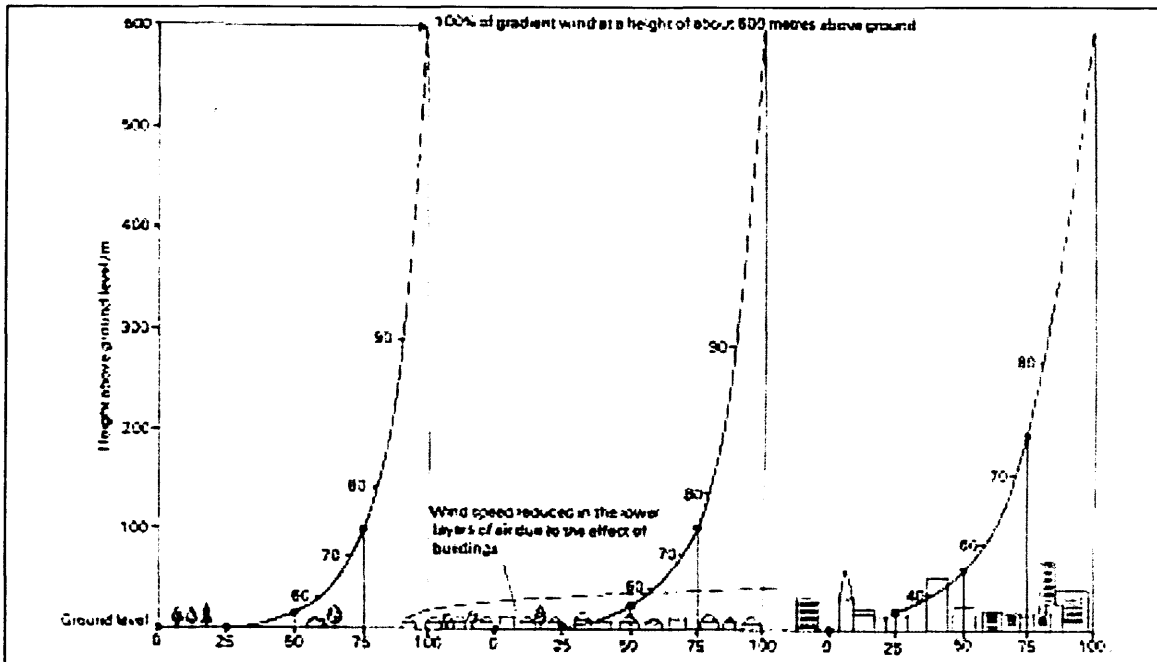
\* Source : Nevers [1].

The greater surface roughness encountered in urban areas, due for example to buildings, generally acts to increase turbulence, and hence enhance dispersion. As shown in **Figure 1.8**, the wind speed has been reduced in the lower layers due to the effects of the buildings and it is the reverse in open areas where the wind speed steadily. This is exceptional during periods of very light winds, when the air effectively stagnates close to the ground, especially in locations such as street canyons. However, it can have the opposite effect for elevated point sources, such as individual chimney stacks, as increased turbulence brings the plume down to ground more rapidly, giving rise to higher concentrations than would be found around a similar source in a rural area.

The conditions that created pollution episodes in urban areas involve [8] low wind speeds, stable atmosphere conditions and low mixing heights. These meteorological conditions normally occur during anti-cyclonic weather and mainly at night-time. During the day, the temperature inversion is likely to break up as the sun warms the ground. However, during the winter months, it is possible for inversions to persist throughout the day and they may survive for several days before breaking up.

In the latter part of the 20<sup>th</sup> century similar conditions were responsible for the pollution episode in London in December 1991. This recent episode, which saw the highest concentrations of air pollution ever recorded, occurred during the night-time.

**Figure 1.8 : Profiles of Wind Speed in the United Kingdom.**



## 1.5 Airborne Particulate Matter

Airborne particulate matter is considered as one of the most unique and complex sources of atmosphere air pollution. It occurs in a wide range of particle sizes and many different chemical compositions. It is produced from either primary or secondary sources in our surrounding environment. Generally, coarse particulate matter (PM) [7] is made up of primary particles, while fine PM is dominated by secondary particles according to the Air Quality Expert Group in the *Particulate Matter in the United Kingdom* report [10].

An aerosol particle [11] is defined as a single liquid, solid, or mixed phase particle or an ensemble of suspended particles. Hydrometeor particles are defined as an ensemble of liquid, solid, or mixed-phase water particles suspended in or falling through the air and contain more water than aerosol particle. These liquids [11] in

aerosol and hydrometeor particles may be pure or may consist of a solution. A *solution* is homogenous mixture of substances that can be separated into individual components on change of state (e.g., freezing). A solution also consists of *solvent*, such as water, and one or more solutes dissolved in the solvent. Pure water and solutes dissolved in water are known as aqueous (dissolved in water) and are denoted as “(aq)”. Followed by gaseous as “(g)” and solids as “(s)”. **Table 1.2** Describe the physical characteristics of gaseous, aerosol particles and hydrometeor particles.

**Table 1.2 : Characteristics of gaseous, aerosol particles, and Hydrometeor Particles.**

	Typical diameter (µm)	Number Concentration (Molecules or Particles/cm <sup>3</sup> )	Mass Concentration (µg/m <sup>3</sup> )
Gas molecules	0.0005	$2.45 \times 10^{19}$	$1.2 \times 10^9$
Aerosol particles			
Small	<0.2	$10^3$ - $10^6$	<1
Medium	0.2-2.0	$1$ - $10^4$	<250
Large	>2.0	<1-10	<250
Hydrometeor particles			
Frog drops	10-20	1-500	$10^4$ - $10^6$
Cloud drops	10-200	1-1,000	$10^4$ - $10^7$
Drizzle	200-1,000	0.01-1	$10^5$ - $10^7$
Raindrops	1,000-8,000	0.001-0.01	$10^5$ - $10^7$

\* Source : Jacobson [11].

The main determinant of the behaviour of an atmospheric particle is its size. This is usually expressed in terms of its ‘aerodynamic diameter’, which refers to a unit density spherical particles with the same aerodynamic properties, such as falling speed [7]. In practice, except for very dense materials and clusters, the aerodynamic diameter is very similar to the geometric diameter as might be measured with a light microscope or electron microscope. PM<sub>10</sub>, refers to particulate matter less than 10 µm aerodynamic diameter (or, more strictly, particles which pass through a size selective inlet with a 50 % efficiency cut-off at 10 µm aerodynamic diameter) [7,8,12]. PM<sub>2.5</sub>, refers to particles passing a size-selective inlet of a sampling instrument designed to exclude particles greater than 2.5 µm aerodynamic diameter.

The distribution of particle size in the atmosphere [8] can be divided up into three groups of particles (or modes), as shown in the schematic diagram **Figure 1.9**. These are the *Nucleation mode*, *Accumulation mode*, and *Coarse mode*.

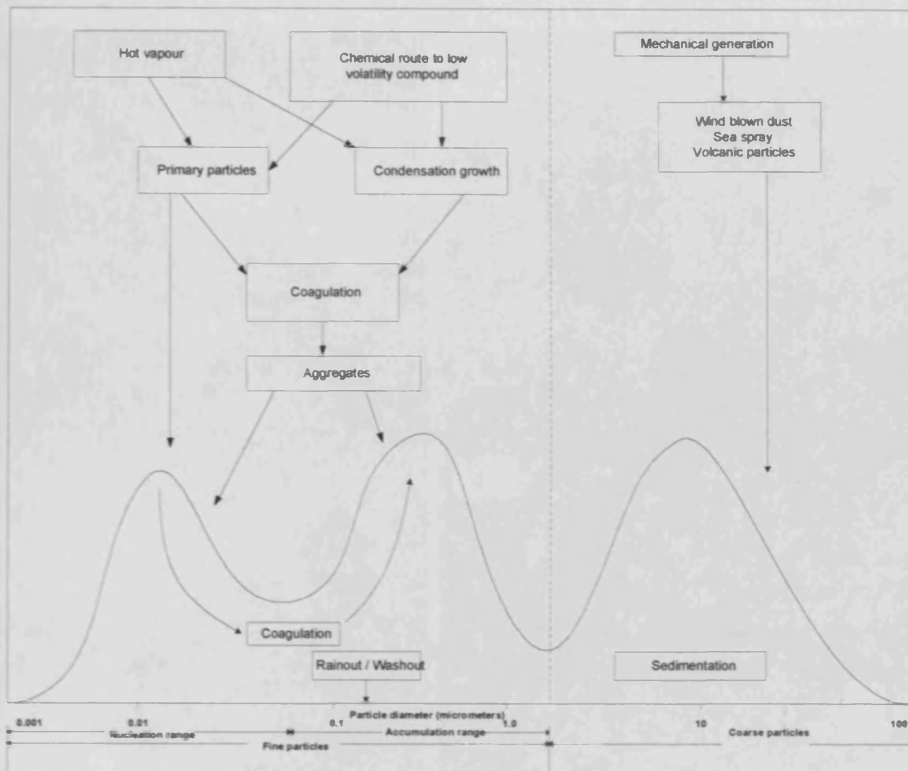
*Nucleation mode, < 0.2 µm diameter* : include particles which were recently emitted from processes involving condensation of hot vapours (eg. incinerator, smelter), or particles freshly formed within the atmosphere by gas to particle conversion (eg. sulphuric acid particles from sulphur dioxide oxidation). Nucleation mode particles have rather transient existences, as they rapidly coagulate into larger particles; hence in many situations the nucleation mode is not found.

*Accumulation mode, particles 0.2 to 2 µm diameter* : This mode comprises particles which have grown from the nucleation mode by coagulation or condensation of vapours. These are the most stable and long-lived of atmospheric particles with a lifetime of some 7 to 30 days, as they are not subject to efficient removal by gravitational settling, scavenging by rain, or any of other mechanisms, which remove smaller and larger atmospheric particles.

*Coarse mode, > 2 µm* : These particles are mainly formed by mechanical attrition processes, and hence soil dust, sea spray, and many industrial dusts fall within this mode. This is due to their large size and high settling speeds, their atmospheric lifetime tends to be short.

A simple distinction is drawn between fine particles, usually < 2 µm diameter and coarse particles, > 2 µm. Fine particles are those most commonly connected with adverse health effects, whilst the latter may make a major contribution to soiling due to their rapid deposition, and the disamenity consequent upon it. In years gone by, deposition of coarse particles from industry and mining activities was a major cause of local soiling problems; fortunately due to stricter controls such problems now occur infrequently.

**Figure 1.9 : Typical Size Distribution for Atmospheric Particles, Indicating Some Formation Pathways.**

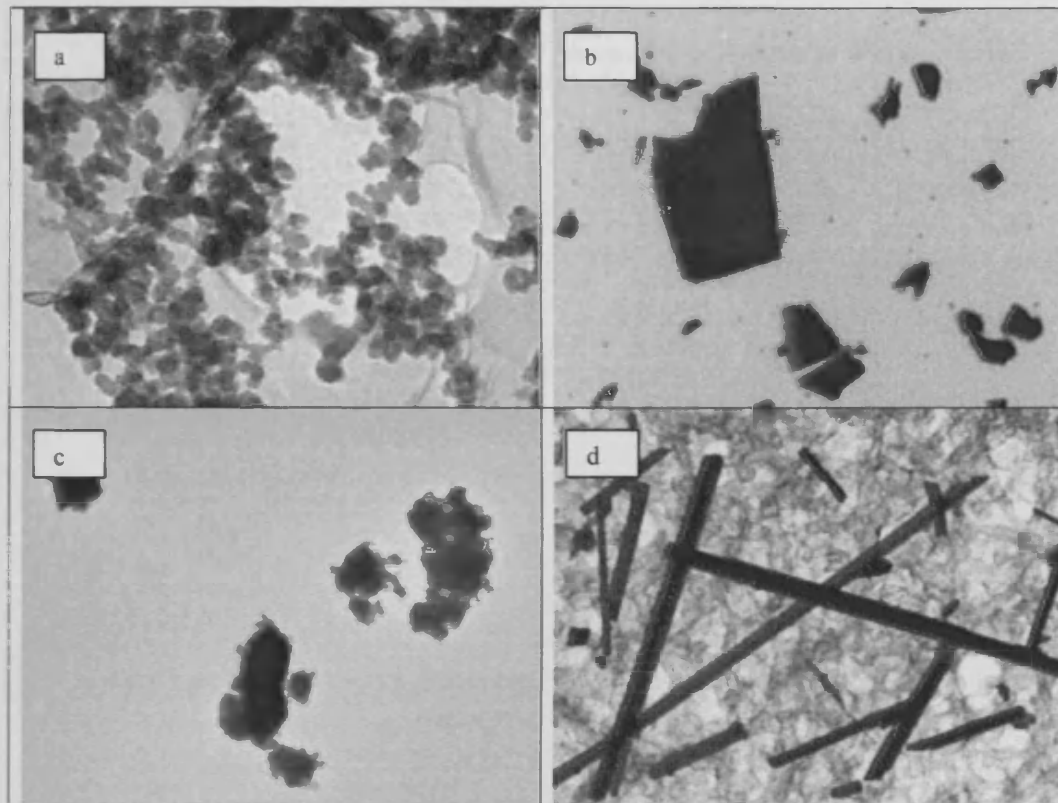


\* Source : QUARG [8].

### 1.5.1 Morphology of Particulates

The morphologies (structures) and shapes of aerosol particles vary with composition. The older an aerosol particle, the greater the number of layers and attachments the particle is likely to have. If the aerosol particle is hygroscopic, it absorbs liquid water at high relative humidities and becomes spherical. If ions are present and relative humidity decreases, solids crystals may form within the particle. Some observed particles are flat, others are globular, others contain layers, and still other are fibrous [11]. Some occur as single particles, some as an aggregates, some could be longer and slender shape, which depends on the source from which they originate. There are many shapes of particles, ranging from compact particle to fibrous particles. Examples of compact particles and fibrous particles are shown in **Figure 1.10** together with single and aggregate particles.

**Figure 1.10 : Electron Micrographs of Various Particles : a). Combustion Particles, b). Coal Dust Particles, c). Limestone Dust Particles, and d). Amosite Fibres.**



### 1.5.2 Sources of Particulate Pollution

There are two types of airborne particulate source. Firstly from natural sources, and secondly, from anthropogenic sources. All air contains natural contaminants such as pollen, fungi spores, bacteria, viruses, protozoa, plant fibres, rusts, dust particles from forest fire and volcanic eruptions. And anthropogenic sources such as fly ash, smoke, soot particles, metallic oxides and salts, oily or tarry droplets, acid droplets, silicates, and other inorganic dusts, and metallic fumes [4].

These two sources of particulate atmospheric pollution are summarized in **Table 1.3** and **Table 1.4**. There are situations when identical particulates can be produced from natural or man-made sources such as naturally occurring vegetation fires and manufactured combustion sources. The hazardous nature of airborne particulates from a health point of view is initially dependent upon their physical size.

If particles are too large they may be unable to enter the human body and precipitate a biological response.

**Table 1.3 : Summary Sources of Man-Made Airborne Particulates.**

<b>Industrial Process</b>	<b>Sources</b>	<b>Pollutants</b>
Material handling	Road mix plants, grains elevators	Mineral and organic particles
Combustion processes	Home heating and power plants, cars, trucks, busses, municipal / industrial incinerators, open burning	Smoke / fly-ash particles, particles
Manufacturing processes	Smelters, steel mills, aluminium refineries, car manufacturing	Metal fumes (Zn, Pb, Cu), particles
Industrial processes	Metal scrap yards, rendering plants	Smoke, soot
Chemical process	Fertilizer plants, organic processing plant	Particles
Agricultural operations	Pest control	Hydrocarbons, smoke and soot, mineral parts

**Table 1.4 : Summary of Primary and Secondary Sources of Natural Airborne Particulates.**

<b>Natural Process</b>	<b>Sources</b>	<b>Pollutants</b>
Geological activity	Including catastrophic events i.e. volcanic eruptions, associated igneous activity, erosion, soil dust emissions	Organic matter (C,H,O,N), sodium (Na <sup>+</sup> ), calcium (Ca <sup>2+</sup> ), magnesium (Mg <sup>2+</sup> ), potassium (K <sup>+</sup> ), sulfate (SO <sub>4</sub> <sup>2-</sup> ), chloride (Cl <sup>-</sup> ), silicon (Si), aluminium (Al), iron (Fe), black carbon (C)
Meteorological activity	Sea spray emissions	Organic matter (C,H,O,N), sodium (Na <sup>+</sup> ), calcium (Ca <sup>2+</sup> ), magnesium (Mg <sup>2+</sup> ), potassium (K <sup>+</sup> ), sulfate (SO <sub>4</sub> <sup>2-</sup> ), Chloride (Cl <sup>-</sup> )
Natural combustion	Forest fires, biomass burning	Black carbon (C), organic matter (C,H,O,N), ammonium (NH <sub>4</sub> <sup>+</sup> ), sodium (Na <sup>+</sup> ), calcium (Ca <sup>2+</sup> ), magnesium (Mg <sup>2+</sup> ), potassium (K <sup>+</sup> ), sulfate (SO <sub>4</sub> <sup>2-</sup> ), chloride (Cl <sup>-</sup> ), nitrate (NO <sub>3</sub> <sup>-</sup> ), iron (Fe)
Biological activity	Biological particles lifted by wind	Pollens, spores, plant debris, viruses

The activities that accounted for most of the overall air contaminants in the USA in 1980 are shown in **Table 1.5**. It will be noted that transportation was the single largest source of air pollution, while fuel combustion in stationary sources (for



power and heating) was the second major contributor. Power generation and heating accounted for about 80 percent of the oxides of sulphur and 51 percent of the oxides of nitrogen emitted to the ambient air, while industrial processes contributed 50 percent of the hydrocarbons and oxides of nitrogen.

Meanwhile the total emissions (million tonnes per year) of the five major pollutants for 1977 are illustrated in **Table 1.6**. Of these pollutants, transportation produced approximately 83 percent of the total carbon monoxide, 41 percent of the total hydrocarbons, 40 percent of the nitrogen oxides, 9 percent of the particulates, and 3 percent of the sulphur oxides emitted. In 1980, transportation produced a slightly lower percentage of total carbon monoxide and hydrocarbons, a slightly higher percent of nitrogen oxides, and significantly higher percent of particulates. Transportation was also responsible for 56 percent (by weight) of all contaminants emitted to the atmosphere in 1977, as compared to 55 percent in 1980 [14].

**Table 1.5 : Sources of air pollutants in the United States in 1980\***

Source	Pollutants					
	CO	Particulates	SO <sub>x</sub>	HC	NO <sub>x</sub>	Total
Transportation	69.1	1.4	0.9	7.8	9.1	88.3
Fuel combustion from stationary sources (power, heating)	2.1	1.4	19.0	0.2	10.6	33.3
Industrial processes	5.8	3.7	3.8	10.8	0.7	24.8
Solid-waste disposal	2.2	0.4	0.0	0.6	0.1	3.3
Miscellaneous (forest fire, agricultural burning, etc.)	6.2	0.9	0.0	2.4	0.2	9.7
<b>Total</b>	<b>85.4</b>	<b>7.8</b>	<b>23.7</b>	<b>21.8</b>	<b>20.7</b>	<b>159.4</b>

\* In million tonnes per year.

\* Source [14]

**Table 1.6 : Pollution emissions in the United States in 1977\***

Pollutants	Sources	
	Transportation	Other
Sulphur oxides (SO <sub>x</sub> )	0.8	26.6
Carbon monoxides (CO)	85.7	17.0
Particulates	1.1	11.3
Hydrocarbons (HC)	11.5	16.8
Nitrogen oxides (NO <sub>x</sub> )	9.2	12.8
<b>Total</b>	<b>108.3</b>	<b>84.5</b>

\* Emissions in million tonnes per year.

\* Source [17]

The information highlighted in both **Table 1.5** and **Table 1.6** here is to show the status of particulates pollution sources since the 1970 s and 1980 s. Even though, particulates contribute only a small amount to overall atmospheric pollution, it can however be considered as one of the most significant, complex, and unique components. Particulates have a different character depending upon what sources it comes from, either primarily or secondary particulates. But also the size distribution, chemical composition, and lifetime is affected by the source from which it originates together with the interaction of meteorological factors.

### **1.5.3 Primary Particulates**

Primary particulate matter (PM) comprises those particles emitted directly to the atmosphere from natural and anthropogenic sources as explained in the previous section. Primary particulates come from distinct sources and not from any chemical reactions in the atmosphere. Primary PM consists of carbon (soot), emitted from cars, trucks, heavy equipment, forest fires, burning waste, crustal material from unpaved roads, stone crushing, construction sites, and metallurgical operations [7]. Since primary particulate matter is emitted by various sources, these situations make it more difficult in quantifying their emissions.

### **1.5.4 Sources of Primary Particulates**

In the UK, according to the report produced by *Airborne Particles Expert Group* [10,15,16] there are three main primary sources i.e. from road transport, stationary combustion, and industrial processes with road traffic or road transport as the major contributor to primary particulate matter emissions. Particulate matter is emitted from a variety of sources besides fuel combustion, which increases the difficulty and uncertainty in quantifying their emissions. These emissions come from stationary combustion and road transport are certainly major sources, but there are also significant emissions from industrial processes, construction and quarrying, and fugitive sources through mechanical break-up, abrasion and erosion (e.g. vehicle tyre

and brake wear). These sources are particularly difficult to quantify and vary both spatially and temporally, particularly construction.

Road transport refers to all road traffic. As mentioned above, emissions come from the exhaust, tyre and brake wear. Other processes contributing such as road surface wear, corrosion of chassis, bodywork, other vehicle components, and also corrosion of street furniture and crash barriers [10]. In general, diesel engined vehicles emit a greater mass of particulate matter per vehicle than those with petrol engine [10,16]. In London for example, it is estimated [10] 77 % of emissions come from traffic without significant emissions from industrial processes or stationary combustion.

Domestic coal burning was traditionally the major source of particulate matter emissions under stationary combustion [15,16]. However, these emissions have declined to 14 % nationally in the UK in 1996. Although some of the big cities have restricted coal combustion by the Clean Air Acts, it is still an important source in small towns and villages for example Northern Ireland and areas associated with the coal industry. Emissions from power generation have also been declining gradually in the move of switching from coal to gas for electricity and due to improvements in the performance of electrostatic precipitators at coal-fired stations. Hence, public power generation is estimated to cause 16 % emission of the national  $PM_{10}$  in 1996 [15].

Industrial processes, includes bulk handling, construction, mining and quarrying activities and it is estimated nationally [15] that these processes contributed 28 % of  $PM_{10}$  emissions in the UK in 1996. These sources are difficult to quantify due to the nature of the source and due to the lack of information on the extent of these activities. Fugitive emission relates to pollutant losses from points in a process not associated with a defined process stream (such as a stack) [16]. Such sources generate particulate matter through two main processes i.e. first, mechanical break-up through pulverization or surface abrasion resulting in the production of dust. This includes tyre and brake wear, mineral processing, wear of wheels and blades and various construction activities. The other one is through the wind-blown dust.

Temporary activities such as construction, creates particles from a wide range of cutting, grinding, and crushing operations especially during land clearing activities. Despite their temporary nature, construction sites can have a substantial impact on local air quality [16]. Other contributors to primary airborne particulates are from the waste treatment and disposal and also agricultural activities.

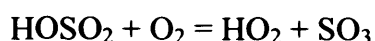
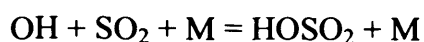
### **1.5.5 Secondary Particulates**

Secondary particulate matter (PM) forms in the atmosphere from gaseous emissions. It could also refer to original gaseous material present as an intimate component of PM<sub>10</sub> [16]. Some of these reactions require sunlight and/or water vapour. It is formed by low volatility species through the action of atmospheric chemical reactions. It could also be formed by gas phase oxidation of emitted precursor gases or a product of the reactions of gaseous species with aerosol or aqueous droplets either wholly or partially in a condensed phase [10]. These low volatility species initially present as gaseous species but ultimately, some distance downwind, become particles or become attached to particles. If they become secondary particles by nucleation of entirely new particles and grow by coalescence, then the particles have been formed by homogenous nucleation. However, there are often the low volatility species attach themselves to pre-existing aerosol species known as heterogenous nucleation [15].

### **1.5.6 Sources of Secondary Particulates**

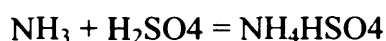
Secondary particulates, includes sulfates, nitrates, and carbon species. Sulfates form from sulphur dioxide emissions from power plants and industrial facilities. Nitrates formed from nitrogen oxide emissions from cars, trucks, and power plants. And Carbon formed reactive organic gas emissions from cars, trucks, industrial facilities, forest fires, and biogenic sources such as trees [7]. These sources produced sulphuric acid and sulphate aerosol particles, particulate ammonium, and particulate nitrate.

Sulphur dioxide is a common constituent of ambient air in the United Kingdom mainly through its emission from coal-burning in large electricity-generating stations and from industrial coal- and oil-burning [15]. Photochemical oxidation of sulphur dioxide is initiated through the following sequence reactions :



Where M represent an atmospheric nitrogen or oxygen molecule, and OH is the hydroxyl free radical. The sulphuric acid,  $\text{H}_2\text{SO}_4$ , vapour then nucleates to form sulphuric acid droplets and by simultaneously condensing water vapours, grows rapidly out of the nanometer size range. These initial nuclei continue growing rapidly by condensing more water vapour, by coalescing with each other by Brownian aggregation and by coagulation with pre-existing in size producing a relatively stable distribution of particles size in the nucleation and accumulation modes, covering the entire 10 nm to 1  $\mu\text{m}$  size range [15].

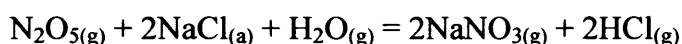
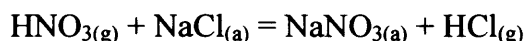
In the case of acidic aerosol droplets, it can take up ammonia,  $\text{NH}_3$ , from the gas phase forming droplets of ammonium sulphates, leading also to a growth in aerosol mass per unit volume, through the reactions :



The main sources of  $\text{NH}_3$  are agricultural in origin through the storage, disposal and application to soils of animal wastes and industrial fertilizers.

The main source of  $\text{NO}_x$  emissions are from motor vehicles exhausts, industrial combustion and power stations. It is conversion to nitric acid, ammonium nitrate and nitrogen pentoxide in a relatively rapid series of daytime and night-time

reactions [15]. Although nitric acid, ammonium nitrate and nitrogen pentoxide have low volatility compared to  $\text{NO}_x$ , from which they have been generated, there are all unable to undergo homogenous nucleation. Instead, they attach themselves to pre-existing particles by heterogenous nucleation. If the pre-existing particle was a sea-salt particle, then additional chemical reactions can occur leading to the liberation of gaseous hydrogen chloride by sea-salt displacement :



### 1.5.7 Fine & Ultra-fine Particulates

In the atmosphere, coarse and fine particles behave in different ways. Larger coarse particles may settle out from the air more rapidly than fine particles and usually will be found relatively close to their emission sources. Fine particles can be transported long distances by wind and weather and can be found in the air thousands of miles from where they were formed [7]. It is generally referred to particle with less than 50 nm in diameter [16].

Fine ( $\text{PM}_{2.5}$ ) and ultra-fine ( $\text{PM}_{0.1}$ ) particulates are more hazardous towards human health than the coarser particulates. Most of the fine and ultra-fine particulates can be characterized as respirable dust. It has been stated [16] that the finer particles are higher in total particle number count but represent lower of the total mass concentration. All this respirable dust will intend to be deposited into the deepest side of the lungs. And this later could cause various biological effects upon human health such as pneumonia, lung cancer, death, etc. The effects of particulates pollution mainly upon human health, flora and fauna, buildings and materials, and the global environment will be discussed in Chapter 2.

## 1.6 General Chemical Characteristics of Airborne Particulates

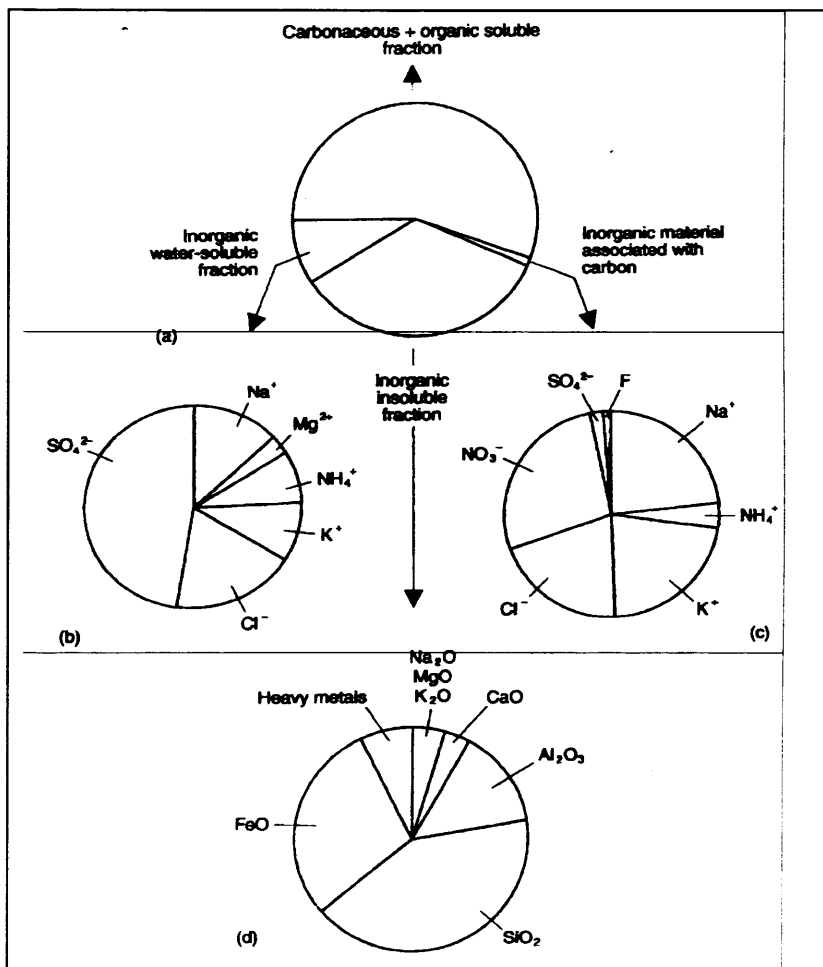
The chemical characteristics of airborne particulates are complex and variable due to the amount, various sources and chemical reactions involved in the atmosphere. It has been stated [18] that there is a close relationship between particle size, shape and chemistry. For example, coarse particles will concentrate different chemical species than finer fractions and heavy metals from metallurgical industries will tend to have a rounded shape owing to condensation of metal vapours. There are a range of different factors, which affect the chemistry of airborne particulate matter i.e. types of source, chemical transformations in the atmosphere, long-range transport effects and removal processes.

The coarse fraction of airborne particulates is formed mainly by minerals and natural salts coming from dust created by wind or marine aerosols, and also from some anthropogenic sources. However, coarse particles represent a small proportion of most atmospheric dust. Finer particulates are the most abundant particle phase and include nitrates, sulphates, heavy metals, organic compounds, and elemental carbon [18]. The finer particles are mainly formed by :

- *Secondary particles* : sulfates, nitrates and chloride salts of ammonium, products of the reaction of SO<sub>2</sub>, NO<sub>2</sub>, hydrochloric acid and ammonium ions under atmospheric conditions;
- *Heavy metals* : originate from anthropogenic sources, such as smelting plants (iron, cadmium, zinc) and combustion processes (in urban locations, combustion of leaded fuel releases lead);
- *Elemental carbon* : a product of incomplete combustion processes, including the combustion of fuels (for transport), coal, and biomaterial. The surface area of elemental carbon particles are considerably increased by their porous structure and their ability to adsorb more airborne chemical substances (such as organic compounds) is greatly enhanced;
- *Organic compounds* : these condense on the surface of carbonaceous material, the small particles of which present a larger surface area for the condensation and/or adsorption of chemical species.

The percentage breakdown of the PM<sub>10</sub> particulate matter in the UK are as follows: ammonium (~5%), sulphate, nitrate and chloride (~30%), carbonaceous material (~40%), metals (~5%) and insoluble material (minerals)(~20%) [8; 16]. While another study of the chemical analysis of airborne PM<sub>10</sub> in Cardiff has given the following results : soluble inorganic matter (40.8%), insoluble inorganic matter (19.2%), organic matter (40%) [19].

**Figure 1.11 : Fractional Semiquantitative Chemical Composition of an Urban (Cardiff) PM<sub>10</sub> sample. (a). Major Fractional Components of an Urban PM<sub>10</sub> sample; (b). Composition of Water-Soluble Fraction; (c). Composition of Inorganic Material Associated with Carbon-Based Fraction; (d). Composition of Inorganic Fraction After Removal of other Components from the sample.**



\* Source : Pooley and Milagros [18].

In general, PM<sub>10</sub> samples can be described most conveniently [18] as a number of individual fractions, each of which is either soluble or insoluble in water or in



organic solvent; the insoluble component is either carbon-based or inorganic material. This fractionation, enables some approximate division of the sample by source. Despite that, information such geographical locations, the contribution of local industrial activity to the airborne particulate pollution can be assessed and distinguished from the natural contributions of the sea and from secondary particulate formation due to atmospheric chemical activity [18]. An example of the composition of a sample taken in a busy town centre (Cardiff, Wales), which represents the fractionation and analysis of PM<sub>10</sub> is illustrated in **Figure 1.11**. The analysis reveals that the sample consists of : > 50% carbon and organic soluble material; 10% water-soluble material; the remainder is insoluble inorganic material. The overall composition of the sample is listed in **Table 1.7**.

**Table 1.7 : Semiquantitative composition of an airborne particulate Sample collected from the Cardiff Area (Expressed As Parts Per Thousand on a Mass Basis)**

	Aqueous soluble species	Aqueous soluble species after ashing	Inorganic insoluble species <sup>a</sup>	Fraction of total
Soluble organic and carbonaceous material	-	-	-	555
Na	12	2	2	16
NH <sub>4</sub> <sup>+</sup>	8	<1	-	8
Mg	3	-	6	8
K	9	2	8	19
Ca	n.d.	-	12	12
F	n.d.	<1	-	<1
Cl	17	2	-	19
NO <sub>3</sub> <sup>-</sup>	<1	3	-	3
SO <sub>4</sub> <sup>-2</sup>	41	<1	-	41
Al	<1	<1	49	49
Si	<1	<1	144	144
Ti	-	-	8	8
Cr	<1	<1	4	4
Mn	-	<1	4	4
Fe	<1	<1	100	101
Co	<1	<1	-	<1
Ni	<1	<1	-	<1
Cu	-	<1	1	1
Zn	<1	<1	4	4
Pb	-	-	3	3
<b>TOTAL</b>	<b>90</b>	<b>9</b>	<b>345</b>	<b>1000</b>

\* Note : i. n.d. = not detectable

ii. a - The components of this fraction are expressed as elemental oxides. Crystalline and adsorbed water are neglected.

\* Source : Pooley and Milagros [18].

### 1.6.1 Organic Chemistry of Airborne Material

*Organic compounds* are those compounds that are emitted, and are formed by chemical reactions in the atmosphere. The main sources of organic compounds are fuel evaporation or spillages, natural gas leakage, solvent usage, industrial and chemical processes, and the use of bitumen and road asphalt.

It has been stated [18] that organic compounds can be classed as volatile (a property associated with a low molecular weight), semivolatile and non-volatile. This characteristic, which is closely related to the molecular weight of the compound, will influence their behaviour in the atmosphere and their association with airborne particles. Normally, it exist only in gaseous form can be carried by PM<sub>10</sub> particles. Organic compounds with high molecular weight are the ones that will be associated with particles, while those with lower molecular weight (and therefore more volatility) remain in the gaseous form.

Toxic organic micropollutants (TOMPs) have received special attention because of their health effects. These compounds include polynuclear aromatic hydrocarbons (PAH), polychlorinated biphenyls (PCB) and dioxins. They are frequently referred to in terms of toxic equivalent (TEQ) [18].

### 1.6.2 Inorganic Chemistry of Airborne Particulates

The *inorganic compounds* of particulate material in urban samples, consists of particulate elemental carbon or carbon black (which comes from road traffic and is associated with organic compounds in smoke particles) and water-soluble or insoluble inorganic compounds.

The elemental carbon particles result from the incomplete combustion of fuels and lubricating oils and are generally small, forming part of the finer fraction of PM<sub>10</sub> matter. They have a porous surface that increases the area available for adsorption processes. Organic compounds, heavy metals and soluble inorganic material can be

carried by elemental carbon particles. Health concerns were originally focused on this fact, but it is now recognized that elemental carbon can be dangerous by itself [18].

Soluble inorganic compounds can be divided into several categories as follows [18]:

- *Aerosol acids* : Result from partial neutralization of the airborne acid species present in the atmosphere (nitric acid, sulfur acid, bisulfates) owing to an insufficient quantity of basic species, i.e. ammonium ions.
- *Sulfates* : Soluble sulfate salts ( $\text{CaSO}_4$ ,  $\text{Na}_2\text{SO}_4$ ,  $(\text{NH}_4)_2\text{SO}_4$ ) are common in airborne samples. High percentages of sulfate (up to 85%) are likely to be found in  $\text{PM}_{10}$  samples, especially in the finer fraction  $\text{PM}_{2.5}$ .
- *Nitrates* : The finest  $\text{PM}_{10}$  fraction has the majority of the nitrate contents. This fraction is formed by an oxidation process like sulfates, but from  $\text{NO}_2$ .
- *Chlorides* : Result from reaction between hydrochloric acid and the ammonium ions released by pollutant sources (industries). Sodium chloride mainly enters the atmosphere from marine aerosols in coastal areas, and is mainly found in coarse particles.
- *Ammonium compounds* : Result from combined with sulfate, nitrate, and chloride forming acids. Mostly found in  $\text{PM}_{2.5}$  fraction.
- *Other cations* : Sodium (associated with chloride, sea salt, typical marine aerosol, and may occur in the form of nitrates and sulfates); calcium (as carbonates and sulfates); and magnesium (from formations forming carbonates and chlorides close to the sea).

*Insoluble inorganic* material is typically associated with the coarse fraction of  $\text{PM}_{10}$  matter and is formed by soil-derived particles. It includes compounds such as  $\alpha$ -quartz ( $\text{SiO}_2$ ), calcite ( $\text{CaCO}_3$ ), epsomite ( $\text{MgSO}_4 \cdot 7\text{H}_2\text{O}$ ), gypsum ( $\text{CaSO}_4 \cdot 2\text{H}_2\text{O}$ ), feldspar ( $\text{KAlSi}_3\text{O}_8$ ), chlorite, kaolinite and montmorillonite.

*Metals*, can be found in a variety compounds and exist in both a soluble and insoluble elemental state. They are difficult to detect and analyze due to their low concentrations in air. Trace heavy metals, are generally anthropogenic in origin, e.g.

the combustion of fossils fuels, waste incineration and high temperature processes (metal smelting industries). During the latter processes, heavy metals become vaporized and condense preferentially onto the surface of smaller ambient particles owing to their larger surface area/mass ratios.

## **1.7 Conclusion**

It can be seen that the atmosphere is a complex and dynamic gaseous system with a continuously varying composition of pollutants, which include trace gases and particulates. The concentration of these pollutants vary and they often have very short half lives. Of most importance from an environmental impact perspective are those pollutants from anthropogenic sources. Monitoring and characterizing such materials is of great importance in understanding their subsequent environmental impact.

## **CHAPTER 2 :**

### **THE ENVIRONMENTAL IMPACT OF AIRBORNE PARTICULATES**

#### **2.1 Introduction**

Pollution of the atmosphere from natural sources is a continuous process. With the exception of catastrophic pollution events, the ecosystem has evolved to handle natural pollution of the atmosphere. With the addition to this of man-made pollution, the natural balance has been altered, resulting in an increased detrimental impact on the environment. This manifests itself in a number of ways, which include an increase in detrimental effects on human health, flora and fauna, and the built environment. If the magnitude of the emissions is significant, then an influence on the global environment ensues.

Of major concern are those episodes of pollution that can be linked to the deterioration of human health, which result mainly as a consequence of the inhalation of polluted air. It will be shown in the following sections that this is of particular concern in the case of those people exposed to occupational pollution, often employed in the mineral-related and other heavy industries. These workers may over many years be exposed daily to a range of particulates and gaseous pollutants, which can also be dispersed into the surrounding environment to affect a local population.

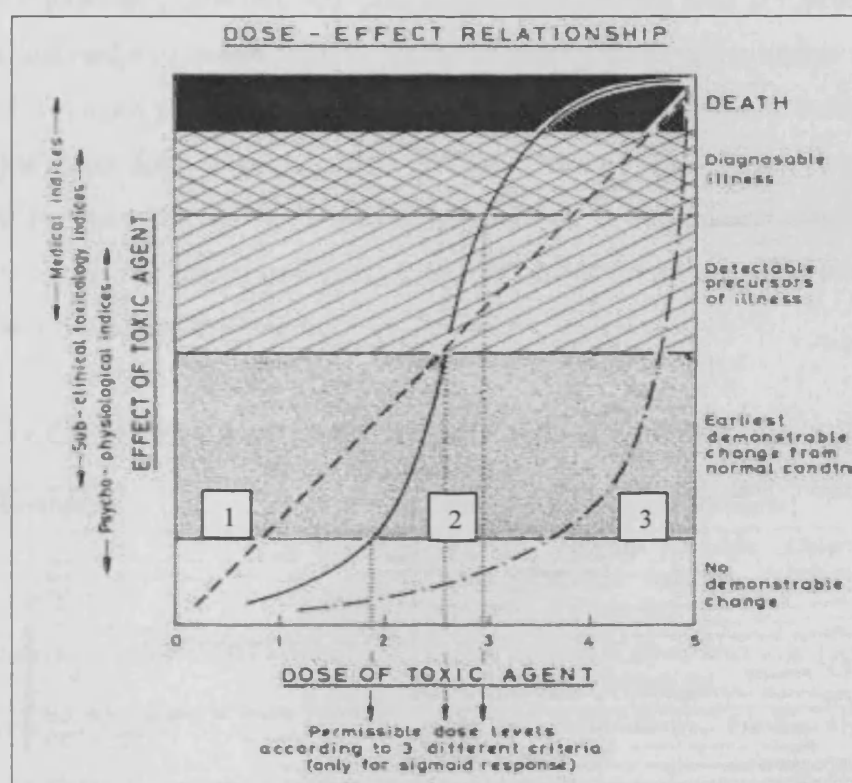
The impact of atmospheric pollution depends to a large extent on geographic location, the sources of pollution, and regional meteorological conditions, which effect its concentration and impacts. The understanding and determination of the physical and chemical characteristics of airborne pollution, especially particulate matter, is an important requirement in understanding its impact, sources, and control.

#### **2.2 The Impact of Gaseous Atmospheric Pollution on Human Health**

In order to affect human health, pollutants in the atmosphere must first be taken into body. The main point of entry of both gaseous and particulate pollutants is via the respiratory tract, by inhalation, although it is also possible for them to gain

entry by absorption through the skin and via the gastro-intestinal tract by ingestion. Inhalation of contaminated air gives gaseous and particulate pollutants direct entry to the human body via the lungs.

**Figure 2.1 : The Physiological Dose - Effect Relationship of Toxic Agents.**



\* Source : Schröder [20].

The physiological dose-effect relationship of toxic agents is illustrated in **Figure 2.1**, and there are three forms that it takes: In the first instance, the effect is linearly proportional to the dose (1):(- - - -); in the second the effect increases as the doses increases (a hyperbolic curve or non-linear relationship)(2):(- · · · ·); and lastly the effect is “all-or-none” and known as the sigmoid curve (3):(—). In the first case, where the effect is in linear proportion to the dose, as the dose of particular toxic agents begins to increase, the effects increase in correlation from a level of ‘no demonstrable change’ to the level ‘death’. The second instance is well understood, as when the dose of the toxic agents begins to increase, the human exposed will experience the effects increasingly, and further increase can cause death. The third case, of the sigmoid curve, illustrates that when the dose of toxic agents begins to

increase there is at first little effect, then the effects begin to increase rapidly with increased dose, and illness levels rise sharply towards death.

Gases and vapours may react immediately with the human biological system and at high levels an instantaneous effect can be produced. The biological response caused by gaseous pollutants are concentration-dependent and compound-specific. The type and range of responses that can be caused by gaseous pollutants are listed in **Table 2.1**. Gaseous pollutants are of greater concern in confined environments, which prevent the gases from dispersing and diffusing into the atmosphere. It is rare that a sufficient concentration of toxic gases can build up in the general atmosphere, and when this occurs the situation does not tend to persist for an extended period of time due to the influence of the weather.

**Table 2.1 : Classification of Health Hazards Associated with Gases and Vapours.**

Health Hazards	Examples of Gases and Vapours
Irritants	Ammonia, Sulphur Dioxide, Chlorine Oxide, Ozone, Dimethyl Sulphate, Nitrogen Dioxide, Nitrogen Tetroxide, etc.
Asphyxiants (a).Simple and (b).Chemical	Carbon Dioxide, Carbon Monoxide (combine with haemoglobin), Methane etc.
Anaesthetics & Narcotics	Acetylene Hydrocarbons, Paraffin Hydrocarbon, Ethers, Esters, etc,
Carcinogens	Aromatic Amines, Arsenic, Asbestos, Petroleum Oil, Radiations, etc.
Mutagens	Pesticides, ionizing radiation, radioactive isotopes, chemicals, etc.
Teratogens	X-ray exposure, Carbon Monoxide, etc.
Systemic Poisons	Halogenated Hydrocarbons, Fluorides, etc.

\* Source : *Schröder [20]*.

From **Table 2.1**, gases and vapours in the category *irritants* can be classified as i). affecting the upper respiratory tract (e.g.: ammonia; chromic acid, sulphur dioxide, etc.); ii). affecting both the upper respiratory tract and lung tissue (e.g.: chlorine oxides, ozone, dimethyl sulphate, etc.); and iii). affecting primarily the terminal respiratory passages and air sacs (e.g.: arsenic trichloride, nitrogen dioxide, nitrogen tetroxide, etc.).

*Asphyxiants* are materials that exert their effects by reducing the supply of oxygen to the tissues, and can be classified into the following categories i). simple asphyxiants, which are physiologically inert gases that act principally by dilution of the atmospheric oxygen, and as a consequence the oxygen in the blood, thus depriving the tissue of oxygen (e.g. : carbon dioxide, methane, etc.); ii). chemical asphyxiants, which act through chemical action and either prevent the blood from transporting oxygen from the lungs, or prevent normal oxygenation of the tissue, even though the blood is well oxygenated (e.g. : carbon monoxide (combines with haemoglobin)).

*Anaesthetics* and *Narcotics* produce simple anaesthesia without serious systemic effects and have a depressant action on the central nervous system governed by their partial pressure in the blood supply to the brain (e.g. : Acetylene hydrocarbons (acetylene), aliphatic alcohol (e.g. ethyls, butyl)).

*Carcinogenics*, under favourable conditions act through direct or indirect action, either externally or internally, on healthy tissue cells to cause a rapid proliferation of the cellular elements and the development of structural abnormalities in the form of cancer (e.g. : arsenic, heavy metals, organic compound (benzene)).

*Mutagens* are substances that produce changes in the body's genetic material, such as the genes and chromosomes of cells. They can be linked to the mutation of cells e.g. cancer, or the mutation of micro-organisms, which can alter the development of offspring, causing abnormalities such as mental retardation, congenital blindness, etc. Examples of mutagens include: ionizing radiations, radioactive isotopes, chemicals, anti-cancer drugs, pesticides, etc.

*Teratogens*, are compounds that can produce abnormal foetuses in pregnant women and the effects occur after conception, while the organism is still unborn. They are mainly produced by X-ray exposure at the pelvis of pregnant women, German measles, carbon monoxide, strong steroids, etc.

*Systemic Poisons* consist of a range of compounds and elements encountered in modern society, examples of which are: halogenated hydrocarbons, materials damaging the hematopoietic system, heavy metal (Pb, Hg, Cd, etc.), and nonmetal



inorganic compounds such as As, P, Se, S and fluorides.

The London Black Smog Tragedy of 1952, which has become a critical starting point in the study of air pollution epidemiology is a good example of gaseous as well as particulate air pollution because of the scale of its effect, with an estimated 4000 deaths [21; 22; 23; 24; 25]. Thereafter far greater consideration was given to air pollution, and the requirement to control its production and impacts, both gaseous and particulate, has subsequently increased. This has especially been so with regard to airborne particulates, and in particular fine ( $PM_{2.5}$ ) and ultra-fine ( $PM_{1.0}$  &  $PM_{0.1}$ ) particulates, which, as it will be shown, have significant potential for damaging the human respiratory system. The inhalation deposition and retention of particulates in the lungs is normally related to a linear dose effect response situation.

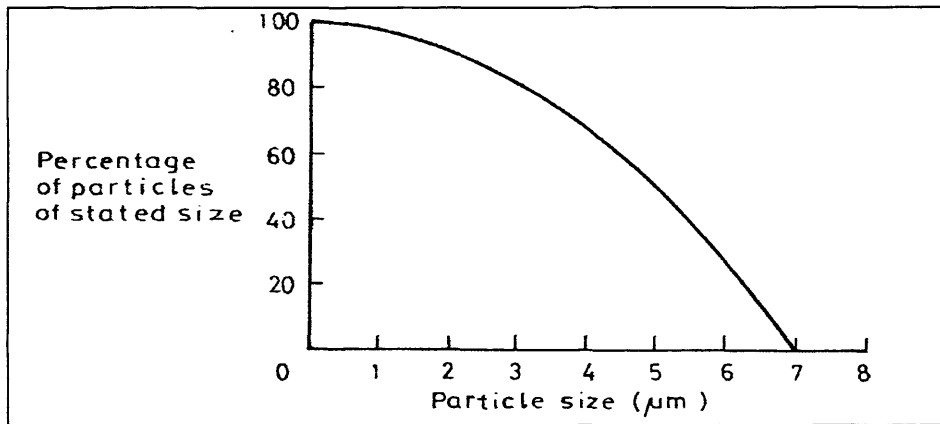
### **2.3 The Impact of Particulate Atmospheric Pollution on Human Health**

Not all airborne particulates are hazardous and they do not all cause the same immediate impact as gaseous atmospheric pollution. Particulate pollution is hazardous in a different way to gases and vapours, mainly because of its potential to accumulate and react in the lungs, consequently producing a variety of health effects. The physical and chemical characteristics of airborne particulates are extremely variable. They are derived from a wide range of sources and are classified as either primary or secondary in origin. They may be solid or liquid in composition and may consist of soluble or insoluble materials. They can be further classified into particulates that have a natural origin, and those derived as a result of the intervention of man i.e. anthropogenic (man-made) particulates, as explained in Chapter 1.

The impacts of airborne particulates upon human health are closely related to the size of the airborne particulates inhaled, as only particles under a certain size are deposited in the lungs. The particles deposited in the lung as a result of inhalation are known as 'respirable' particles. In general, the smaller the particle, the more serious the effects they can produce, especially if deposited in the deepest part of lungs and thus affecting the human respiratory system, as outlined in a recent EPA report [26]. Based on the respirable sampling curve recommended by the International

Pneumoconiosis Conference in Johannesburg in 1959 as illustrated in **Figure 2.2**, the following percentages of particles inhaled, are deposited in the lungs: 100% of the dust particles of a size  $< 1\mu\text{m}$  aerodynamic diameter, 50% of particles of size of  $5\mu\text{m}$  aerodynamic diameter, 20% of particles of size of  $6\mu\text{m}$  aerodynamic diameter, and 0% of particles of a size of  $7\mu\text{m}$  aerodynamic diameter [20]. The largest particle that can enter the lung has been estimated as  $7.07\mu\text{m}$  in diameter (based on the BMRC convention).

**Figure 2.2 : Respirable Sampling Curve Defined at the International Pneumoconiosis Conference in Johannesburg, 1959.**



\* Source : *Schröder [20]*.

Fibrous particles are defined as having parallel sides and an aspect-ratio (length-to-diameter) of 3:1. The aerodynamic diameter and aerodynamic behaviour of a fibrous particle are more dependent on its diameter than its length. Therefore, the finer the fibrous particle becomes, the higher the possibility for it to penetrate into the deepest parts of the lung i.e. the pulmonary air spaces. For example, fibres in the range from  $50$  to  $200\mu\text{m}$  in length and  $3\mu\text{m}$  in diameter can be found in the human lung [20], however, towards the deepest part of lung, only the thinner particles are deposited. These can cause lung diseases such as emphysema, fibrosis, chronic bronchitis, chronic obstructive lung disease, and many others, depending on the minerals contained in the fibrous particles, as summarized in **Table 2.2**.

**Table 2.2 : Classification of Health Hazards Associated with Airborne Particulates.**

<b>Health Hazards</b>	<b>Examples of Airborne Particulates</b>
Coal worker's pneumoconiosis	Coal
Benign pneumoconioses i.e. siderosis, stannosis, barytosis	Inert metal dusts i.e. iron, tin, barium
Talcosis	Talc
Severe fibrosis of the lungs	Mineral silicates i.e. mica, kaolin, zeolites
Chronic bronchitis i.e. coughing, could cause death, emphysema	Cigarette smoke
Silicosis, chronic obstructive lung disease	Crystalline silicates
Asbestosis	Asbestos fibres i.e. chrysotille, amphiboles
Collagenous pneumoconioses	Cobalt dust i.e. tungsten carbide
Zinc ague/brass founder's ague, appreciable mortality	Metallic dusts or fumes i.e. zinc oxide, manganese, vanadium, cadmium, beryllium
Lung cancer, bronchogenic cancer, mesothelioma	Cigarette smoke, Asbestos, Iron oxides

\* Source : Schröder [20]; Pan et.al. [27]; Hedley et.al. [28]; Deschamps et.al [29].

The three principal forms of exposure to airborne particulate pollution are environmental exposure, occupational exposure, and indoor air exposure. Often, exposure to a particular polluting material is not confined to one form of exposure only. In the following subtopics, it will be explained how people who have been exposed to these forms of pollution, especially through occupational exposure, have a higher risk of contracting any of the diseases related to hazardous particulate materials.

### **2.3.1 Particulates Deposition in Human Lungs**

Airborne dust consists of a mixture of a larger "coarse particle" and a smaller "fine particle." Coarse particles have diameters ranging from about 2.5µm to 40µm and above, while finer particles, which are also known as PM<sub>2.5</sub>, include particles with diameters equal to or smaller than 2.5µm. PM<sub>10</sub> include coarse particles that are "inhalable" ranging in size from 2.5 to 10µm, which can penetrate the upper regions of the body's respiratory defence mechanism [7]. It has also been stated [16] that the pattern of respiration also needs to be taken into consideration in this respect. In relation to the effects of these particulates upon health, the study of coagulation,

retention and deposition of particulates is vital to our understanding of the effects they produce in the inner parts of the lungs.

The effects of inhaled particles are dependent on where they are deposited in the respiratory tract. The penetration and deposition of particles is dependent on wind speed and direction, physical variations in individual breathing rate, and whether one is breathing through the nose or mouth. Besides that, the sizes of these particulates can also determine the location at which they will be deposited in the upper or lower respiratory tracts. The largest particles do not penetrate very far in to the lungs, and thus tend to cause fewer harmful health effects. Some researchers have shown that fine and ultra-fine particulates are deposited with greater ease in the deepest part of lungs and that they can subsequently cause lung cancer. These tiny particles come in many shapes and sizes, and can be composed of hundreds of different types of chemicals [7]. It has been stated [30] that our understanding of these smaller particles is crucial, as they are generated in abundance by the most significant pollution sources, which are those related to combustion processes. The size of the particles generated from the combustion processes is usually around  $0.01\mu\text{m}$  to  $0.3\mu\text{m}$  [30]. Even though they are an insignificant contribution to the mass of airborne particulates (approximately 9%), in terms of their size these particles comprise the vast majority of all the airborne particles on a number basis. Besides this numerical prevalence, knowledge of the lung deposition of combustion aerosols and – more generally – aerosol in urban air, is important because of the combination of the particle abundance and toxicity, and its effect on human health.

The aerodynamic diameter of a particle is the diameter of a sphere of density  $1\text{gm/cm}^3$  ( $1\text{kg/dm}^3$ ) with the same aerodynamic properties in the air as the particle. It is considered that the inhalation of an airborne particle (in this case, aerosol) decreases with an increase in its aerodynamic diameter ( $d_{AE}$ ). Therefore, many smaller particles are prone to be inhaled in comparison to larger particles. These factors are very important especially when considering the collection of health-related airborne particulates in locations, where the inhalable hazardous airborne particles are generated.

The estimated typical quantity of particles in the PM<sub>10</sub> range deposited in an adult lung is about 250µg per day. This value is considered to be a small dose in terms of a traditional toxicology of inhaled particles. Some experimental studies on animals expose at high concentrations of dust show that mixtures of particles with pollutant gases such as SO<sub>2</sub>, NO<sub>2</sub> or O<sub>3</sub> have greater effects than those of the components inhaled separately. It is not clear whether these results would apply at the low concentrations normally present in the environment [16]. The absorption of such gases, metals and acid-sulphates on the surface of particles may be important. Animal studies also indicate a potentially important role for ultra-fine particles (< 0.05µm diameter). They are cleared only very slowly from the lung and they can penetrate the pulmonary interstitium, inducing inflammatory responses. It has been suggested that allergenic material may be carried into the lung in association with particles, though evidence is lacking [16]. The mechanisms of particle deposition will be further discussed in Chapter 3 with the review of instruments for the collection and characterization of airborne particulates.

### **2.3.2 Lung Diseases and Affected Groups**

The symptoms experienced as a result of exposure to the same form of pollution may vary from person to person. This variation may be related in particular to their levels of health. People with e.g. lung disease, asthma or heart disease, may experience different symptoms and to a different extent, than those experienced by a normal healthy person. The following groups of people may be more or less susceptible to dust exposure: healthy people, younger people, people with critical illnesses, older people, pregnant mothers. A healthy person will generally experience temporary symptoms from temporary exposure to elevated levels of particles. The symptoms are: irritation of the eyes, nose, and throat; coughing; phlegm; chest tightness; and shortness of breath. If the person has lung disease, they may not be able to breathe deeply as normal, and may experience respiratory symptoms such as coughing, phlegm, chest discomfort, wheezing, shortness of breath, and unusual fatigue, while a person with asthmatic problems might experience similar symptoms to those described before. For person with a heart disease problem, the effects may be serious, such as a heart attack, with no warning symptoms. Other symptoms may

include chest pain or tightness, palpitations, shortness of breath, and unusual fatigue. These may indicate serious problems [26]. These symptoms may gradually increase, resulting in death.

All the examples of effects mentioned above can be caused by particulates inhaled in a range of particle sizes and originating from various sources. Many factors can contribute towards an increase in symptoms i.e. increases of traffic flows, development of the new industrial areas, open burning, cigarette smoke, passive smoke, building materials, chemical fumes, etc. As explained in Chapter 1, meteorological factors have played a significant part in atmospheric pollution concentrations, which can vary from hour to hour and one day to another [8; 16]. These include changes in temperature, which can affect the same health endpoints [16].

It is suggested [16] that the following are indicators of ill-health (acute effects): day-to-day variations in mortality, time at school or work, respiratory symptoms, exacerbations of asthma, changes in lung function, and also pneumonia. At present, the research with most consistent results has been done on a day-to-day variations in mortality. This report suggests that nobody is immune from being affected by diseases related to inhalation of airborne particulate pollution, but that the following groups of people are more susceptible: newborn babies, children, older people, especially those with critical illnesses [16].

As a result of exposure to airborne particulate pollution, instances of people admitted to hospital has increased. It has been proposed [26; 31] that the findings of the epidemiological research of the last decade, which indicated that exposure to air pollution, at the level of urban environments is associated with an increase in mortality and variety of health conditions, including emergency room visits and hospital admissions for respiratory and cardiovascular diseases. In relation to the symptoms and factors contributing towards the health effects in humans mentioned above, the effects will tend to be greater for those who suffer from heart or lung disease, or diabetes, and for older people and children. A person taking part in physical activities is also often more susceptible to the effects of particulate pollution, as an increase in breathing rate and depth generally means that they will take more

particles into the lungs.

People who already have heart or lung diseases, such as coronary artery disease, congestive heart failure, asthma, and chronic obstructive pulmonary disease (COPD) are at risk of the effect of particle inhalation, which can aggravate these diseases. People with chronic obstructive pulmonary disease (COPD) have an obstructed air flow which may cause more particles to deposit in their lungs. People with diabetes are at risk of serious effects, possibly because of underlying cardiovascular disease [26].

Older people are at increased risk from particles, not least because of the possibility of having undiagnosed heart or lung disease or diabetes. Numerous studies have provided evidence that older people are more likely to be hospitalized as a consequence, and that some may die from aggravated heart or lung diseases. People who are more prone to heart attacks because of their personal risk factors, may also be at greater risk from high particle levels. Among the factors are: age, family history of heart disease, smoking, high blood pressure, high blood cholesterol, obesity, physical inactivity, and diabetes [26].

Children are also at a risk from particles, for a number of reasons. They may be more vulnerable to particles as their lungs are still in the process of development. Children also tend to spend more time at higher activity levels, which can lead to a greater quantity of particles being deposited in their lungs. Also, they are more susceptible to asthma and acute respiratory disease, which can be aggravated by particulate exposure [26]. In healthy children and adults, exposure to elevated particle levels for short periods of time may cause minor irritation and the temporary symptoms described above, however, for most healthy people, they will recover quickly from these effects and are unlikely to experience long-term consequences. Long-term exposure to particles has been associated with reduction in lung function and the development of chronic bronchitis.

Evidence is inconsistent as to whether pregnant women could represent another significant sensitive group as mentioned above. Some studies have suggested that breathing high particle levels over long periods of time may be associated with

low birth weight in infants, pre-term delivery, and foetal and infant mortality.

### **2.3.3 Occupational Pollution**

Occupational or 'work-related' pollution is generally caused by airborne particulate pollutants, especially fibrous particles. The excessive accumulation of these types of particles in the lung, together with the tissue reaction is referred to as pneumoconiosis. The Occupational Disease in Mines and Works Act (No.78 of 1973) defines pneumoconiosis as "a permanent lesion of the cardio-respiratory organs caused by the inhalation of dust in the course of the performance of risk work." **Figure 2.3** and **2.4** is an illustration of a comparison between a thin section of normal human lung, with a thin section of coal worker's pneumoconiosis lung. As it can be seen, the coal worker's lung has accumulated considerable mineral dust which has dramatically influenced its efficiency to transfer oxygen into the blood stream.

Non-fibrogenic dusts cause little or no reaction of any kind, and are usually classified as biologically inert dusts. They do not generally cause pulmonary fibrosis, physical impairment, or disease because any inorganic dust tends to evoke a defence mechanism if only the mobilization of macrophages, in order to expel the inhaled particles. Macrophages are pleopotential cells responsible for the defence of the lower respiratory tract. It has been shown [20] that inert metal dusts such as iron, tin and barium can cause benign pneumoconiosis, iron can cause siderosis, while tin oxide tends to cause stannosis and barium sulphate causes barytosis.





**Figure 2.3 : Thin Section of a Normal Human Lung.**





**Figure 2.4 : Thin Section of a Coal Worker's Pneumoconiosis Lung.**

Carbonaceous substances, such as coal, carbon black, and graphite produce dust foci characterized by the production of reticulin fibres but little or no collagen [20]. The black-lung disease, known as Coal Worker's Pneumoconiosis (CWP) was one of the major health-related concerns in respect of occupational pollution in the

UK. It is caused primarily by coal dust that tends to begin to accumulate in air sacs of the lung, producing scars and making breathing difficult. An average of 2000 coal workers per year have died since 1831 [32]. Example of a lung affected from the black-lung disease is shown in **Figure 2.4**.

Biologically active dusts such as free crystalline silica and asbestos decrease the active life of macrophages, which causes a less controlled accumulation of dusts in the alveolar region. This is followed by an increased number of fibroblasts, which then creates masses of interlacing collagen fibres (scarring) with mature fibrosis being characterized by the deposition of hyalin [20]. **Table 2.2** illustrates the effects of the fibrogenic dusts that cause some of the pneumoconiosis diseases. All collagenous pneumoconioses are caused by fibrogenic dusts, which bring about many pulmonary changes, such as the reduction of the elasticity of lung tissues, thus lowering oxygen uptake and lessening its efficiency. This is characterized clinically by breathlessness, decreased lung expansion, and a lessened capacity for work. **Figure 2.5** illustrates an example of the effects of kaolin inhalation on the human lung.

Certain dusts, mainly from metallic compounds, if inhaled can cause acute inflammation of the lung tissue or bronchioles. These effects could be caused during gassing accidents where the inhaled material has changed form into fumes. Following such exposure, the victim may develop an illness, with symptoms similar to pneumonitis. The least severe pneumonitis is caused by the inhalation of zinc oxide fumes and can cause “zinc ague” or “brass founder’s ague”. Symptoms experienced may be similar to an attack of malaria or influenza. Metallic dusts and fumes of manganese, vanadium, cadmium, and beryllium on the other hand have graver consequences and can cause severe attacks and in some cases death. Normally, however, survivors tend to recover completely, even after a long period of illness [20]. Another example is of people who work in the steel manufacturing factory, who are more likely to inhale more iron oxides into their lungs.





**Figure 2.5 : Thin Section of Lung of an Individual Heavily Exposed to Kaolin Dust.**

Another type of pulmonary fibrosis caused by the inhalation of dust containing free crystalline silica is known as silicosis. Silicosis can cause clinical shortness of breath, decreased chest expansion, lessened capacity for work, absence of fever, and increased susceptibility to tuberculosis [20]. Silicosis is caused by the free crystalline silica, in contrast to silicates, which are the main constituents of clays and fireclay and

do not appear to affect the lungs. If the intensity and duration of exposure to free crystalline silica is too high and of a higher toxicity, macrophages can not clear the lungs effectively. This causes respirable sized particles to accumulate in the alveolar region, and focal deposits also containing increased fibroblasts and interlacing reticulin are formed. These foci will go on to develop masses of interlacing collagen fibres. This disease progresses, individual nodules may fuse together to form larger masses and its extreme development is known as “progressive massive fibrosis.” Unless the fibrosis is very intensive, silicosis in and of itself is not a severe crippling or life-shortening disease. Morbidity and death are not caused directly by the formation of discrete nodules characteristic of silicosis, but are due mainly to the adverse effect of the tissue reaction to crystalline silica, on the tissue defences against the tubercle bacillus and similar mycobacteria [20]. This increased susceptibility to tuberculosis has in the past caused many miners to succumb to the coexisting silicosis and tubercolosis. Further progressive development of silicosis can cause death, for example in the case of the miners in the South African Gold Mines.

Crystalline silica exists as quartz, tridymite, cristobalite and stishovite where stishovite is one type which is nonfibrogenic, while cristobalite and tridymite grouped under fibrogenic dusts and are more fibrogenic than quartz. Quartz, if heated between 860 to 1470 °C, is converted to tridymite, and if heated above 1470°C will create cristobalite [20]. Therefore, the calcining or sintering of materials which contain silica produce highly dangerous dusts.

While natural occurring dusts, which contain silica, e.g. flint, is highly dangerous, it is even more dangerous in the case of freshly fractured silica than that of old dust. The milling of quartzitic ore or sandblasting, with sand containing free crystalline quartz, may lead to highly dangerous freshly fractured quartz becoming airborne dust. It can also lead to acute silicosis from the sandblasting activities, which has a tendency to develop rapidly, often within less than a year, and the results can be fatal. Natural amorphous (non-crystalline) silica, such as diatomaceous earth (kieselguhr) appears to have a low fibrogenic activity and from calcining activities, amorphous silica may also produce highly active forms.

Among the serious impacts of particulate atmospheric pollution due to occupational exposure are: chronic obstructive lung disease, emphysema, chronic bronchitis, asbestosis, bronchial cancer, and death. Chronic obstructive lung disease is a type of lung impairment and is observed in individuals with simple silicosis. The causes of this disease are difficult to determine as it can be caused either by chronic bronchitis or destructive emphysema or a combination of the two. Moderate to severe symptoms might occur such as a cough, sputum production or breathlessness on exertion, and a measurable alteration of pulmonary function. Chronic obstructive lung disease can be caused by the free crystalline silica other co-existing dusts and fumes from cigarette smoking in the workplace, which can lead to the development of obstructive emphysema [20].

Emphysema is defined as the rupture of inter-alveolar cell membrane distal to the terminal bronchioles due to the excessive pressure build-up, which may be due to a restriction in the respiratory airways [20]. Rupture usually occurs during coughing, causing the formation of larger air spaces formed of individual alveolar sacs. Emphysema has been found in 5 percent of the lung in about 50 percent of all males over 50 years old age. In some 10 to 20 percent of these individuals it represented moderate to severe cases of increase in airway resistance, which can lead to abnormal breathlessness on exertion (dyspnea).

Chronic bronchitis is defined as periodic or persistent bouts of coughing and if frequency increases can cause death [20]. The primary cause of such bronchitis is cigarette smoking and its assessment is difficult at the place of residence, medical care and air pollution may also overshadow any demonstrable influence of industrial dusts, fumes or gases. **Figure 2.6** shows examples of a lung affected by cigarette smoking.

Asbestosis is one type of pneumoconiosis caused by the inhalation of asbestos fibres, which are a naturally occurring inorganic mineral fibres, consisting mainly of silicate chains. It has been indicated [20] that asbestos is classified into two groups, based on physical and chemical properties i.e. chrysotile, and amphiboles. Chrysotile is known as the most abundant fibrous silicate, and it represent 90 percent of the world's production. The shapes are curly, tough, compressible, and stand a great deal of mechanical handling. However, they are easily broken down by weak acids but are



not easily decomposed by alkalis. In general, chrysotile is the softest type of asbestos and is used widely for spinning and weaving to produce asbestos cloth and tape.



**Figure 2.6 : Thin Section of a Lung Affected by Cigarette Smoking.**

Another group of asbestos minerals are the amphiboles, which can be found embedded in tabular deposits of sedimentary origin and occurring in extremely hard

rock. They are of a long shape, and are stiff and brittle, and require gentle handling in order to avoid degradation, which can result in a dust hazards [20]. They usually have a minimum diameter of 0.1µm and lengths in excess of 150 mm have been found with approximately 50 percent of it longer than 20 mm. In contrast to chrysotile, amphiboles are more resistant to acids and are also not easily decomposed by alkalis. The subgroups actinolite (greenish) and tremolite (white), even though less commercial, occur in small amounts naturally as contaminants in talc. Another subgroup, the anthophyllite (white) is mined in Finland, while amosite brown (grey-brown) and crocidolite (cape asbestos, riebeckite, blue-lavender) have been mined extensively in the northern Transvaal and north-west Cape respectively in South Africa.

There has also been increasing concern in instances of the exposure of naturally occurring asbestos (NOA) on human health around the world, examples of which are the chrysotile and also tremolite in California [27], which has caused malignant mesothelioma among the workers in California and also in Da-Yao, China due to the exposure to natural crocidolite ore, known as 'blue clay' by the local people [33]. Mesothelioma is a rare diffuse cancer which spreads over the surface of the lung i.e. pleura and the abdominal organs i.e. peritoneum. Similar cases have also been recorded in Turkey from the exposure of carcinogenic tremolite and erionite, a fibrous zeolite, which is present in the volcanic tuffs that are used as building stones [34]. In the town of Libby, Montana, vermiculate (clay mineral) is mined and was used widely by the insulation manufacturers and installers from 1950s to 1990. In the 1980s and 2000, according to Jacobson [11], 192 people out of 2700 people died and 375 others were diagnosed with asbestos-related lung problems, especially in cases where the mine workers exposed the asbestos to their family when they brought their clothes, permeated with asbestos-laden dust into their homes. A lung exposed to the hazardous fibres is illustrated in **Figure 2.7**

Bronchial cancer has been associated with excessive exposure to asbestos and also from cigarette smoke, which can contribute towards the production of bronchial tumours. Furthermore, uptake of carcinogens appears to be asbestos-mediated in that the carcinogens are adsorbed onto the fibre surface from where they are transferred to the lung tissue on inhalation of the carrier fibre [20]. People who work in the mining



industries, for examples in France, have been exposed to carcinogenic agents, which can cause lung cancer [29]. Some of the carcinogenics agents are described in **Table 2.3** given by the *International Agency for Research on Cancer (IARC)*.



**Figure 2.7 : Thin Section of Lung of an Individual Exposed to Asbestos Dust.**

**Table 2.3 : Major Known Human Carcinogens Linked to Cancers.**

<b>Carcinogenic Agents</b>	<b>Sites of Cancer</b>
Aromatic Amines	Bladder
Arsenic	Liver, Liver (angiosarcoma), skin
Asbestos	Lung, Mesotheliomas
Benzene	Leukaemia
Bischloromethyl Ether	Lung
Chromium	Lung, Nasal Cavity
Ionizing Radiation (radon and its decay products)	Lung
Iron Oxides	Lung
Mineral Oils	Skin
Nickel	Lung, Nasal Cavity and Ethmoid
PAHs (coal tar – soots)	Lung, Bladder, Skin
Vinyl Chloride	Liver
Wood	Nasal Cavity and Ethmoid

\* Sources : *Deschamps et.al. [29]*.

### 2.3.4 Effects of Particulate Environmental Exposure

The London Smog and Los Angeles Smog are two examples that represent environmental pollution. Known as ‘urban pollution’, it normally occurs in large, developed and industrialized cities, as a result of burning of wood, vegetation, coal, natural gas, oil, gasoline, kerosene, diesel, waste, and chemicals [11]. The sources of environmental pollution creates high concentration of airborne particulates i.e. the primary and secondary particulates that, once mixed up in the atmosphere, as stated earlier, is known as emitted smoke. Chemically formed pollution is known as photochemical smog. Both types of smoke is produced generally from vehicles, factories, and industries.

Airborne particles smaller than 10µm in diameter can cause asthmatic and chronic obstructive pulmonary diseases [35], while particles smaller than 2.5µm in diameter, tend to cause the most severe problems for human health. This type of particle is produced in the atmosphere by emissions and nucleation. **Jacobson [11]** has indicated that in the air, the number concentration and size change by coagulation, condensation, chemistry, water uptake, rainout, sedimentation, dry deposition, and transport. The effects from the exposure to environmental pollution caused by the fine

particles are asthma morbidity and mortality, coughing, inflamed lungs, choking or even death as a result of heart attacks brought on by the difficulty in breathing [5]. It is stated [36] that finer particles can also contribute to a variety of cardiopulmonary problems, including an increase of mortality, increased disease, and decreased lung function in adults and children.

The focus of most air quality legislation standards, emission control regulations and other legislation is on the protection of mainly human health and also on the prevention of harm towards the environment. Among the aspects of air pollution that often causes most direct concern to the public is the nuisance effects arising from fumes, odours, dust, and dirt [8].

Traffic is known as the most widespread source of these nuisance effects, despite other certain industries and construction / demolition activities can contribute to localized effects. This is strongly supported by the study run by **Mackie and Davies** [37] for the Transport Research Laboratory on the environmental effects of a number of schemes that changed traffic flow. These studies show a strong link between nuisance and both the number of lorries and the change in total traffic flow. They discovered that the road schemes that reduced traffic by 60 percent on average, were found to reduce the number of people bothered by dust and dirt at home, either 'very much' or 'quite a lot', by half, from 56 percent to 28 percent. In another case, the percentage bothered by dust and dirt was reduced from 55 percent to 16 percent following the implementation of scheme that reduced lorry traffic, but which did not reduce total traffic flow. The significant role of lorries identified in this study probably represents a combination of effects, including noise / vibration and the perceived physical danger. It is also likely to relate to the more smoky and odorous nature of emissions from diesel engines.

Dust and dirt caused by traffic includes direct exhaust emissions of particulates (mainly from diesel) as well as dust re-suspended from the road by passing traffic. The re-suspended material will include soil material, and the following, that pre-dominate on road surfaces: product of vehicle wear i.e. rust, vehicle tyre rubber etc; and de-icing salt in winter months. The nuisance effects of these types of dust and dirt are related to deposition onto surfaces. These can be seen easily on windows and

window sills, on cars, and on washing and indoor fabrics. The soiling effects of the carbonaceous particulates emitted from diesel engines is considered to be particularly important, however little is known in respect of which sources of dust and dirt are most important [8].

Meanwhile, fumes and odours are less significance as source of nuisance. The term 'fumes', though hard to define, refers to gases as well as fine aerosol particles i.e. less than 2µm in diameter, and it often implies the odorous component of these. Odour from vehicles will contribute the unpleasantness of being in the vicinity of traffic. It is the nature of the perception of odours that response is derived from exposure over period of few seconds, and concentrations over this time period can be a factor of 10 to 20 times higher than those measured over one hour. Among the sources such as aldehydes, benzaldehyde, marker pens, diesel exhaust odorant, and also hydrogen sulphide from catalytic converters [8].

### **2.3.5 Effects Produced by Indoor Air Pollution Exposures**

The normal working hours of a person is between 9.00 am and 5.00 pm, which, followed by overtime, means that they can spend up to 10 to 12 hours per day in their offices. Humans tend to spend nearly 70 percent of their time indoor and they are exposed to any of the airborne particulates mentioned earlier. This situation has increased the potential of the building occupants to be exposed to either direct or indirect effects of indoor air pollution. This has resulted in an increase of short-term and long-term effects experienced by building occupants. One study perform in the USA has shown that indoor air pollution is worse in comparison to outdoor air pollution. A report by the EPA [26] has stated that when particle levels are high outdoors, they can also be high indoors. Particles can enter buildings through doors, windows, and even the ventilation system causing a higher particulate-concentration indoor than the outdoor. IAP is complex as the relationship between the contamination sources in a building, the ventilation rate, and the dilution of indoor air contaminant concentrations with outside air can worsen the situation.

There are two groups of IAP pollutants i.e. gases, and aerosol particles. The gaseous pollutants identified are: carbon dioxide, carbon monoxide, nitrogen dioxide, ozone, sulphur dioxide, formaldehyde, volatile organic compounds, and radon. The aerosol particles are: allergens, asbestos, fungal spores, bacteria, viruses, and polycyclic aromatic hydrocarbons. Other pollutants such as tobacco smoke, wood stoves, fireplaces, outdoor air, etc. Passive smoke has been identified as one of the contributor to IAP, which can cause heart disease and is known to have caused lung cancer in the catering industry in Hong Kong [28]. This relationship is further complicated by outside air sources entering the buildings and being used for diluting air and pollution sinks that may modify or remove contaminants. Another example of the health hazard linked with airborne particles is the indoor-burning of biomass and coal, which is caused by cooking activities and home heating by a large part of population around the world. Out of 2.7 million people who died every year by the atmospheric pollution, 1.8 million come from rural areas as a result of indoor-burning of biomass and coal as estimated by the World Health Organization [38]. Among the effects on human health are: eye irritation threshold, throat irritation threshold, biting sensation in nose and eye, tearing eyes, lung effects, inflammation of lung (pneumonitis), odema, respiratory distress, danger to life and even death.

#### **2.4 Atmospheric Particulate Pollution Impact on Flora and Fauna**

Flora and fauna are second in the hierarchy of those most affected from pollution by atmospheric particulates pollution. They can be exposed both in urban and rural areas and are subjected to the impact of particulate pollution in the form of dry acid deposition ( $\text{SO}_2$ ), carbon particles, carbonaceous material, etc. Being part of the ecosystem, flora are affected based on the range of the pollutant concentration and environmental conditions. Also, the impacts depends on many factor i.e. plant species, age, nutrients, soil, temperature, humidity, and sunlight.

Urban vegetation is characterized by amenity trees as found in public parks and alongside roads, and herbaceous plant species also typical of public parks, in addition to private gardens and allotments. Since the implementation of the Clean Air

Act in 1956, urban air quality has been altered considerably, as both SO<sub>2</sub> and smoke levels have sharply declined [8]. Prior to this legislation very few trees were able to grow and thrive in urban areas, whereas nowadays a much greater diversity of trees can be seen. The colonization of lichen species, which has been observed in some areas in London is consistent with falling SO<sub>2</sub> levels. However, this improvement in urban air quality has been negated to a large extent by the dramatic increases in vehicle exhaust emissions, resulting in elevated levels of NO<sub>x</sub> and hydrocarbons, both precursors of O<sub>3</sub>. Both NO<sub>2</sub> and O<sub>3</sub>, have been demonstrated to affect tree growth and performance at concentrations typical of those recorded during pollution episodes which characterize urban air quality. At the moment, it has not been possible to quantify the contribution made by air pollution to the damage of amenity trees. This is a complex problem as it is difficult to separate effects attributable to air pollution from those caused by other stress factors such as road salt, drought, and pest infection [8]. These other stresses may in fact predispose trees to damage by air pollutants or vice-versa.

In rural areas, forests are being affected by atmospheric particulate pollution in a range from beneficial to detrimental. In the agriculture sector, the impacts is believed to come from the dry deposition and wet deposition of airborne particulates, which consist of various chemical components with the major components being e.g. sulphates, ammonium and also nitrates and many other toxicity chemicals. Dry deposition from the air onto the leaves may prevent the sun from reaching the plants, reducing their photosynthetic capabilities and eventually leading to their death as a result of a lack of exposure of photosynthetic cells to the sun. In the case of wet deposition, the airborne particulates can e.g. enter the drainage system during precipitation, which can cause an increase in the chemical components absorbed by the plants, which in larger doses can slowly kill them. Looking further afield, such pollution, can affect the income of farmers and food processing companies. An example of the direct effect of this precipitative pollution on plants is when sulfuric acid deposits onto the leaf or needle, it forms a liquid film or low pH that erodes the cuticle wax, leading to the drying out (desiccation) of and injury to the leaf or needle [11].



The impact on fauna is seen to a greater extent in the forest, as part of the ecosystem, where the animals are at risk when they eat plants, trees, or crops, contaminated by airborne particulates through dry or wet deposition. The fauna is also at risk in its intake of contaminated groundwater formed by raindrops contaminated by acidic materials.

## **2.5 Impact of Air Pollution on Buildings and Materials**

Acid deposition originally contributed by sulphuric acid from sulphur dioxide ( $\text{SO}_2$ ) and also some from nitric acid from nitrogen oxide (NO) in the air has been causing many effects on buildings and materials. Acid deposition, which is contained in gases, aerosol particles, fog drops, or rain, falls onto the buildings, affecting materials such as sandstone, limestone, marble, copper, bronze, and brass [11]. Other contributors to the effects are fine carbon, hydrocarbon, ozone, etc.

The soiling of buildings remains a problem, even though smoke levels in urban areas have reduced extensively over the past thirty years [7; 8]. The problem is mainly caused by diesel emissions, with the rich source of very fine carbon particles known as Particulate Elemental Carbon (PEC). Nowadays, PEC is known as the main source of soiling in most European towns.

These particles are very small and sticky due to their hydrocarbon content. A diesel particle has a greater propensity than others to cling to surfaces. It is also much less wettable than a suspended soil particle, and thus is less readily removed by rain.

The surface tension properties of PEC have implications for potentially damaging reactions, which may occur within the patina of building's façade. Patinas are defined as any fine layer on the surface; in this case the building surface layers. Acidic gases such as sulphur and nitrogen oxides can become easily absorbed onto the surface of such particles and once deposited on a soiled stone surface may act synergistically with it. Also, PEC may aid the catalytic conversion of such acidic gases to the sulphate and nitrate forms respectively.

The enhanced erosion of certain building stones, and the greater corrosion of metals, due to sulphur dioxide deposition, is well established. As is to be expected, the steady reduction of sulphur dioxide in urban areas has been due to decreasing corrosion rate of metals [8]. However, the same cannot be said of the erosion rates of stone. This may be due to a 'memory effect', whereby the erosion rate is determined by previous exposure. It is also possible that the increased urban concentrations of nitrogen oxides have compensated for the decline of sulphur dioxide, although there is clear evidence as to the role, if any, that nitrogen oxides play in the stone erosion.

Despite causing soiling and enhanced corrosion / erosion of building materials, air pollutants can affect a wide range of other materials used in urban areas. Among those highlighted, ozone is perhaps the most important. It is a very reactive gas, which causes the ageing of rubber. This ageing process can be reduced by using anti-oxidants, but this may increase the material cost by 10 to 25 percent [8]. This type of pollution may lead to considerable economic costs. For example, the cost of such damage in the United States of America was estimated in the 1970s to be in the region of \$900 million per year (approximately equivalent to \$2,650 million in 1991). Other damages which can be caused by ozone are: on the cellulose in textiles, reducing the strength of certain items, and also, causing the fading of fabrics. If most of the textiles are kept indoor, the damage caused by such pollution tends to be low as the ozone levels are low. In this context, particular attention is paid to the protection of valuable paintings in art galleries from damage due to ozone.

## **2.6 Impact of Air Pollution on the Global Environment**

Amongst the effects of airborne particulates on the global environment are global warming issues, icebergs melting and increases of worldwide sea level, hurricanes due to the increases of the sea surface temperature, floods, haze, decreasing of visibility, fogs, etc. Airborne particulates have been identified to play a role in causing these problems. The pollution of the troposphere and stratosphere layer of our atmosphere could come from various sources such as from natural or anthropogenic, organic or non-organic sources, which react during the photochemical process from primary to the secondary particulates which can then create toxicity particulates in the



air as explained in Chapter 1. Other effects on the global environment could also be caused by an episodic events, such as biomass burning, temperature inversions, and also dust storms [7].

Biomass burning can either be a human-initiated event, such as in the burning of vegetation for land clearing or land use change, or a natural event, as in the wildfires resulting from lightning. Biomass can significantly increase PM levels in local areas and sometimes more distant areas and air can also carry the smoke half-way around the earth. Organic carbon compounds usually dominate the  $PM_{2.5}$  concentration profile during these fire episodes.

Topography and meteorological conditions make some areas more susceptible to episodic events. In mountain regions, temperature inversions sometimes trap polluted air during winter. Wintertime  $PM_{2.5}$  and  $PM_{10}$  can be more than three times higher than other seasonal averages. Woodstove smoke, containing large amounts of organic carbon, is often identified as a significant source of the elevated wintertime PM concentrations.

Arid desert conditions in the South-western United States make this region more vulnerable to wind-blown dust than other regions of the nation. Most dust events are caused by passage of weather fronts and troughs and down mixing of upper-level winds. Cyclone development and thunder-storms result in the most dramatic dust clouds with the lowest visibilities. Dust related events are typically dominated by large, coarse particles, but fine particle levels also increase.

The effects of dust storms also can be seen globally. Giant sand storms originating from Sahara Desert can blow across the Atlantic to South America, the Caribbean, and the southeastern United States, transporting several hundreds million tons of dust every year. Movement of dust from Africa has increased since 1970 because of an increase of dry weather in the Saharan region. Sandstorms also originating from China's Gobi Desert occasionally cross the Pacific to the United States. Transport from Africa typically occurs in summer, and transport from Asia typically occurs in the spring season.

Another global environmental effect of atmospheric pollution is that on visibility. This can cause haze problems, which can effect the economies of countries in the regions affected. Also known as trans-boundary effects, it can affect the productivity of human resources. For example, if lots of workers are taken ill due to respiratory or pulmonary disease related to airborne particulate materials, the productivity of human resources is susceptible to drop drastically as a consequence. This could lead to a national emergency alert. Among other effects are: increase in hospital admissions, closure of schools, delay or cancellation of flights as a result of decreased visibility, etc. In addition, there is the possibility of the tourist industry being affected by a decrease in the number of tourists following the news of such pollution.

Based on the Particulate Pollution Report on the *Current Understanding of Air Quality and Emissions through 2003* produced by EPA [7], of all types of air pollution, pollution by airborne particulates is considered to be the most complex. Some particles or particulates, such as dust, dirt, soot, or smoke, are large or dark enough to be seen with the naked eye. Others are so small, they can only be detected using a transmission electron microscope (TEM).

**QUARG [8]** has indicated that one of the most obvious impacts of air pollution is loss of visibility; and for many people the associated loss of comfort is of serious concern. Air pollution reduces visibility by introducing particles and gases, which absorb and scatter light, between the observer and the observed object. This visibility impairment is experienced in the form of a haze that limits the distance we can see and that degrades the colour, clarity, and contrast of the view [7]. The particles that cause haze are the same particles that contribute to serious health problems and environmental damage.

Fogs are most extreme instance of visibility loss, and there is much evidence that air pollution increases especially with pollution by airborne particles, which act as nuclei for the condensation of fog droplets. Smogs of the classical London type, which could reduce visibility to a few metres, are now a thing of the past. However, there are less intense winter smogs that still occur occasionally, related largely to the build-up of traffic related pollutants. Nowadays, reduced of visibility are more commonly

associated with summer smogs due to photochemical air pollution (Los Angeles type smog). The effects of visibility will be discussed in the next subtopic which, will be introduced the haze problems as part of the trans-boundary effects.

In the United States, visibility impairment and the concentration of particles that cause it are generally worse in the East than it is in the West [7]. Despite that, humidity has been identified as contributing to a significant increase in visibility impairment, by causing some particles to become more efficient at scattering light. Average relative humidity levels are higher in the East (70 percent to 80 percent) than in the West (50 percent to 60 percent). In the East, reduced visibility is mainly attributable to sulphates, organic carbon, and nitrates. Poor visibility is caused by high sulphur concentration, which dominates the composition of these visibility-impairing particles and contributes to light extinction than they do to fine particle concentrations. In the West, organic carbon, nitrates, and crustal material make up a larger portion of total particle concentrations than they do in the East

In the case of visibility effects, fine particles are the major source of haze that reduces visibility in many parts of United States, including in their National Parks for example the Yosemite National Park (California) and also the Shenandoah National Park (Virginia). National parks are the best known examples of the most obvious effects of air pollution occurrence in urban areas and the countryside. Visibility at both national parks was recorded under bad and good visibility conditions with the visual range of Yosemite National Park 111 kilometres during bad conditions and greater than 208 kilometres during the good conditions. The same trend is in evidence at Shenandoah National park with visual range of 25 kilometres and 180 kilometres during bad and good visual conditions respectively [7]. This demonstrates that airborne particulates can cause worse visibility effects depending on related factors in different such as chemical compositions, humidity, wind flow, etc. Therefore, regional haze reduction plan among the related agencies has been seen as the best plan at the moment in reducing the visibility effects for the future.

## **2.7 Conclusion**

It has been shown that atmospheric particulate pollution has a considerable environmental impact especially with regard to human health. In order to understand the health effect of airborne particulates, it is necessary to sample and characterize the material. This is necessary in order to define or detect these fractions of airborne particles, which represent the most hazardous size of particles. By understanding of the physical and chemical characteristics of the airborne particulates, more efficient dust sampling instruments can be designed and techniques developed to monitor and control any pollution problems.

**CHAPTER 3 :**  
**INSTRUMENTS FOR INHALABLE AND RESPIRABLE**  
**AIRBORNE PARTICULATES SAMPLING**

**3.1 Introduction**

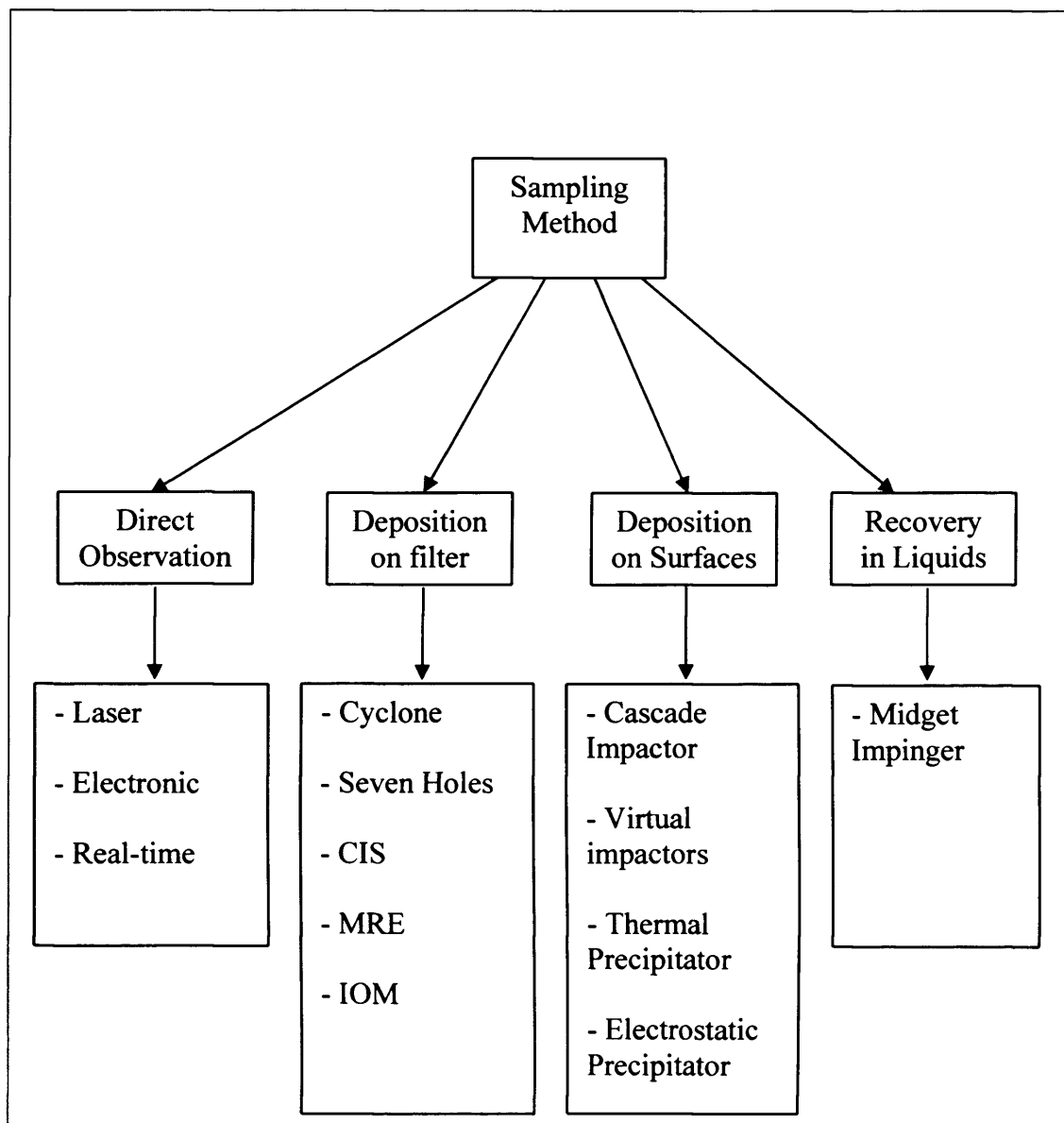
In this chapter the basis of the design of instruments for the collection and characterization of airborne particulates is considered. In designing instruments for the purpose of sampling airborne particulates, there needs to be clear objective in mind by the manufacturer. Manufacturers normally have to consider criteria such as the purposes and sizes of airborne particulates they are going to sample. The size of particulates sampled is based on standards and an understanding of particulate deposition mechanisms in the respiratory system tract. The purpose of sampling may be for identifying the source of airborne particulates or for dust control purposes. The instrument should therefore be capable of physical collection so that characterization of particulates such as mass or number concentration, size distribution, optical imaging, and chemical composition can be performed. Most importantly, the design must be based on an acceptable standard such those recommended by the British Medical Research Council (BMRC), American Conference of Governmental Industries Hygienists (ACGIH) and also the International Commission of Radiological Protection (ICRP). These standards are based upon an understanding of particle deposition mechanisms within the respiratory system.

**3.2 Review of Design of Sampling Instruments**

Airborne dusts consist of a range of materials of particle sizes derived from multitude of sources either natural or anthropogenic. With particulates varying in size, their sampling or collection is a challenging task. As reviewed in Chapter 1, this research has blossomed from simple suspended particulates measurements (SPM) to the detailed characterization of ultra-fine particulates. This increased interest has been promoted by the study of health effects of pollution and other atmospheric environmental problems. In the sampling of airborne particulates, a variety of methods can be used including the collection of dust onto filters, surfaces or liquids, for

particle mass, number and/or size determinations. **Figure 3.1** outlines the various methods available.

**Figure 3.1 : The Summary of Methods used in Sampling of Airborne Particulates.**



Many types of filters are employed and they are the most popular type of media used in sampling aerosol particles. The two most common filter media used are the fibrous and porous filters. Fibrous filters are made of fine fibres (usually glass) arranged perpendicular to the direction of airflow. These filters have 70 to greater than 99 percent porosity air and can be designed to select particles from submicrometer

size up to 100  $\mu\text{m}$ . Some fibrous filters are manufactured from cellulose fibres. Others from glass, and also various plastics materials such as polyvinyl chloride (PVC). The porous types of filters have a different structure and a porosity less than fibrous filters. The gas flow through the filter often follows irregular pathways through the complex pore structure. Porous membrane types of filter are manufactured from cellulose esters, sintered metals, PVC, Teflon<sup>TM</sup>, and other plastics. The capillary pore membrane filter (Nuclepore<sup>®</sup>) is another example of membrane filter, which has a uniform diameter of cylindrical holes approximately perpendicular to the surface of filter. To capture airborne particles, air is simply drawn through filters onto which particles can be collected for further examination.

The methods of sampling onto surfaces is commonly used in instruments such as the cascade impactor, thermal precipitator, electrostatic precipitator, and etc. The cascade impactor employs the impaction concept where an aerosol sampled is passed through a nozzle and the output stream (jet), which is directed against an impaction plate. This flat impaction plate, deflects the flow to form an abrupt  $90^{\circ}$  bend in the streamlines. Particles [39] (whose inertia exceeds a certain value are unable to follow the streamlines and collide (impact) on the flat plate, by assuming that particles stick to the surface. Smaller particles will follow the streamlines and avoid hitting the impaction plate. Each stage in the cascade impactor is assumed to capture all particles reaching it and are larger than its cutoff size. Therefore, smaller particles are captured by the previous plate and the larger particles are captured by the following stages. Examples of instruments using this concept are the Marple Personal Cascade Impactor (Series 290) and the Anderson Cascade Impactor (Mark II) which will be described in Chapter 4. Another type of impactor is the virtual impactor where the difference is that particles larger than the cutoff size and those smaller than the cutoff size are collected on separate surfaces where the larger particles are carried by the minor flow onto the filter and the smaller particles are carried radially by the minor air flow onto the other filter.

Another example of collection of particles on surfaces is that of the Thermal precipitator. This device employs the thermophoretic concept to force particles in the direction of decreasing temperature and allowing them to be deposited onto suitable surfaces for examination. Electrostatic precipitators using the concept of electrostatic

forces to collect charged particles onto surfaces is another example of a surface collection method.

Collection of particles in a fluid is a well-established method. The Midget impinger is one example of such a device employing a dust-counting cell to determine the number of particles collected. This method of measurement has been used in the past to correlate with the incidence of respiratory disease observed in mines and other dusty trades [39]. The impinger operates like an impactor, except the jet is immersed in water or alcohol. Normally, particles larger than 1  $\mu\text{m}$  are captured by inertial mechanisms and end up suspended in the liquid. Of known volume, diluted particles are brought back up to standard volume and an aliquot of the liquid is examined in a dust-counting cell, which can be analysed by light microscopic examination. The number of particles collected are obtained on the basis of the ratio of the liquid volume counted in an area using an eyepiece graticulate or by a grid etched on the cell base, to the total volume of liquid. Therefore, the number concentration is calculated by dividing the total number of particles collected by the volume of air sampled, as for filter samples. This method has now been extensively replaced by respirable mass sampling.

It is obvious that before one starts dust sampling one should be quite clear as for what the sample will be used. The purpose for which sampling is performed will greatly affect the way in which the samples are taken. It will affect the way in which they are assessed, and the accuracy which can be obtained. There are two main objectives of sampling. The first, to provide quantitative feedback on the quality of the atmospheric environment for positive engineering control of the atmosphere. To allow dilution with fresh air, filtration, dust suppression, the use of barriers, or a combination of these measures; and/or secondly, to assess the exposure of personnel to airborne particulates. Based on these two considerations, a number of sampling systems can be identified.

(a) *Routine sampling*

Routine sampling should be simple and inexpensive employing a single parameter such as mass concentration of dust particles to compare concentrations at



fixed stations or for spot samples. For example, sampling limestone dust or coal dust particles conducted in the environmental dust chamber using various simple sampler heads such as the cyclone sampler and the seven holes sampler for determination of respirable and inhalable dust fractions in a short period of time.

(b) *Sampling to measure full-shift exposure (TWA)*

This assessment is conducted on a survey basis to estimate dust exposures for epidemiological studies of work-related respiratory diseases and known to as time weight assessment (TWA). On site, the assessment was conducted by highly-trained observers operating several sampling instruments used to take up 8-hours up to 24-hours sampling, with intervals throughout the shift and assessed in the usual fashion to give mass and number concentrations.

(c) *Sampling to determine risk*

This sampling objective conducted mainly to measure dust levels and the pathogenicity of the various mineral dusts, and is used to assess occupational health risk in the working area for example in mining, factory, office building, construction, etc. In determination of the risk of dust exposure, a range of instruments can be used including the thermal precipitator, respirable samplers (i.e. cyclone sampler, MRE gravimetric sampler, etc), inhalable sampler (i.e. seven hole sampler, CIS sampler, etc). Instruments like the RespiCon sampler can also be used, which can sample respirable, thoracic, and inhalable dust fractions simultaneously or the cascade impactor, which has many stages with each stage having a cut-off aerodynamic size for dust particles collected. The results gained are then compared with the BMRC, ISO, and ICRP size conventions for further recommendation or action to be taken to assess the risk of exposure.

For routine sampling and assessment of airborne dust, most of the hand-held type of samplers have been used or developed by hygienists working in the mineral industries. Generally, in designing and manufacturing a sampler, certain requirements are needed for hand-held instruments as follows [20]

- i) known sampling characteristics under a full range of atmospheric conditions experienced in working places;
- ii) suitability for sampling the best single descriptive parameter (or parameters) of the particulate clouds found in working places;
- iii) ease and accuracy of assessment, and preferably on-the-spot display of measured values;
- iv) simple to operate under difficult environmental conditions;
- v) intrinsically safe in case of use in explosive atmosphere;
- vi) rugged to withstand unavoidable rough treatment in use and in transit, and resistant to moisture and extremes of temperature;
- vii) low first cost, easily serviced, and spare parts readily available

### **3.2.1 Environmental Size Classification of Airborne Particulates**

As shown in Chapter 2, classification of airborne particulates ranges from consideration of total suspended particulates (TSP) to the ultra fine components of air samplers. Of major concern are those size fractions of dust, which cause health effects when inhaled. For health purposes, the respiratory tract can be treated as three regions: the heady airways region, the tracheo-bronchial region of the lungs including the trachea and ciliated airways, and the alveolar region of the lungs including non-ciliated airways and alveolar sacs. Some materials may be toxic wherever they deposit in the respiratory tract and others only if they are deposited in a particular region, and some particles may be so large that they are lost from the inhaled air before reaching the region where they must deposit to exert their toxic effect. The toxic effects of particulate materials are therefore a size dependant evaluation of the hazard associated with particulates, which contain toxic material this evaluation is usually performed by measuring their airborne mass concentrations. Some experts believe it is better to evaluate the hazard if particles, which do not contribute to mass concentration are excluded from the concentration measurement. An understanding of the inhalable, thoracic and respirable fractions in a dust is important to exclude those particles, which are too large to contribute significantly to the hazard posed by a particular material. **Figure 3.2**, illustrated the location of deposition of the inhalable, thoracic, and respirable dust fractions.

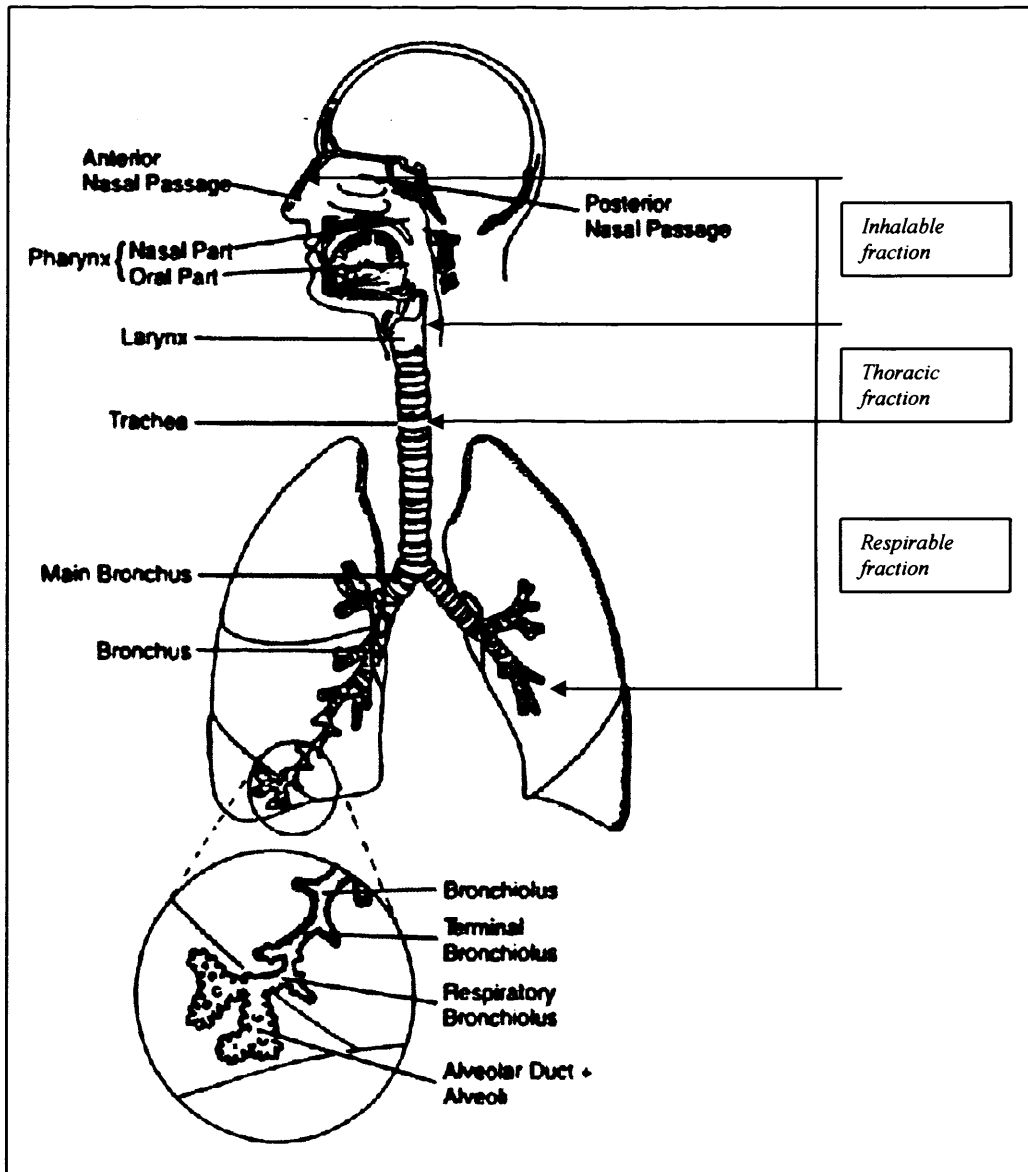
### 3.2.1.1 The Inhalable Fraction

The inhalable fraction (also called inspirable fraction) is intended to include the portion of the ambient aerosol, which passes the nares or lips and enters the head inhalation [40]. Collection of this fraction may be suitable for evaluating the potential effects of airborne materials, which may exert an adverse effect wherever they are deposited in the respiratory tract. The inhalable fraction is also defined as the fraction of airborne material that enters the nose and mouth during breathing, and may cause damage in the respiratory tract. The characteristics of the inhalable fraction depends on the prevailing air movement around the exposed person (wind speed and direction, and whether breathing takes place using the nose or mouth [41]. The inspirable fraction [42] is defined as the available set of measurements of the fraction of airborne particles, which enters the nose or mouth of a human model in a wind tunnel. A simple mathematical function [43] to describe the inhalable fraction for sampling purposes is as follows

$$SI(d_{AE}) = 0.5 (1 + e^{-0.06d_{AE}}),$$

where  $SI$  is the sampling efficiency of an ideal inhalable sampler, defined as the ratio of the concentration measured by an ideal sampler to the ambient concentration for a monodisperse aerosol, and  $d_{AE}$  is the particle aerodynamic diameter. Based on average inspirability, it has been demonstrated that this formula is mainly applicable for particles with aerodynamic diameters up to 100  $\mu\text{m}$  [44]. Another standard [42] considers particles up to 155  $\mu\text{m}$  in size to be included in this inhalable fraction.

**Figure 3.2 : The respiratory system. Adapted from the International Commission on Radiological Protection [45].**



### 3.2.1.2 The Thoracic Fraction

The thoracic fraction is defined as those particles, which are small enough to pass the larynx and enter the lungs during inhalation and may be of use in evaluating the hazard associated with airborne materials, which exert an adverse effect when they deposit in the lungs [40]. The thoracic fraction has been defined as a subdivision of the inspirable fraction [42], which can be represented by the following mathematical function

$$\frac{ST\{ISO\}}{SI\{ISO\}} = 1 - F(x),$$

with

$$x = \frac{\ln(d_{AE}/\Gamma)}{\ln(\Sigma)}, \Gamma = 10 \mu\text{m}, \Sigma = 1.5$$

where  $x$  is the dummy value has been used [40] in calculating  $ST\{ISO\}$ ,  $SI\{ISO\}$ , and  $F(x)$  where  $ST\{ISO\}$  refers to sampling efficiency of an ideal collector of the thoracic fraction which was given by ISO [42],  $SI\{ISO\}$  stands for the sampling efficiency of an ideal collector of the inspirable fraction (inhalable fraction) which was given by ISO [42], and  $F(x)$  is the cumulative probability function of a standardized normal random variable. While  $d_{AE}$ , stands for particle aerodynamic diameter,  $\Gamma$  represents a parameter with unit length which is sometimes used when calculating the thoracic or respirable fraction, and  $\Sigma$  is a unitless parameter which is sometimes used when calculating the thoracic or respirable fraction.

and

$$F(x) = \int_{-\infty}^x \frac{dx}{\sqrt{2\pi}} e^{-x^2/2}$$

A convenient algebraic expression for  $F(x)$  is given in the **Appendix A**. For a particle with aerodynamic diameter near to 8.5  $\mu\text{m}$ , one-half of the ambient particles would be included in a thoracic fraction [42]. While the Environmental Protection Agency [46], have adopted the  $\text{PM}_{10}$  sampling criterion which specifies that the particle aerodynamic diameter at which one-half of the particles in the air sampled are collected should be  $\pm 0.5 \mu\text{m}$ , and also requires that for a size distribution which is specified [45] that the mass concentration which a sampler can be expected to measure must be between 129.5 to 158.3  $\mu\text{g}/\text{m}^3$ . The ACGIH [43] have also adopted a definition of thoracic fraction which specifies that one-half of the 10  $\mu\text{m}$  particles in the air sampled will be collected :

$$ST\{ACGIH\} = 1 - F(x),$$

where

$$x = \frac{\ln(d_{AE}/\Gamma)}{\ln(\Sigma)}, \Gamma = 10 \mu\text{m}, \Sigma = 1.5.$$

A slight modification of these definitions was proposed by Soderholm [40] :

$$ST(d_{AE}) = SI(d_{AE})[1 - F(x)],$$

where

$$x = \frac{\ln(d_{AE}/\Gamma)}{\ln(\Sigma)}, \Gamma = 11.64 \mu\text{m}, \Sigma = 1.5.$$

where  $x$  is the dummy value used in calculating  $ST\{ACGIH\}$ ,  $ST(d_{AE})$ ,  $SI(d_{AE})$  and  $F(x)$  [40] where  $ST\{ACGIH\}$  stands for sampling efficiency of an ideal collector which was given by ACGIH [43],  $ST(d_{AE})$  represents the for sampling efficiency of an ideal collector of the thoracic fraction which was proposed by Soderholm [40],  $SI(d_{AE})$  is the sampling efficiency of an ideal collector of the inspirable fraction (inhalable fraction) which was proposed by Soderholm [40], and  $F(x)$  is the cumulative probability function of a standardized normal random variable. A convenient algebraic expression for  $F(x)$  is given in the **Appendix A**. While  $d_{AE}$ , represents the particle aerodynamic diameter  $\Gamma$  is a parameter with unit length which is sometimes used when calculating the thoracic or respirable fraction, and  $\Sigma$  is a unitless parameter which is sometimes used when calculating the thoracic or respirable fraction. **Table 3.1** gives the values of : (i) the proposed thoracic fraction as a function of aerodynamic diameter; and (ii) the efficiency which would be required of an instrument to collect downstream of an inlet which has an efficiency matching the definition of the inspirable fraction.

The proposed form of  $ST(d_{AE})$  guarantees that it is smaller than  $SI(d_{AE})$  at all particle sizes. And the proposed definition of the thoracic fraction [40] had satisfies the EPA  $PM_{10}$  criteria, since an ideal thoracic sampler would collect 50% of particles having an aerodynamic diameter of 10  $\mu\text{m}$  and would measure a mass concentration of 148  $\mu\text{g}/\text{m}^3$  if it sampled the size distribution [46].

The choice of a function to define the thoracic fraction is guided by the available set of measurements of the deposition of airborne particles in the head during inhalation through the nose or mouth. Particles with larger aerodynamic diameters are removed effectively from the inhaled air by the airways in the head can be excluded from the thoracic fraction. Author [47] has explained that, the airways in the head consists of the nasal passages, mouth, pharynx and larynx, and deposition of

inhaled particles there occurs mainly in the nasal passages during nasal breathing and in the larynx during oral breathing.

**Table 3.1 : Proposed values of inspirable fraction, thoracic fraction and thoracic fraction as a subdivision of inspirable.**

Particle aerodynamic diameter (µm)	Inspirable fraction [SI]	Thoracic fraction [ST]	Thoracic as subdivision of inspirable [ST]/[SI]
0	1.000	1.000	1.000
2	0.943	0.943	1.000
4	0.893	0.890	0.996
6	0.849	0.805	0.949
8	0.809	0.666	0.822
10	0.774	0.500	0.646
12	0.743	0.349	0.470
14	0.716	0.232	0.324
16	0.691	0.150	0.216
18	0.670	0.095	0.141
20	0.651	0.059	0.091
22	0.634	0.037	0.058
24	0.618	0.023	0.037
26	0.605	0.014	0.024

\* Proposed by Soderholm [40].

### 3.2.1.3 The Respirable Fraction

The respirable fraction is intended to include those particles, which are small enough to enter the alveolar region of the lungs during inhalation [40]. The respirable fraction is also known to be the appropriate size fraction for evaluating the hazard associated with materials, which exert an adverse effect only if they deposit in the alveolar region. Nowadays, most size-selective sampling of particles in the workplace consists of measuring the respirable fraction according to the BMRC, ACGIH or ISO conventions. Hence, respirable dust is given as the estimated fraction of airborne material that penetrates to the gas exchange region of the lung [41]. Definition of the maximum size of respirable dust particles are given by the following expressions.

The BMRC definition for respirable dust [48] is given as follows :

$$SR\{BMRC\} = 1 - \left( \frac{d_{AE}}{7.07} \right)^2$$

The ACGIH [43] definition :

$$SR\{ACGIH\} = 1 - F(x),$$

and

$$F(x) = \int_{-\infty}^x \frac{dx}{\sqrt{2\pi}} e^{-x^2/2}$$

where

$$x = \frac{\ln(d_{AE}/\Gamma)}{\ln(\Sigma)}, \quad \Gamma = 3.5 \mu m, \quad \Sigma = 1.5.$$

Followed by Soderholm [40] proposed definition :

$$SR(d_{AE}) = SI(d_{AE})[1 - F(x)],$$

where

$$x = \frac{\ln(d_{AE}/\Gamma)}{\ln(\Sigma)}, \quad \Gamma = 4.25 \mu m, \quad \Sigma = 1.5.$$

where  $x$  is the dummy value used in calculating  $SR\{BMRC\}$ ,  $SR\{ACGIH\}$ , and  $F(x)$  where  $SR\{BMRC\}$  stands for sampling efficiency of an ideal collector (sampler) of the respirable fraction which was given by Orenstein [48],  $SR\{ACGIH\}$  stands for sampling efficiency of an ideal collector (sampler) of the respirable fraction which was given by ACGIH [43],  $SR(d_{AE})$  represents the sampling efficiency of an ideal collector (sampler) of the respirable fraction which was proposed by Soderholm [40],  $SI(d_{AE})$  is the sampling efficiency of an ideal collector (sampler) of the inspirable fraction (inhalable fraction) which was proposed by Soderholm [40] and  $F(x)$  is the cumulative probability function of a standardized normal random variable. A convenient algebraic expression for  $F(x)$  is given in the **Appendix A**. While  $d_{AE}$ , stands for particle aerodynamic diameter,  $\Gamma$  is a parameter with unit length which is sometimes used when calculating the thoracic or respirable fraction, and  $\Sigma$  is a unitless parameter which is sometimes used when calculating the thoracic or respirable fraction.

Both the BMRC and ACGIH definitions are based on the collection efficiencies of the samplers and the inlet efficiency when sampling is conducted. This is due to the unpredictability of the inlet efficiency of samplers with variation in



atmospheric conditions. Normally, great care is undertaken to minimize the effects of wind speed and orientation of the sampler with respect to the wind.

**Table 3.2** lists the proposed fractional values of the respirable dust with variation of particle aerodynamic diameters and collection efficiencies. Dust sampling instruments would need to have in order to sample the respirable fraction downstream of an ideal inspirable inlet or an ideal collector of the thoracic fraction. The proposed definition also specifies that 50% of ambient particles with an aerodynamic diameter of 4  $\mu\text{m}$  would be included in the sample [40].

**Table 3.2 : Proposed values of respirable fraction collected and the respirable fraction as a subdivision of inspirable and thoracic fraction.**

Particle aerodynamic diameter ( $\mu\text{m}$ )	Respirable fraction [SR]	Respirable as a subdivision of inspirable [SR]/ [SI]	Respirable as subdivision of thoracic [SR]/[ST]
0	1.000	1.000	1.000
1	0.971	1.000	1.000
2	0.914	0.968	0.968
3	0.739	0.805	0.805
4	0.500	0.559	0.562
5	0.300	0.344	0.351
6	0.168	0.198	0.208
7	0.090	0.109	0.122
8	0.048	0.059	0.072
9	0.025	0.032	0.044
10	0.013	0.017	0.027

\* Proposed by Soderholm [40].

The respirable concentrations ( $R$ ) of airborne particles is therefore calculated by integrating, over all particle aerodynamic diameters, the product of the differential size distribution and the sampling efficiency for each size [40]. In order to get the value of the respirable concentration using the BMRC definition, the proposed definition need to be multiplied by a factor of 0.67 and 1.0 for log-normal size distributions for which geometric standard deviation,  $\sigma_g > 2$  and for which at least 10 % of the ambient aerosol is respirable by the BMRC definition. The value of respirable concentration using ACGIH definition, it has to be multiplied by a factor of 1.0 and 1.3 for log-normal size distribution for which the geometric standard deviation,  $\sigma_g > 2$  with at least 10 % of the ambient aerosol being respirable by the ACGIH definition [40]. The choice of a function to define the respirable fraction is guided by the available sets of measurements of the deposition of airborne particles in

the head and tracheo-bronchial region of the lungs during inspiration through nose or mouth. Therefore, particles with aerodynamic diameters large enough to result in their being removed from the inhaled air by the conducting airways can be excluded from respirable fraction. In **Table 3.3**, the inhalable, thoracic, and respirable fractions given by ACGIH are listed.

**Table 3.3 : Inhalable, thoracic, and respirable fractions.**

Aerodynamic Diameter ( $\mu\text{m}$ )	Inhalable Fraction	Thoracic Fraction	Respirable Fraction
0	1.00	1.00	1.00
1	0.97	0.97	0.97
2	0.94	0.94	0.91
3	0.92	0.92	0.74
4	0.89	0.89	0.50
5	0.87	0.85	0.30
6	0.85	0.81	0.17
8	0.81	0.67	0.05
10	0.77	0.50	0.01
15	0.70	0.19	0.00
20	0.65	0.06	0.00
25	0.61	0.02	0.00
30	0.58	0.01	0.00
35	0.56	0.00	0.00
40	0.55	0.00	0.00
50	0.52	0.00	0.00
60	0.51	0.00	0.00
80	0.50	0.00	0.00
100	0.50	0.00	0.00

\* Given by ACGIH [49].

Nowadays, the new proposed definition of inspirable (inhalable) fraction, thoracic fraction, and also respirable fraction [40] has been accepted and widely use as the standard by many manufacturers for designing dust sampling instruments for the characterisation of airborne particulates. For example, *TSI*, an American based company has designed an instrument called the *RespiCon*, which is one of the highest sampling efficiency instruments for health-based particle-size-selective sampling. A further explanation on the instruments used will be discussed in Chapter 4.

### 3.2.2 Particle Deposition Mechanisms

In Chapter 2, a short review had been made of the airborne particulate deposition in the lungs together with the BMRC particle deposition conventions, in

relationship to the effect of dust inhalation on human health. However, in this chapter, it will be discussed in more detail to help understand the concept of how and why sampling instruments for the characterization of airborne particulates were design in the past, present, and will be in the future.

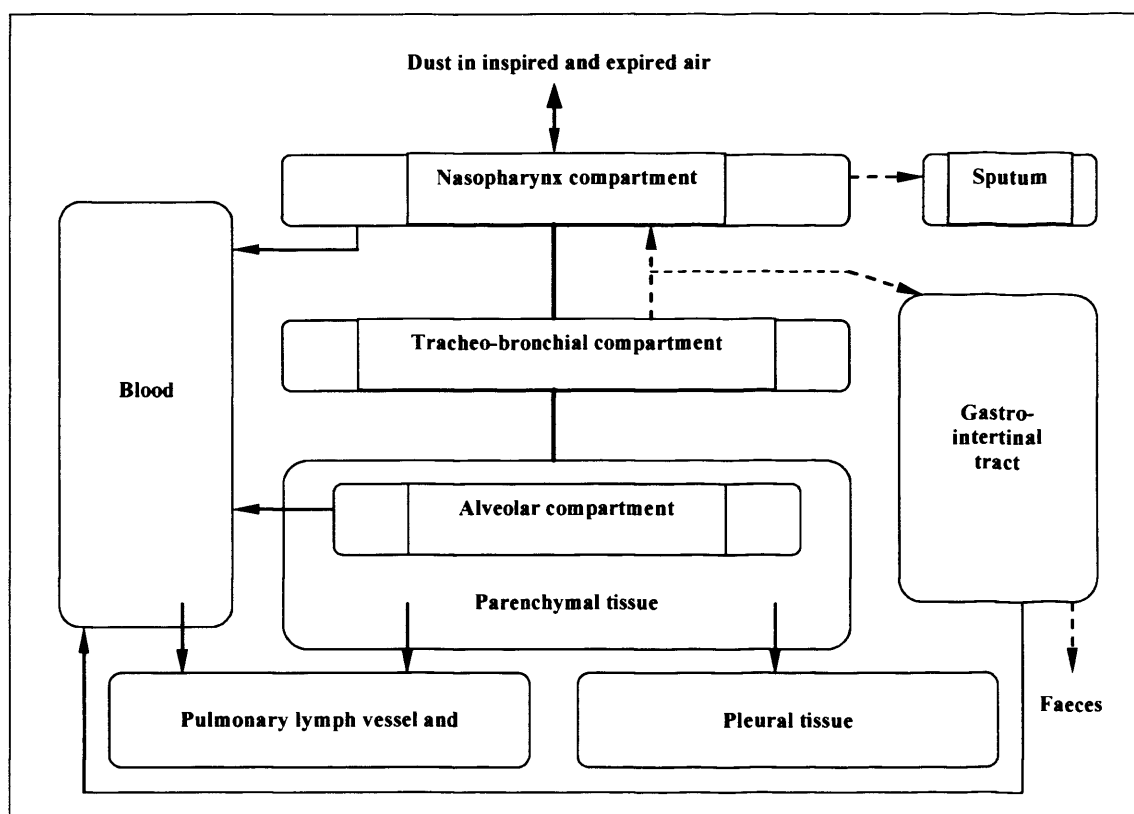
It has been stated [41] that particles which enter the human respiratory system vary in size depend upon their aerodynamic behaviour, deposition location and also their removal or relocation. Once located, the particulates elicit a response in the lungs, which relies on the nature and size of the particle. Other physical properties must also be taken into account i.e. the size distribution, density, shape, and surface area of particles, which influence their penetration into the respiratory tract and also their subsequent deposition in the conducting airways from nose to lung parenchyma. It is with these physical properties and the surface-chemical reactions they produce which, precipitate the magnitude of the biological response to the deposition and retention of particles in lungs. The size distribution of particulates is considered to be the most important parameter influencing their pathological potential.

According to some investigators [50], the site of the particle deposition and injury in the respiratory tract ultimately define the rates of clearance, and potential for retention or dissolution of particulates in respiratory tissues. Information has been gained using radio-labeled aerosols as surrogates for respirable particulates and spatial radiation detectors, which have been to gauge regional particle deposition and retention i.e. nasopharyngeal, tracheobronchial and pulmonary regions.

When inhalation takes place, airborne particulates are drawn into the airways of the lungs and are transported with the airflow deep into the lung. Once a particle touches the fluid lining of the airways, then it is said to have deposited and is not exhaled. Whether the particles deposits, or not, depends on its size, mass and also shape. Due to the heterogeneity of the tissue structure, it has been noted [51] that with the difference in cell types in different parts of the tracheo-bronchial tree, the site where the particles is be deposited will dictate the subsequent rate of clearance and, hence, the dose rate to that region of the lung. In addition, the cell types present will determine the cellular response and mode of any pathobiological response that will occur particles deposited in different locations will produce differences in health

effects. Authors [39,51] have noted that the extent and location of particle deposition depends on the particle density and morphology, airway geometry, and individual breathing patterns. A position agreed to by other works [40]. However, deposition characteristics may be quite different for others, such as children or people with respiratory disease. **Figure 3.3** showing the general scheme for deposition, clearance, translocation and retention of particles, derived from the International Commission Radiological Protection (ICRP) lung model.

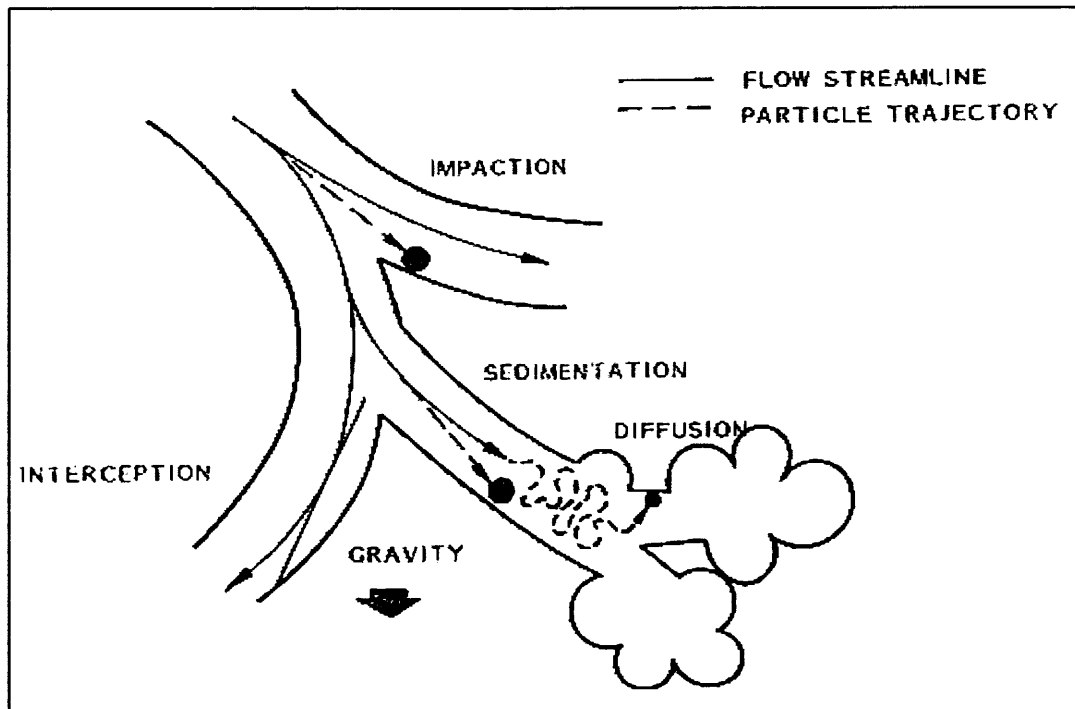
**Figure 3.3 : General scheme for deposition, clearance, translocation and retention of particles, derived from ICRP lung model. (Heavy arrows – deposition; light dotted arrows – clearance pathways; light arrows – translocation pathways).**



It has been proposed [39,50] that there are five depositional mechanisms for particles in the lung. These include inertial impaction, settling, diffusion, interception, and electrostatic deposition. The first three mechanisms are considered as the most important. The last two deposition mechanisms, are only considered important in certain situations. All the deposition mechanisms mentioned above are applicable for

all types of aerosol deposition in the lung. **Figure 3.4** illustrates the mechanisms of deposition.

**Figure 3.4 : Diagram Illustrating the Mechanisms of Particle Deposition in the Lung.**



### 3.2.2.1 Inertial Impaction

Inertial impaction is the mechanism of the particles moving down an airstream that suddenly, changes direction the particles carried by the stream will continue to travel in the inertial direction of the airstream for a short distance, and may encounter and impact on the surface [50]. The probability of impaction is therefore dependent on the particle's momentum, i.e. its mass and its velocity, and also on the aerodynamic forces acting on it [51]. Hence, the probability of impaction is also dependent on the particle's shape and its volume (or given mass and density). A greater mass and more compact shape will increase the probability of impaction as will the greater airflow speeds in the upper airways.

The effectiveness of this mechanism depends on the particle stopping distance and upon the airway velocities, which are comparatively low. Impaction is limited to the deposition of large particles that happen to be close to the airways walls. Nonetheless, the mechanism typically causes most aerosol deposition on a mass basis [39]. The greatest deposition by impaction typically happens at or near the first carina, the dividing point of the tracheal bifurcations. This is because the streamlines bend most sharply at bifurcations and pass close to carina.

### 3.2.2.2 Settling

While settling is the mechanism where the particles with densities greater than the air experience a downward force due to gravity [50]. These gravitational settling becomes a dominant deposition mechanism for particle with aerodynamic diameter,  $d_{AE} > 0.5 \mu\text{m}$ . It has been postulated [39] that, settling is most important in the smaller airways and the alveolar region, where flow velocities are low and airways dimensions are small such as in the distal airways (those farthest from the trachea). However, hygroscopic particles grow as they pass through the water-saturated airways, and this increase in size favours deposition by settling and impaction in the distal airways.

### 3.2.2.3 Diffusion

For particles with aerodynamic diameter,  $d_{AE} < 0.5 \mu\text{m}$ , gravitational settling is less important than deposition by diffusion or *Brownian movement* [51]. Diffusion becomes important for particles with geometric dimension that are of a dimension close to the mean free path of gas molecules. The diffusion mechanism relates to the random collisions between gas molecules and submicrometre-sized particles. It will push the particles in an irregular manner that is called *Brownian movement* [50]. *Brownian movement* [39] considered as the irregular wiggling motion or more known to be as a movement from side to side [52], of an aerosol particle in still air caused by random variations in relentless bombardment of gas molecules against the particle. Diffusion of aerosol particles is the net transport of these particles in a concentration gradient, from a region of higher concentration to a region of lower region. Also, diffusional deposition becomes more important as particle size decreases. A most

important factor is that particles will deposit on airways walls, especially in the smaller airways, where distances are short and residence times comparatively long [39].

#### **3.2.2.4 Interception**

Interception has been described [51] as the situation where a particle's trajectory, defined or calculated for its central point, would escape contact with an adjacent surface, but some extremity of the particle would make contact. For deposition in the respiratory tract, this is an important consideration for elongated particles such as fibres as suggested by [50], but is negligible for compact particles that are small (generally  $< 10 \mu\text{m}$ ) compared with the smallest airways with diameters of  $100 \mu\text{m}$ .

It has also been proposed [39] that interception also depends on the proximity of the gas streamlines to the airway surface and on the ratio of particle to airway diameter, which is usually small even in the smallest airways. Although fibers may be very large in one dimension, they may have small aerodynamic diameters. Long fibers can readily traverse the tortuous path to the small airways, where they have a high likelihood of interceptive deposition.

#### **3.2.2.5 Electrostatic Deposition**

Electrostatic deposition, may be an extremely important mechanism in the deposition of dust in the lung, but its effect is difficult to quantify because it requires knowledge of the charge on the particle surface [39]. Electrostatic deposition is often neglected unless the charge on the particle or on the fibre surface can be quantified. When particles are charged, they tend to be attracted to oppositely charged particles by coulombic attraction. A neutral particle also can be attracted to a charged particle by induction. These situations will occur when the electric field created by the charged particle induces a dipole, or charge separation, in the particle. In the nonuniform field around the neutral particle, the near side of the particle experiences an attractive force that is greater than the repulsive force on the far side; hence a net force exists in the direction of the charged particle, and the neutral particle migrates in

that direction. The charged particle produces an equal and opposite charge on neutral particles surface and thus creates its own field of attraction. Theories on particle collection, by other charged surfaces, and charged particles have been extensively reviewed [53].

### 3.2.3 Lung Structure and Airflow in the Lungs

The respiratory system has been studied extensively in humans, and also in rats, because of the importance of dosimetry for interpreting toxicological data on the effects of particles. Although humans and animals, such as the rat, are obviously very different in overall size, but the dimensions of the terminal airways and the aveoli are similar [51]. However, it has been noted [54] that, the structure of the bronchial tree is markedly different, with humans having an approximately symmetrical pattern (bipodal) with each bronchus dividing into two approximately equal daughter bronchi at similar angles to the parent, whereas rodents have a clearly asymmetrical pattern (monopodal) with single daughters separating at a greater angle. Although these differences are quite marked, the size of particles which reach rodent and human lungs are relatively similar [55]. This remarkably small difference in deposition is due to the changes in scale of the respiratory systems, which have largely counteracting and counterbalancing effects, with the main parameters affecting deposition, airways diameter, breathing rate, etc.

The nature of airflow has important consequences for several mechanisms of deposition of particles. When the air passes deeper into the lung during inspiration, it is travelling towards a “blind-end” through ever-narrower tubes, and the flow of air will start to slow down to zero by the time it reaches the terminal bronchioles [54]. The flow through the airways may be laminar, where dominating forces in the fluid are viscous, or turbulent where inertial forces dominate the flow. The regions corresponding to these different flow types are assessed by *Reynolds number*, which is the ratio of inertial to viscous forces. The *Reynolds number* is proportional to airways diameter and air velocity, so it decreases as the flow passes beyond the first few generations of bronchi, as both velocity and airway diameter decrease. Consequently, inertial forces would be expected to determine deposition of particles of large enough



size in the upper airways, and at slow or zero airflow in the lung periphery, diffusion will dominate deposition.

#### **3.2.4 Particle Types and Sizes Deposited in the Lungs**

Once deposited, particles will be retained in the lung for a certain periods, depending on their physicochemical properties, their location within the lung, and type of clearance mechanism involved [39]. The airway surfaces of the first two respiratory regions, the head and lung airways, are covered with a layer of mucus that is slowly propelled by ciliary action to the pharynx, where subconsciously swallowed to the gastrointestinal tract. This mucociliary escalator transports particles deposited in the airways out of the respiratory system within a few hours. This clearance mechanism can be accelerated by low doses of irritating gases or aerosols, or it can be slowed by high doses of such materials or by overloading with particles. Because of its gas exchange function, the alveolar region does not have this protective mucus layer. Hence, insoluble particle deposited in this region are cleared very slowly, over a period of months or years. It has been proposed [39] that dissolved particles pass through the thin alveolar membrane into the bloodstream. Solid particles may dissolve slowly or be engulfed by alveolar macrophages (phagocytic cells) and dissolved or transported to lymph nodes or mucociliary escalator. While for fibrogenic dusts, such as silica, interfere with this clearance mechanism and cause gradual scarring or fibrosis of the alveolar region. It showed that, difference types of particles will have different types of clearance mechanism in the lungs depends on the location where it was deposited as mentioned earlier.

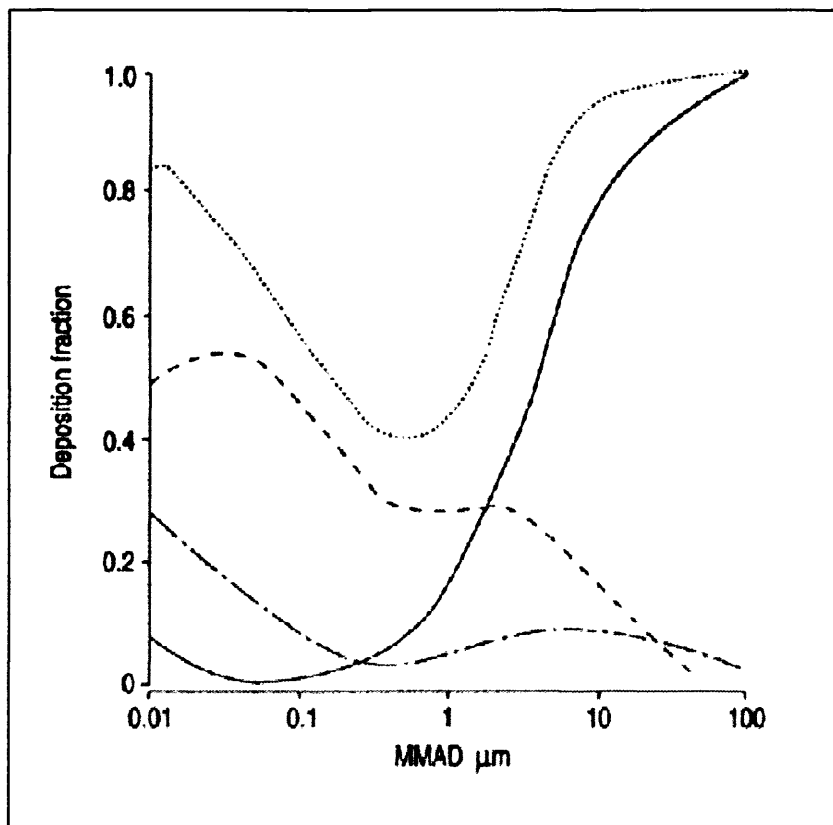
The actual size of airborne mineral particles, which are capable of penetration and deposition in the various compartments of the respiratory system is extremely difficult to predict because of the heterogenous nature of particles formed by different minerals when they are mechanically produced.

In order to estimate regional deposition of inhaled particles in the lungs, a reliance is placed upon theoretical models. These have been produced employing anatomical detail of the lung relating to the size of conducting airways and

physiological factors including breathing patterns, airflow dynamics, temperature, and humidity in the respiratory tract.

Models have also assumed that particles inhaled were insoluble spheres with a density of  $1 \text{ gm/cm}^3$ . These parameters are used extensively to compare the motion of airborne particulate materials in a description referred to as aerodynamic equivalent diameter. The concept of aerodynamic behaviour is the most useful one of relating the physical nature of particles to their deposition. The aerodynamic behaviour of particles is generally described as the “aerodynamic diameter” ( $d_{AE}$ ), defined as being the diameter of a sphere with the same density of water (“unit density”,  $1 \text{ gm/cm}^3$ ) mentioned earlier, and the same gravitational settling speed as the original particle [51].

**Figure 3.5 : Average deposition model for normally distributed (log) aerosols with given mass median aerodynamic diameters (MMAD). The results are calculated for tidal volumes of 750 mL at 15 breath/min. The deposition fraction is relative to the aerosol inhaled at nose. ·····: inhalable ———: extrathoracic; ———: respirable; - - - : tracheobronchial. Modified from the Task Group on Lung Dynamics, 1966 [51].**



This settling speed is determined by an equilibrium between gravitational force (proportional to density multiplied by volume) and the aerodynamic resistance (proportional to particle diameter multiplied by the square root of density). That is, the spherical particle diameter,  $d_l$  and spherical particle density,  $\rho_l$  has an aerodynamic diameter of :

$$d_{AE} = d_l \sqrt{(\rho_l / \rho_0)}$$

where  $d_{AE}$  is an aerodynamic particle diameter and  $\rho_0$  is unit density ( $1 \text{ gm/cm}^3$ ).

**Figure 3.5** shows a conventional model of the deposition characteristics of variously sized inhaled particles in different parts of the respiratory system.

### 3.2.5 Human Respiratory Patterns

The respiratory flow rate during inspiratory and expiratory phase of breath cycle influence the particle deposition by velocity-dependent mechanisms [50], i.e. inertial impaction, which usually occurs for particles with diameters larger than  $3 \mu\text{m}$ . For particle with diameters  $< 3 \mu\text{m}$ , time-dependent mechanisms such as sedimentation and diffusion are the most significant mechanisms for deposition of particles. Thus, the respiratory pattern (depth of tidal volume and breathing rate) has a strong influence over the size of the particle that deposits, the regional location of deposition, and mechanisms that favour deposition in the respiratory tract. Physical activity with attendant changes in the breathing pattern affects particle deposition. In other reviews of this subject, people who had more physical activity outdoor are more exposed to the health effects especially for the critical groups of age and also with critical illness i.e. children, people with chronic disease, older people, etc [26]. These groups of people, are more prone to inhale more particulates as their breathing rates are increased while performing sport activities outdoor. As a result, it will increase the percentage of particles deposited in the lungs.

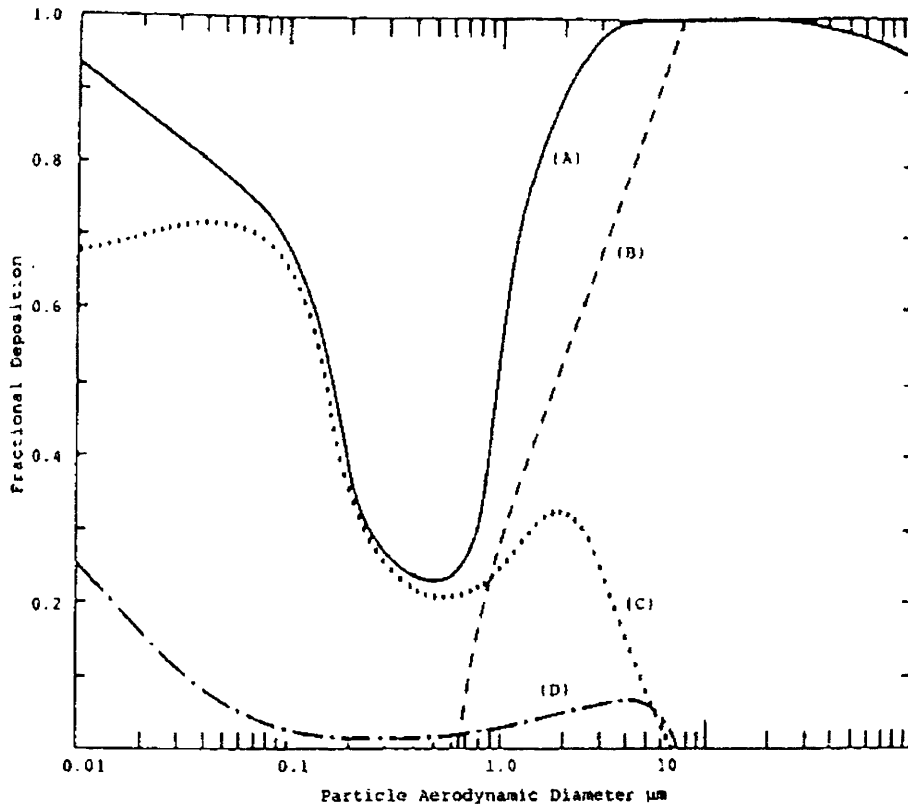
### 3.2.6 Regional Fractional Deposition of Inhaled Particles

The most well-known model of fractional regional deposition with respect to particle size in the lungs is that produced by the International Commission on Radiological Protection (ICRP) Task Group on Lung Dynamics. Their estimations for regional fractional deposition of inhaled unit density spherical particles is illustrated in **Figure 3.6** for standard breathing conditions of 15 breaths per minute and a tidal volume of 1.45 liters.

It is a basic fact that the potential health effect from the inhalation of airborne mineral particles will depend upon which locations in the respiratory tract they are deposited. Location of particle deposition in either conductive airways or the pulmonary gas exchange regions of the lung will effect either their translocation to other sensitive cells and areas, or their clearance from the lungs. Particles of different aerodynamic sizes will therefore have the potential to react with different tissues and their biological potential to cause disease must then be considered independently.

As for the fractional deposition of fine and ultrafine particles, they are deposited by sedimentation or impaction whilst ultrafine particles are expected to be deposited in the lung by diffusion [51]. Although the total lung deposition values are generally comparable for ultrafine *versus* fine or coarse particles [52], it is likely that the regional deposition will vary between ultrafine and the larger particles. From **Figure 3.4**, it can be seen that particles with median diameters  $< 0.1 \mu\text{m}$  would have a deposition fraction of  $\sim 50\%$  in the respiratory zone. However, particles with  $10 \mu\text{m}$  median diameter would have a deposition fraction  $< 20\%$  in this region. Figures for deposition of ultrafine particles in human volunteers have been reported [57]. For a range of particles in the ultrafine size range ( $0.04\text{-}0.10 \mu\text{m}$ ), a peak deposition fraction of 10-30% occurs in the lung regions, which encompass the transition zone between the conducting airways and the alveolar region. Moreover, this peak deposition fraction increases with decreasing particle size within the ultrafine size range. Thus, far from being breathed out, as is sometimes erroneously believed, very small particles deposit in the lungs more than large coarse particles [57].

**Figure 3.6 : Fractional deposition of inhaled spherical particles in various compartments of the lung predicted by the *International Commission on Radiological Protection Task Group on Lung Dynamics*. (A) Total deposition in the respiratory tract; (B) Nasal deposition; (C) Pulmonary deposition; (D) Tracheobronchial deposition.**



### 3.2.7 ISO Health-related Particle Sampling Conventions

Depending on the aerodynamic diameters,  $d_{AE}$  and air flow characteristics in the lung, particles will deposit in different regions of the respiratory tract. Particles of different size will therefore produce different adverse effect in the lung when deposited. Occupational hygienists have developed the *International Standards Organizations (ISO) Conventions* to show the quantitative relationships between particle aerodynamic diameters,  $d_{AE}$  and the fraction of particles penetrating to the different regions of the respiratory tracts under average conditions. These fractions are defined in **Table 3.4** and as referred to graphically in **Figure 3.7**. These conventions describe the aerodynamic size fraction of airborne particles that should be collected using a sampler with these specified conventions. The conventions provide rational specifications for health-related sampling instruments that allow correlations between

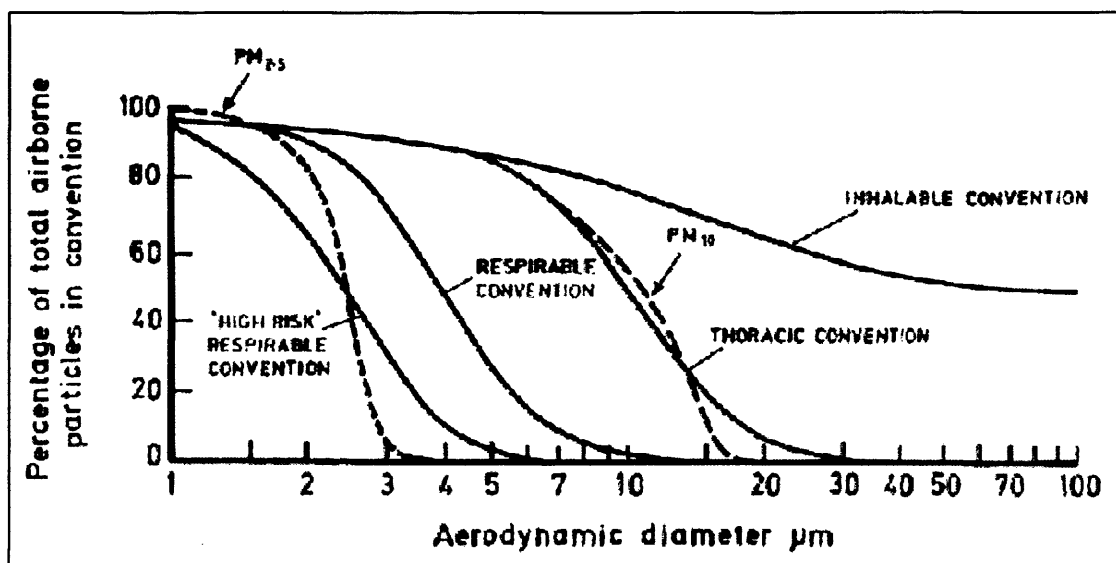
airborne particle concentration and health effects [52]. In considering particles that might impact on asthma, the thoracic fraction should be sampled since asthma is a disease of the airways [51]. Particles important in producing diseases of the lung parenchyma, such as silicosis, are best sampled using the respirable convention, since the fraction is small enough to penetrate to the alveolar region if asthma is of concern a disease of the airways then the thoracic sampling convention should be employed. These conventions are the most useful guidelines for sampling and relating airborne particles to specific health effects.

**Table 3.4 : Mass deposition fractions according to the International Standards Organization (ISO).**

ISO convention	Mass Fraction
Inhalable	Inhaled through the nose or mouth
Extrathoracic	Failing to penetrate beyond the larynx
Thoracic	Penetrating beyond the larynx
Tracheobronchial	Penetrating beyond the larynx but failing to penetrate to the unciliated airways
Respirable	Penetrating to the unciliated airways

\* From ISO [42].

**Figure 3.7 : Curves defining inhalable, thoracic and respirable particle fraction.**



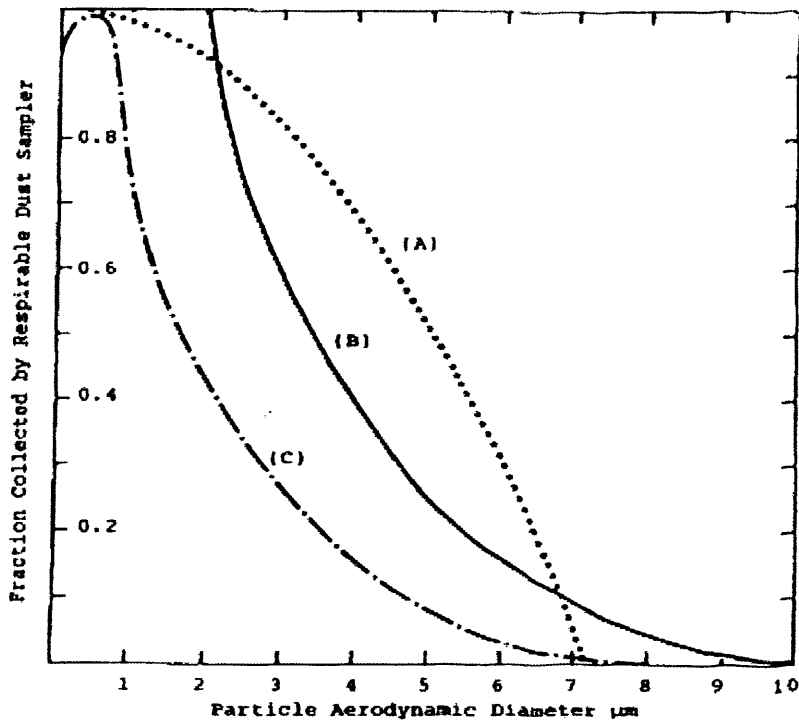
The sampling conventions with 50% sampling efficiency for particle with aerodynamic diameters of  $<2.5 \mu\text{m}$  ( $\text{PM}_{2.5}$ ) and  $<10 \mu\text{m}$  ( $\text{PM}_{10}$ ), are the global environmental standards for measuring the mass of airborne particles [16]. The  $\text{PM}_{10}$  sampling convention approximates to the ISO thoracic convention whilst the  $\text{PM}_{2.5}$  convention corresponds approximately to the ISO respirable convention.

The total mass concentration of dust in the air does not usually have a meaningful correlation with the incidence of respiratory disease. However, measurement of inhalable, thoracic and also respirable dust particles in air by aerodynamic fractions have been found to correlate more closely to the incidence of respiratory disease than those of total dust in air. In the former case, measurements relate to the finer which is dust fraction most likely to deposit in the pulmonary regions of the lung, while in the later case, measurements of total airborne dusts are more closely linked to larger particles which do not reach the deeper lung to cause pulmonary disease.

The criteria employed for defining the sampling of the finer fractions of airborne dust particles were conceived as representing the size classification that occurs in the upper respiratory tract during breathing. The equipment developed in the U.K. by the British Medical Research Council (BMRC) was based upon the ability of particles to penetrate a horizontal parallel plate elutriator, known as MRE respirable sampler. It was designed to cut all particles with an aerodynamic diameter,  $d_{\text{AE}}$ , larger than approximately  $7 \mu\text{m}$ . While in U.S.A. a small cyclone separator with aerodynamic cut size (50%) equivalent to  $3.5 \mu\text{m}$  aerodynamic diameter,  $d_{\text{AE}}$ , was chosen for the respirable dust sampling.

The curves representing the proportion of respirable dust particles of different sizes capable of penetrating the devices are given in **Figure 3.8** together with the proportion of particles capable of penetration and deposition to the pulmonary regions of the lung predicted by the ICRP Task Group on Lung Dynamics. The sampling results obtained with the cyclone device produced a basic result, which was modified by the American Conference of Governmental Industrial Hygienists (ACGIH) to represent their recommended aerosol sampling curve to define respirable airborne fractions of dust.

**Figure 3.8 : Fraction of airborne dust collected by sampling device vs. particle aerodynamic diameter based on (A) *British Medical Research Council* recommendations, (B) *American Conference Governmental Industrial Hygienists* recommendations, (C) Predicted efficiency of pulmonary deposition based on the *International Commission on Radiological Protection Task Group on Lung Dynamics*.**



The curves represented in **Figure 3.8** are employed extensively in environmental control, inhalation toxicology and risk assessment of exposure to airborne particulates materials. However, they do not refer directly to the physical characteristics of airborne dust particles produced by specific minerals and materials, and the variations that may exist between actual respirable size fractions of similar materials. They have also not been correlated with the actual size of airborne particulate detected in lung tissue samples. Mainly, because of the difficulty of assessing irregular shapes of particle.



### 3.3 Conclusion

It has been established that many factors need to be considered when designing dust particulate sampling instruments, for risk assessment and occupational-health sampling purposes. In defining inhalable, thoracic, and respirable dust fractions, aerodynamic particle size has been used extensively to characterize the size distribution of fine particles (i.e. the respirable dust fraction), which are capable of penetrating the human lung and may cause lung diseases. The conventions representing the size ranges of particles, which may be inhaled and their deposition efficiency in the various compartments of the lung have all been derived theoretically with no reference to real particulate dimensions. Several conventions have been proposed and these include the British Medical Research Council (BMRC), International Standards Organization (ISO), American Conference of Governmental Industries Hygienists (ACGIH) and also the International Commission of Radiological Protection (ICRP) convention. No concerted attempt has been made in the past to compare actual with theoretical size distributions of inhaled deposited and retained airborne particulates. In this thesis an attempt has been made to alter this situation.

## CHAPTER 4 : METHODS, MATERIALS, AND APPARATUS

### 4.1 Introduction

Characterisation of airborne particles involves an investigation of their physical and chemical properties. This information on particles is required to estimate the possible influence these may have on human health and the environment. For physical characterization, the mass concentration, number airborne concentration, size distribution, and morphology of particles are important parameters to monitor in order to estimate the health hazard relating to such particles. The chemical characterisation of particles, including their elemental composition and structure, are important in determining the subsequent biological response once particles have entered the body.

The main objective of airborne particulate characterisation is to gain a better understanding about the toxicological and pathological effects of dust inhalation. Fine and ultrafine particulates, can be transported very readily over long distances by the weather from the sources where they were generated [16]. They can be inhaled and retained in lungs and they are more hazardous towards human health than the large Aeolian particles. At very low mass concentrations, they can produce pathological effects because of their large number per unit volume and also their extremely high surface area / volume ratio [10]. Overall, characterizations of airborne particulates is therefore very important in the study of environmental health problems associated with dust inhalation.

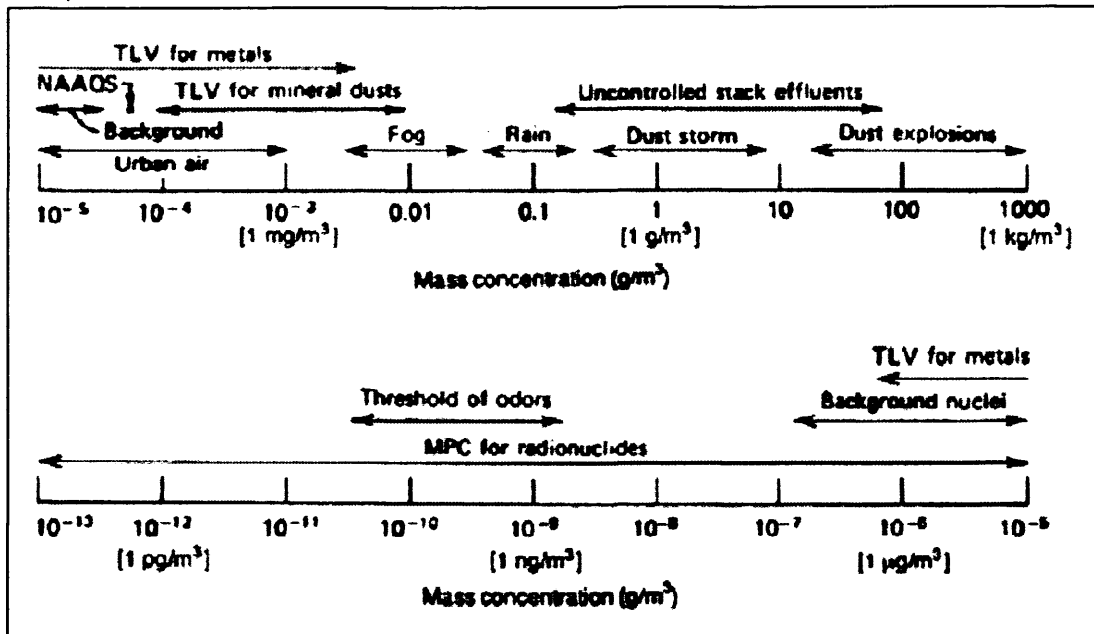
Mass concentration of particles per unit volume of air is recognized as one of the most easily measured aerosol properties. It is defined in common units such as  $\text{g}/\text{m}^3$ ,  $\text{mg}/\text{m}^3$ , and  $\mu\text{g}/\text{m}^3$ . Even though mass concentration is equivalent to the density of the ensemble of aerosol particles in air, density is not used to define dust concentrations because of possible confusion with true particle density [39]. Number concentration is defined as the number of particles per unit volume of aerosol, usually given as  $\text{number}/\text{cm}^3$  or  $\text{number}/\text{m}^3$ . An older unit expressed dusty conditions in terms of million of particles per cubic foot (mppcf). Normally, bioaerosol particles and fibres concentration are stated in terms of number concentration [39]. Volume ratio or

mass ratio or parts per million (ppm) are not used to describe aerosol clouds due to the two distinct phases that are involved and aerosol concentrations are numerically very low when expressed in this manner.

At present, mass concentration and number concentration are the terms most widely used around the world, with terms such as the U.S.  $PM_{10}$  annual average values. Occupational exposure limits for nuisance dusts are sometimes used to define exposure conditions from uncontrolled emissions for control purposes as shown in **Figure 4.1** and they refer to the concentration of dust that may be hazardous. Measurement of particulates concentration is conducted in both the indoor and outdoor environments. Most particulate collection is conducted using a direct measurement, known as gravimetric analysis [39]. Various filters are used in integrating particle mass overtime to give average aerosol concentrations over a period ranging from minutes to hours and may sometimes days. These are known as TWA values (Time Weighted Average). The number concentrations of most aerosol clouds normally decrease with increasing particle size as shown in **Table 4.1**. With mass and number concentration values, the information obtained is used for provision of information on current concentrations of air pollution. This provides the means to evaluate whether air pollutant concentrations exceed health-based standards and guidelines, and estimate public health impacts. The data is used to provide information to the public and is the basis on which to implement short-term remedial strategies and long-term plans to improve air quality. It is also a means of determining trends in air pollution and the effectiveness of control strategies. Mass and number concentration information has been used widely in producing various reports from both the environment and health related governmental agencies, and industries around the world.

In Chapter 3, particle size was established as the most important parameter to define the hazardous nature of a dust, but it is rarely monitored on a routine basis. What is more usually performed when sampling dust clouds is the size selective collection of particles for mass concentration determination and collection of respirable, thoracic, inhalable dust fractions or total suspended particulates (TSP).

Figure 4.1 : Range of aerosol concentrations.



\* From Hinds [39].

Table 4.1 : Relationship Between Size / Number and Mass Concentration.

	Typical Diameter ( $\mu\text{m}$ )	Number Concentration (Molecules or Particles / $\text{cm}^3$ )	Mass Concentration ( $\mu\text{g}/\text{m}^3$ )
Gas molecules	0.0005	$2.45 \times 10^{19}$	$1.2 \times 10^9$
Aerosol particles			
Small	<0.2	$10^3$ - $10^6$	<1
Medium	0.2-2.0	$1$ - $10^4$	<250
Large	>2.0	<1-10	<250
Hydrometeor particles			
Fog drops	10-20	1-500	$10^4$ - $10^6$
Cloud drops	10-200	1-1000	$10^4$ - $10^7$
Drizzle	200-1,000	0.01-1	$10^5$ - $10^7$
Raindrops	1,000-8,000	0.001-0.01	$10^5$ - $10^7$

Date are for typical lower tropospheric conditions.

\* From Jacobson [11].

In understanding the types of chemical compounds, especially the fine and ultrafine particles, which can be deposited in the deepest part of human lungs, researchers, scientists, and the public, have gained new and updated knowledge such as the source location, possible health effects of dusts, precautions can then be made to reduce the pollution.

In this chapter, the methods, materials and apparatus that were employed to investigate mass and size of airborne particles are discussed. The apparatus was selected to represent a range of dust sampling instruments, which are employed to monitor pollution in ambient or occupational environmental situations. They represent equipment that is capable of collecting total or size selective samples by a variety of means. To compare the performance of these instruments and methods, experimental dust clouds of compact and fibrous particles were generated in an environmental chamber and also by dust generation in a confined dust propagator when dust particles were considered to be hazardous.

Dust samplers were assessed by a variety of techniques, including weighing, sizing, counting, and the data obtained analyzed. This allowed a performance comparison of instruments to be made. The results between instrumental sampling a biological sample and theoretical predictions of hazardous dust sizes were also performed.

## **4.2 Description and Operation of Airborne Sampling Instruments**

### **4.2.1 The Casella MRE Sampler**

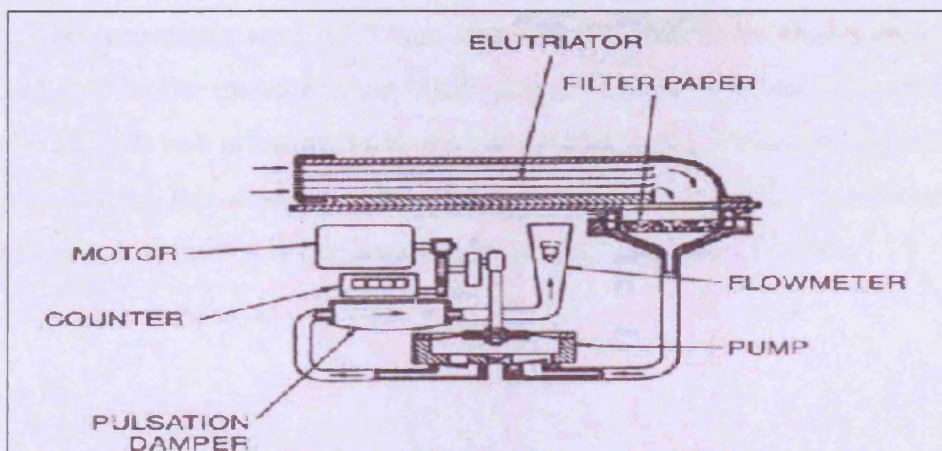
A Mining Research Establishment (MRE) sampler was employed to obtain respirable dust samples using Milipore filters of size 56 mm diameter. The MRE sampled at a flow rate of 2.5 Litre per minutes (L/min). The MRE sampler is a respirable sampler employing a horizontal elutriator concept [39; 58] as illustrated in **Figure 4.2a and b**.

**Figure 4.2a : The Casella MRE sampler.**



The horizontal elutriator can be used [39; 58] either as a separator to size fractionate an aerosol stream or as an aerosol spectrometer to measure the distribution of particle size. For separation, an aerosol is passed at low velocity through a horizontal duct having a rectangular cross section (referred to Figure 4.2b). Particle settling perpendicular to the gas streamlines. Particles reaching the floor of the duct are removed from the aerosol stream. This situation is viewed as an attenuation in particle concentration that is greater for larger particles than for the smaller ones.

**Figure 4.2b : Schematic Diagram of MRE sampler.**



\* Source : Hinds [39].

Operation instructions for the MRE sampler :-

1. Three weights of filter were taken using a calibrated balance. The filter was then inserted into a metal holder and inserted into the MRE sampler. The filter paper and holder were screwed into place at the exit of the elutriator before the start of sampling. The weight accuracy of filters and dust were recorded to 5 decimal points.
2. Then, the sampler was placed inside the environmental dust chamber, which was sealed. Limestone dusts were generated for various periods. This was followed by sampling periods of various lengths.
3. After sampling, three consecutive weights of the filter were recorded.
4. With the average weight before and after sampling, the mass of limestone dust was obtained, mass concentration values were calculated and recorded in  $\text{mg/m}^3$ .

#### 4.2.2 The Cyclone Sampler

The cyclone sampler has evolved with a similar function to the MRE to sample respirable dust. A cutaway illustration of the cyclone sampler is given in **Figure 4.3a** and **b**. The instrument uses a 25 mm diameter type of filter. Dust samples were collected in a similar manner to the MRE sampler. The sampler operates with a flow rate of 2.2 L/min and is known to be the most widely used device for respirable dust sampling. During this study, a comparison of results of operating the instrument at five different flow rates was performed to investigate sampling efficiency.

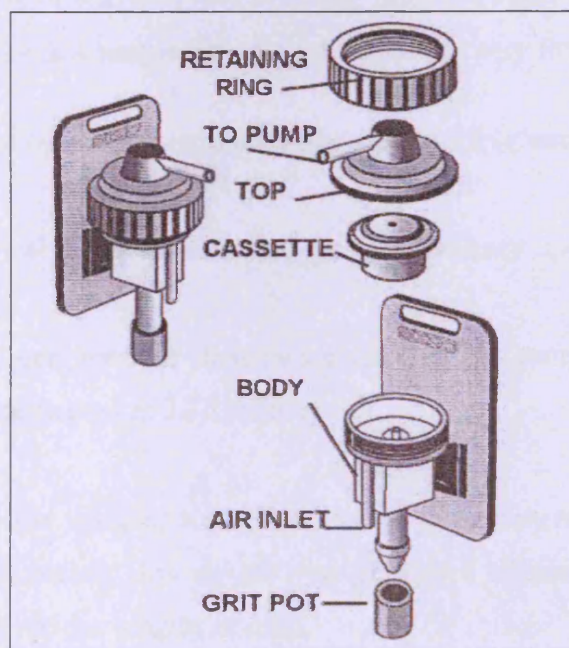




**Figure 4.3a : The Cyclone sampler.**



**Figure 4.3b : Schematic Diagram of Cyclone Sampler.**



\* Source : SKC [59].

Below are the operation instructions for cyclone sampler :-

1. Filter were weighed 3 times before use with accuracy up to 5 decimal points.
2. Cyclone sampler was then connected with its pump and the flow rate through the device set at 2.2 L/min.



3. The cyclone sampler was placed in the environmental dust chamber and the door was sealed. Dust clouds were generated for several minutes followed by sampling for various lengths of time.
4. After sampling, the filtered dusts were again weighed 3 three times.
5. The average weighed before and after the sampling of dust were calculated and mass concentration values were determined in  $\text{mg}/\text{m}^3$ .

#### **4.2.3 The Seven Hole Sampler**

The Seven Hole sampler is known as a total inhalable sampler. It is illustrated by **Figure 4.4a** and **b**. It also employs a 25 mm filter to collect dust at a flow rate of 2.0 L/min. This device is a simple filter holder which has very little design input.

Below are the operation instructions for a Seven Hole sampler :-

1. Filters were weighed 3 times before use with accuracy up to 5 decimal points.
2. Seven Hole sampler was then connected with its pump and the flow rate through the device set at 2.2 L/min.
3. The Seven Hole sampler was placed in the environmental dust chamber and the door were sealed. Dust clouds were generated several minutes followed by sampling for various lengths of time.
4. After sampling, the filtered dusts were again weighed 3 three times.
5. The average weighed before and after the sampling of dust were calculated and mass concentration values were determined in  $\text{mg}/\text{m}^3$ .

**Figure 4.4a : The Seven Hole sampler.**

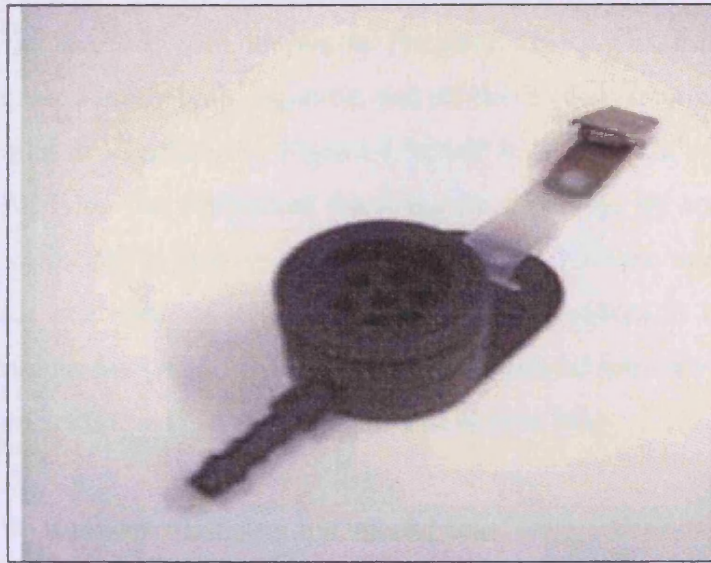
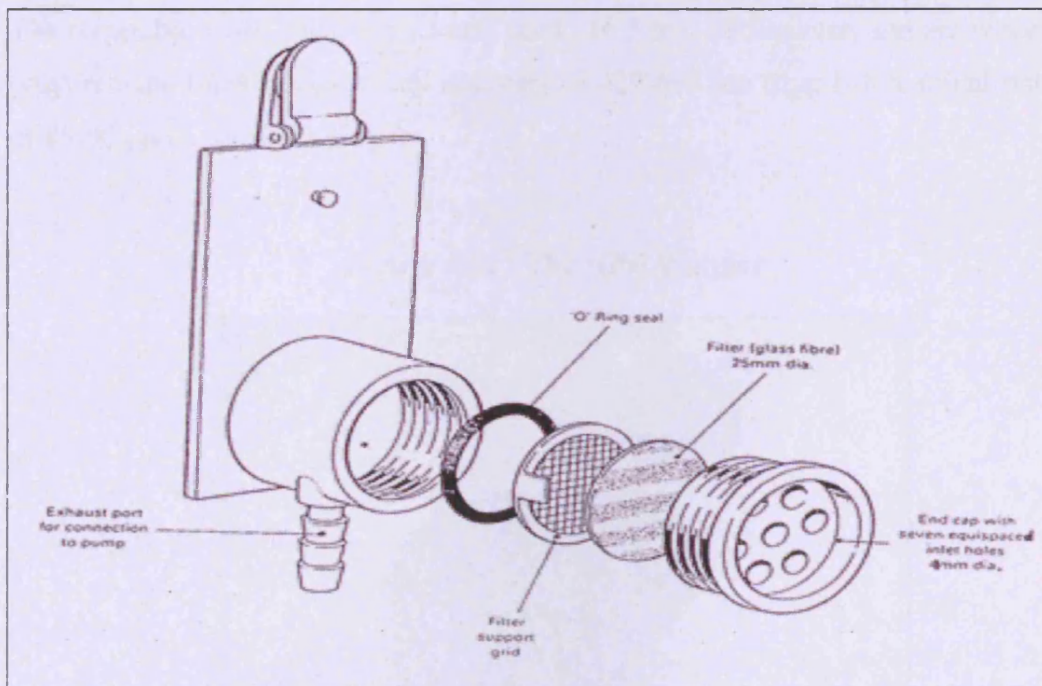


**Figure 4.4b : Schematic Diagram of Seven Hole sampler.**



\* Source : MDHS 14 [60].



#### 4.2.4 The IOM Sampler

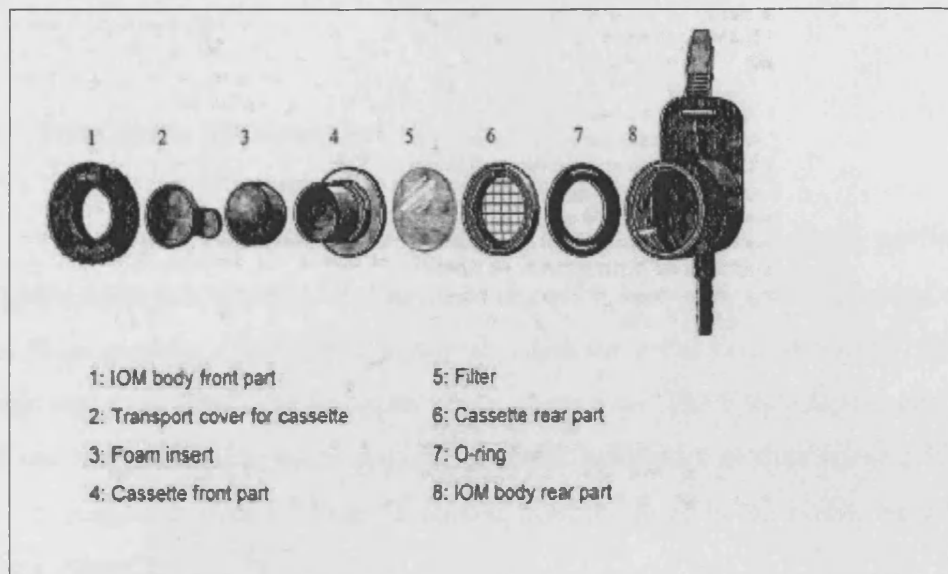
The IOM sampler, also known as the Institute for Occupational Medicine (IOM) sampler, can sample both respirable and inhalable (dual-fraction) dust fractions in a single sampler as illustrated by **Figure 4.5a and b**. Its also can be used to capture thoracic dust fraction. The individual fractions are separated by employing porous sponge inserts calibrated to remove non respirable or non thoracic sized particles. The advantage of the dual-fraction version is that it is not required to handle the foam insert during analysis by weighing. The cassette is separated into two halves, with the foam in the front portion and the filter in the final portion [61].

The IOM sampler used was the plastic type produced by SKC, Inc., of the USA. The filters used were the same as those employed in the Seven Hole sampler and the cyclone sampler, that is the 25 mm diameter. The flow rate needed to operate the IOM sampler is 2.0 L/min. The IOM sampler consists of a cassette, filter, head and foam. The white foam was used to sample respirable and inhalable dust particulates. The respirable foam plugs are 12 mm thick, 16.5 mm in diameter, and are made with polyurethane foam having a cell diameter of 420-460  $\mu\text{m}$  (that is a nominal porosity of 85-90 pores per inch) [61].

**Figure 4.5a : The IOM sampler.**



**Figure 4.5b : Schematic Diagram of IOM Dual-Fraction Dust sampler and the Components of the Foam Cassette.**



\* Source : SKC [59].

For the measurement of the mass concentration using the IOM sampler, the filter, the lightweight cassette and also the foam are weighted together so that any particles that deposit in the inlet are included in the sample weight.

Below are the operation instructions for the IOM sampler :-

1. The filter together with the cassette were weighed 3 times. After inserting the foam, a further 3 readings of weight were obtained with an accuracy taken were up to 5 decimal places.
2. The IOM sampler was then connected to a personal pump and the flow rate set at 2.0 L/min.
3. The IOM sampler was placed in the environmental dust chamber and the door were sealed. Dust clouds were generated several minutes followed by sampling for various lengths of time.
4. After completing the sampling, filter, cassette and the foam were again weighed 3 times.



5. With the average weigh before and after the sampling of limestone dusts were obtained, the mass concentration value were calculated in  $\text{mg}/\text{m}^3$ .

#### 4.2.5 The Casella CIS Sampler

The Conical Inhalable sampler (CIS) is another inhalable sampler as illustrated by **Figure 4.6a**. It is capable of sampling inhalable dust to give similar results as the Seven Hole sampler. The CIS sampler also has the capability to sample inhalable, thoracic and respirable dust fractions at the same time. The CIS sampler used  $\text{PM}_{2.5}$ ,  $\text{PM}_{10}$  and respirable samples to produce different categories of dust particle fractions. The CIS sampler utilizes a 37 mm fibreglass filter mounted in reloadable cassette with the flow rate of 3.5 L/min.

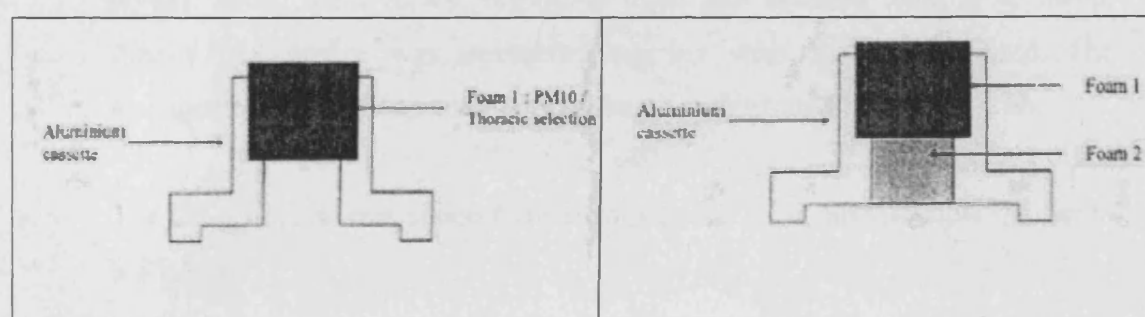
**Figure 4.6a : The Casella CIS sampler.**



There are two ways of measuring an inhalable dust fraction with this device. The first uses the filter, cassette and the cover with holes as shown earlier, while the second uses the filter, cassette holder, respirable foam and thoracic foam. For the second method, a different cassette holder is used as this cassette can hold both respirable and thoracic foam as illustrated by **Figure 4.6b**. Before starting to use the foam, it needs to be cleaned using the sonic water shaker. The twin foam respirable

PUF selectors are used to sample the respirable fraction, which is collected on the filter, while the thoracic fraction is collected by the filter and both foams together [62]. The inhalable fraction is determined by weighing (or otherwise analysing) both the filter and the foams. In inserting the foams, clean, sterilized, tweezers and plastic gloves are to be used if they are to be chemically analysed following sampling.

**Figure 4.6b : Cassette Holding a Foam for PM<sub>10</sub> / Thoracic (Left) and Cassette Holding a Twin Foam of Thoracic (Foam1) and Respirable (Foam 2)(Right).**



\* From Li and Lundgren [61].

The weight losses for the CIS sampler holders were found to be [63] typically greater than those for the IOM plastic cassette. Therefore, the accuracy of the weight of dusts sampled by the CIS sampler is lower than the IOM sampler.

In removing the foam after sampling, the foam or the PUF plugs from their cassettes prior to analysis, clean, sterilized, tweezers and plastic gloves should be used to remove them. Where the two foams are used in the same cassette, as in respirable sampling, then the foams should be extracted in opposite directions to reduce cross contaminations of the fractions.

Below are the operation instructions for the CIS sampler (inhalable, thoracic and respirable sampling simultaneously) :-

1. The foam treatment process took approximately 10 times their volume of distilled water and the twin foams were cleaned separately using an ultra sonic water bath for 20 minutes. The foams were thoroughly rinsed in

approximately 10 times their volume of distilled water for further 3 times before being dried at 70°C for 24 hours. Then the clean foams were stored in a clean desiccator. Before start taking the foams from the desiccator, the desiccator need to be open for few minutes with the purposes to expose the foams to the room temperature.

2. Three weights of new filter together with their filter holder, were recorded. Then, three readings for the filter holder, filter, foam holder and respirable foam were taken together. Followed with another three reading for the filter holder, filter, foam folder, respirable foam and thoracic foam were taken. Finally, the device was assembled together with the sampler head. The arrangement of the filter and the twin foams is illustrated by **Figure 4.6b**.
3. The CIS sampler were connected with a personal pump and the flow rate set to 3.5 L/min.
4. The IOM sampler was placed in the environmental dust chamber and the door was sealed. Dust clouds were generated for several minutes followed by sampling for various lengths of time
5. After complete the sampling, again three weight of the filter, the twin foams and the cassette holder were recorded as explained in step (2).
6. With the average weight before and after sampling, the mass concentration of dust particles concentration values were calculated in  $\text{mg/m}^3$ .

#### **4.2.6 The RespiCon Sampler**

The RespiCon sampler is a special sampler which can sample respirable, thoracic and also inhalable dust simultaneously as illustrated by referred **Figure 4.7a**. Designed by TSI Inc. of the USA as a multi-stage impactor, it is suitable for either a personal or an area sampler. Particles collected on the first stage of the RespiCon represent the respirable fraction of airborne particulate matter. Particles collected on



the first and second stages represent the thoracic fraction, and particles collected on the first, second, and third stages represent the inhalable fraction [64; 65].

**Figure 4.7a : The RespiCon sampler.**



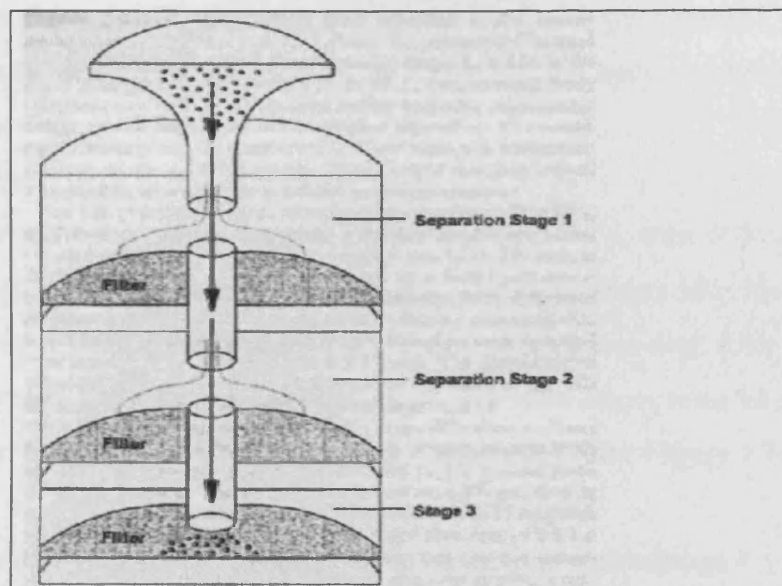
The RespiCon uses 37 mm filters, two with central holes and one complete filter paper. It has the capability of sampling very efficiently, although the preparing of the device may take some time before any sample can be collected. The first two stages required filters paper with centre holes of 4.3 mm (0.017 inches) in diameter for use in collection stages one and two, while the third stage filter has no center hole filter for dust collection.

Virtual impactors differ from conventional impactors because the impaction surface is replaced by a virtual space of stagnant or slow-moving air. According to **TSI Manual Model 8522 [65]**, an aerosol passes through an accelerating nozzle toward a collection probe. Near the collection probe, a major portion of the airflow is directed away from the probe. As shown in **Figure 4.7b**, small particles with low inertia follow the flow streamlines and are carried away with the major flow to be deposited on a filter. The separation efficiency curve is determined by the ratio of the major and minor flows and by the dimensions of the accelerating nozzle and



collection probe. Another characteristic of the virtual impactor is that particles smaller than the cut-size of the impactor remain in both the major and minor airflows [64].

Figure 4.7b : The RespiCon MultiStage Virtual Impactor.



\* Source : Tatum et.al. [64].

The RespiCon design is based on the American Conference of Governmental Industrial Hygienists (ACGIH) / International Organisation for Standardization (ISO) / CEN definition for inhalability. The instrument also samples inhalable, thoracic and respirable dust fractions in the manner proposed by Soderholm [40]. The particles collected on the stage one, the filter will be  $4 \mu\text{m}$  in aerodynamic-equivalent diameter ( $d_{\text{AE}}$ ), whereas the stage two filter will contain a much smaller percentage of particles  $4 \mu\text{m}$  ( $d_{\text{AE}}$ ) plus the majority of the particles in the 4 to  $10 \mu\text{m}$  ( $d_{\text{AE}}$ ) range. At stage three, the filter would be expected to contain yet smaller percentage of the particles less than  $10 \mu\text{m}$  ( $d_{\text{AE}}$ ) and the majority of the percentage greater than  $10 \mu\text{m}$  ( $d_{\text{AE}}$ ) [64].

Before operating the RespiCon particle sampler, it is necessary to 1) Prepare the filters and 2) verify the flow rates. Below are the operation instructions for the RespiCon sampler :

1. RespiCon sampler was disassembled by removing the inlet head by pressing down slightly and turning counter-clock-wise. Then, the body were placed on the removal cylinder and cover with removal disk (**refer Figure 4.7c**).
2. Using the palm of the hand, the removal cylinder were pressed down on the removal disk, filter stages became loose and the body can be pushed down (**refer Figure 4.7d**).
3. After the three stages were removed from the body, then followed the filter holder were moved from each stages. The filter stages identified by ring(s) inscribed around the perimeter where filter #1 has one ring, filter stage #2 has two rings, and filter #3 has three rings. The filter stages must be assembled in order with stage #1 on top and #3 on the bottom (**refer Figure 4.7e**).
4. Before putting the filter on the filter holder, the filters (stage # 1 and #2 with holes, and stage #3 without the holes) had to be pre-condition and weighing using an approved mass balance. Three weighs each for the filter at stage one, two and three were taken with it own filter holder using the mass balance.
5. With the top ring removed, the 37-mm filter with no holes was placed in the filter folder. Before replacing the top ring, the filter holder based was placed into filter stage #1. Then, the side of the filter stage was tapped to allow the filter to center itself on the impactor nozzle located in then center of the stage (**refer Figure 4.7f**). Next, the top ring were aligned and gently pressed into place using both hands. These processes were repeated for the second filter and filter stage #2 and stage #3.
6. For assembling the RespiCon sampler, all three filters stages were stacked with stage #1 on top and stage #3 on the bottom. The exterior of the filter stages were examined to ensure that the two O-rings on each stage were intacted. Then, the body unit were placed over the removal cylinder. Followed by placing the stacked filter stages onto the removal cylinder and the body unit were lift up (**refer Figure 4.7g and 4.7h**).

7. The removal cylinder were inverted and using the removal cylinder, it was pressed firmly down on the top of the filter stage stack until the three stages were seated tightly at the bottom of the body unit (**refer Figure 4.7i**).
8. The RespiCon sampler was then connected with a personal pump with the flow rate set at 3.1 L/min. Prior to that, the total flow checker were attached and placed on the body unit by turning it clock-wise. The tube was then attached to the flow checker using a suitable rotameter. After the total flow checker was removed from the body unit, the inlet head was placed onto the body unit and tightened by turning clock-wise. Now the RespiCon sampler is ready for sampling.
9. The RespiCon sampler was put inside the environmental dust chamber and the door was sealed. Next, the limestone dusts were generated (DGP) first for 2 or 3 minutes. This followed by sampling the limestone dusts, which had been generated by the dust disperser for 5 or 10 minutes depends on the mass concentration that were looking at that time.
10. After complete the sampling, again three weights of the filter for each stages with its holders, were taken and noted.
11. With the average weight before and after the sampling of limestone dust, the mass concentration was calculated in  $\text{mg/m}^3$  using the Microsoft Excel worksheet provided when the sampler was bought.

**Figure 4.7c : Place Body Unit on Removal Cylinder. Cover with Removal Disk.**



**Figure 4.7d : Press Down to Remove Filter Stages.**



**Figure 4.7e : Filter Stage #1 with Filter Holder.**

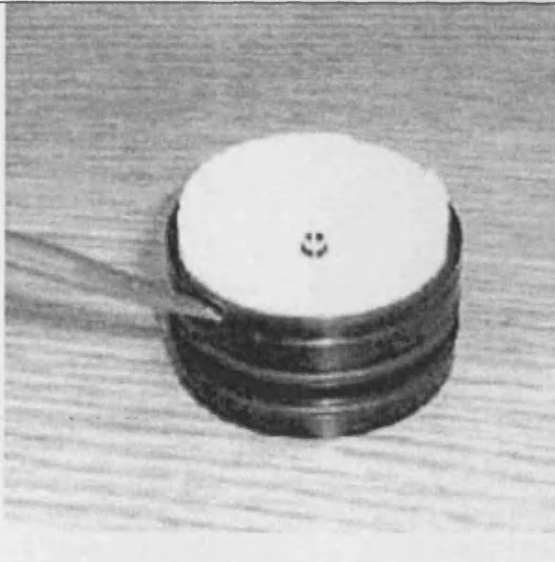


**Figure 4.7f : Tap Side of Filter Stage to Center Filter Over Nozzle.**

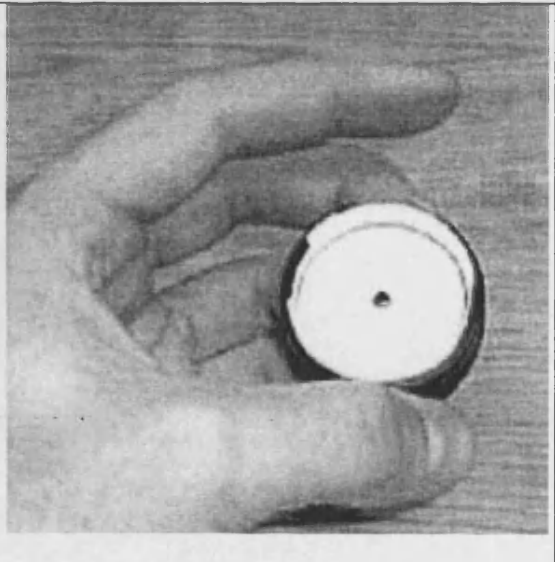


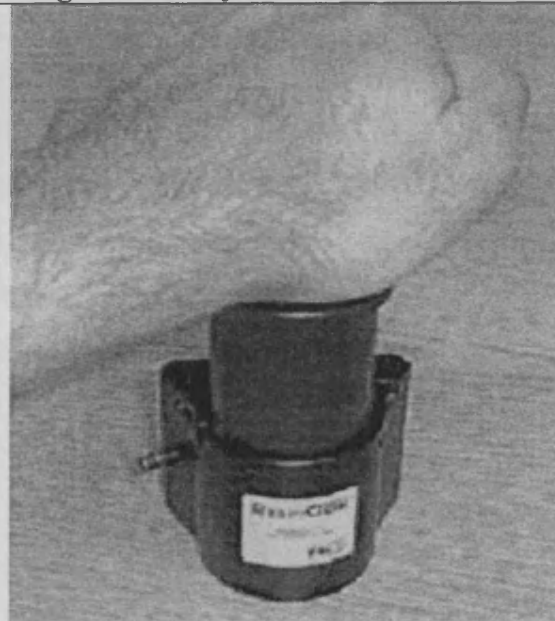
**Figure 4.7g : Place Body Unit Over Removal Cylinder. Place Stacked Filter Stages into Body Unit.**



**Figure 4.7h : Lift Body Unit to Cover Filter Stages.**



**Figure 4.7i : Press Down to Seat Filter Stages into Body Unit.**

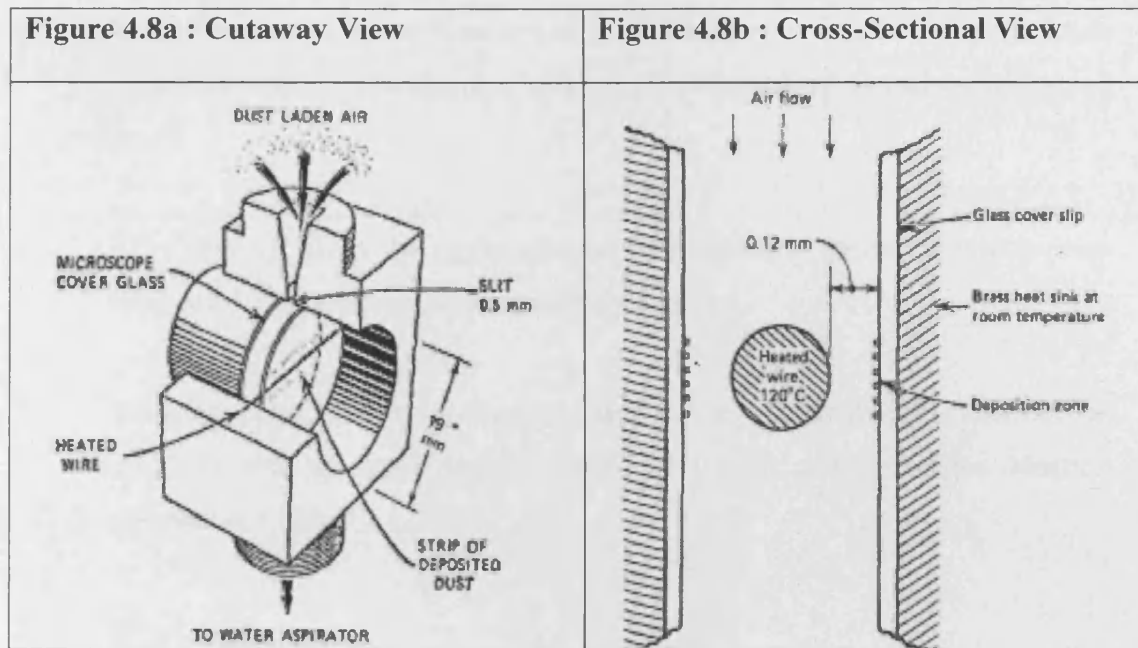


*\* Note : Figure 4.7c to 4.7i were from TSI Manual Model 8522 [65].*

#### 4.2.7 The Thermal Precipitator

The Thermal Precipitator is a sampler, which collects particles using the thermophoresis concept to deposit the particles onto a surface. Thermophoresis is defined as the movement or force exerted on aerosol particles in a gas in the direction of decreasing temperature in the presence of a temperature gradient. The movement occurs when a cold surface is in proximity to a warm gas, which causes particles in the gas to be deposited onto the surface. This may occur in 2 ways i.e. hot gas flowing through a metal tube or a warm flow of air over a cold surface.

These devices employ a heated element, such as wire, ribbon, or plate; air passes the aerosol between the heated element and an ambient-temperature surface, onto which particles may deposit, as illustrated by **Figure 4.8a** and **b**. For the purposes of sampling of particulates, a gold carbon coated grid was used as the sampling surface located adjacent to a heated wire. The spacing between the heated element and the collection surface is usually about 120  $\mu\text{m}$ . This produced a temperature difference that provided large temperature gradients. Thermophoretic velocity does not decrease with particle size and these devices are very efficient in collecting small particles. For a properly designed precipitator, the collection efficiency is virtually 100 percent for particles less than 5 or 10  $\mu\text{m}$  [39; 66]. The Thermal precipitator runs at very low sampling rates of 10 cubic centimetres per minute ( $\text{cm}^3/\text{min}$ ). Therefore, it is suitable for collecting small quantities of particles for observation in both the phase contrast optical microscope (PCOM) or transmission electron microscope (TEM).



\*Courtesy By British Crown Copyright [39].

As the thermophoretic effect velocity for small particles is greater than that for large particles, there is some size segregation of the collected particles in a wire-and-plate thermal precipitator. The smallest particles are deposited first, followed by the large particles farther downstream. This problem can be minimized by using a heated plate instead of a heated wire or by slowly moving the deposition surface relative to the wire. For a heated plate, the temperature gradient does not need to be as great, because the particle is exposed to the thermal force for a longer time.

A Thermal Precipitator can be used for both counting and sizing of particles using a microscope, and also for chemical analysis. The operating instructions for the Thermal Precipitator are given below :

1. Gold carbon coated grids were placed on top of one of the metal insert, while a microscope cover glass was placed on top of the facing metal insert.
2. The metal inserts were put into the sampler. After that, both plates adjacent to the heated wire and locked in place as shown in **Figure 4.8a**.

3. The thermal precipitator flow was set at 10 cm<sup>3</sup>/min to sample dust particles in the environmental dust chamber and samples were taken for various periods of time.
4. After removal from the environmental dust chamber, the metal inserts were removed for careful examination of the samples.
5. The glass cover slide were examined with a phase contrast optical microscope (PCOM) and the gold carbon coated grid with a transmission electron microscope (TEM).

#### **4.2.8 The Marple Personal Cascade Impactor (Series 290)**

The Small Cascade Impactor sampler used was the Series 290 Marple Personal Cascade Impactor, which is a product of New Star Environmental and is shown in **Figure 4.9a**. The Marple cascade impactor is a precision instrument capable of giving an accurate aerodynamic particle size distribution. The Marple cascade impactor used in this study was an 8 stages impactor cut-points ranging from of 21 to 0.5 microns. It is operated at a nominal flow rate of 2 L/min. The Marple cascade impactor is used for sampling wood dust, coal dust, silica dust, respirable dust sampling, inhalation toxicology, aerobacteriology, indoor air pollution, low-cost multi-point sampling and for aerosol research as well [67].

It has an inlet visor and cowl, which prevents large wood chips, cigarette ash and other debris from entering the device. Air enters the inlet cowl and accelerates through the six radial slots in the first impactor stage. Particles larger than the cut-point of the first stage give an impact on the collection substrate used. The air then flows through narrower slots in the second impactor stage, where smaller particles impact on the second collection stage and so on. The widths of the radial slots are constant for each stage, but are smaller for each succeeding stage. Higher jet velocity is needed for each succeeding stage and smaller particles acquiring sufficient



momentum to impact on one of the collection substrates. After the last impactor stage, the remaining fine particles were collected by a final 34-mm filter.

Substrate materials available include Mylar and Stainless steel and various back-up filters of 5-micron pore size. The pump for the Marple Personal Impactor must have a constant flow controller, which maintains the pre-selected flow rate constant as the pressure drop through the back-up filter increases with particulate loading and also it must have a sufficient vacuum capability to maintain the pre-selected flow rate over the entire sampling period in **Table 4.2** below are cut-point for Marple Personal Impactor are given.

**Table 4.2 : Series 290 Impactor Cut-Points at 2 L/min.**

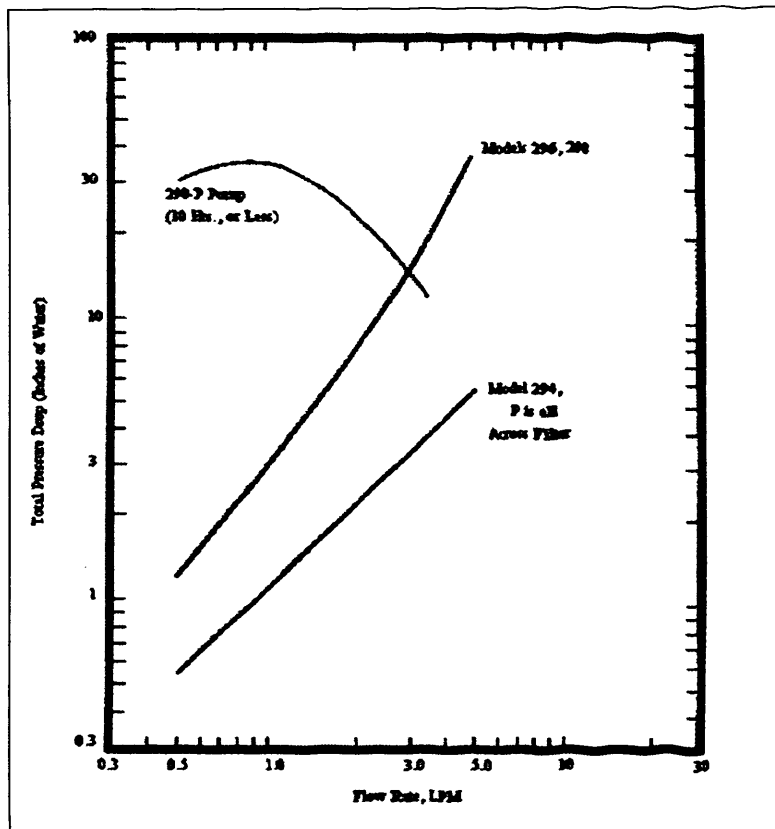
Impactor Stage Number	Cut-Point Diameter, Dp ( $\mu\text{m}$ )
1	21.3
2	14.8
3	9.8
4	6.0
5	3.5
6	1.55
7	0.93
8	0.52

*\* From New Star Series 290 Manual [67].*

**Figure 4.9a : Marple Personal Cascade Impactor (Series 290)**



**Figure 4.9b : Pressure Drop Across the Series 290 Impactors with Clean 34 mm 5-micron PVC Back-Up Filter.**



\* From New Star Series 290 Manual [67].

The operating procedures used with the Marple Personal Impactor are as follows

1. From **Figure 4.9b**, the sampling flow rate based on the particle cut-points desired and the vacuum capability of the sampling pump was selected.
2. All collection substrates and back-up filters had to be pre-weighed and recorded. A balance with a sensitivity between 0.00001 mg was used to weigh the blank and the sampling substrates before and after sampling was conducted. The substrates and the final filter have to be equilibrated with the lab environment for approximately 24-hours at a relative humidity of 50 percent, or less, before weighing.
3. The cascade impactor was then assembled.

4. The instrument was connected to the sampling pump and set to the desired sampling flow rate. The flow rate used was recorded at 2 L/min and the pump flow was tested using an airflow calibrator.
5. After the desired sampling period, the pump was switched off and the sampling time (or elapsed time) was recorded.
6. For best results, the fully assembled impactor was transported in the upright position and sealed on the inlet to prevent sample contamination. In the lab, all collected substrates and the back up-filter were weighed and recorded.
7. The air volume, total net weight of dust, the percentage in size range and also the mass concentration were calculated.

#### **4.2.9 The Anderson Cascade Impactor (Mark II)**

The large cascade impactor used in this study is the Andersen 1 ACFM Ambient Particle Size Sampler (Mark II) as shown by **Figure 4.10a**. It is a multi-stage, multi orifice cascade impactor, which is normally used in the environmental working area to measure the size distribution and total concentration levels of all liquid and solid particulate matter on the basis of their aerodynamic diameter [68].

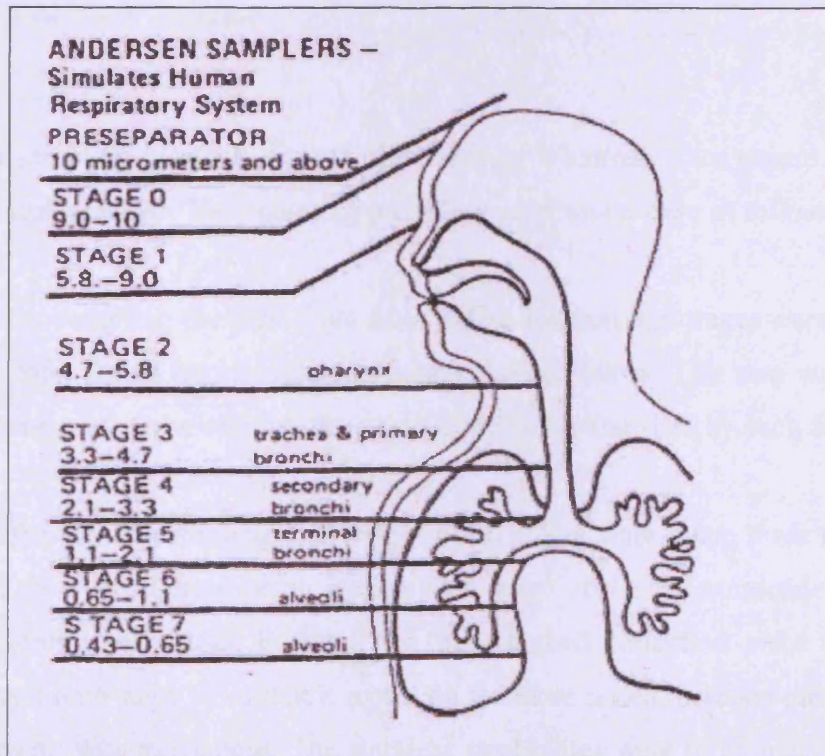
The aerodynamic result obtained can be used to determine compliance with existing Threshold Limit Values (TLV) and Occupational Safety and Health Administration (OSHA) Regulations in the USA. The fraction of inhaled dust retained in the respiratory system and the site of deposition vary with size, shape, and density. The correlation of impactor stages with deposition locations in the lung are illustrated by **Figure 4.10b**.



**Figure 4.10a : Anderson Cascade Impactor (Mark II) with Personal Pump and L-Shape Tube.**



**Figure 4.10b : Anderson Cascade Impactor Simulates Human Respiratory System.**



\* From New Star NV Manual [68].

The impactor, consists of eight aluminium stages. Stages 0 and 1 have integral inlet sections that contain 96 orifices arranged in a radial pattern. Stages 2 to 6 have integral air inlet sections that contain 400 orifices arranged in a circular pattern. Stage 7 contains 201 orifices arranged in a circular pattern. The orifices are progressively smaller from top to bottom stages, ranging from 0.1004 inch diameter on stage 0 to 0.0100 diameter on stage 7. Each stage has a removable stainless steel collection plate. The exhaust section of each stage is approximately 0.75 inch larger in diameter than the collection plate, allowing unimpacted particles go to go around the plate and into the next stage stage. The top two stainless steel collection plates have  $\frac{7}{8}$  inch holes in the center to allow airflow through the center also. In **Table 4.3** below are the cut-points at each stage for the Anderson Cascade Impactor.

**Table 4.3 : Anderson Cascade Impactor Cut-Points at 28.3 L/min.**

Impactor Stage Number	Cut-Point Diameter, Dp ( $\mu\text{m}$ )
0	9.0
1	5.8
2	4.7
3	3.3
4	2.1
5	1.1
6	0.7
7	0.4

\* From New Star NV Manual [68].

For sampling purpose, a glass fibre filter or Whatman filter papers were used for each sampling stage. The operating procedures employed were as follows :-

1. Before sampling the glass fibre filter papers for the eight stages were put in the desicator for 24 hours in the environmental laboratory. This step was taken to stop any influence of humidity or moisture being absorbed by each filter.
2. On the day of sampling, the weight of all filters were taken three times each and recorded, before being put on each stage of the large cascade impactor, beginning with stage F. Next, the pre-weighed collection plate no. 7 was placed onto stage F, so that it rested on the three raised, notched metal seats to prevent plate movement. The stainless steel plates were to be placed with the curved lip down so that a raised, smooth surface was to be exposed for particle

impingement. This was followed by stage 7, collection plate 6, stage 6, and so on until the inlet cone or pre-separator or the L-shape tube was positioned last. Then, three spring clamps, which extending from the base were used to hold the 8 stages impactor.

3. After all the filter was measured and put on each stage of the large cascade impactor, it was interconnected with tube, flow pump and also the rotameter. This was to ensure that the airflow passed through the impactor and through the pump at the same flow rates when the experiments were conducted. The pump flow was running at 28.3 L/min throughout the whole sampling processes.
4. The Anderson cascade impactor was placed inside the environmental dust chamber and the door was sealed. Next, the limestone dusts were generated, (DGP) first for 2 or 3 minutes. This was followed by sampling of the limestone dusts, which had been generated by the dust disperser for 5 or 10 minutes depends on the mass concentration that were looking at that time.
5. After completing the sampling, again three weighs of the filter for each stage were taken and noted. Prior to that, all filters used in the impactor were pre-conditioned before weighing in a desicator.
6. The average weight before and after the sampling of limestone dusts were obtained, the mass concentration was calculated in  $\text{mg/m}^3$  using the Microsoft Excel worksheet supplied when the sampler were bought.

### **4.3 Materials used in this study experimental**

#### **4.3.1 Types of Dust**

At the early stage of the laboratory works, coal dust was used in order to check the sampling efficiency. However, due to its character, it could not be disperse easily.

As a result, limestone dusts were used in place of the coal dust. Limestone dust has a smaller size distribution than coal dust, which made it easy to disperse and produce a minimum of aggregation. The limestone dust was produced by ball milling standard quarry aggregate.

### 4.3.2 Types of Filter

Fibrous and porous membrane filters, known to be the most important filters in aerosol sampling. The glass fibre filter at different magnifications is shown in **Figure 4.11a**. As for the porous membrane filters, it has different filter structure and less porosity between 50 to 90 percent from fibrous filters as shown on **Figure 4.11b**.

Each membrane filters have their own capillary pore. **Figure 4.11c** showed the Nuclepore filter microscopic cylindrical holes of uniform diameter, approximately perpendicular to the surface of the filter.

Various filters can be used for sampling but they has to reach the objective of sampling in the first place. For instance, membrane filters are most suitable for gravimetric sampling to obtain mass concentration values, while nuclepore filters (0.2  $\mu\text{m}$  pore size) is the most suitable for size distribution sampling i.e. sizing and counting using the transmission electron microscope (TEM).

**Figure 4.11a : High-Efficiency Glass Fibre filter at 4,150 X.**

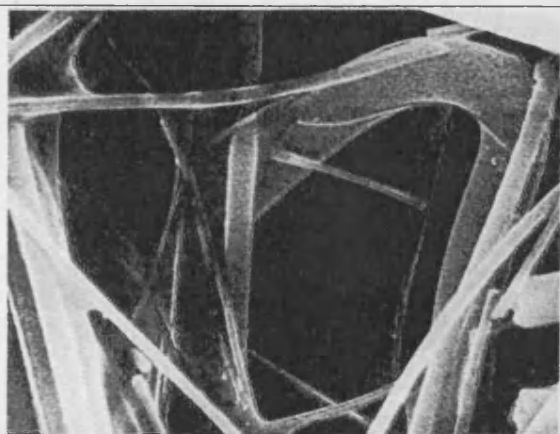
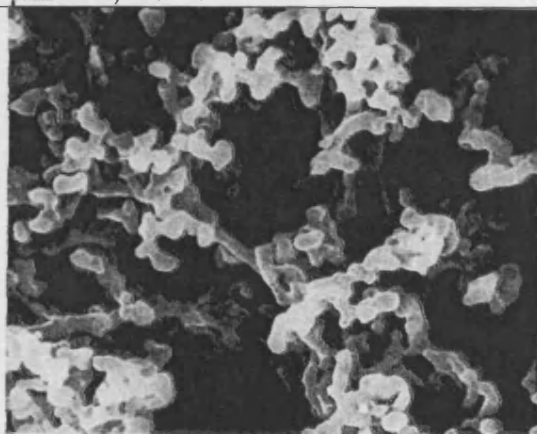
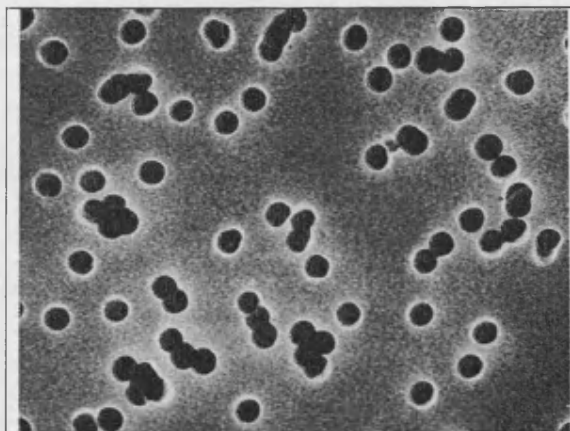


**Figure 4.11b : Cellulose Ester Porous Membrane filter with a pore size of 0.8  $\mu\text{m}$  at 4,150 X.**



\* Image Using Scanning Electron Microscope. From Hinds [39].

**Figure 4.11c : Capillary Pore Membrane Filter with a Pore Size of 0.8 $\mu$ m at 4,150 X.**



*\* Image Using Scanning Electron Microscope. From Hinds [39].*

In regard of the aerosol particles, which are going to be analysed by chemical methods, the concern is with interferences caused by the filter material, or contaminant in the filter. For example, fibreglass filters often contain organic binder of up to 5 percent by weight, which can interfere with the analysis of certain organic compounds. It can also suffer from the formation of artifacts; specifically, the glass fibres have slightly alkaline surface that reacts with SO<sub>2</sub> gas to form sulphates on the fiber surface. While special organic-free “microquartz” filters have a low sulphates artifact formation for analytical methods that require ashing by incineration or dissolution in acid. Consideration must also be given to the amount and type of filter residue. The extraction of soluble aerosol particles with a solvent requires solvent-stable filter material. The depth at which particles are captured is an important consideration for radioassay of alpha-emitting particles, because of alpha absorption by the filter material. For the characterizations of airborne particulates, **Table 4.4** lists the filter used for each sampler head depends on the requirements and sampling objective i.e. the physical or chemical characterisation of particles.



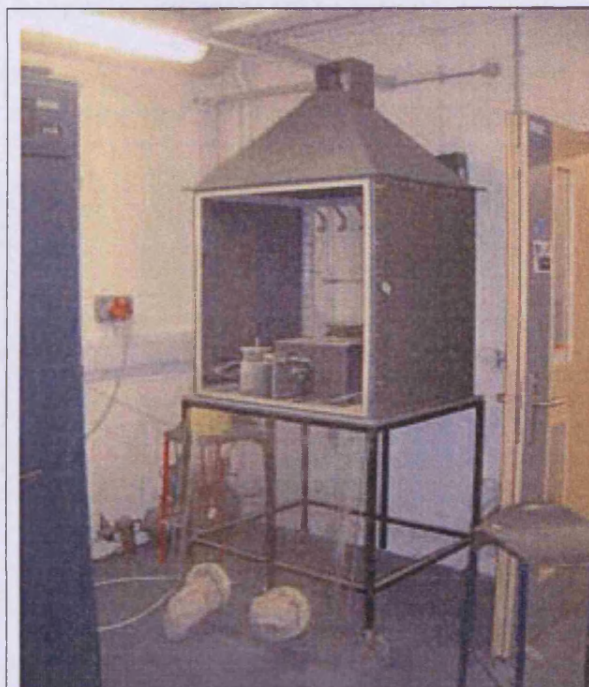
**Table 4.4 : Summary of Airborne Sampling Equipments Descriptions.**

No.	Equipment	Filter Diameter	Air Flow	Type of Filter and Pore Size	Description
1.	Casella MRE Sampler [Respirable]	56 mm	2.5 Litre/min	Whatman Filter, 11.0 µm / Milipore Membrane Filter, 1.2 µm.	Refer 4.2.1
2.	Cyclone Head Sampler [Respirable]	25 mm	2.2 Litre/min	Milipore Membrane Filter, 0.8 µm.	Refer 4.2.2
3.	Seven Hole Sampler [Inhalable]	25 mm	2.0 Litre/min	Milipore Membrane Filter, 0.8 µm.	Refer 4.2.3
4.	IOM Sampler [Respirable & Inhalable]	25 mm	2.0 Litre/min	Milipore Membrane Filter, 0.8 µm.	Refer 4.2.4
5.	Casella CIS Sampler [Inhalable, Thoracic, Respirable]	37 mm	3.5 Litre/min	Glass Fibre Filter, 1.6 µm / MCE Filter 5.0 µm.	Refer 4.2.5
6.	Respicon Sampler [Inhalable, Thoracic, Respirable]	37 mm	3.1 Litre/min	Mixed Cellulose Esther (MCE) With Hole Filter, 5.0µm.	Refer 4.2.6
7.	Thermal Precipitator [Respirable]		10.0 cc/min	Circle Glass Slide & Gold Grid with Filter.	Refer 4.2.7
8.	Small Cascade Impactor [Series 290-Marple Personal Cascade Impactor]	34 mm	2.0 Litre/min	Glass Fibre Filter With Slit.	Refer 4.2.8
9.	Large Cascade Impactor [Anderson 1 ACFM Ambient Particle Sizing Sample]	81 mm	28.3 Litre/min	Glass Fibre Filter.	Refer 4.2.9

### 4.3.3 Environmental Dust Chamber Design

In this study, an environmental dust chamber was used to run dust sampling trials using various dust sources. The chamber with dimensions of 0.85 m X 0.7 m X 0.91 m is illustrated by **Figure 4.12**. The chamber was manufactured from Poly Vinyl Chloride (PVC) on a steel stand. The chamber was designed so that it could be vented easily from the top or the base. During dust sampling experiments, the samplers were placed inside the chamber on the steel stands and the sampling pump outside. They were connected with plastic tube connected through service holes designed for that purpose. The chamber had a removable side with glove apertures so that manipulation of samplers could be performed when the chamber was sealed.

**Figure 4.12 : Environmental Dust Chamber.**



#### **4.3.4 The Mechanical Dust Dispenser**

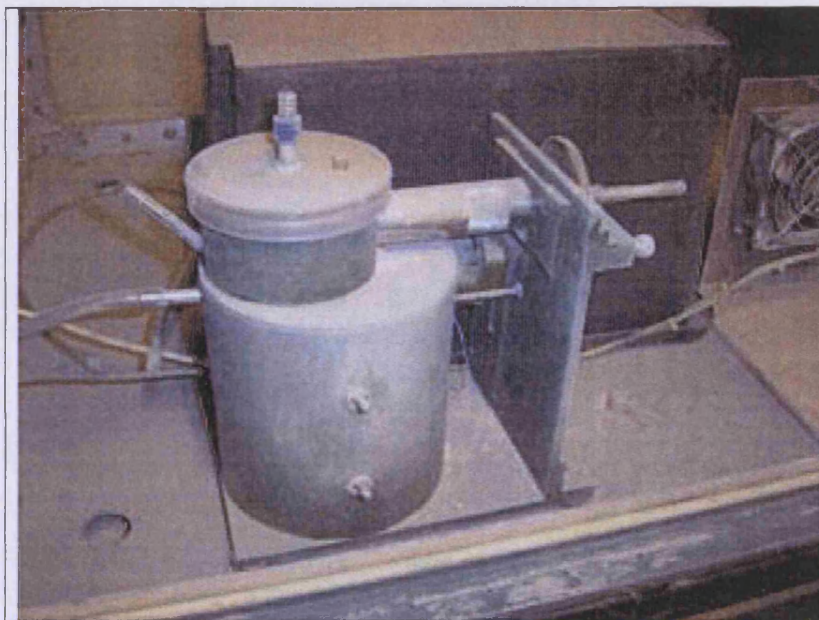
The mechanical dust dispenser was purpose built to disperse efficient and consistent quantities of fine material. It was constructed with two mechanisms : first, a feed mechanism and secondly, a dispersing chamber in which the dust flocks were broken down until particles were sufficiently small for them to pass through the exhaust. The device is illustrated by **Figure 4.13a**. The design of the dispenser is based on a study outlet concerned by with the generation of dust clouds from samples of asbestos.

The feed mechanism is a piston-cylinder arrangement, the cylinder being preloaded with a limestone dust to make a uniformly packed plug. The threaded piston rod screws into a hole tapped in the boss of the gear wheel, which thereby acts as a nut. This gear wheel is held captive on the face of a supporting plate by a bridge piece, and engages with a second gear wheel fixed to the final shaft of an electric motor; advance of the piston rod is obtained when the motor is powered. A weighted arm



prevents the rod rotating during operation of the dispenser but allows it to be rotated manually to set the position of the piston when loading the dust reservoir.

**Figure 4.13a : Mechanical Dust Dispenser.**



The feed mechanism delivers the dusts into the dispersing chamber, which contains a specially shaped rotor driven by an electric motor. Each time either extremity of the rotor hits the end of the dust plug being expelled from the cylinder it shaves off a small amount of material. Since the plug advances only about  $0.05 \mu\text{m}$  during each revolution of the rotor, the dusts are detached mostly as single particles or minute flocks. The appearance of the interior of the chamber as seen through transparent top is of dusts whirling around the wall, with particles being separated from one another by a gentle rubbing of material against material.

Air is supplied to the dust dispenser chamber through a side tube by a small pump or from a compressed air supply. The airflow has two functions. The first is to prevent the circular motion of the dusts from becoming too regular. Preliminary experiments demonstrated that keeping the material in continuous and irregular motion both the air stream and the rotor are necessary, and that if only one of these agents is present a channel may develop in the material and cause an interruption of the dust emission. The second function of the airflow is to expel particles from the

dispersing chamber and to provide, in conjunction with the circular motion, aerodynamic particle classification. As the flocks are dispersed the aerodynamic drag exerted on released particles by the general motion of the air towards the exhaust tube may overcome the tendency of the rotation to keep them at the outer wall of the chamber [67]. With a suitable choice of feed rate, rotor speed, and airflow rate to the dispenser, and by always leaving in the dispersing chamber the material left at the end of the previous run, a balance between input and output is rapidly achieved on starting the apparatus.

The components of the dispenser are described separately as: (a). syringe with shaped flange, (b). bayonet fitting for the syringe, (c) piston and piston rod, and (d) banjo plate. The cylinder of the feed mechanism is a 50 ml syringe of 1 1/8 in.(29 mm) nominal internal diameter, attached to a nozzle with its end sawn off. The purpose is to facilitate rapid removal of the syringe, and it is held to the supporting plate by a bayonet-type fitting : the flange of the syringe is adapted for this purpose by cutting down it to shape illustrated in **Figure 4.13b** (a). While the female part of the bayonet is shown in **Figure 4.13b** (b). **Figure 4.13b** (c), shows the piston retained by a screw on a spigot machined on the end of the piston rod in such manner that the rod can be rotated for setting the position of the piston when loading the syringe without the piston also rotating. **Figure 4.13b** (d) shows the mounting of the motor on a 1/8 in. thick banjo plate, which enables various pairs of gear wheels to be employed to give a series of piston speeds. The banjo plate is separated from the supporting plate by 1/2 in. long spacers; it can be rotated about a pivot bolt to bring the gear wheels into mesh and then secured by a bolt through the slot.

The thread is removed from the free end of piston rod so that the drive becomes disengaged when the piston is 5 mm from the ejection end of the syringe. This ensures the dust plug does not become so thin at the end of a run that it may collapse into the dispersing chamber and cause an abrupt rise in dust emission. It also allows the dispenser to be set for a predetermined period. **Figure 4.13c** showing the dispersing chamber profile and the metal plate to form the rotor.

**Figure 4.13b : Components of the Dispenser.**

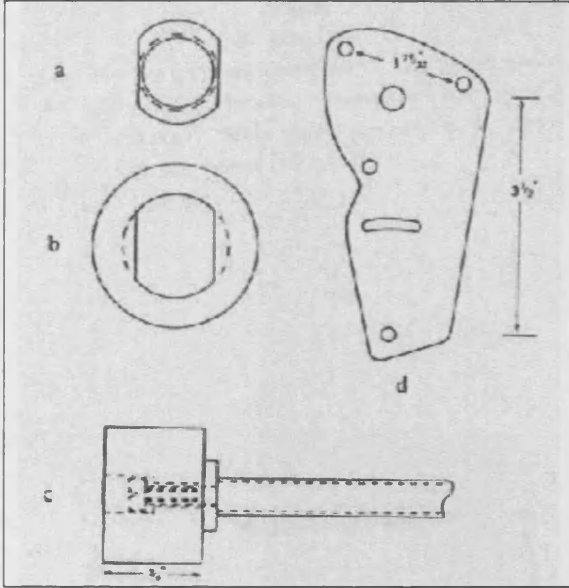
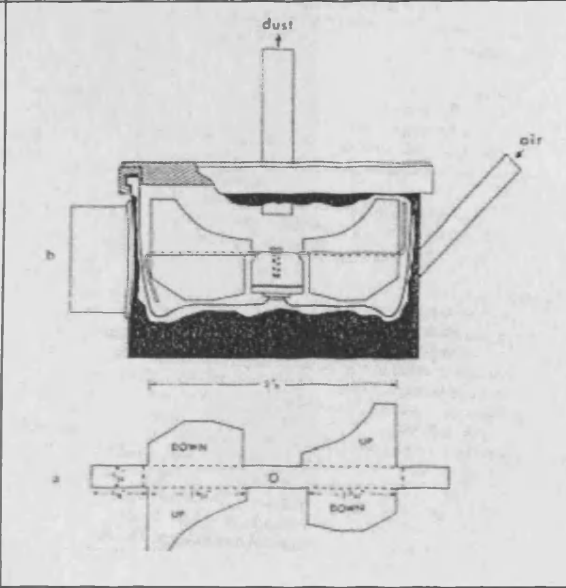


**Figure 4.13c : (a) Metal Plate to Form the Rotor, and (b) Dispensing Chamber**



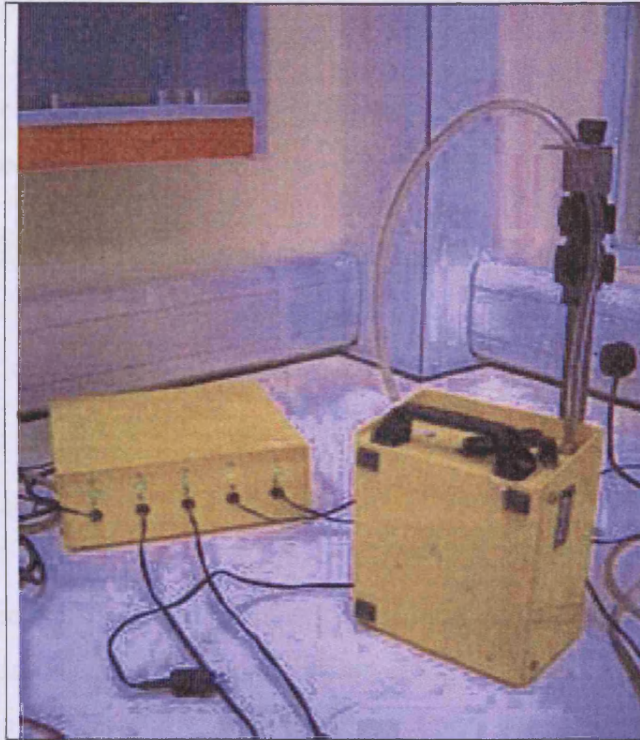
\* From Timbrell et al., [69].

#### 4.3.5 Dust Pump Flow

All sampling instruments listed in sections 4.2.1 to 4.2.9 were operated using a pump with maximum flow rate of 10 L/min as illustrated by **Figure 4.14**. The flow rate was adjusted before each sampling operation to ensure correct sampling conditions. flow rate. The Anderson Cascade Impactor, Casella MRE sampler, and Thermal Precipitator are supplied with their own pumps. The Anderson Cascade Impactor, was operated at 28.3 L/min. The flow rates at which each sampler operated are given in **Table 4.4**. Compressed air was used to supply air to the dust dispenser to produce dust particles inside the environmental dust chamber.



**Figure 4.14 : Personal Pump and Charger.**



#### **4.3.6 Flow Measurement**

An anemometer was used to check pump flow rates for each sampling instrument and also to monitor the airflow generated by the air compressor. Before performing any samplings, the flow of air to the instruments was checked. The purpose of these steps was to ensure that the flow before and after sampling were the same and to make sure each sampler sampled at the correct flow to obtain a good sample.

#### **4.3.7 Measurement of Sample Weight.**

To obtain the weight of dust for gravimetric analysis, filters were weighed before and after dust sampling. For this study, a Metler AE50 balance reading to 5 decimal places and reading up to 0.000001g, which was calibrated before being used. Before using the balance, it was stabilised where the height of the balance being

adjusted using the four levelling screws on the balance base. The balance was then calibrated before it was used.

Samplers and filters were dried in an oven when required and stayed in a desiccator when necessary to prevent moisture adsorption.

Data including sampling times, locations, flow rates and other operating information were recorded in a laboratory handbook.

#### **4.3.8 Other Ancilliary Equipment Employed.**

A low temperature ashing device was used to burn filter paper (which contain carbon) using oxygen ( $O_2$ ) plasma for a certain period to obtained dust particles only and produce carbon dioxide ( $CO_2$ ) at a low temperature where the filter was burned slowly. The dust particles obtained were diluted, filtered on nucleopore filter, carbon coated and floated on the gold grid and ready to used on transmission electron microscope (TEM).

The *Ultra Sonic Water Bath* was used for dispersion of dust particles evenly into suspension, which is to avoid aggregates for certain purposes. Besides that, it was used in cleaning of sampler foams for examples the respirable and thoracic foam of Casella CIS sampler purpose to shake any impurities inside the foam during when it was manufactured in the factory.

#### **4.4 Description and Operation of Instruments for Measurement of Particle Size and Concentration.**

Both phase contrast optical microscope (PCOM) and a transmission electron microscope (TEM) were used for fibres and particles counting and sizing. Images were recorded using the transmission electron microscope and were then analysed using the *AnalySIS* proprietary software. Microscopic methods for determining

particle size distributions are normally tedious, and require consistency skill, and careful preparation. Once mastered with the technique, the counting and sizing particles would be easier.

#### **4.4.1 The Phase Contrast Optical Microscope (PCOM).**

Particles were prepared directly on a glass slides by sedimentation, electrostatic precipitation, or thermal precipitation and viewed directly in a microscope. Powders or bulk dust samples can be spread out on the slide by gentle smearing with a toothpick. The procedure for viewing particles captured on a filter is to cut out a small pie-shaped piece of the filter and place it on a clean glass microscope slide. The filters made cleared using acetone vapours for dust particles and fibres samples to make it transparent.

Even though a total magnification of 2500 X can be obtained with standard objectives and eyepieces, the size of the smallest observable particle is governed not by magnification but by the resolution, which is controlled by the wavelength of light and the characteristics of the objective lens. The resolution is the smallest scale of detail that can be observed in the magnified image. Although greater magnification produces a larger image, however it does not increase the observable detail beyond the limit of resolution. Resolution is usually defined as the minimum separation distance required for two dots to be observed as two separate dots rather than as one elongated dot. The microscope employed in this investigation was the Leitz Diaplan.

#### **4.4.2 The Transmission Electron Microscope (TEM).**

The transmission electron microscope had the ability to examine particles smaller than the limit of resolution of an optical microscope. Transmission electron microscope, known to be the most analogous compared to the optical microscope, and another of its type, i.e. scanning electron microscopes [39]. In this study, the transmission electron microscopes used were the Philips 400T and the Philips Tecnai.



The typical acceleration voltage of 80 kV, could generated wavelength of the electron beam is  $4.5 \times 10^{-6} \mu\text{m}$ , or 100,000 times smaller than the wavelength of the light. The resolution, however, is not 100,000 times smaller than that use in an optical microscope, because of the small value of angular aperture used in electron microscopes to minimize distortion. The limit of resolution of a typical transmission electron microscope is less than  $0.001 \mu\text{m}$ .

The transmission electron microscope permits the smallest aerosol particles to be measured, but these instruments can be used only for solid particles that do not evaporate or degrade under the combined effects of high vacuum and heating by the electron beam. Particle must be deposited on specially prepared 3-mm-diameter grids mounted in a grid holder and inserted into the microscope. The grids are 200 mesh electrodeposited screen with a thin film of carbon covering the screen openings. The film are sufficiently thin, compared to the particles, that is causes only slight attenuation of the electron beam to form a high-contrast silhouette image. Particles can be deposited directly onto the film surface of a grid by electrostatic precipitation using the miniature type of precipitator. In some cases, replication or transfer procedures can be used to deposit particles or their replicas from another surface onto a grid. Sizing of particles was done from images captured with a Charge-Couple Device (CCD) camera.

#### **4.4.3 Asbestos Fibres Sampling, Counting, and Sizing.**

Asbestos mineral possesses some unique properties that cause lung injury and necessitate microscopic methods for evaluating its hazard. The characteristic fibrous shape of asbestos enables them to get past respiratory defense mechanisms and cause asbestosis (scarring of lung tissue), mesothelioma (cancer of the lining of the lung), and lung cancer. Microscopy is used to identify asbestos fibres whose size and shape enable them to cause these diseases. **Table 4.5** below shows the specific size range of fibre and the health related disease it could caused.

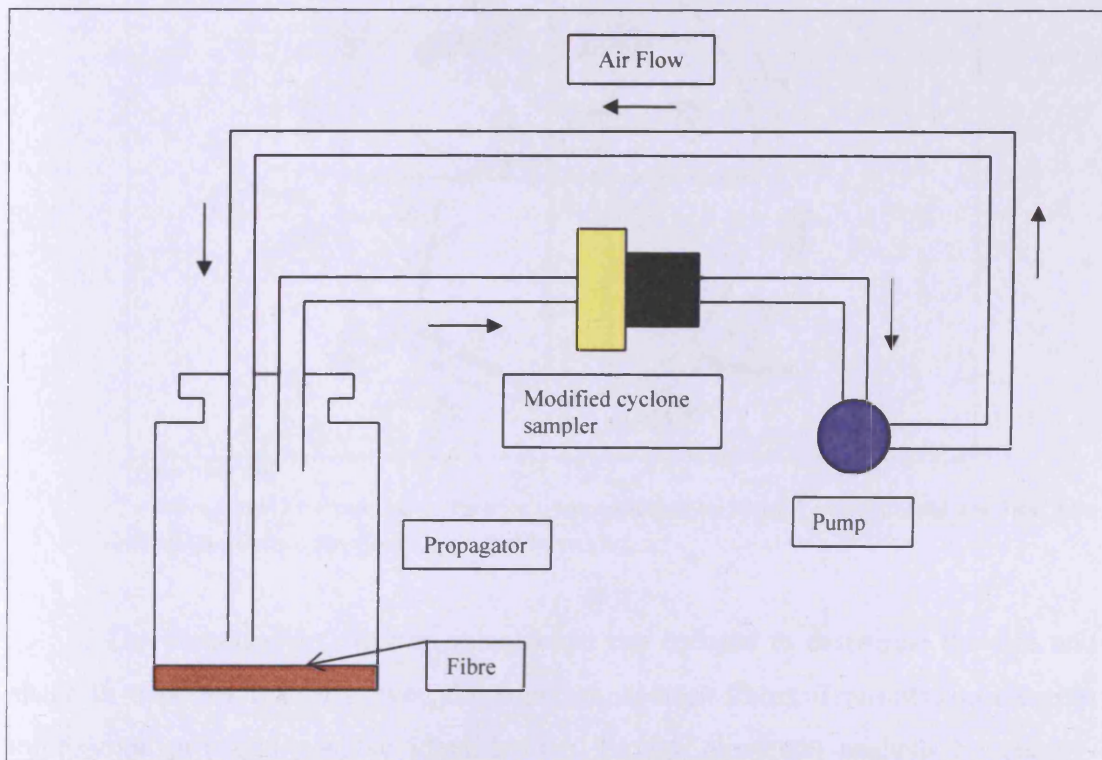
**Table 4.5 : Fibres and Health-related Diseases.**

Size Range of Fibres	Health related Disease Caused
< 5 $\mu\text{m}$ (length)	Cleared by normal clearance mechanisms
0.15-3 $\mu\text{m}$ (diameter), 2-100 $\mu\text{m}$ (length)	Asbestosis
< 0.1 $\mu\text{m}$ (diameter), 5-100 $\mu\text{m}$ (length)	Mesothelioma
0.15-3 $\mu\text{m}$ (diameter), 10-100 $\mu\text{m}$ (length)	Lung cancer

\* From Lippmann [70].

In sampling respirable asbestos fibres, 3 instruments were used i.e. a propagator (contain asbestos fibre samples), a modified cyclone, and a personal pump as illustrated by **Figure 4.15**. Set at 2 L/min flow rates, the pump was switch ON for few seconds as only small amount of fibres were needed to be resolved and magnified using the PCOM and TEM analysis techniques. In this study, 3 types of asbestos were sampled and analyse for their physical properties and characterizations i.e. amosite fibre, crocidolite fibre, and also chrysotile fibre obtained airborne and from the lung tissue.

**Figure 4.15 : Respirable Asbestos Fibres Sampling Process.**





#### 4.4.4 Mass Concentration Sampling

The measurement of mass concentration conducted was based on gravimetric analysis technique [60; 71]. Gravimetric analysis can be considered to be the most accurate and direct way to determine aerosol mass concentration by knowing the volume of the aerosol drawn through a filter and determining the increase in mass of the filter due to the aerosol particles collected. Usually high-efficiency filters with collection efficiency of nearly 100 % for all particles sizes were sampled.

The filters used in each sampler were weighed before and after the sampling process. During the weighing process, three readings of the weigh of the filter before and after sampling were taken. Later, the average value were calculated and used to produce the weigh of dust particles sample at a certain period.

All the samplers used were performance tested before mass concentration tests were conducted. For accurate sample weights, the volume sample must be adjusted. The sampling of the weigh, the sample volume must be adjusted, so that the collected mass of dust is large compared with the variability in filter weights.

For calculation of the mass concentration values, the differences between the weight of dust divided by the pump flow, and multiplied by a sampling period to obtain the mass concentration ( $\text{mg}/\text{m}^3$ ) values for each sampler. Filters, which had already been weighed were properly stored and labelled for further investigation such as determination of size distribution. In this phase calculation, the individual and comparison graph, Microsoft Excel software were used. During this period, the understanding of the calibration techniques, operations, cleaning and also maintaining all the samplers and others instruments to be used was very important.

A wide range of dust sampling equipment and sample analysis techniques have been employed in this investigation. All results obtained were carefully recorded and where appropriate statistically appraised.

#### 4.4.5 Size Distribution Samples Preparation

In this study, the asbestos fibres examined were obtained from airborne and human lung tissue samples. For determination of size distribution of dust particles using the TEM, any preparation is not necessary when particles are deposited directly onto the carbon-coated grid using thermal precipitator. However, preparation is necessary if the dust particles are deposited on membrane filters or on nuclepore filters [73; 74]. The methods used [76] are based on the ISO 13794 [75] and WHO, IARC Scientific Publications No.109 [77] to recover dust particles from specimens and to observe them individually, where the fibrous asbestos particles may be identified and counted. The purposes of determining the asbestos concentration in the lung is to assess past exposure from various types of asbestos and to investigate the relationship between dust inhaled and retained in the lungs, and the incidence of asbestos-related diseases [76].

For lung tissue samples, a known weight of wet lung tissue is digested in a solution of alkaline potassium hydroxide to dissolve organic material and release its occluded mineral content. If necessary, any remaining organic material maybe further reduced by secondary treatment of the digested residue as in Procedure 1 [76]. Final residues are then filtered and made ready for examination with an analytical transmission electron microscope. Preparation of tissue for TEM if lung is available are as follows :

1. Each piece of lung tissue collected from the three sites: apex of upper lobe; apex of lower lobe; base of lower lobe is halved.
2. Form two portions each consisting of one of the halves from each of the three sites.
3. Weigh each portion in a small aluminium foil cup and record the wet weight.
4. Dry one portion to a constant weight at a temperature of 100° C and record weight.
5. Transfer the other wet portion into a clean new Pyrex test tube suitable for

centrifuging (see apparatus in **Appendix B**).

6. Mark the test tube with laboratory sample number using a diamond marker.
7. Add a volume of 40 % alkaline potassium hydroxide to the tube so that the tissue in the tube is covered. (approx: 5 ml).
8. Place the tube in a heating block at 100 °C until all the lung tissue is seen to have disintegrated (see apparatus in **Appendix B**).
9. Centrifuge the digested residue at 1000 g for 20 minutes to recover liberated dust particles.
10. Decant supernatant and re-suspend the pellet at the bottom of the tube in filtered distilled water.
11. Re-centrifuge to remove residual potassium hydroxide (this washing to be repeated twice) before producing the final dust residue.
12. Place tube with final dust residue in a heating block at 350°C for at least 4 hours to remove residual organic material that may remain in the pellet (temperatures check frequently with thermometer).
13. Re-suspend the dust residue in 10ml of filtered distilled water and add a few drops concentrated HCL this will remove residual ferritin and calcium phosphate in the tissue.
14. Filter known aliquots of the suspension through polycarbonate filters (25 mm diameter 0.2 µm pore size ) in Sartorius filter holder, to collect the residue. The size of aliquots filtered are dependent on the quantity of residue produced.
15. The filters from each lung sample are secured in a different Petri dish and allowed to dry, the dried filters are then coated with a layer of carbon in a vacuum coating unit.
16. A suitable volume of chloroform is placed in a glass petri dish to produce a pool 4-5 mm in depth.

17. A gold E.M. grid 150 mesh is held in a pair of tweezers and moistened in the chloroform. A small section of the carbon-coated filter, enough to cover the 3 mm grid, is placed on the moistened grid.
18. The grid is then held in the chloroform with the underside of the grid touching the chloroform for 5 minutes.
19. The chloroform dissolves the filter material leaving the tissue extract to adhere to the carbon filter.
20. Examine the prepared grid in the E.M. to establish its suitability for analysis.
21. The digestion procedure shall be performed with blanks on a frequent basis to check for contamination while centrifuge tubes are only used once.
22. For 1 in 20 specimens each TEM analysis will be performed by two members of staff independently. In the events of a discrepancy between findings both staff would repeat the procedure in the presence of an audit officer.

While the preparation of asbestos air samples collected on cellulose acetate filters is stated in Procedure 3 [76] as follows :

1. Evaporate carbon onto filters in a coating plant.
2. Place a sheet of sponge in a glass petri dish and soak with acetone.
3. Place a clean TEM grid onto the soaked sponge.
4. Cut a portion of the carboned filter on the grid and leave for 10 minutes.
5. Most of the filter will dissolve leaving the dust sandwiched between the carbon and the remaining filter.
6. Lift the grid off the sponge which is now ready for TEM analysis.



## **4.5 Conclusion**

Because of the chemical and physical complexity of atmospheric pollution particles, their characterization is very complex. There is no simple technique, which will provide a comprehensive description of such material. A careful choice has to be made in selecting the collection method and analytical techniques to be employed for particulate characterization. Of prime importance is the requirement to preserve and realistically measure the properties of the particles sampled from the atmosphere. The sampling procedure itself should not modify the properties of the dust during its collection and should if required capture particles in such manner that both the physical and chemical properties of individual particles can be independently assessed. This presents a challenging task for the environmental engineer and may require novel development of sampling and analytical procedures to provide information for the determination of risks associated with the environmental exposure to fine particulate materials.

## CHAPTER 5 : **RESULTS OF MASS CONCENTRATION ANALYSIS**

### **5.1 Dust Dispersion**

To study the efficiency and performance of the various dust sampling instruments employed in this investigation, generating a well-dispersed dust cloud was important. There are a number of factors to be taken into consideration and a consistent concentration was necessary in generating dust clouds inside the environmental chamber. These include types of dust employed, the manner of dust dispersion, a consistent supply of compressed air, circulation of the dust cloud, and sampler location inside the environmental dust chamber.

In the early stages of laboratory work, coal was used as the dust source for sampling purposes. However, due to its physical characteristics which included the difficulty of producing fine particulate feed samples for dust generation and the inability to produce dust clouds with a consistent concentration, a switch was then made to a limestone sample which was more easily reduced in size by milling to minus 20  $\mu\text{m}$ . Tests performed with dust dispensing system revealed that this material was most suitable for creating dust clouds in the environmental chamber. They also posed no significant health and safety risks whereas coal dust clouds do have a potential to ignite and cause explosions in confined spaces.

In generating the dust clouds inside the environmental dust chamber, the mechanical dust dispenser was used through out all the laboratory work. Initially attempts were made to generate dust clouds with a simple dreschel flask but it was not possible to produce consistent dust clouds in this manner. The environmental chamber was cleaned between sampling periods and the device loaded with limestone dusts to make a uniformly packed plug for dispersion. To compare sampling instruments, it was necessary to ensure that a consistent dust cloud could be generated repeatedly.

The mechanical dust dispenser was connected to an air compressor to generate dust clouds. Before starting dust dispersion, the compressor was switched ON for at least 15 to 20 minutes to fill the air reservoir and ensure that the air compressor would

provide enough air to generate limestone dusts from the mechanical dispenser at a maximum of 50 L/min. During the sampling period, the air compressor was set to supply air at 10 L/min. Of major importance was the requirement to supply a consistent flow of compressed air to the dust dispenser. An inline flow meter was used to check frequently to ensure that this was the case.

Inside the environmental dust chamber, a small fan was used to increase the circulation of the limestone dusts once dispersed from the dispenser throughout the sampling period. This gave more consistent mass concentration results from the samplers. The fan was normally switched ON together with the dispenser when generation of dust was initiated. Once the initial dust generating period (DGP) was completed, any samplers inside the environmental dust chamber were switched ON simultaneously and the sampling period (SP) initiated.

The purpose of having an initial dust generation period was to make sure that before sampling was started, the environmental chamber was charged with limestone dust. Two DGP periods were investigated i.e. 2 and 3 minutes periods. While for sampling, 5 minutes and 10 minutes periods were chosen and the results compared.

All the samplers used are described in Chapter 4. They were connected to individual sampling pumps, some of which were built into the instrument. The description of the flow rates, types of filters and size of the filters used for each sampler have been listed in **Table 4.4**. When operating the personal pumps, the flow rates before and after the sampling were checked to make sure that each sampler operated at the desired flow rate. Inconsistency of the flow rates was found to produce large variations in the mass concentration results determined between samplers. A consideration of these flow rates is also very important in obtaining reliable mass concentration results.

Finally, the location of the samplers inside the environmental dust chamber also played an important part in obtaining consistent results. The height of all samplers had to be adjusted to the same level to overcome possible dust concentration differences in height in the chamber. Once all these factors had been taken into account, more consistent results were obtained from the dust sampling experiments.

The major objective of the operation to produce a dust cloud in the environmental chamber was to ensure a consistent airborne source of dust, which could be reproduced repeatedly to compare the sampling capability of the instruments investigated. No attempt was made to vary the dust cloud concentration.

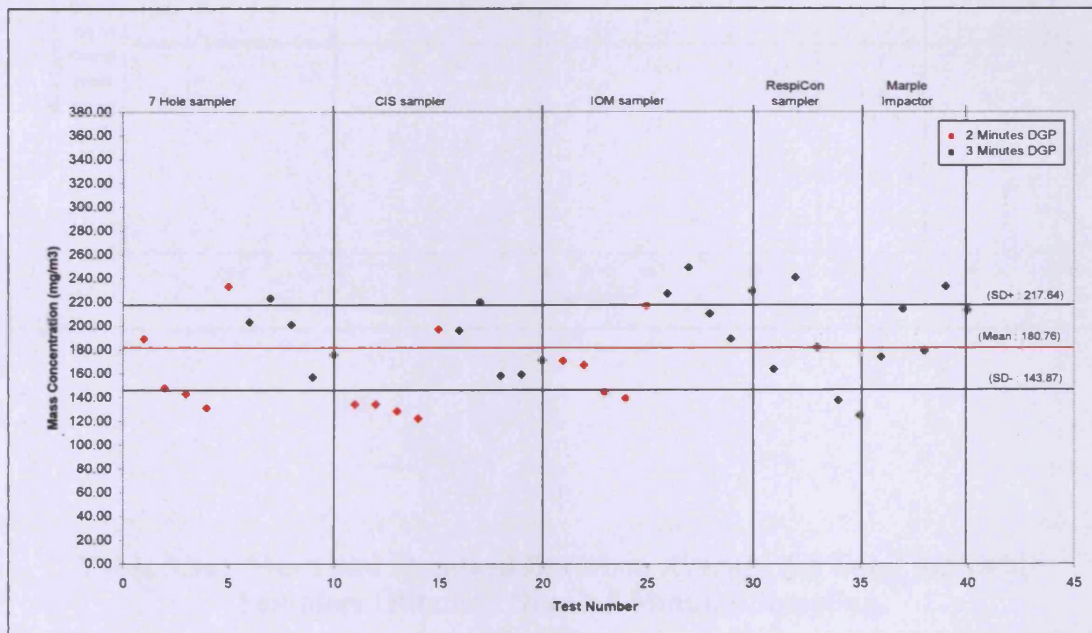
## **5.2 Comparison of Mass Concentration Results Obtained Using Several Total Inhalable Dust Samplers**

In sampling of the limestone dusts inside the environmental dust chamber, several total inhalable sampling samplers were used. These were Seven Holes sampler, Casella Conical Inhalable sampler (CIS), IOM sampler, RespiCon sampler, and the Marple Impactor. The descriptions and operation techniques of these total inhalable samplers were explained in Chapter 4. The instruments were used to sample dust over 5 and 10 minutes sampling periods. These sampling periods were sufficient to provide samples, which were easily determined gravimetrically without over loading the dust filters. The gravimetric results obtained for each instrument are listed in **Appendix C**. These results together with information relating to the volumes of air drawn through the filters were used to calculate mass concentrations of dust in the air sampled. These data are represented for ease of comparison in **Figure 5.1** and **Figure 5.2** for 5 and 10 minutes sampling periods. Also included in the graphs are the values of overall mean and standard deviation (SD) value ranges.

The most obvious difference between the two figures is the fact that the scatter of points about the overall mean value of mass concentration is much greater for samples collected for only 5 minutes rather than 10 minutes. In the two diagrams results calculated from those samples collected after an initial dust generating period of 2 minutes are represented by red points while those collected after a generating period of 3 minutes are represented by green points. Only three instruments were employed to sample dust clouds with initial dust generating periods of 2 and 3 minutes these were the 7 hole, CIS and IOM samplers. From the diagram presented it can be seen that there is an apparent cyclic variation in the results with the 2 minutes dust generating period values being visibly lower than the 3 minutes results. In **Table 5.1a**, the difference is highlighted by a comparison of the mean values of mass concentration calculated for the 2 and 3 minutes DGP for these instruments, these are

159.97 mg/m<sup>3</sup> and 197.94 mg/m<sup>3</sup> respectively with average standard deviation values of 21.50 % and 12.75 % respectively. It is apparent from these results that a 2 minutes dust generating period before sampling was not sufficient to establish an initial dust concentration in the environmental chamber suitable for sampling i.e. the dust concentration had not built up to a large enough value to initiate sampling.

**Figure 5.1 : Variation of Mass Concentration Values Determined Using 5 Total Inhalable Dust Sampling Devices Each Result Obtained Over a 5 Minutes Sampling Period.**



The results for the 10 minutes sampling period are illustrated by **Figure 5.2**. As mentioned previously, there is reduction in the scatter of points in this diagram. The overall average of mass concentration results is larger than that obtained for the 5 minutes sample period while the overall average value of SD is also smaller these being 180.76 mg/m<sup>3</sup> SD 36.88 % for 5 minutes sampling and 197.76 mg/m<sup>3</sup> SD 26.84 % for the 10 minutes sampling results. A similar cyclic variation in the 10 minutes sampling results for the 7 Hole, CIS and IOM samplers was observed for results calculated from the 2 and 3 minutes dust generating period results. From **Table 5.1b**, the average and SD values for the 2 and 3 minutes DGP for the three instruments were 192.84 mg/m<sup>3</sup> SD 9.77 % and 204.02 mg/m<sup>3</sup> SD 13.0 % respectively.



**Figure 5.2 : Variation of Mass Concentration Values Determined Using 5 Total Inhalable Dust Sampling Devices Each Result Obtained Over a 10 Minutes Sampling Period.**

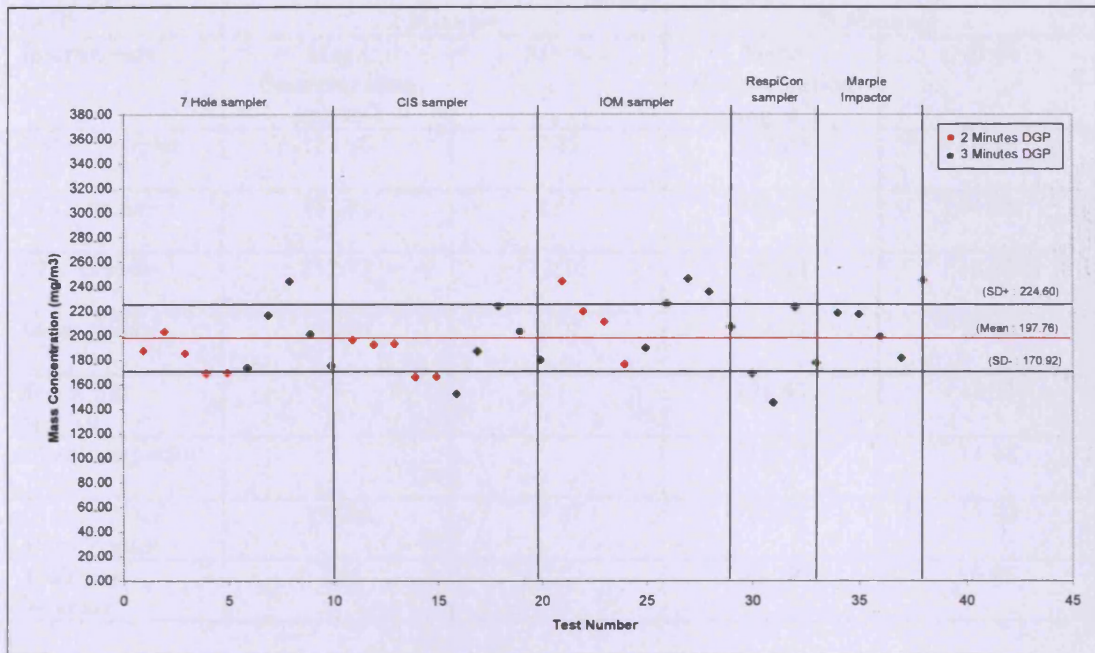


**Table 5.1a : Mean and Standard Deviation Average for Total Inhalable Samplers Obtained Over a 5 Minutes Sampling.**

Sampling DGP	5 Minutes Sampling			
	2 Minutes		3 Minutes	
Instruments	Mean Concentration (mg/m <sup>3</sup> )	SD %	Mean Concentration (mg/m <sup>3</sup> )	SD %
<i>7 Hole sampler</i>	168.80	24.88	192.00	13.39
<i>CIS sampler</i>	143.32	21.27	181.03	14.67
<i>IOM sampler</i>	167.78	18.36	220.80	10.20
<i>Mean Values</i>	159.97	21.50	197.94	12.75
<i>RespiCon sampler</i>			169.72	26.74
<i>Marple Impactor</i>			202.60	12.43
<i>Overall Total Mean Values</i>	159.97	21.50	193.23	15.49
<i>Anderson Impactor</i>			75.79	32.39

**Table 5.1b : Mean and Standard Deviation Average for Total Inhalable Samplers Obtained Over a 10 Minutes Sampling.**

Sampling	10 Minutes Sampling			
	2 Minutes		3 Minutes	
DGP	Mean Concentration (mg/m <sup>3</sup> )	SD %	Mean Concentration (mg/m <sup>3</sup> )	SD %
<i>7 Hole sampler</i>	182.90	7.75	202.00	14.68
<i>CIS sampler</i>	182.91	8.41	189.31	14.11
<i>IOM sampler</i>	212.71	13.16	220.74	10.22
<i>Mean Values</i>	192.84	9.77	204.02	13.00
<i>RespiCon sampler</i>			178.57	18.31
<i>Marple Impactor</i>			212.10	11.18
<i>Overall Total Mean Values</i>	192.84	9.77	200.54	13.70
<i>Anderson Impactor</i>			67.29	39.96

The difference between the 2 and 3 minutes dust generating periods is not as pronounced for the results calculated from 10 minutes samples. This to be expected as the dust concentration in the environmental chamber would tend to stabilize over the longer dust dispensing period, added airborne dust from the generator being balanced by dust deposition within the chamber. The 10 minutes sampling results indicate it is possible to produce a consistent dust cloud, which can be sampled over short periods of time to compare the results provided by different sampling instruments.

The inhalable dust sampling results obtained for the individual instruments investigated are illustrated by **Figure 5.3** and **5.4**. In **Figure 5.3**, the results calculated from 5 minutes sampling periods some with initial dust generating periods of 2 and 3 minutes show that the average results for each instrument are very comparable. The exception being the average value obtained for the Anderson Impactor which is much lower. This difference can be explained by a comparison of the sampling rates of the various instruments. In order there were as follows :



7 Hole sampler	: 2.0 L/min
CIS sampler	: 3.5 L/min
IOM sampler	: 2.0 L/min
RespiCon sampler	: 3.11 L/min
Marple Impactor	: 2.0 L/min
Anderson Impactor	: 28.3 L/min

The volume of the environmental chamber is 0.541 m<sup>3</sup> and the dust volume generated per minute was set at 10.0 L/min. This means that when operating the Anderson Impactor with a sampling rate at 28.3 L/min it was removing dust from the chamber faster than it was being generated. This is illustrated by comparing the results for that instrument obtained from the 5 and 10 minutes sampling periods which were 75.79 mg/m<sup>3</sup> SD 32.39 % and 67.29 mg/m<sup>3</sup> SD 39.96 % respectively. The larger sampling period effectively reducing the dusts concentration in the environmental chamber.

**Figure 5.3 : Average Mean and Standard Deviation Values of Mass Concentration of 6 Total Inhalable Dust Sampling Devices Over 5 Minutes Sampling Period.**

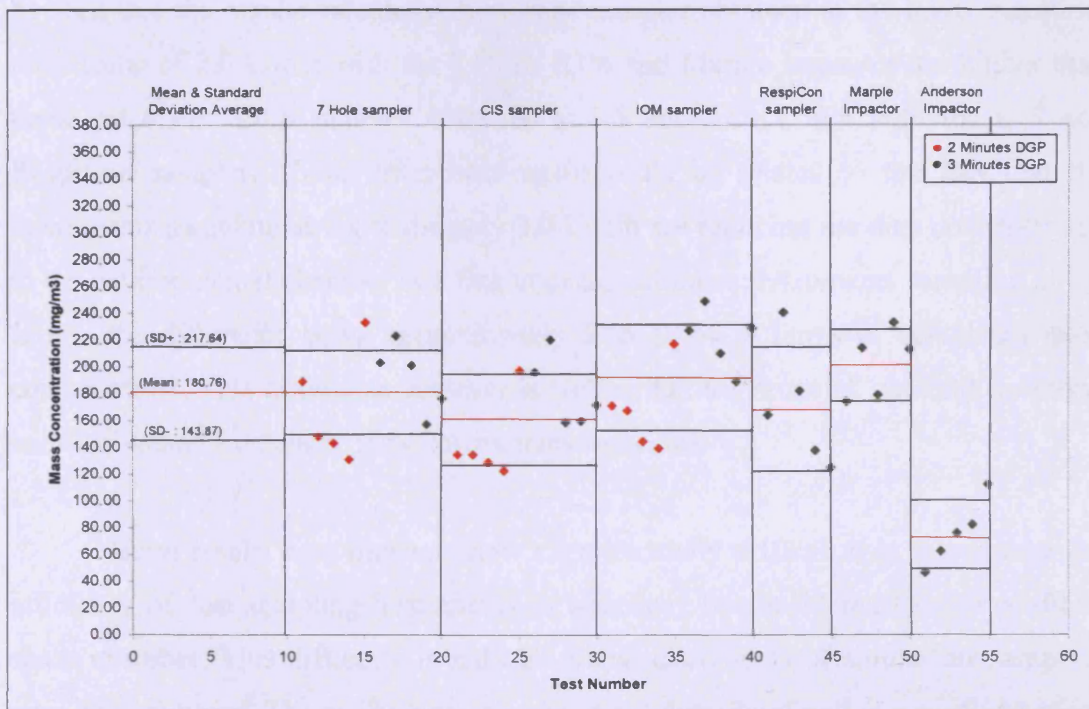
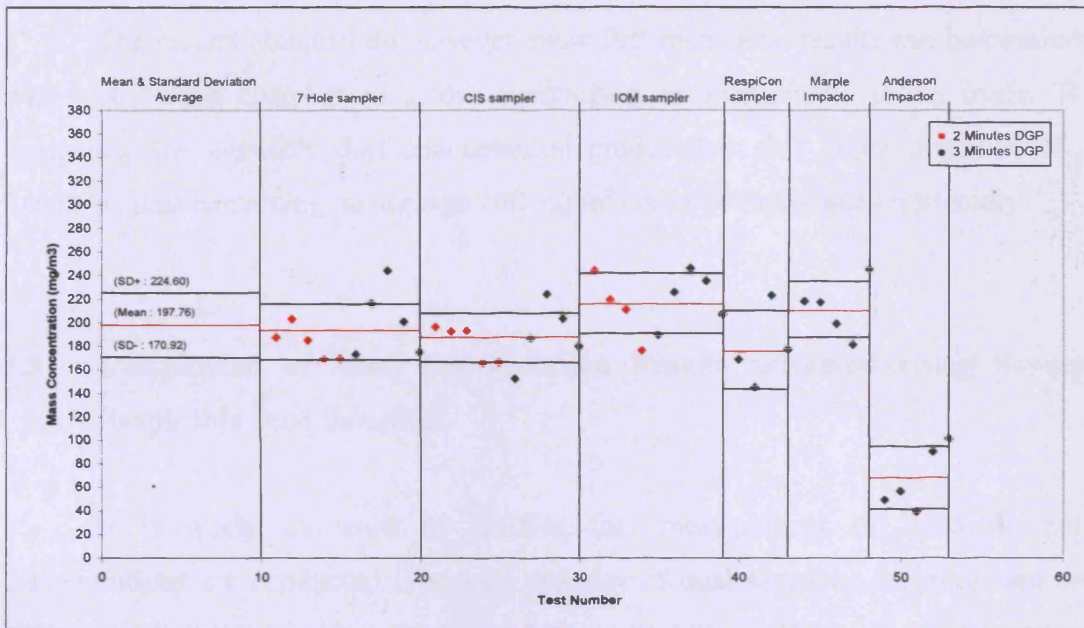


**Figure 5.4 : Average Mean and Standard Deviation Values of Mass Concentration of 6 Total Inhalable Dust Sampling Devices Over 10 Minutes Sampling Period.**



From **Table 5.1a** and **5.1b**, the results obtained for the instruments with the lower sampling rates can be seen to be much more comparable. However, again it can be seen that the results calculated from dust sampler obtained at the lower sampling rates value of 2.0 L/min with the 7 Hole, IOM and Marple Impactor are higher than those calculated from samples collected at 3.5 and 3.11 L/min with the CIS and RespiCon sampler. These differences again could be related to the fact that the instruments sampling at approximately 3.0 L/min are reducing the dust concentration in the environmental chamber at a rate in excess of those instruments sampling at 2.0 L/min, the difference being approximately 5 to 10 % in terms of calculated mass concentration. This difference however is well within the range of standard deviation values obtained from each of the instruments individually.

These results now illustrate how experimentally difficult it is to compare the efficiency of dust sampling instruments in what may be considered to be a confined space chamber. This difficulty is reduced when instruments of similar air sampling rates are compared. The production of a consistent dust cloud within a confined space chamber can also be a problem. The ideal situation for instrumental comparison



purposes would be to compare them in a through flow system where dust is generated continuously at one end of a chamber and removed at the other.

The results obtained do however show that repeatable results can be obtained with a confined chamber to allow comparison of instruments to be made. By comparing the inhalable dust concentration produced in this experimental work a limestone dust containing on average  $200 \text{ mg/m}^3$  could be reproduced repeatedly.

### **5.3 Comparison of Mass Concentration Results Obtained Using Several Respirable Dust Samplers.**

It is rarely the case in practice that measurement of inhalable dust concentrations are conducted. The vast majority of dual sampling measurement are taken to indicate respirable or thoracic dust concentration. These measurements are taken usually for control purposes but are often employed to perform risk analysis estimates in situations where environmental pollution has occurred. From the results of instrumental sampling of the inhalable fraction of experimental dust clouds created in the laboratory environmental chamber it was established that a repeatable dust concentration conditions could be created. These conditions could therefore be employed to compare the sampling efficiency of a number of samplers designed to collect size selected respirable and thoracic dust samples. An identical experimental procedure was adopted to that need for collecting inhalable samples. Dust samples were collected for 5 and 10 minutes periods employing 2 and 3 minutes initial dust generating periods. **Figure 5.5** and **5.6** illustrated the calculated mass concentration of respirable dust obtained from samplers taken over 5 and 10 minutes sampling periods. Again those results relating to 2 minutes and 3 minutes dust generating periods are represented by red and green data points respectively.

**Figure 5.5 : Variation of Mass Concentration Values Determined Using 5 Respirable Dust Sampling Devices Each Result Obtained Over a 5 Minutes Sampling Period.**

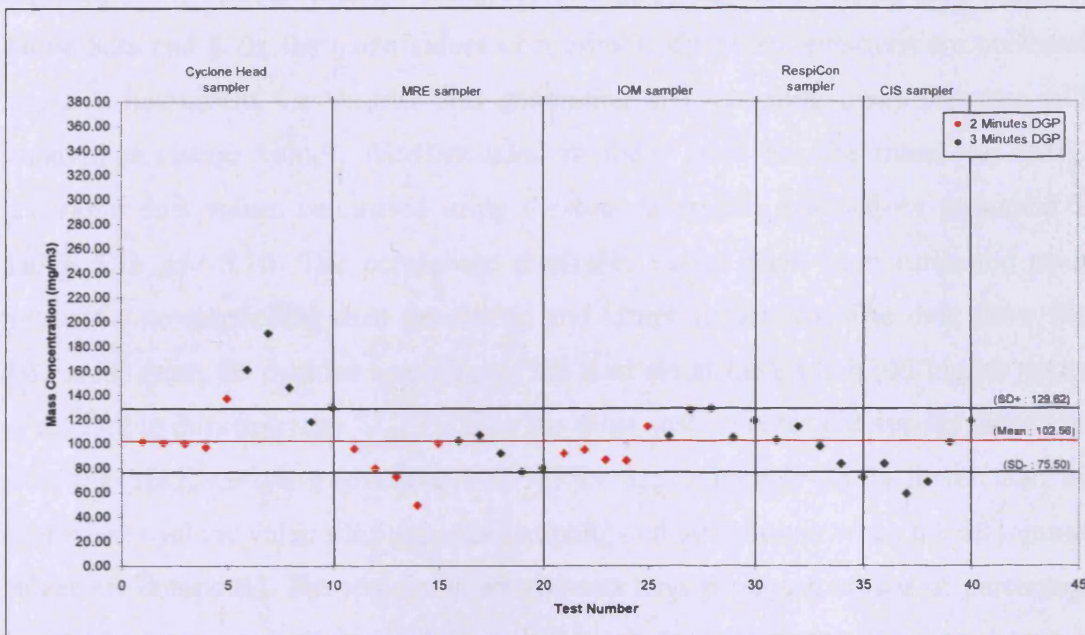
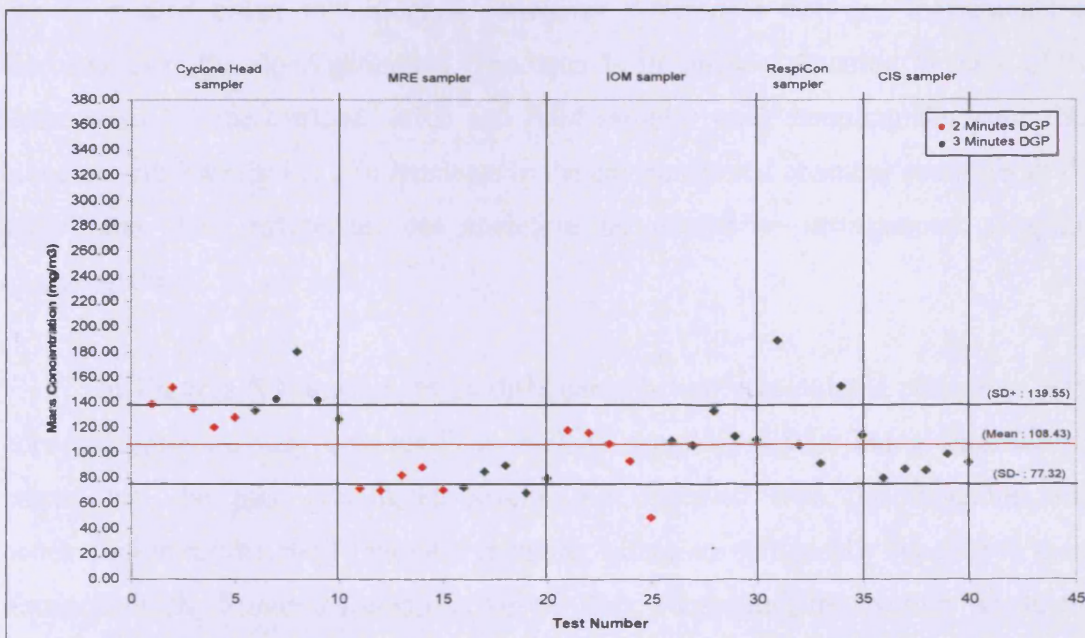


**Figure 5.6 : Variation of Mass Concentration Values Determined Using 5 Respirable Dust Sampling Devices Each Result Obtained Over a 10 Minutes Sampling Period.**



A similar cyclic response can be observed when comparing the instrumental results obtained for the 2 and 3 initial dust generating periods a fact which is to be expected if the results from the inhalable dust sampling experiments are correct. In **Table 5.2a** and **5.2b**, the mean values of respirable dust concentrations are presented for each instrument for various dust generating and sampling times together with standard deviation values. Also included in these table are the mean percentage respirable dust values calculated using the total inhalable dust values presented in **Table 5.1a** and **5.1b**. The percentage respirable values have been estimated using results for corresponding dust generating and sampling periods. The data show that the results from the cyclone sampling of the dust cloud have produced higher values of respirable dust (average 71.7 %) than the other instruments. The results calculated from the MRE samplers (average 44.2 %) are approximately 25 % lower than the equivalent cyclone value for 5 minutes sampling and 30 % lower when the 10 minutes values are compared. The remaining instruments have produced values of percentage respirable dust concentrations which fall between these average values as shown in the tables with values ranging from 44 to 60 % respirable. The variation in calculated mass concentration values of respirable dust are much larger than variations observed in the concentration of inhalable dust samplers previously discussed. The differences can be related either to collection efficiency differences between instruments or fluctuations in the cloud generated. The latter is an unlikely situation as three of the instruments i.e. the cyclone, MRE and IOM sampler were sampling the same dust cloud simultaneously i.e. 3 instruments in the environmental chamber sampling at the same time. The differences can therefore be related to instrumental sampling characteristics.

In **Figures 5.7** and **5.8**, these differences between calculated respirable mass concentrations are very obvious. The cyclone sampling results being significantly larger than the other calculated results. As observed with the inhalable dust concentration results, the 10 minutes sampling values are statistically superior to those obtained by the 5 minutes sampling period tests. Neglecting the cyclone result, the overall average of % respirable dust determined from the 10 minutes sampling and 3 minutes initial dust generating period was 52.5 % with a range of values from 39.5 to 65.2 %. The cyclone result producing a value of 72.4 %. The variation in these %

respirable dust values can be mainly explained by the mechanism of dust collection for each of the instruments employed.

**Table 5.2a : Mean and Standard Deviation Average for Respirable Samplers Obtained Over a 5 Minutes Sampling.**

Sampling	5 Minutes Sampling					
DGP	2 Minutes			3 Minutes		
Instruments	Mean Concentration (mg/m <sup>3</sup> )	SD %	Mean Respirable %	Mean Concentration (mg/m <sup>3</sup> )	SD %	Mean Respirable %
<i>Cyclone sampler</i>	107.45	15.59	67.17	149.29	19.02	77.26
<i>MRE sampler</i>	79.76	25.45	49.86	91.68	14.57	47.45
<i>IOM sampler</i>	94.80	12.15	59.26	117.32	10.07	60.72
<i>Mean Values</i>	94.00	17.73	58.76	119.43	14.55	61.81
<i>RespiCon sampler</i>				93.90	17.56	48.59
<i>CIS sampler</i>				86.25	28.09	44.64
<i>Overall Total Mean Values</i>	94.00	17.73	58.76	107.69	17.86	55.73

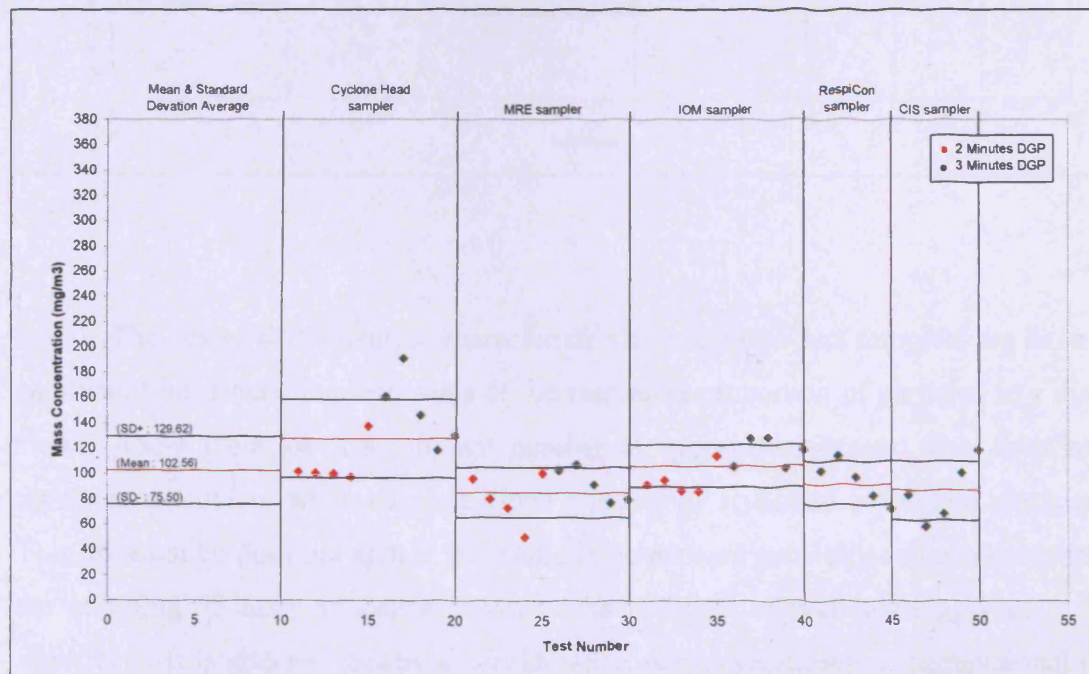
**Table 5.2b : Mean and Standard Deviation Average for Respirable Samplers Obtained Over a 10 Minutes Sampling.**

Sampling	10 Minutes Sampling					
DGP	2 Minutes			3 Minutes		
Instruments	Mean Concentration (mg/m <sup>3</sup> )	SD %	Mean Respirable %	Mean Concentration (mg/m <sup>3</sup> )	SD %	Mean Respirable %
<i>Cyclone sampler</i>	134.91	8.72	69.96	145.16	14.32	72.38
<i>MRE sampler</i>	76.88	10.80	39.87	79.28	11.13	39.53
<i>IOM sampler</i>	96.76	29.27	50.18	114.62	9.47	57.16
<i>Mean Values</i>	102.85	16.26	53.33	113.02	11.64	56.36
<i>RespiCon sampler</i>				130.73	30.40	65.19
<i>CIS sampler</i>				89.12	7.87	44.44
<i>Overall Total Mean Values</i>	102.85	16.26	53.33	111.78	14.64	55.74



The MRE sampler employs a horizontal plate elutriator to remove what are considered to be non respirable dust particles by sedimentation from a non turbulent flow of air. The interference with airborne particulates in the process of sampling can therefore be considered to be minimal. It is appropriate therefore that this instrument produced the lower calculated mass value of respirable dust. The IOM and CIS sampler employ foam filters to remove non respirable particles from air being drawn into the samplers. The IOM employs a single foam filter while the CIS utilizes a two stages foam filtration arrangement. The air flow through these foam filters can not be considered to be non turbulent due to the range of pore sizes and non linear direction of the pores. Particles sampled will therefore be subjected to a very of sheer forces in pores of different dimensions and considerable inertial forces due to changes in direction of the air flow through the foam. There is therefore considerable opportunity for particles to collide and impact on surfaces in the foam thus allowing aggregates of particles, which may be non respirable to break up into smaller respirable size particles.

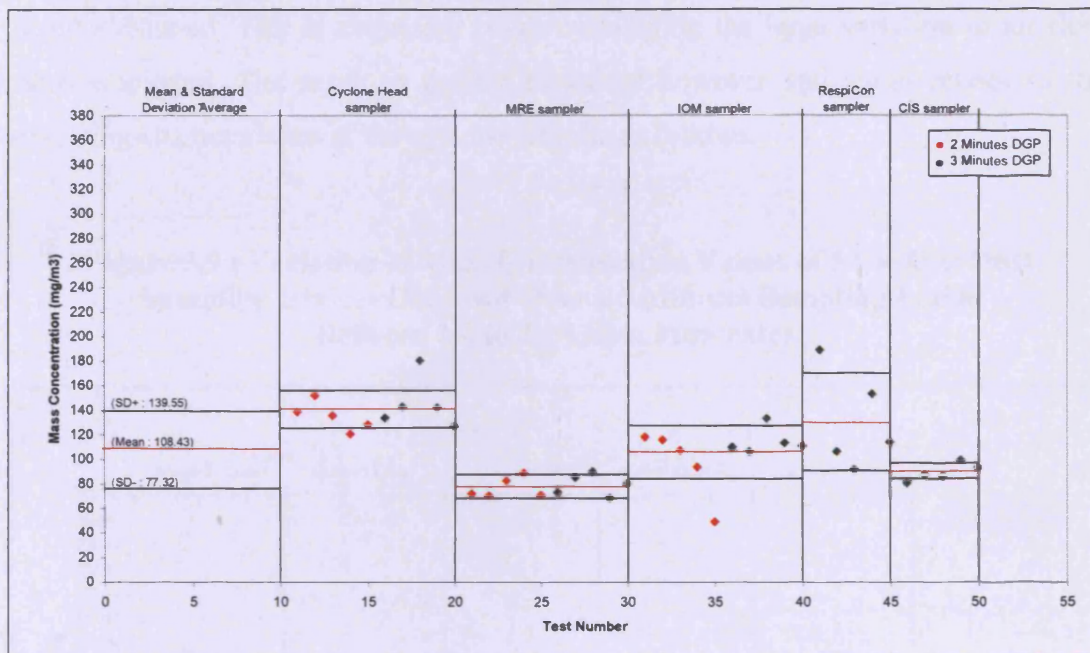
**Figure 5.7 : Average Mean and Standard Deviation Values of 5 Respirable Dust Sampling Devices Each Result Obtained Over a 5 Minutes Sampling Period.**





The cyclone sampler represent a unique device which relies upon centrifugal force to separate respirable and non respirable particles. This is achieved in the cyclone design of the sampler which subjects airborne particles to considerable shear forces within a rapidly rotating air flow. There is the opportunity to dramatically break up aggregates of particles into smaller aggregates or individual particles thus reducing them to a respirable size as opposed to inhalable or thoracic dimensions.

**Figure 5.8 : Average Mean and Standard Deviation Values of 5 Respirable Dust Sampling Devices Each Result Obtained Over a 10 Minutes Sampling Period.**



The design and operating characteristics of respirable dust samplers are have a significant influence upon estimates of the respirable proportion of particles in a dust clouds where there are a significant number of aggregates present. This does not represent a problem when the dust cloud consists of separated individual particles. This information does not appear to be taken into account generally when considering the sampling of dusty atmospheres where the presence of particulate aggregates is significant. It is also not usually a consideration when application of occupational or environmental control values are being enforced.



The use of cyclone samplers for monitoring personal exposure has been extensive in industry. But its unique sampling characteristics require it to be operated with care. The cyclone sampler has no moving parts but its efficient operation is very dependant upon sampling at the designed air sampling rate. To investigate what effect deviation from the designed sampling rate might have upon the performance of cyclone, a series of tests were performed in which the sampling rate was varied. Samples were collected using five air sampling rates varying from 1.6 to 2.4 L/min with the designed sampling rate for the cyclone being 2.2 L/min. These tests were repeated 5 times. The results obtained are illustrated by **Figure 5.9**, **Figure 5.10** and **Table 5.3**. It can be seen that there is very little variation in the mass concentration results obtained. This is surprising result considering the large variation in air flow rates employed. The result is readily explained however and again relates to the operating characteristics of the cyclone sampler as follows.

**Figure 5.9 : Variation of Mass Concentration Values of 5 Cyclone Dust Sampling Devices Obtained Over a 5 Minutes Sampling Period Between 1.6 to 2.4 L/min Flow rates.**

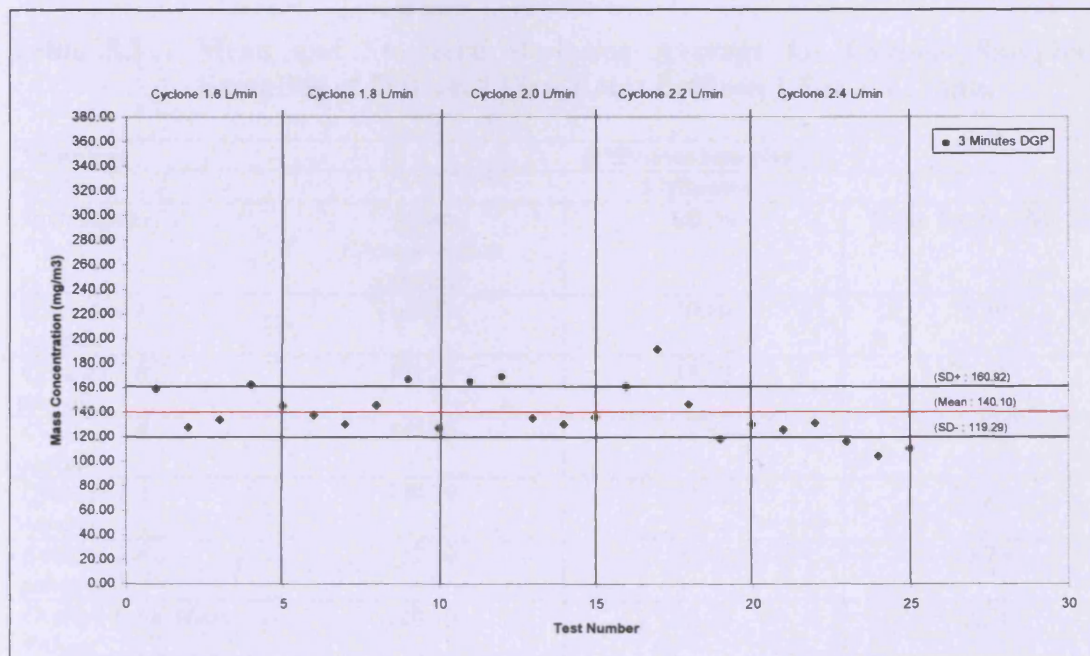


**Figure 5.10 : Average Mean and Standard Deviation Values of Mass Concentration Values of 5 Cyclone Dust Sampling Devices at Different Flow Rates Between 1.6 to 2.4 L/min.**

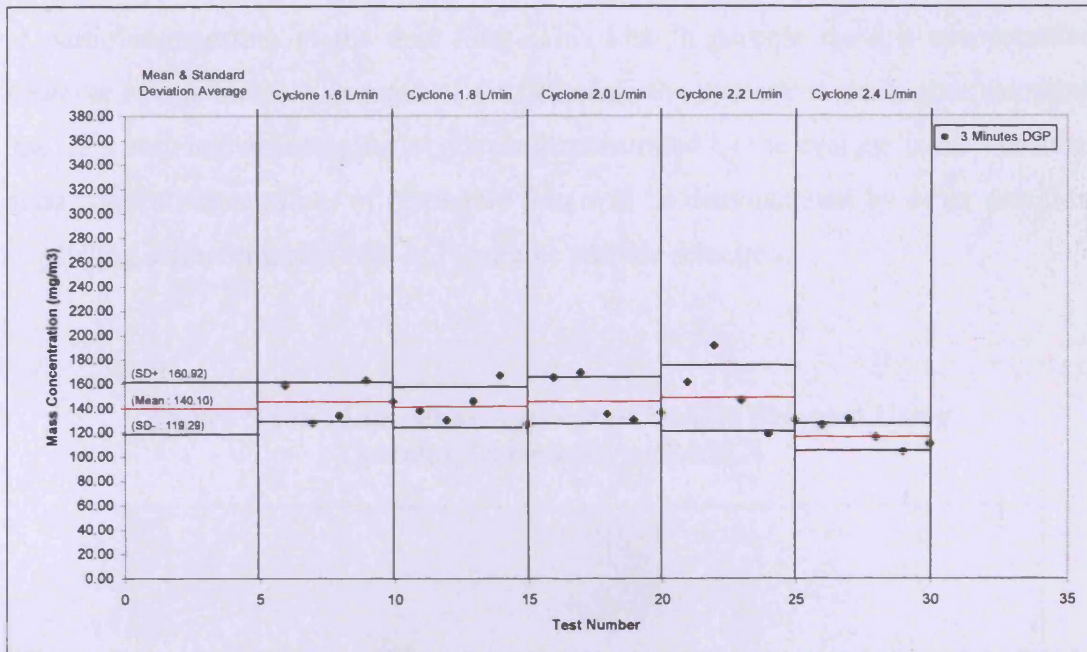


**Table 5.3 : Mean and Standard Deviation Average for Cyclone Samplers Sampling at Different Flow Rates Between 1.6 to 2.4 L/min.**

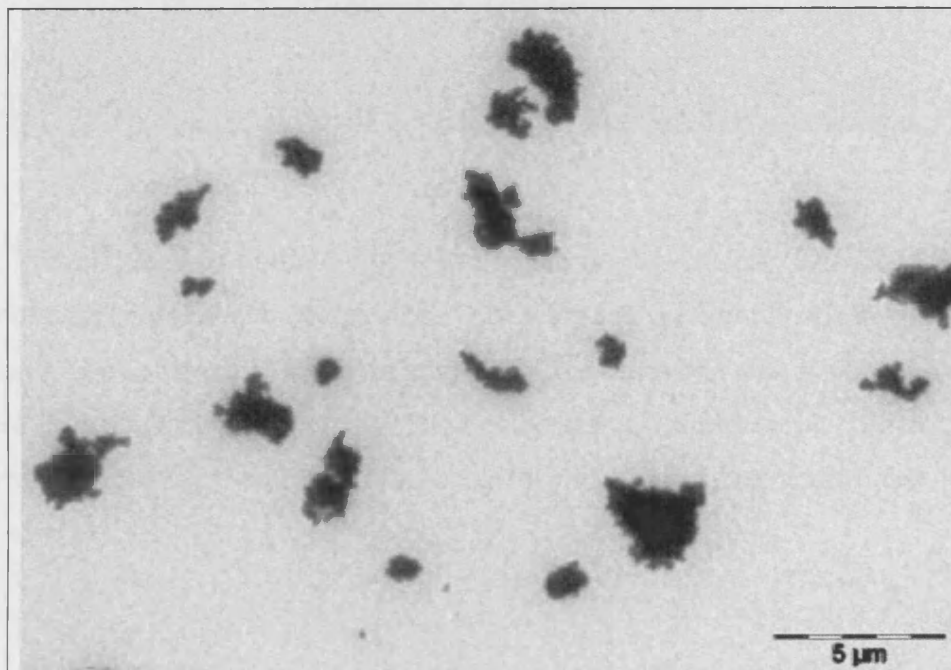
Sampling DGP	5 Minutes Sampling		
	3 Minutes		
Instruments	Mean Concentration (mg/m3)	SD %	Mean Respirable %
<i>Cyclone 1.6 sampler</i>	145.50	10.46	75.30
<i>Cyclone 1.8 sampler</i>	141.34	11.28	73.15
<i>Cyclone 2.0 sampler</i>	147.00	12.55	76.08
<i>Cyclone 2.2 sampler</i>	149.29	19.02	77.26
<i>Cyclone 2.4 sampler</i>	117.39	9.33	60.75
<i>Overall Total Mean Values</i>	140.10	12.53	72.51

When sampling flow rates are reduced, the size selective action of the cyclone is reduced allowing larger particles to be collected on the dust filter. A reduction in



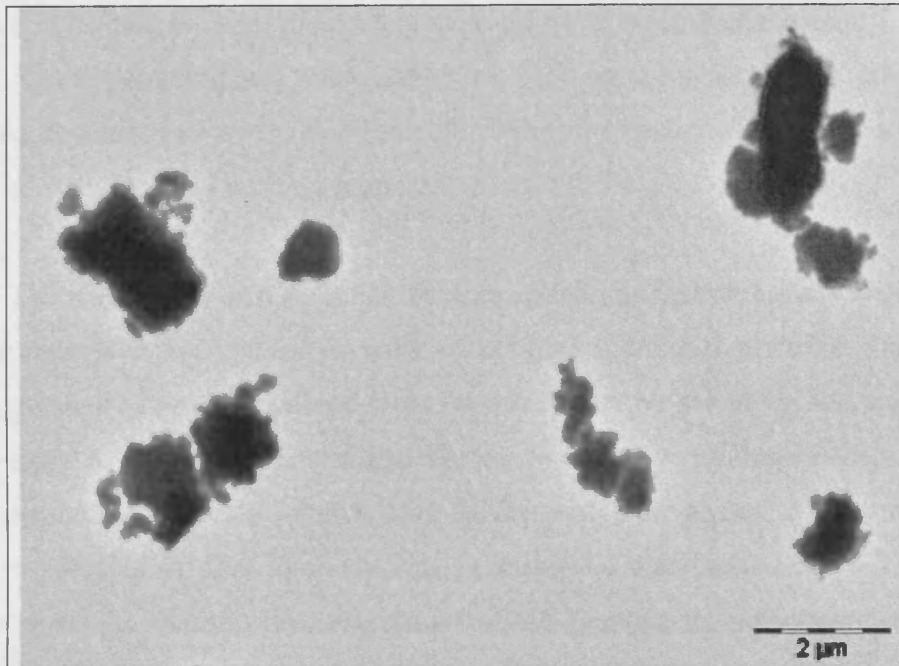
the volume of air and therefore particle mass is therefore balanced by an increase in the proportion of the dust reporting to the filter. When the air flow rate exceeds the designed value, the size of selective action of the cyclone increases reducing the size of particles reporting to the dust filter. This loss in particle mass is compensated however by the increase in mass of dust entering the cyclone at the higher sampling rate. It is certain that instrumental effects demonstrated by the cyclone upon measured mass concentration values of respirable dust will be demonstrated by other samplers employing different techniques of respirable particle selection.

**Figure 5.11a : Limestone Aggregates Images Sampled Using Thermal Precipitator at 2,050 X.**



In **Table 5.2b**, the RespiCon dust sampler produced a respirable dust result which was higher than the IOM and CIS sampler at 65.2 % approaching that of the cyclone. This value again been influenced by the collection characteristics of the device in which inertial and shear forces are employed to separate particles into specific aerodynamic size fractions. Aggregates will be dispersed during this process producing fewer particulate phases and an increase in respirable sizes of particles.

**Figure 5.11b : Limestone Aggregates Images Sampled Using Thermal Precipitator 4,400 X.**



The presence of particle aggregates in the limestone dust dispersed into the experimental environmental chamber has been observed and are illustrated by **Figure 5.11a and 5.11b.**, which is photo micrograph of the limestone dust collected using a Thermal Precipitator in the chamber. This instrument collects airborne particles in an unaltered state so that the physical characteristics of actual airborne particles can be observed.

#### **5.4 Comparison of the Particulate Size Distributions of Inhalable, Thoracic, and Respirable Dust Samples.**

Although mass concentration is the parameter most commonly used to monitor and characterize airborne particulates, of more significance from a health perspective is the particle size distribution of the dust. It is the size distribution of particulates, which dictate how far into the respiratory tract they can penetrate where they will be deposited and how they will be retained to produce a biological response. The toxicity of dust particulates produced from a particular material is therefore size dependent

varying from completely non toxic to highly toxic with only a small change in aerodynamic diameter from 10 to 1  $\mu\text{m}$ . Determination of airborne particle size distribution of dust are very difficult to measure for a number of reasons. The first is related to the sampling and presentation of dust particles for sizing purposes. A sampling device is required which can collect airborne particles and allow them to be examined individually for sizing purposes.

The majority of dust sampling devices collecting dust on a mass basis require that the sample be redispersed in order to examine individual particles. This means that aggregates of particles, which have been collected by sampling instruments will be dispersed and the original size distribution of the airborne dust particles altered. Resuspension in water may remove some of the particulate phases by dissolution, also compact particles of clay minerals will be dispersed and broken down into much smaller particulate phases. It can be plainly stated therefore that any interference with airborne particulate material after sampling will produce minor to major changes in its physical characteristics especially size distribution.

Besides the problems associated with the collection of airborne particles for sizing purposes difficulties can arise when considering how the dimensions of the particles themselves are to be obtained. A microscopic technique has to be employed which can either be light or electron optical in nature. Light microscopic techniques have a limited application to the sizing of airborne particles because of resolution problems, which allow the sizing of the smallest particles to a practical limit of approximately 0.5  $\mu\text{m}$ . With electron optical techniques, particles of all sizes can be observed. Sizing of individual particles is a tedious process, which is impractical because of the irregular shapes displayed by dust particles. Sizing is therefore performed by grouping particles into size fractions defined by regular subdivision of the size range over which the sizes of particles occur. The choice of particle sizing parameter can then be defined (e.g.: equivalent circular diameter, maximum length, chord length in a particular direction etc.) to meet the objectives of the particle sizing investigation. For the measurement of the limestone dust, the parameter equivalent circular diameter was chosen to define the size of particle as they were compact in appearance and a circle best described their average shape. For the actual sizing of particle images, an image analysis software program was utilized to interpret magnified

images collected with a C.C.D. camera attached to a transmission electron microscope (TEM). Dust samples were prepared for examination with the TEM as explained in Chapter 4. The TEM was chosen for producing pictures of particles as they were black images of particles on a white background, which were convenient to size. Optical sizing was not considered for the limestone dust as many of the particles were translucent and did not provide sufficiently contrasting images for particle sizing purposes.

#### **5.4.1 Calibration of the Transmission Electron Microscope System and Sizing Software.**

Before utilizing the TEM and image analysis software to size preparations of limestone dust samples the system was calibrated using a latex particle standard. The standard consisted of spherical latex particles with a quoted mean particle diameter of 1.036  $\mu\text{m}$  and SD 0.0161  $\mu\text{m}$ . These particles are illustrated by **Figure 5.12a** and **5.12b**. Images of the spheres were recorded at a magnification of 2100 X and these were used to calculate mean and standard deviation values for the particles to compare with the quoted values of the standard. The variation in the particle size distribution obtained from the standard are illustrated by **Figure 5.13** and **5.14** in which the particles can be seen to be very closely distributed in size. The presence of some broken spheres and overlap of spherical particles produced small tails in the to fine and coarse ends of the size distribution curve but the bulk of the particles were observed to occur between 0.9 to 1.0  $\mu\text{m}$  in size. The average value obtained from the instrumental configuration was 0.951  $\mu\text{m}$  with a standard deviation of 0.045  $\mu\text{m}$ . This is a lower mean value than that quoted for the latex standard, which was 1.036  $\mu\text{m}$ . The difference was small and would have little effect upon the determination of the size distribution of the airborne limestone dust particles, which were to be sized using this instrumental configuration. The difference between the measured and quoted size of the latex particles was 8.2 %.



**Figure 5.12a :Standard Latex Spheres Image Taken Using TEM at 2,100 X Magnification Before Analyse using the AnalySIS Software.**

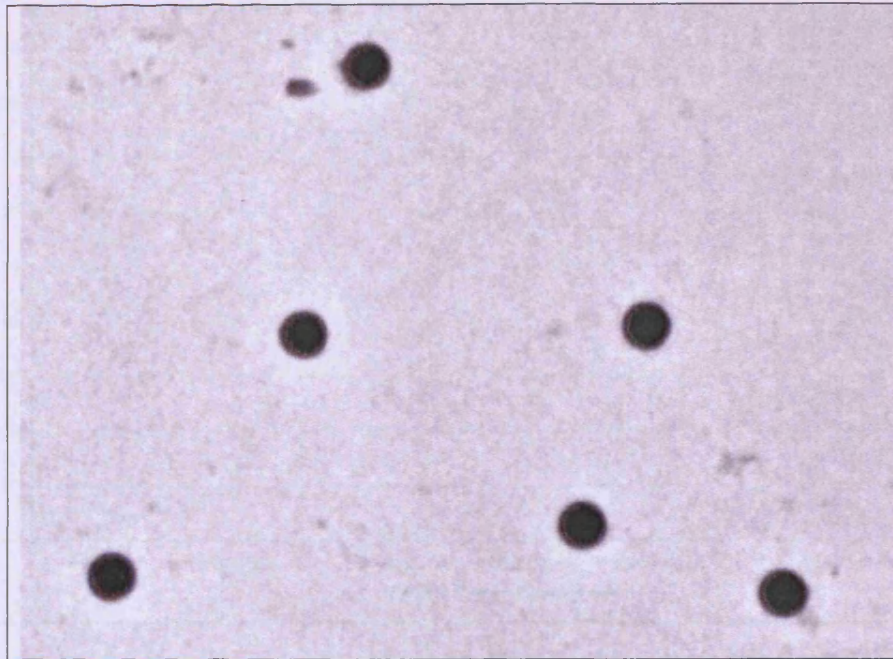


**Figure 5.12b : Standard Latex Spheres Image Taken Using TEM at 2,100 X Magnification After Analyse using the AnalySIS Software.**

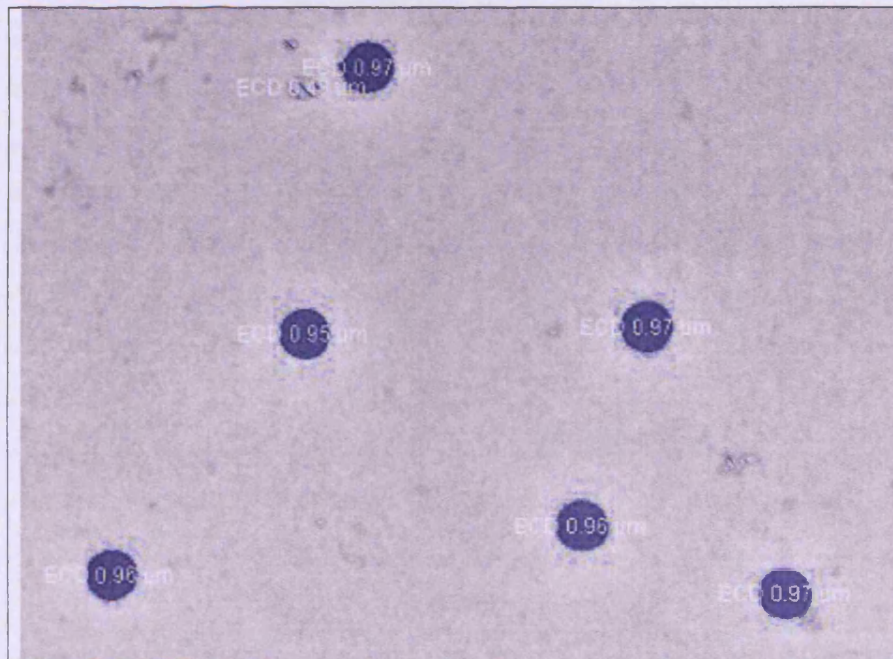


**Figure 5.13 : Latex Sphere Standard Particle Number Frequency Distribution.**

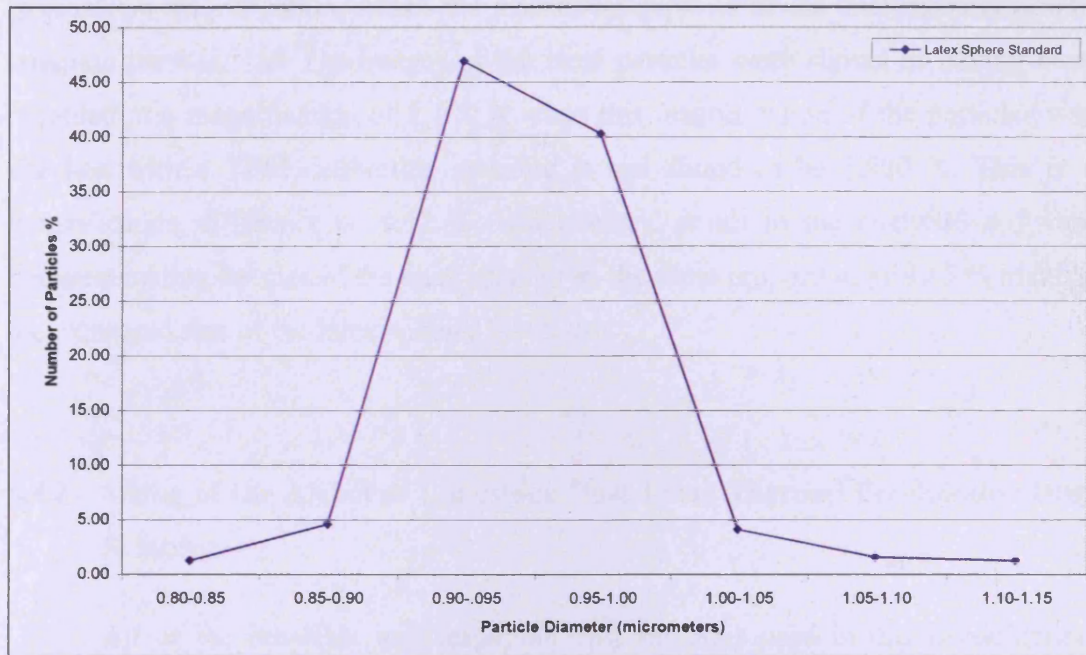
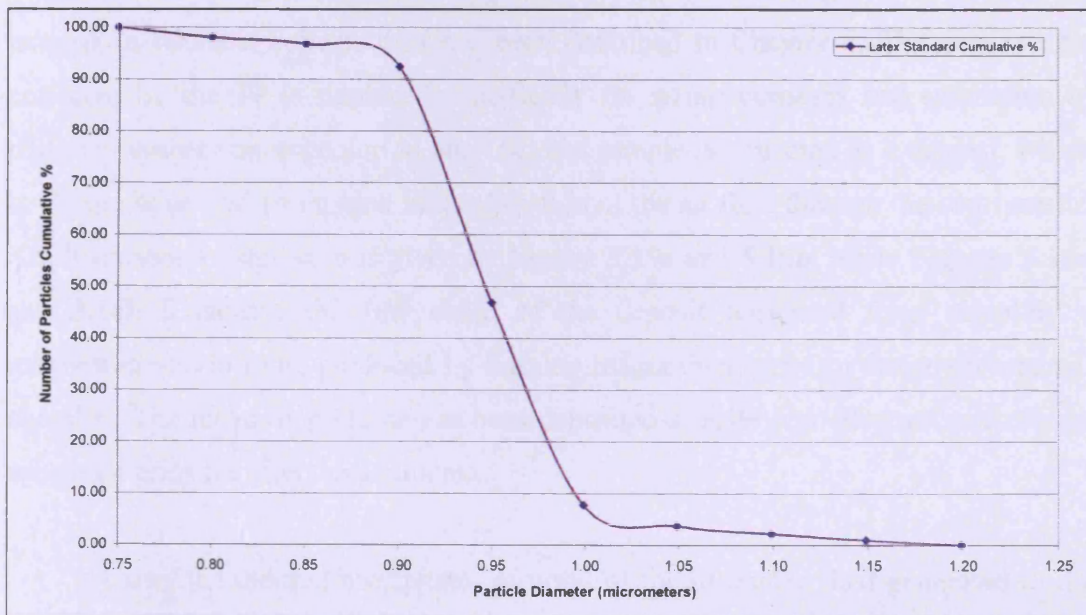


**Figure 5.14 : Latex Sphere Standard Particle Number Distribution Cumulative %.**





The major portion of this difference can be related to the value of electron microscope magnification, which the instrument supplies to the analysis software to compute particle size. The images of the latex particles were shown as having been recorded at a magnification of 2,100 X when this magnification of the particles was checked with a TEM calibration standard it was found to be 1,900 X. This is a magnification difference of 9.52 %, which would result in the analySIS software underestimating the size of the latex spheres by the same proportion of 90.5 % making the measured size of the latex spheres 0.905  $\mu\text{m}$ .

#### **5.4.2 Sizing of the Airborne Limestone Dust Using Thermal Precipitator Dust Samples.**

All of the inhalable and respirable dust samplers used in this investigation were designed for gravimetric sampling. They were not therefore capable of producing samples of airborne dust for sizing purposes. In order to obtain some measure of the true size distribution of the limestone dust airborne cloud produced in the environmental chamber, a thermal precipitator was employed to collect a sample directly onto prepared electron microscope sample grids so that airborne particulates could be examined in an individual and unaltered state. The design of the TP and the manner in which it collects dust has been described in Chapter 4. The dust sample collected by the TP is produced specifically for sizing purposes and estimation of particle number concentration in air. The dust sample is collected as a deposit, which is 10 mm wide and 1 mm long in the direction of the air flow through the instruments. An illustration of this strip is given by **Figure 5.15a** and **5.15b**, while **Figures 5.16a** and **5.16b** illustrated the fine detail of the deposit preserved from sampling a magnesium oxide fume produced by burning magnesium metal in the environmental chamber. The metal oxide fume has been deposited directly onto electron microscope specimen grids for direct examination.

Using the thermal precipitator samples of the limestone dust generated in the environmental chamber were collected and they are illustrated by **Figure 5.11**. The presence of aggregates is apparent in the images recorded while fine particles less than 0.3  $\mu\text{m}$  are absent. A series of images were recorded and particles sized in an identical

manner to that for the latex particles. The results obtained for the sizing are shown in **Figure 5.17** and **Figure 5.18**. In **Figure 5.17** the frequency size distribution of the experimental cloud is compared with sizing data obtained from samples collected with three inhalable dust samplers. To obtain the latter data the limestone dust collected by the three instruments was first dispersed in water to prepare a sample for sizing. This has resulted as shown in the **Figure 5.18** in a large increase in the percentage of fine (0.3 to 0.5  $\mu\text{m}$ ) particles if the sizing data for the three samplers is corrected for the increase by decreasing the percentage of fine particles to that of the thermal precipitator and normal sample 20 to 35 % increased values than a result illustrated by **Figure 5.17** is obtained. This reveals that the comparison of frequency size distribution is very similar for the four instruments the largest difference again being in the second fine size fraction, which was not corrected. The thermal precipitator sizing results have been used to compare sizing data obtained from the three inhalable dust samplers investigated and to establish the most probable size distribution of the dust cloud produced in the environmental chamber.

**Figure 5.15a : Magnesium Oxide Particles End of Thermal Precipitator Deposit taken using PCOM.**

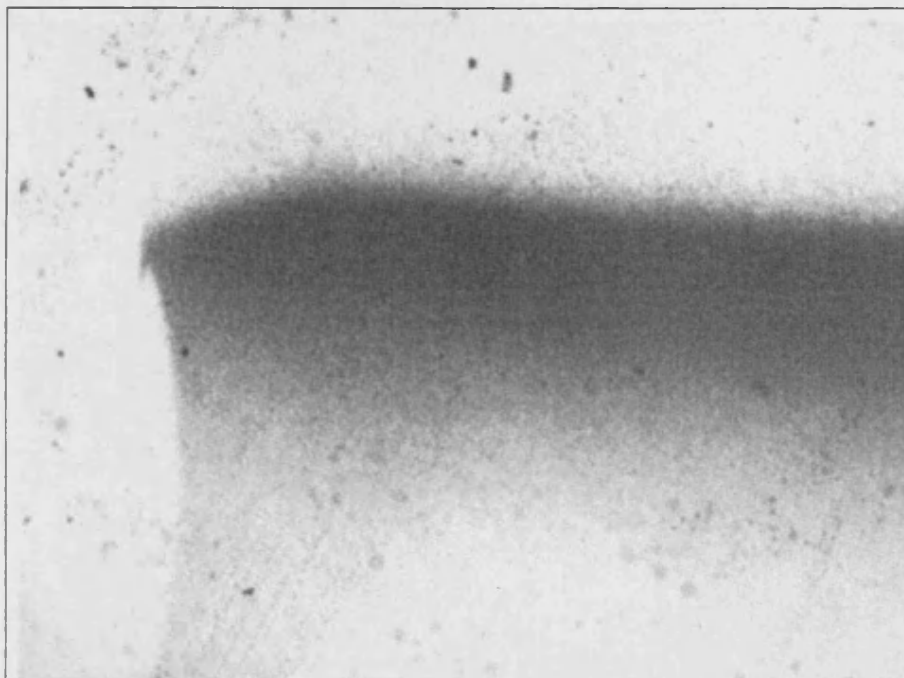


**Figure 5.15b : Magnesium Oxide Particles Middle of Thermal Precipitator Deposit taken using PCOM.**

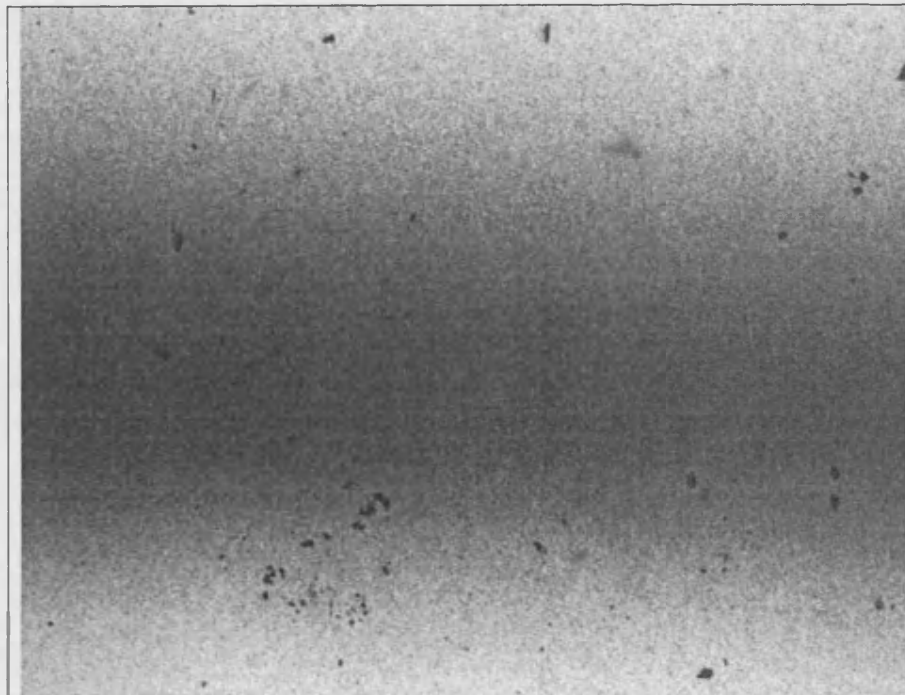


**Figure 5.16a : Magnesium Oxide Particles Sampled using Thermal Precipitator at 4,400 X taken using TEM.**

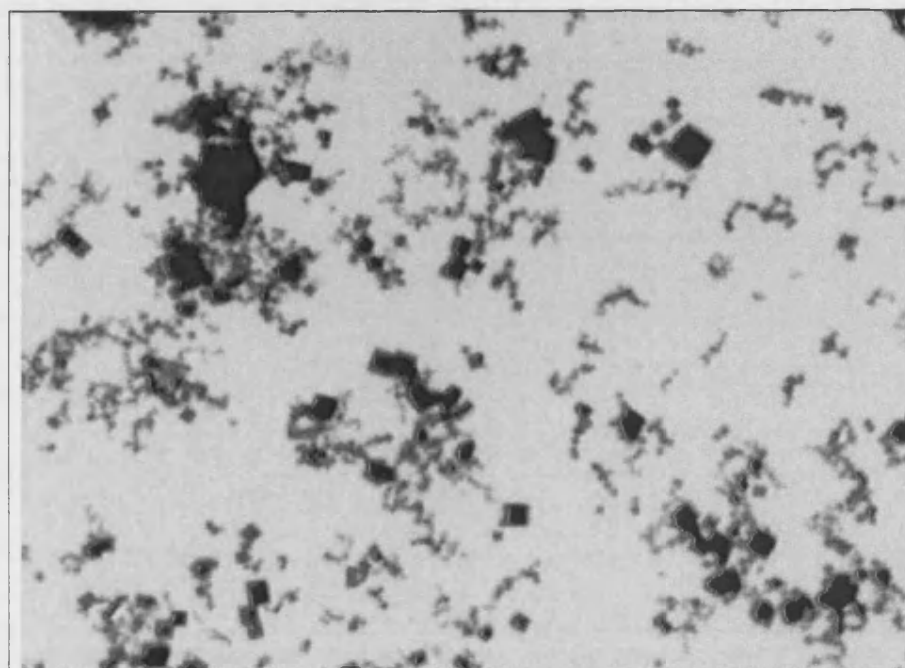


**Figure 5.16b :Magnesium Oxide Particles Sampled using Thermal Precipitator at 26,000 X taken using TEM.**

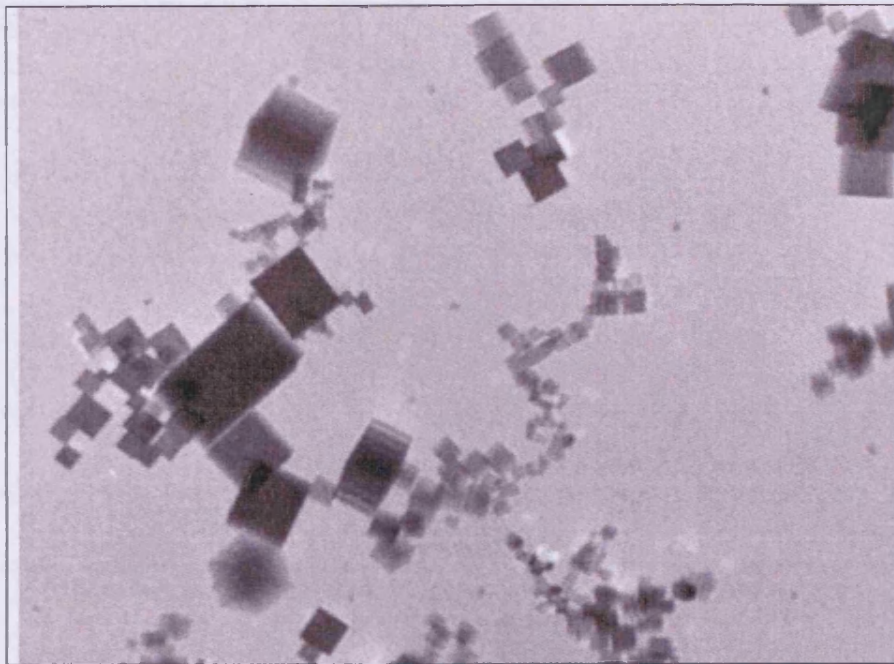


**Figure 5.17 : Comparisons of Number of Particles Frequency Collected by the Total Inhalable Samplers with Thermal Precipitator Unmodified Results.**

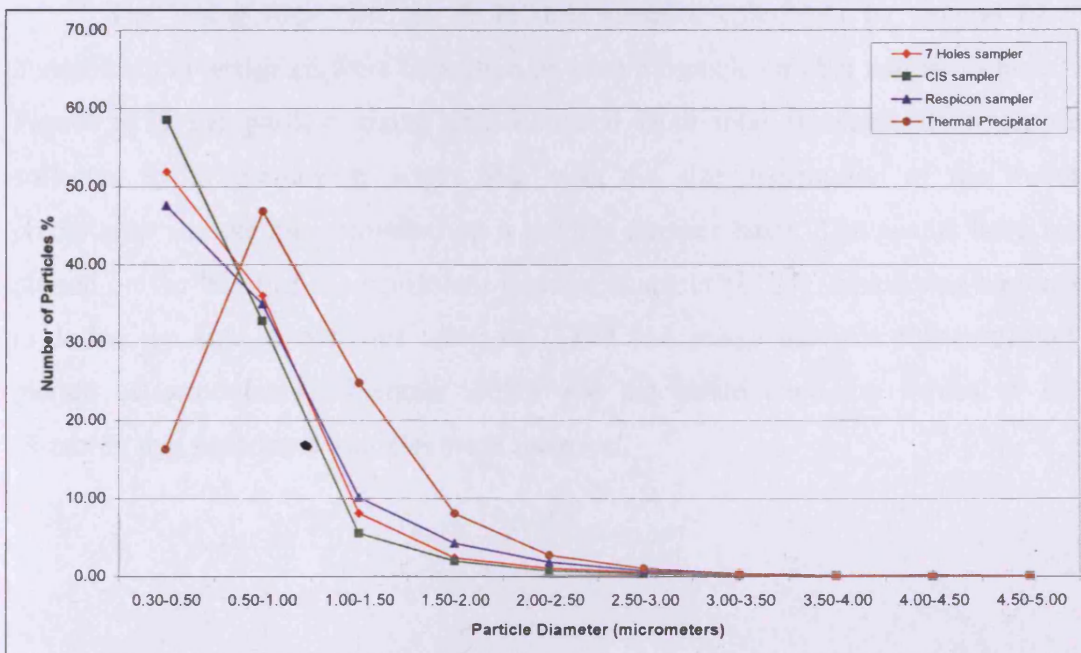
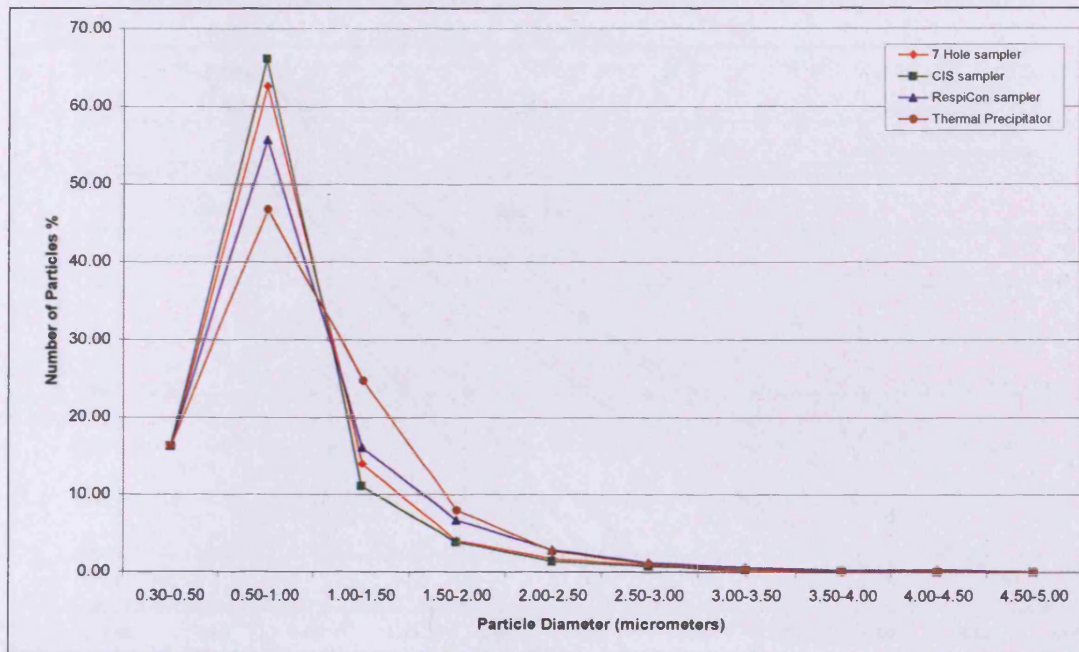




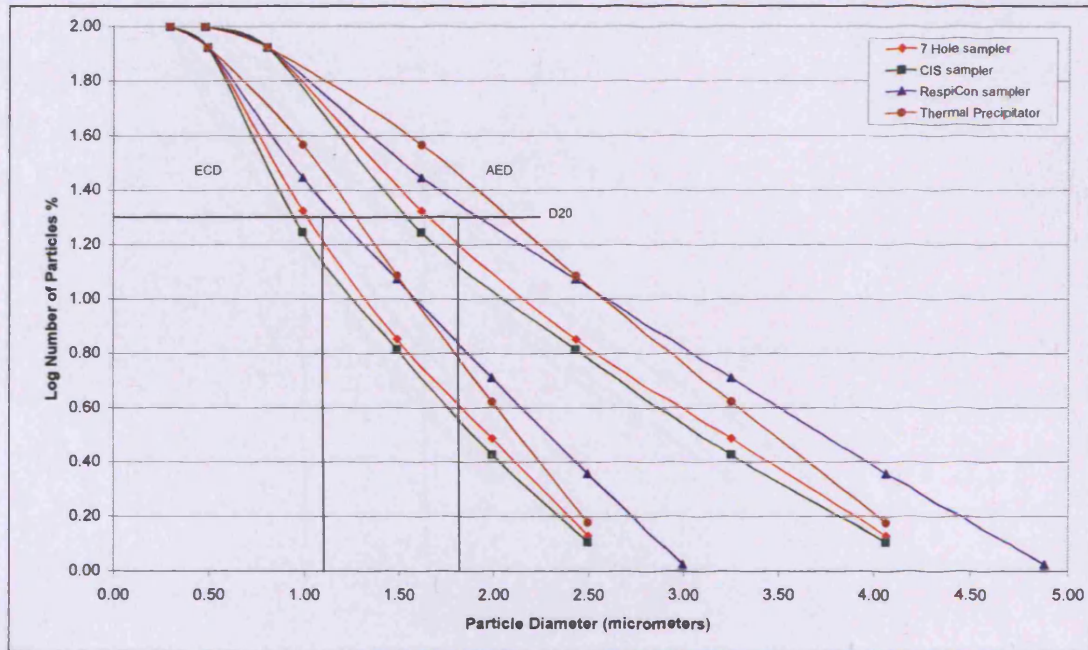
**Figure 5.18 : Comparisons of Number of Particles Frequency Collected by the Total Inhalable Samplers with Thermal Precipitator Modified Results.**



#### **5.4.3 A Comparison of Size Distributions from Dust Samples Collected with Total and Respirable Dust Sampling Instruments.**

The sizing data obtained from dust samples calculated by several of the instruments investigated were compared on both a particle number and mass basis. In **Figure 5.19** the particle sizing data obtained from total inhalable dust samplers collected by 3 instruments larger than with the size distribution of the thermal precipitator sample are compared on a particle number basis. The results have been plotted on the basis of the equivalent circular diameter (ECD) (which was employed to define the size of particles using the TEM and image analysis software) and a picture of aerodynamic diameter which was calculated from the values of ECD assuming that individual particles were spherical.

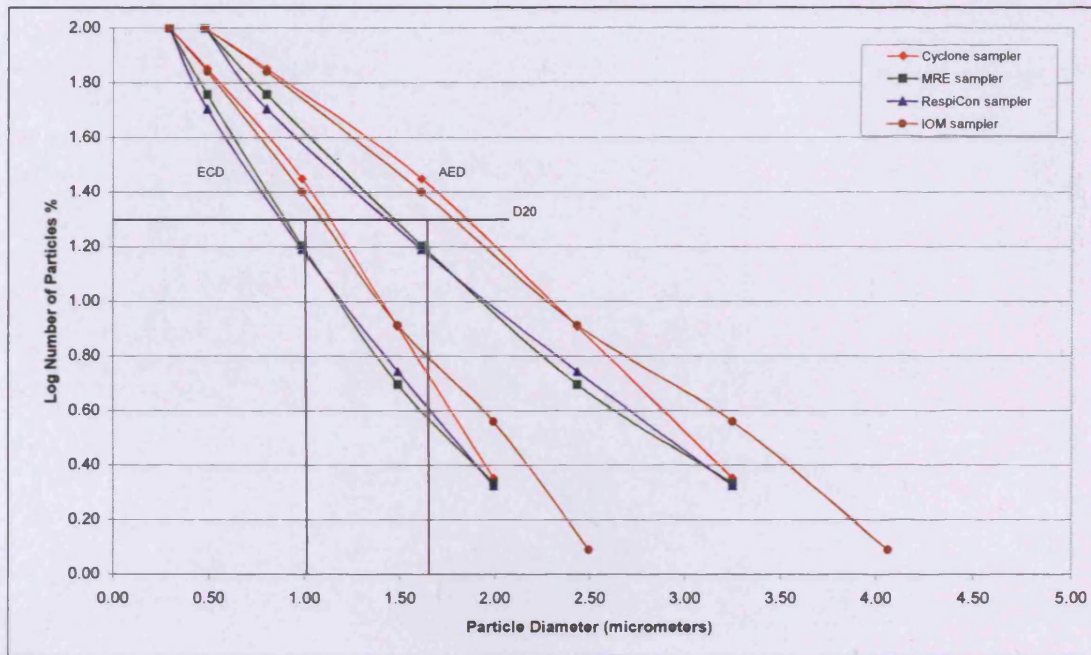
**Figure 5.19 : Comparisons of Cumulative % Particle Size Distributions of the Total Inhalable Samples and Thermal Precipitator Result Expressed in terms of Equivalent Circular Diameter and Calculated Aerodynamic Diameter.**



It can be seen that the trends in particle size distribution are similar for all instruments with the distribution having dominated by the fewer particles sizes. On the basis of ECD the value of  $D_{20}$  was  $1.1 \mu\text{m}$  while the corresponding  $D_{20}$  value for AED was  $1.9 \mu\text{m}$ . In **Figure 5.20** the particle sizing results obtained from respirable dust samples collected by 4 instruments are illustrated on a similar basis of ECD and AED size values. The results again have the same trend but a smaller dispersion of values when compared to the inhalable dust sample results illustrated by **Figure 5.19**. Again on the basis of ECD, the value of  $D_{20}$  for the combined instrumental results was  $1.0 \mu\text{m}$  while the AED value of  $D_{20}$  was  $1.6 \mu\text{m}$ . These are slightly smaller than those values observed for the total inhalable results considering the increased proportion of large particles observed in the size distribution of the inhalable dust. The average size distribution values for inhalable and respirable dust samples investigated are contained in **Figure 5.21** which illustrated the increase of larger particles with size in the average inhalable results. On a number basis, the dust samplers collected by the inhalable samplers therefore have very similar size distribution to those collected by the respirable samplers the latter containing lower numbers of larger particles.



**Figure 5.20 : Comparisons of Cumulative % Particles Size Distributions of the Respirable Samples Result Expressed in terms of Equivalent Circular Diameter and Calculated Aerodynamic Diameter.**



To illustrate this difference between size distributions of the inhalable and respirable samplers, the size distribution data was computed, plotted and compared on the basis of sample mass distribution with size. These results are presented in **Figure 5.22** and **5.23** in which it can be seen that the inhalable dust samples have a much coarser size distribution than the respirable samplers the former having a  $D_{20}$  value of  $3.5 \mu\text{m}$  and the latter  $2.9 \mu\text{m}$  on a mass basis demonstrating the effect of a larger proportion of coarse particles in the inhalable dust. The plotted average values of mass distribution illustrate this difference more clearly as shown in **Figure 5.24**.

**Figure 5.21 : Comparisons of Cumulative % Particle Size Distributions Between Total Inhalable and Respirable Samples Result Expressed in terms of Equivalent Circular Diameter and Calculated Aerodynamic Diameter.**

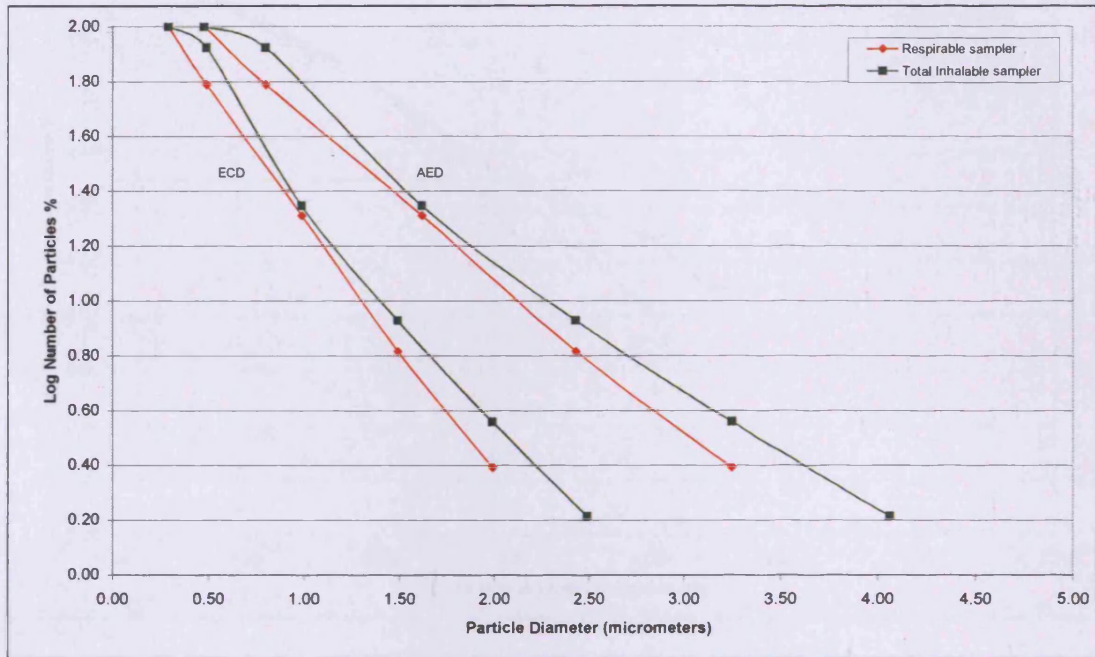


**Figure 5.22 : Comparisons of Particle Mass Distributions of the Total Inhalable Samplers Result.**

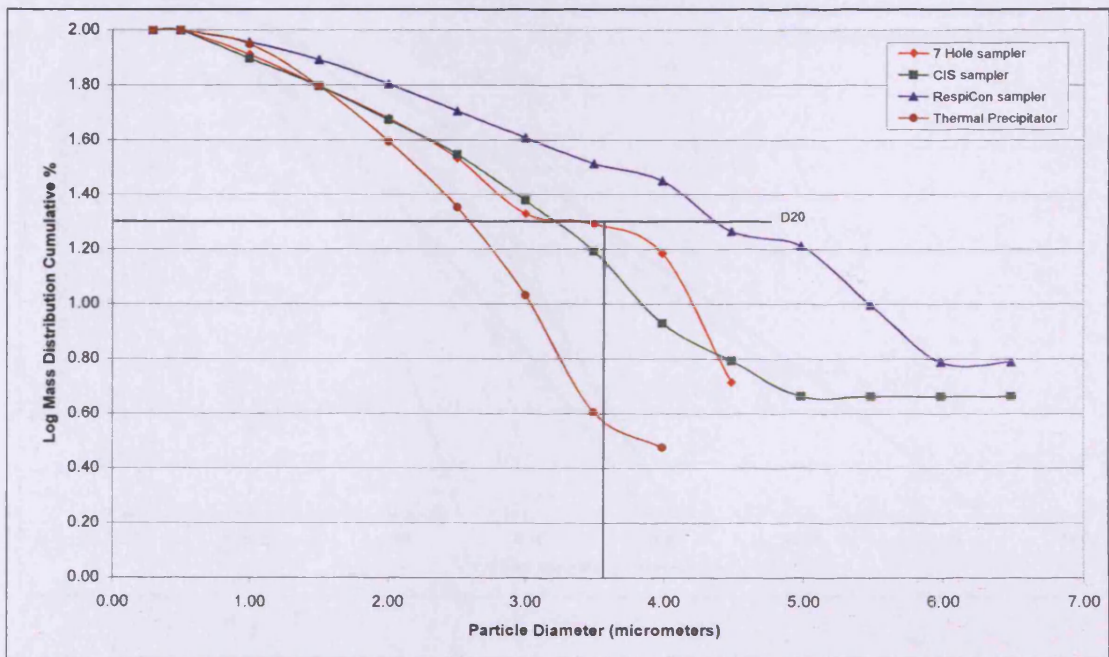




**Figure 5.23 : Comparisons of Particle Mass Distributions of the Respirable Samplers Result.**

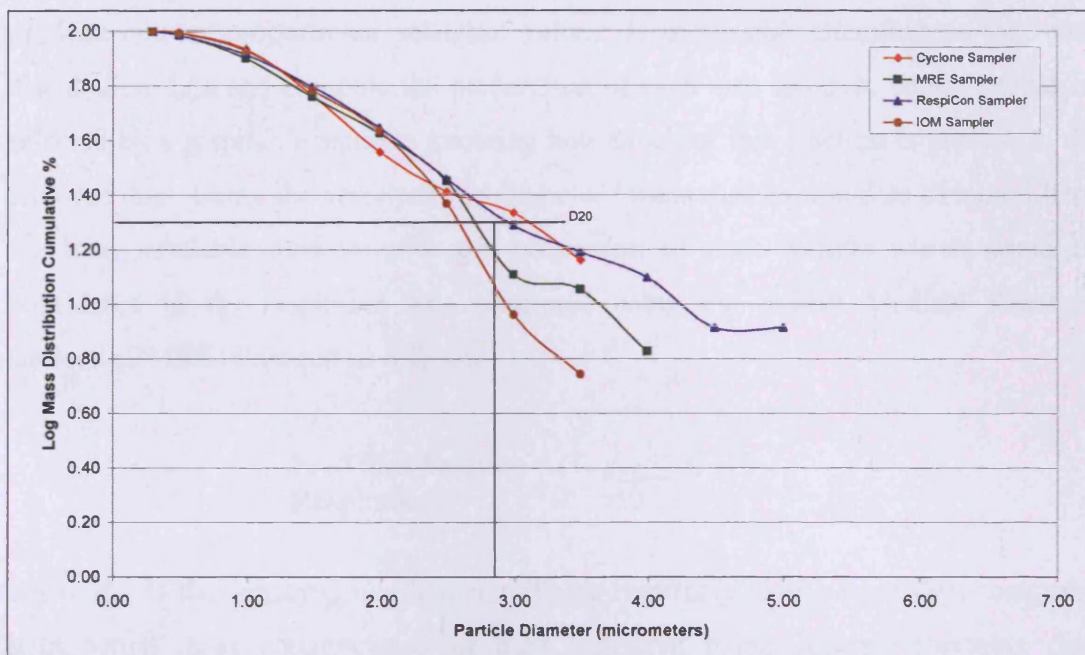
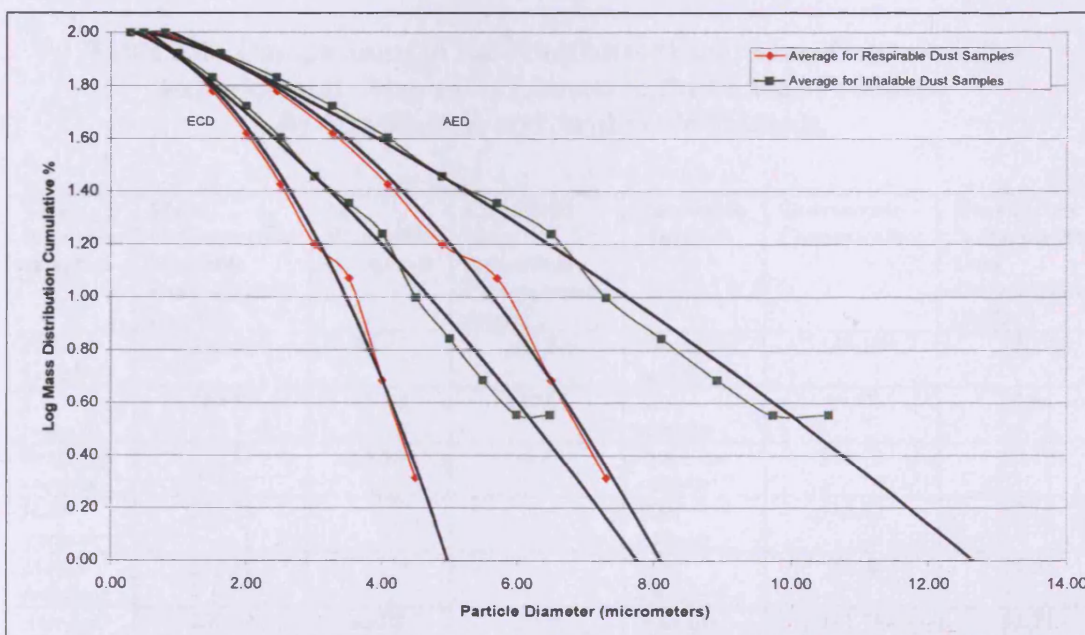


**Figure 5.24 : Comparisons of Cumulative % Particle Mass Distributions of the Average Inhalable and Respirable Samples on the Basis of ECD and AED Values.**



We have seen in Chapter 3 that the selective of respirable dust samplers on aerodynamic size basis is mathematically defined by a number of expression which produce similar proportional selection values. It is possible therefore to take size distribution data and compute the preparation of each size fraction, which should be selected by a respirable sampler knowing how much of that fraction is present in the airborne dust. Using the aerodynamic diameter / mass distribution data obtained from the total inhalable dust samples the proportion of each sample which could be considered to the respirable was computed using the British Medical Research Council (BMRC) function as follows.

$$\% \text{ of Size Fraction Respirable} = \left(1 - \frac{d_{AE}^2}{50}\right) \times 100$$

where  $d_{AE}$  is the aerodynamic diameter. These respirable values were then compared with actual mass concentration of dust measured using several respirable dust sampling instruments. The comparison of results is given in **Table 5.4** from which it can be seen that the % of respirable dust predicted from the inhalable dust size distribution compares favourably with measured values.

**Table 5.4 : Comparisons of the Fractional % and Mass Content of the Experimental Respirable Limestone Dust Cloud Produced By Gravimetric and Arithmetic Methods.**

Total Inhalable samplers	Mass Concentration Inhalable Dust samplers (mg/m <sup>3</sup> )	% Respirable Calculated	Calculated Mass Respirable Concentration (mg/m <sup>3</sup> )	Respirable samplers	Gravimetric Concentration	Gravimetric % Respirable Dust Concentration (mg/m <sup>3</sup> )
7 Hole sampler	202.00	67.27	135.89	Cyclone sampler	145.16	72.38
CIS sampler	189.31	69.10	130.81	CIS sampler	89.12	44.44
RespiCon sampler	178.57	52.86	94.39	RespiCon sampler	130.73	65.19
IOM sampler	220.74			IOM sampler	114.62	57.16
Marple Impactor	212.10			MRE sampler	79.28	39.53
Average Values	200.54	63.08	120.36	Average Values	111.78	55.74



**Table 5.5 : Comparison of Results for Size Selective Sampler i.e. the RespiCon and CIS Sampler for Respirable, Thoracic, and Inhalable Dust Fractions.**

Sampling DGP	5 Minutes Sampling			10 Minutes Sampling		
	3 Minutes			3 Minutes		
Instruments	Mean Concentration (mg/m <sup>3</sup> )	SD %	Fraction %	Mean Concentration (mg/m <sup>3</sup> )	SD %	Fraction %
<i>[I]. Respirable Overall Average</i>	90.07	22.16	55.07	109.93	31.57	57.77
<i>RespiCon sampler</i>	93.90	17.56	55.33	130.73	30.40	63.47
<i>CIS sampler</i>	86.25	28.09	54.81	89.12	7.87	51.05
<i>[II]. Thoracic Overall Average</i>	127.46	23.13	77.93	149.08	28.83	78.34
<i>RespiCon sampler</i>	128.67	20.84	75.81	167.07	34.28	81.11
<i>CIS sampler</i>	126.25	27.81	80.22	131.09	6.26	75.08
<i>[III]. Inhalable Overall Average</i>	163.55	30.68	100.00	190.29	25.45	100.00
<i>RespiCon sampler</i>	169.72	26.74	100.00	205.98	32.78	100.00
<i>CIS sampler</i>	157.37	37.64	100.00	174.59	5.73	100.00

The RespiCon and CIS were the only instruments with which it was possible to determine inhalable, thoracic and respirable dust fractions. The comparison of the mass concentration of these fractions in the experimental dust cloud is given in **Table 5.5**. It was not possible to determine the size distribution of these three fractions from the CIS instrument due to the manner in which they were collected in porous sponge inserts. The size distribution of the RespiCon fraction are however illustrated by **Figure 5.25** on a log mass distribution basis to highlight the differences in coarse particle content between the three fractions. While **Figure 5.26** illustrated the dust particles mass distribution collected from the 7 stages of the Marple Impactor.

**Figure 5.25 : Comparisons of Cumulative % Particle Mass Distributions of the RespiCon sampler.**

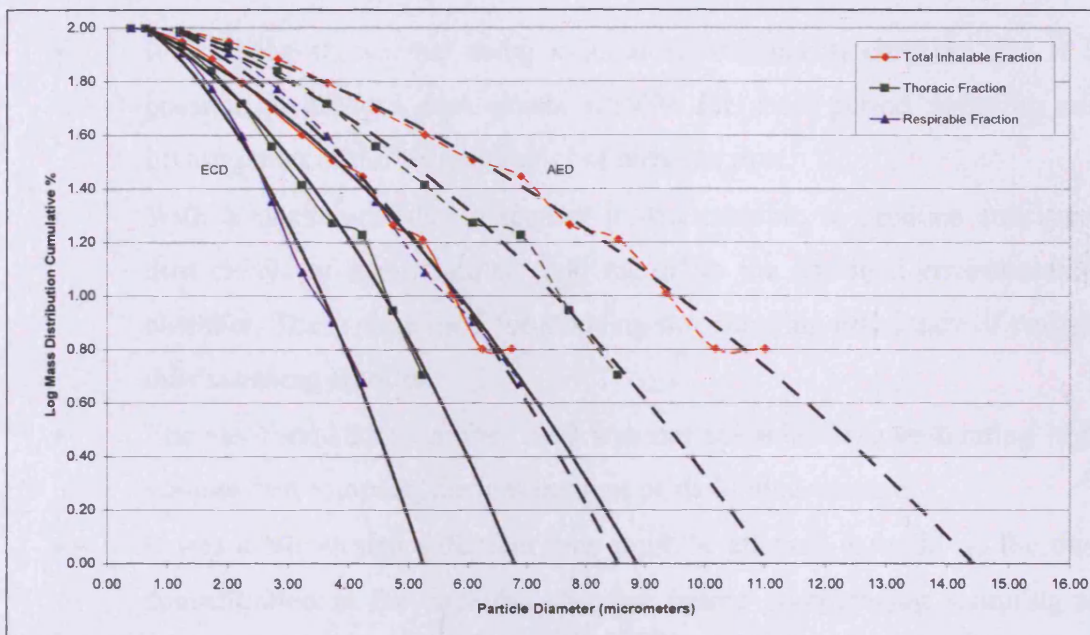
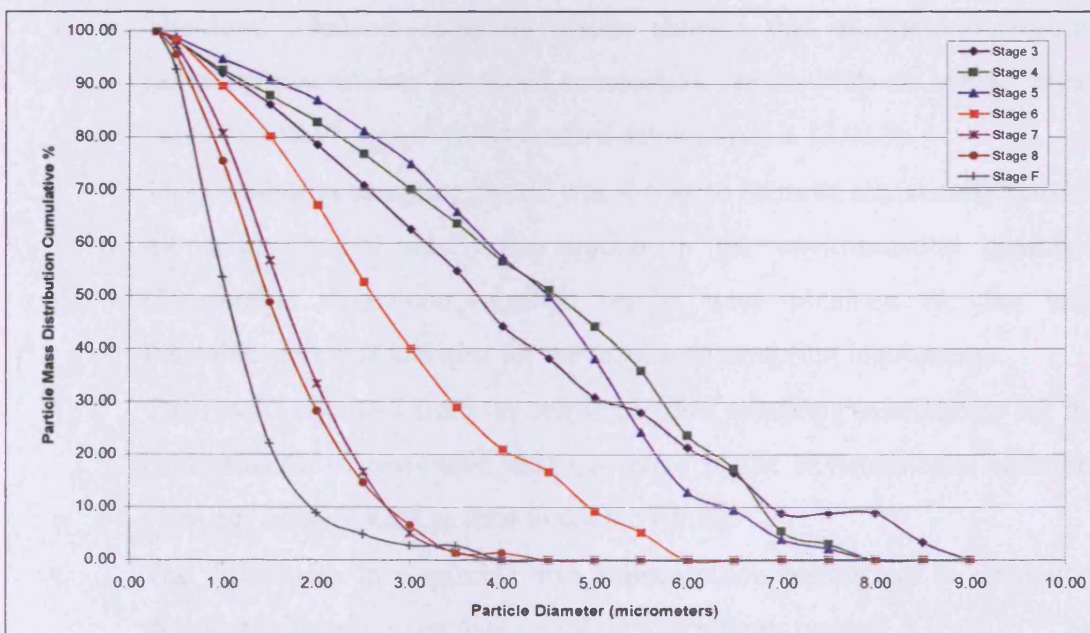


**Figure 5.26 : Comparisons of Cumulative % Particle Mass Distributions of the Marple Impactor.**



## 5.5 Conclusion

- It has been shown that using a small environmental chamber that it is possible to produce dust clouds suitable for short period sampling and investigation of the characteristics of airborne dust.
- With a mechanical dust dispenser it was possible to produce consistent dust clouds of approximately  $200 \text{ mg/m}^3$  in the confined environmental chamber. These were used for studying the sampling efficiency of various dust sampling devices.
- The environmental chamber used was not suitable for investigating high volume dust sampling devices because of its limited volume.
- It was established that sufficient time must be allowed to build up the dust concentration in the enclosed chamber before commencing sampling as demonstrated by comparison of the results for initial dust generating periods 2 and 3 minutes. The 3 minutes dust generated period before sampling produced more consistent sampling results as compared to sampling after 2 minutes of dust generation.
- The total inhalable sampling results showed that all the low volume sampling instruments produced comparable results with an overall mean value of  $208.37 \text{ mg/m}^3$  with standard deviation of  $\pm 12.02 \%$ .
- The 10 minutes sampling period was shown to be more statistically reliable for estimation of dust concentration in the environmental chamber. Comparable mass concentration results were obtained for the total inhalable samplers and also for the respirable sampling instruments.
- The results obtained from the respirable dust sampling instruments for the concentration of respirable dust generated in the environmental chamber were not as consistent as total inhalable values.
- The differences in respirable dust concentration results can be related to the manner in which the dust sampling instruments operate.
- Respirable dust sampling instruments which employ energetic methods for separation of respirable particles can break up particle aggregates and modify the proportion of dust particles considered to be respirable.

- The experimental dust cloud was found to contain on average 55.74 % of respirable dust as defined by 5 different instruments.
- Employing the BMRC convention for the variation of respirable fraction with aerodynamic size distribution of inhalable dust samples a respirable dust content of 63.08 % was calculated.

## **CHAPTER 6 :**

# **THE PHYSICAL CHARACTERISTICS OF ASBESTOS AND COAL DUST FROM AIRBORNE AND BIOLOGICAL SOURCES TOGETHER WITH URBAN ATMOSPHERIC POLLUTION**

## **6.1 Introduction**

The results from an investigation of the physical characteristics of airborne asbestos and coal particles are presented.

The examination of airborne asbestos fibres is particularly relevant for a number of reasons which can be listed as follows :

- The concentration of fibrous particles in air defined by regulations and determined on a particle number basis and not mass which is unique for any mineral dust. Recommended control levels for airborne asbestos dust are quoted in fibres per ml.
- The techniques for sampling of fibrous particles in air for control purpose do not employ a size selective procedure i.e. respirable dust sampling instruments. An open faced filter is employed for sampling which effectively collects total inhalable dust particles.
- There are two accepted microscopic techniques for determination of airborne fibres one which is based upon phase contrast optical microscopy (PCOM) the other on electron microscopical procedures.
- When using the optical microscopic technique for dust control purpose, no attempt is made to discriminate between the various mineral types of airborne fibre which may be collected by sampling.
- Special regulations have been formulated for handling and disposal of asbestos materials capable of generating and acting as a source of fibrous dusts.
- Asbestos fibres are considered to be extremely toxic if inhaled and capable of causing fibrosis and cancer of the lung.

The characteristics of airborne asbestos fibres and those recovered from human lung tissue samples have been compared. The size of those fibres which have been inhaled and retained in the lung and which cause health problems can then be defined.

Coal dust particles collected with inhalable and respirable samples have been compared with coal dust particles recovered from the lung tissue of a coal miner. This investigation was performed to establish the size of coal particles being inhaled and retained in the lungs. The aerodynamic size characteristics of these particles have been determined and compared with the predicted size values of respirable dust particles employed to design respirable dust sampling instruments. After a comprehensive review of the literature, no attempt appears to have been made to determine whether these instruments do sample particles which are representative of those which can deposit in the lung parenchyma.

## **6.2 Size Characteristics of Asbestos Fibres from Airborne and Biological Sources.**

The asbestos samples investigated included dust preparations of an amosite, a chrysotile and two crocidolite samples. Dust clouds of each mineral were generated as described in Chapter 4 and the dust particles sampled using a modified cyclone sampler to represent a respirable fraction of the fibrous dust cloud. Dust particles of each mineral were collected onto milipore filters for sufficient time to allow a gravimetric estimate of the dust on the filter samples to be performed. The dust filters were divided in half and respective portions prepared for optical and electron optical examination. The preparation techniques and instrumental conditions of the microscopic examination have been described (Chapter 4) they conform to National and International standard examination procedures. The objectives of the examination were to produce sizing and fibre counting data, which could be used to compare samples and establish the differences in results obtained between the microscopic techniques and also physical differences between airborne fibres and those retained in the lungs. Using the gravimetric result and fibre concentration per unit area of the

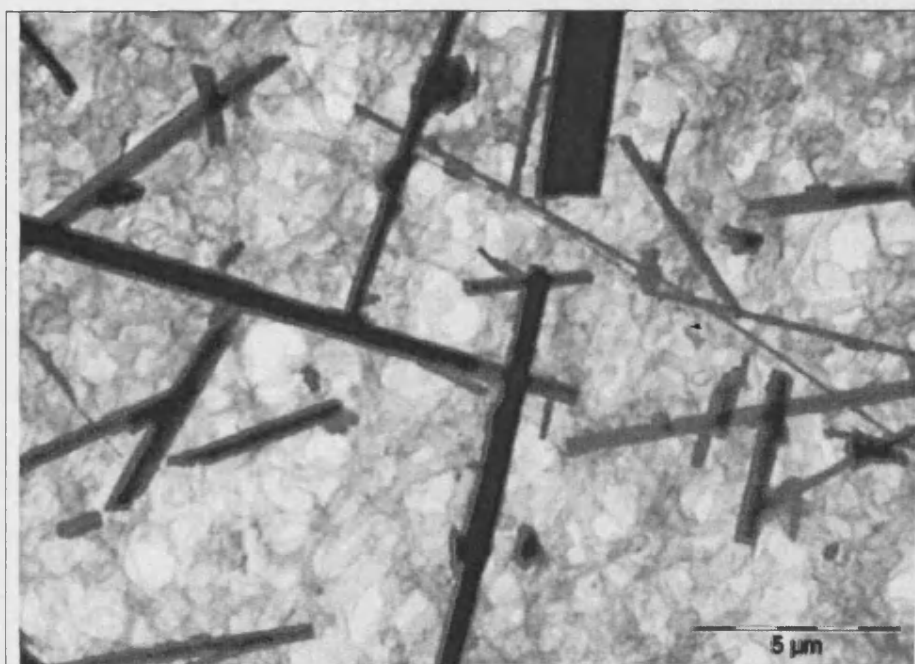


filter relationships between mass concentration of dust collected and fibre number were determined.

### 6.2.1 Characteristics of Airborne Amosite Asbestos Fibres.

The filter preparation of airborne amosite asbestos dust is illustrated by **Figure 6.1**. This is an electron microscope image from which it can be seen that amosite fibres are straight mainly parallel sided particles of variable length and diameter. The weight of amosite fibres on the filter was 0.00005 g or 0.05 mg of material. The concentration of fibres per unit area of filter determined by optical and electron optical counting techniques respectively were 360 and 60 fibres per 10,000  $\mu\text{m}^2$  of filter area. The difference in number concentration per unit area of filter between fibre counts determined by TEM and PCOM is a factor of 5X and can be directly related to the difference in resolution between the TEM and PCOM instruments. A large number of amosite fibres are smaller in one dimension than the working resolution of the optical microscope, which for white light is approximately 0.3  $\mu\text{m}$ . These smaller particles will therefore not be seen using the PCOM. The TEM which uses an electron beam to image particles has no practical limit to its resolution so that all particles can be resolved, observed and counted.

**Figure 6.1 : Filter with Airborne Amosite Fibres Preparation at 2,650 X.**



The size of airborne amosite fibres observed on a fibre length basis by PCOM and TEM analysis are illustrated by **Figure 6.2**. It can be seen from this figure that a larger proportion of the fibres observed by PCOM are longer than 10  $\mu\text{m}$  when compared with the corresponding result for the TEM. In total 42 % were larger than 10  $\mu\text{m}$  by PCOM compared with 10 % larger than 10  $\mu\text{m}$  by TEM. This result demonstrates the fact that a large number of shorter amosite fibres are not observed using the PCOM method because of their finer diameter. The distribution of fibre diameters measured with the TEM for both airborne dust and fibres recovered from lung tissue are illustrated by **Figure 6.5**. From this graph it can be seen that majority of fibres are less than 0.5  $\mu\text{m}$  in diameter. The airborne sample having 15.71 % and the lung tissue fibre 8.1 % of fibre larger than 0.5  $\mu\text{m}$ . The comparison of the length distribution of amosite fibres from lung tissue by PCOM and TEM are illustrated by **Figure 6.4** in which it can be seen that the length distributions are very similar. The fibre lengths are however shorter than those of airborne amosite fibres with few particles being in excess of 30  $\mu\text{m}$  in length. If we compare the amosite fibres found in lung tissue and airborne fibre collected with a cyclone respirable dust sampler and sized with a TEM. The following differences can be observed :

- There is a greater proportion of finer diameter fibre observed in lung tissue than in air which would infer that finer diameter fibres are more readily respirable (**Figure 6.5**).
- The length of amosite fibres from lung tissue are shorter than those observed in airborne dust with very few having lengths in excess of 30  $\mu\text{m}$ .
- The use of PCOM to define the size distribution of amosite fibres by diameter or length is scientifically unsound because of the inability to resolve all fibres.
- The use of the PCOM to quantify fibres in airborne fibres in airborne samples is highly inaccurate as not all fibres can be resolved.
- The respirable fraction of an amosite dust cloud is mainly confined to those fibrous particles less than 30  $\mu\text{m}$  long and less than 0.5  $\mu\text{m}$  diameter.

**Figure 6.2 : Comparisons of the Length Distributions Frequency % of Airborne Amosite Fibres Obtained Using PCOM and TEM Analysis Techniques.**

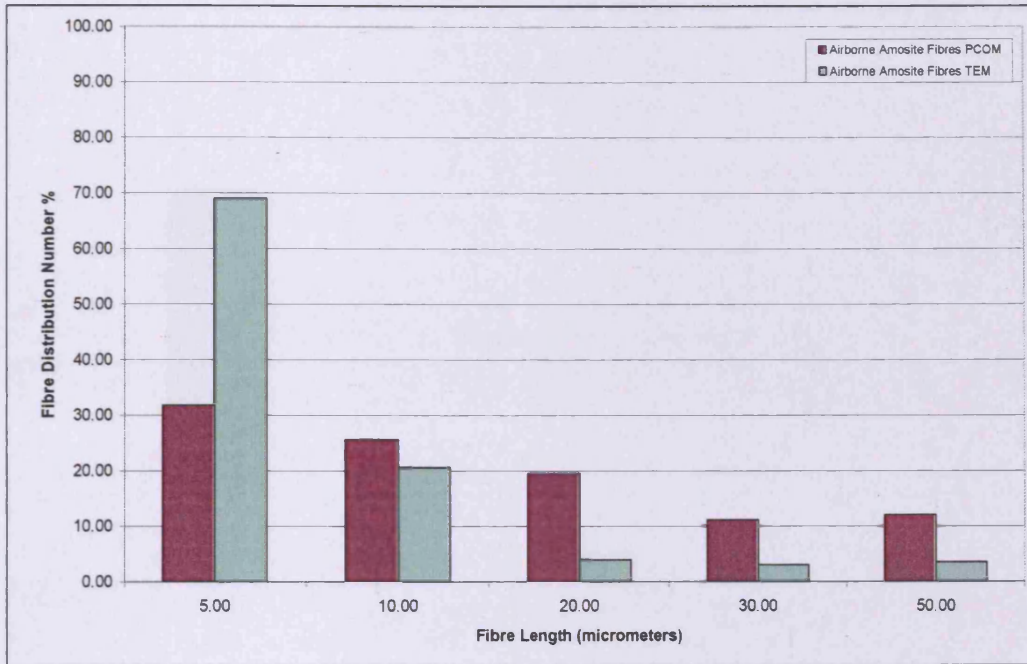


**Figure 6.3 : Comparisons of the Length Distributions Frequency % of Airborne Amosite Fibres and Amosite Fibres from Lung Obtained Using TEM Analysis Techniques.**

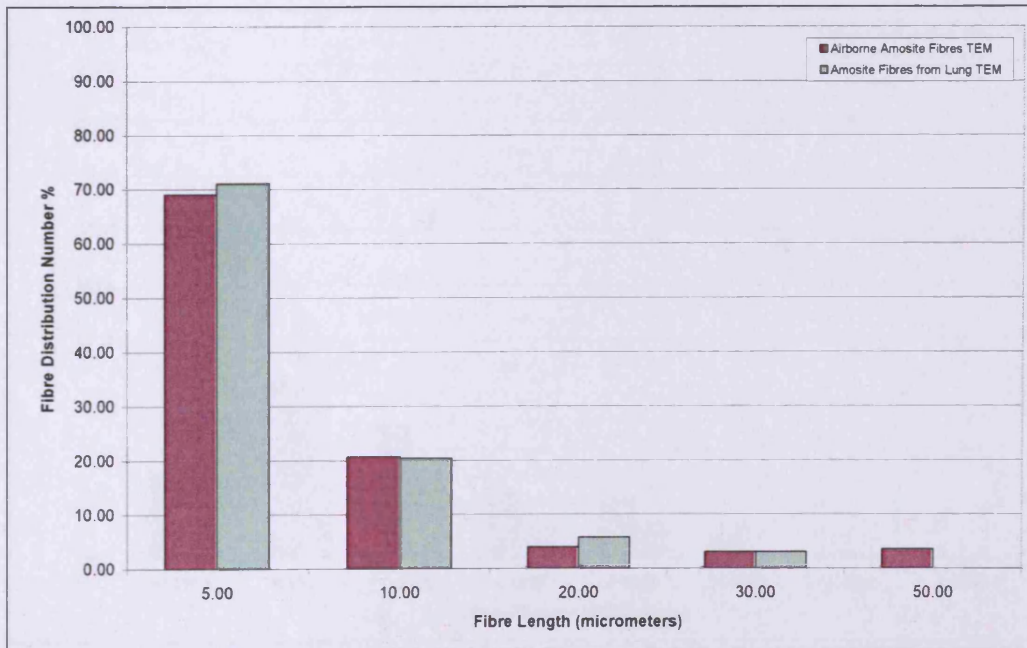


**Figure 6.4 : Comparisons of the Length Distributions Frequency  
% Amosite Fibres from Lung Tissue Obtained  
Using PCOM and TEM Analysis Techniques.**

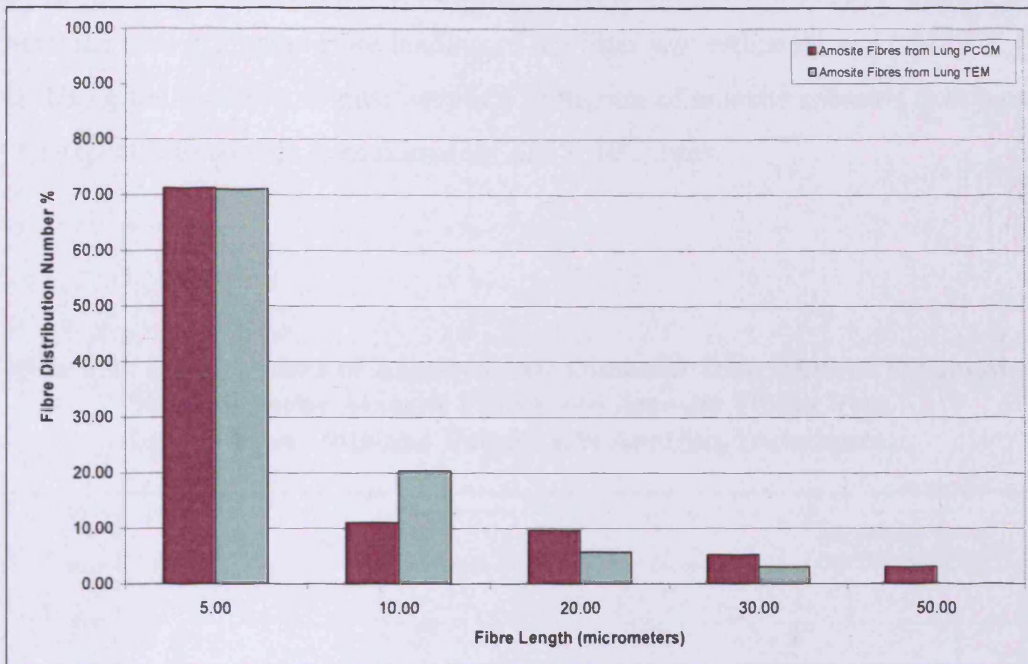
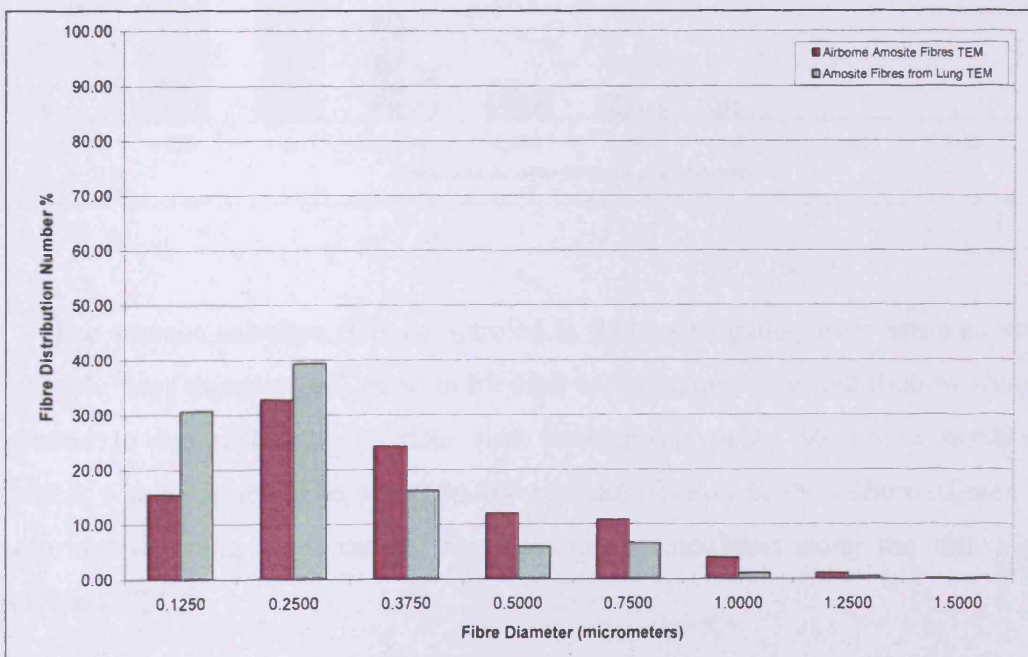


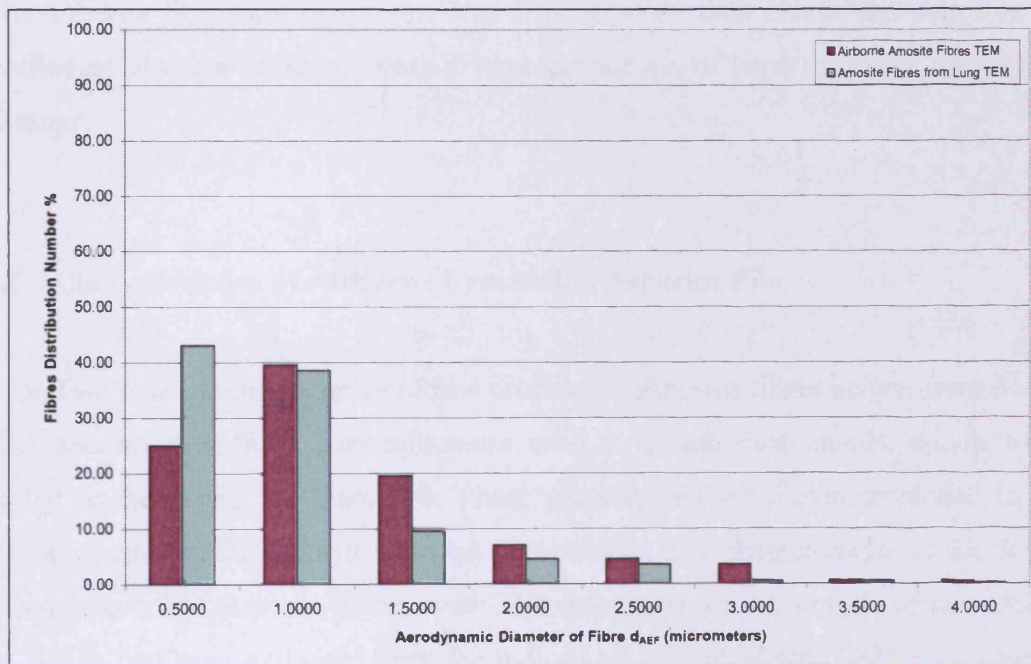
**Figure 6.5 : Comparisons of Diameter Distributions Frequency  
% of Airborne Amosite Fibres and Amosite Fibres from  
Lung Tissue Obtained Using TEM Analysis Techniques.**





The amosite dust sample examined was initially found to have a weight of 0.05 mg and the average fibre concentration per unit area of filter was 360 fibres per 10,000  $\mu\text{m}^2$ . As the active filter area onto which fibres were deposited was 20 mm diameter the total estimated fibre loading of the filter was estimated as  $11.3112 \times 10^6$  fibres. Using the gravimetric dust weight a milligram of amosite asbestos dust would then be expected to contain approximately  $226 \times 10^6$  fibres.

**Figure 6.6 : Comparisons of Aerodynamic Diameter Distributions Frequency % of Airborne Amosite Fibres and Amosite Fibres from Lung Tissue Obtained Using TEM Analysis Techniques.**



The amosite asbestos fibres examined in this investigation were sampled with a respirable dust sampler and their individual aerodynamic size distribution should correspond to the respirable particle size conventions upon which the sampling instrument was designed. The aerodynamic size distribution of the airborne fibres of amosite and the lung fibre sample were therefore calculated using the following expression [78] :

$$d_{AEF} = 1.6d_F \sqrt{(e_F / e_0)}$$

where  $d_F$  = fibre diameter,  $d_{AEF}$  = aerodynamic fibre diameter,  $e_F$  = fibre density,  $e_0$  = unit density.

The calculated results are presented in **Figure 6.6** from which it can be seen that the  $d_{AEF}$  distribution of the two samples are well within the size convention range quoted for respirable dust particles. Because the aerodynamic size of fibrous particles is the main function of diameter it can be seen that the distribution profile is very similar to that of the amosite fibre diameter distribution as shown in **Figure 6.5**. Over 80 % of the fibres in the sample from lung tissue have a  $d_{AEF}$  below 1  $\mu\text{m}$ , while 65 % of the airborne fibres are below this size also. Amosite dust clouds can therefore be classified as ultrafine in nature with a large proportion of particles in the nanometer size range.

## 6.2.2 Characteristics of Airborne Crocidolite Asbestos Fibres

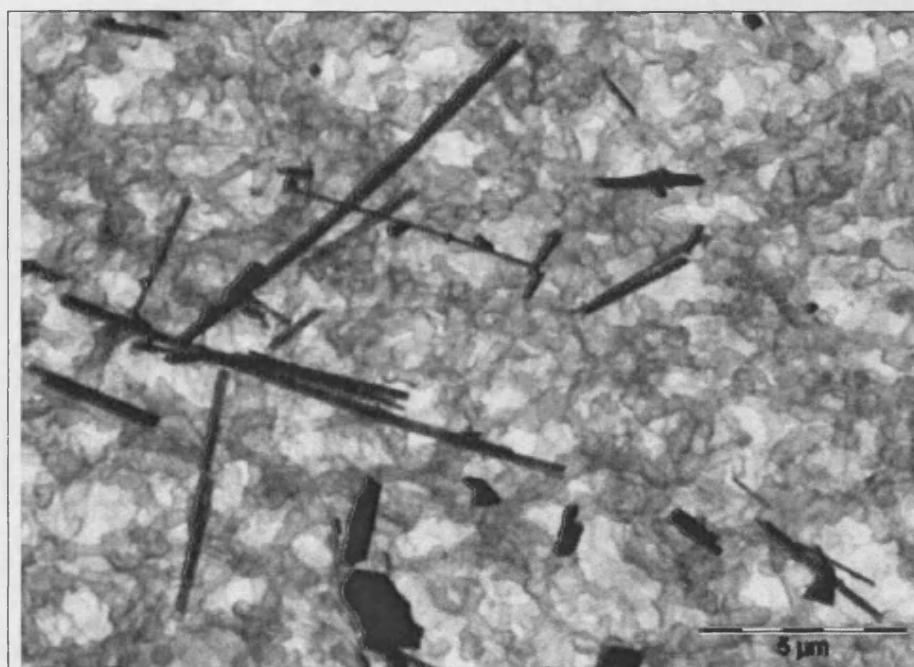
Two commercial samples of raw crocidolite asbestos fibres i.e one from South Africa and another from Australia were used to create dust clouds, which were sampled as described in Chapter 4. These preparations were then examined in an identical manner to the amosite asbestos dust sample. The characteristics of the South African crocidolite airborne fibres were also compared with a sample of crocidolite dust, which had been extracted from the lung of an individual who had been exposed only to crocidolite asbestos from that location. Gravimetric data for the two crocidolite samples was obtained to assess the relationship between fibre number concentration and mass of dust.

The filter preparation of the crocidolite dusts are illustrated by **Figure 6.7**. It can be seen that crocidolite fibres have almost identical morphological features as amosite asbestos fibres. The weight of South African crocidolite fibres on the filter was 0.00006 g or 0.06 mg of material. The concentration of fibres per unit area of filter determined by optical and electron optical counting techniques respectively were



1222 and 144 fibres per 10,000  $\mu\text{m}^2$  of filter area giving a ratio of 7.5 : 1 of TEM to PCOM. This means that 88.2 % of the Koegas crocidolite fibres could not be observed with an optical microscope.

**Figure 6.7 : Filter with Airborne Koegas Crocidolite Fibres Preparation at 2,650 X.**



A comparison of the size distribution of Koegas crocidolite fibres obtained by PCOM and TEM techniques on a fibre length basis are illustrated by **Figure 6.8**. It can be seen that the majority of fibres observed by PCOM and TEM methods are less than 10  $\mu\text{m}$  in length. Over 93 % were less than 10  $\mu\text{m}$  by TEM and 90 % by PCOM. A comparison of the PCOM and TEM results of length distribution for crocidolite fibres from lung tissue are illustrated by **Figure 6.9** which are very similar to each other. When the TEM results for airborne fibres and lung fibres are compared, they are remarkable similar to each other showing that the fibres in the Koegas dust cloud are almost totally respirable in nature as illustrated by **Figure 6.10**.

**Figure 6.8 : Comparisons of Length Distributions Frequency  
% of Airborne Koegas Crocidolite Fibres Obtained  
Using PCOM and TEM Analysis Techniques.**

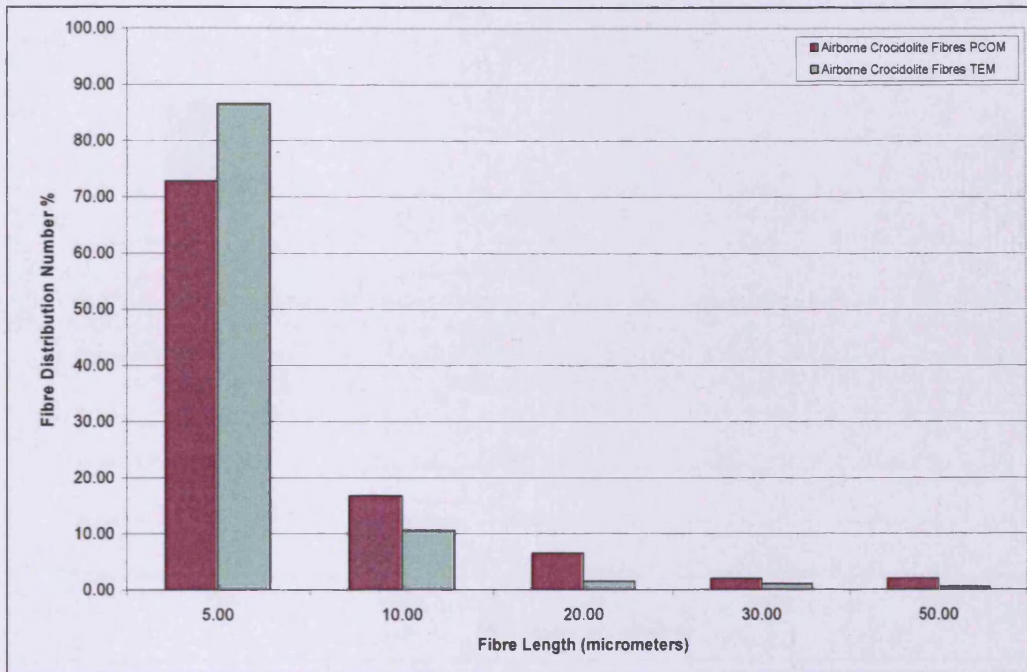


**Figure 6.9 : Comparisons of Length Distributions Frequency  
% of Koegas Crocidolite Fibres from Lung Tissue Obtained  
Using PCOM and TEM Analysis Techniques.**

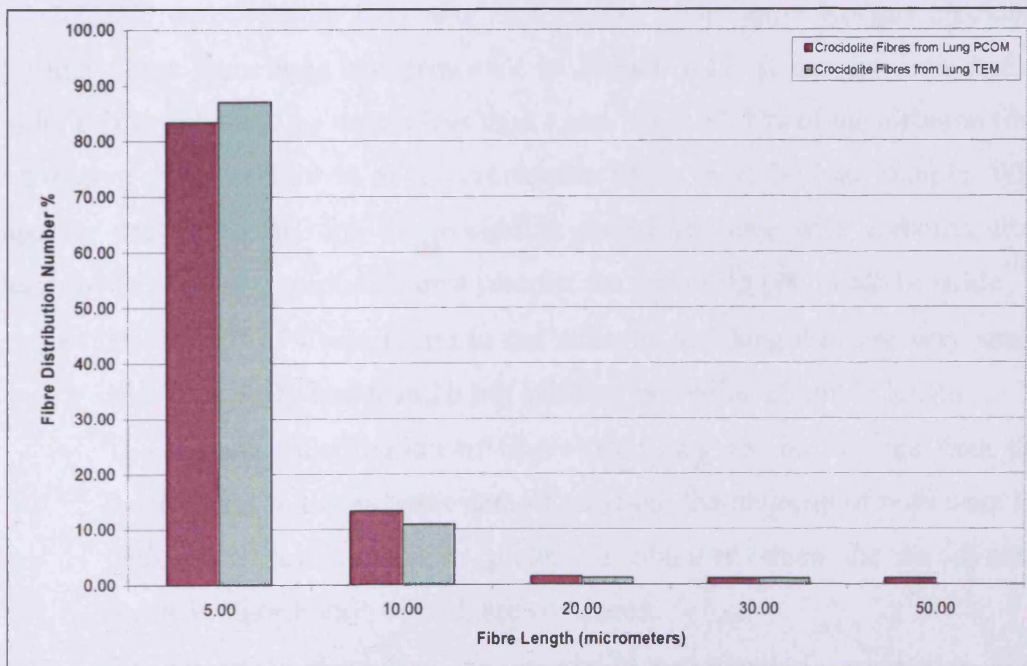
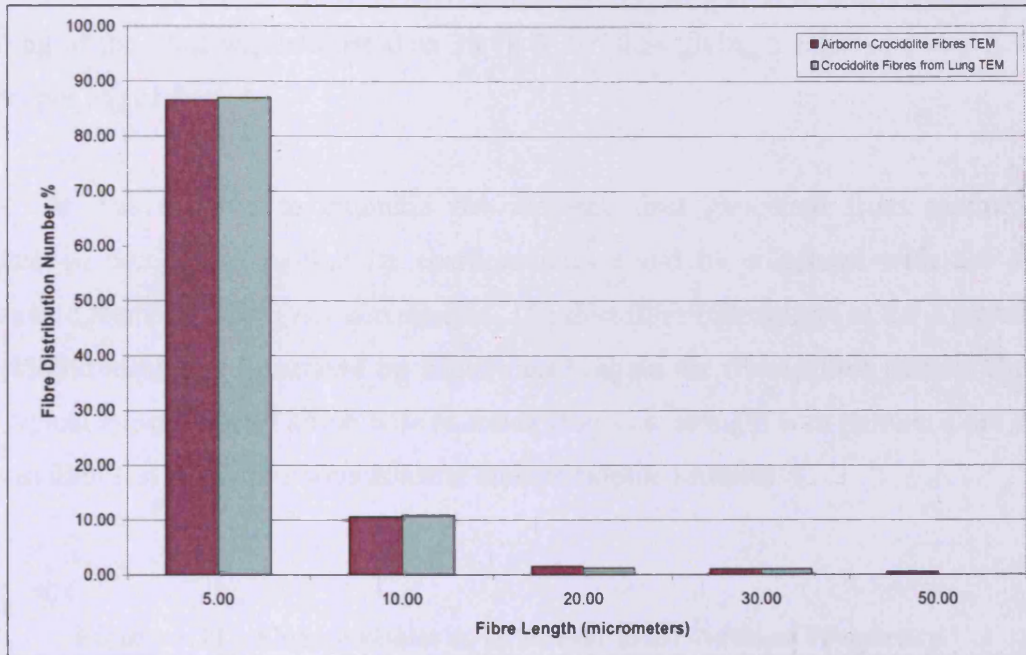




**Figure 6.10 : Comparisons of Length Distributions Frequency % of Airborne Koegas Crocidolite Fibres and Crocidolite Fibres from Lung Tissue Obtained Using TEM Analysis Techniques.**



The diameter distribution obtained by TEM airborne and lung derived crocidolite fibres is illustrated by **Figure 6.11**. This figure shows that the majority of fibres from both sources have diameters, which are substantially finer than  $0.375 \mu\text{m}$ . The calculated aerodynamic  $d_{AEF}$  size distribution of airborne Koegas crocidolite fibres and fibres from lung are presented in **Figure 6.12**. It can be seen that the majority of fibres have  $d_{AEF}$  values less than  $1 \mu\text{m}$ . Over 93.5 % of the airborne fibres had a  $d_{AEF}$  of  $1 \mu\text{m}$  and 99 % of the crocidolite fibres from the lung sample. When comparing the characteristics of crocidolite found in lung with airborne fibres collected with a cyclone respirable dust sampler the following points can be made :

- The length of fibres found in the airborne and lung dust are very similar with a majority less than  $10 \mu\text{m}$  and few exceeding  $20 \mu\text{m}$  in length.
- The diameter distribution of fibres from lung are on average finer than those found in the airborne sample although the majority of both were less than  $0.375 \mu\text{m}$ . A similar picture is obtained when the aerodynamic diameter distribution of both are compared.
- The respirable fraction of the crocidolite dust clouds is confined to fibres less than  $20 \mu\text{m}$  long and less than  $0.375 \mu\text{m}$  in diameter.

The airborne Koegas crocidolite sample was initially found to have a weight of 0.06 mg with an average fibre concentration of 1222 fibres per 10,000  $\mu\text{m}^2$ . As the active filter area onto which fibres were deposited was 20 mm diameter, the total fibre loading of the filter was estimated as  $38.18 \times 10^6$  thus giving a value of  $636.3 \times 10^6$  fibres per mg of dust.

It was decided to examine the airborne dust generated from sample of Australian crocidolite so that its characteristics could be compared with the dust generated from the South African sample. The dust filter preparation of the Australian crocidolite sample is illustrated by **Figure 6.13**, again the fibrous dust particle shave the typical appearance of amphibole asbestos fibres i.e. straight with parallel sides and almost identical to the previous amosite and crocidolite samples.

**Figure 6.11 : Comparisons of Diameter Distributions Frequency % of Airborne Koegas Crocidolite Fibres and Crocidolite Fibres from Lung Tissue Obtained Using TEM Analysis Techniques.**

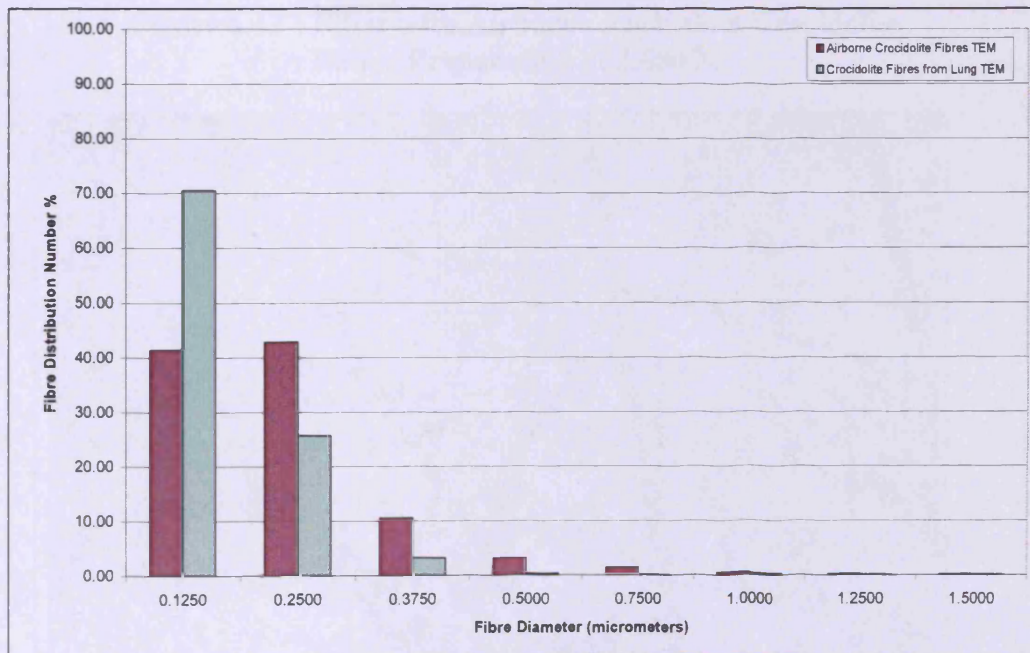




**Figure 6.12 : Comparisons of Aerodynamic Diameter Distributions Frequency % of Airborne Koegas Crocidolite Fibres and Crocidolite Fibres from Lung Tissue Obtained Using TEM Analysis Techniques.**

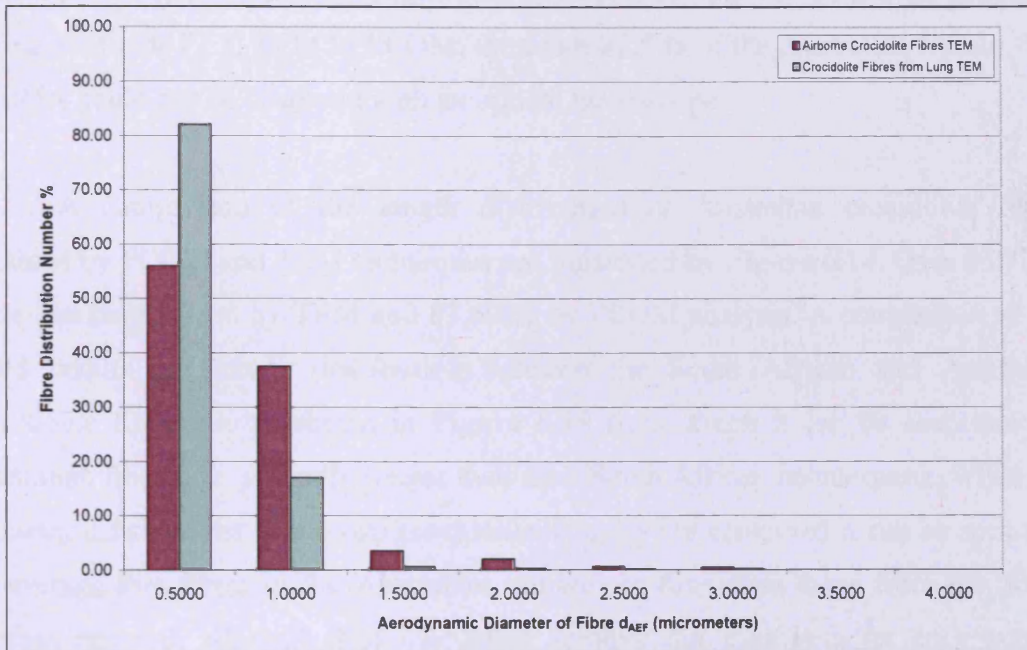
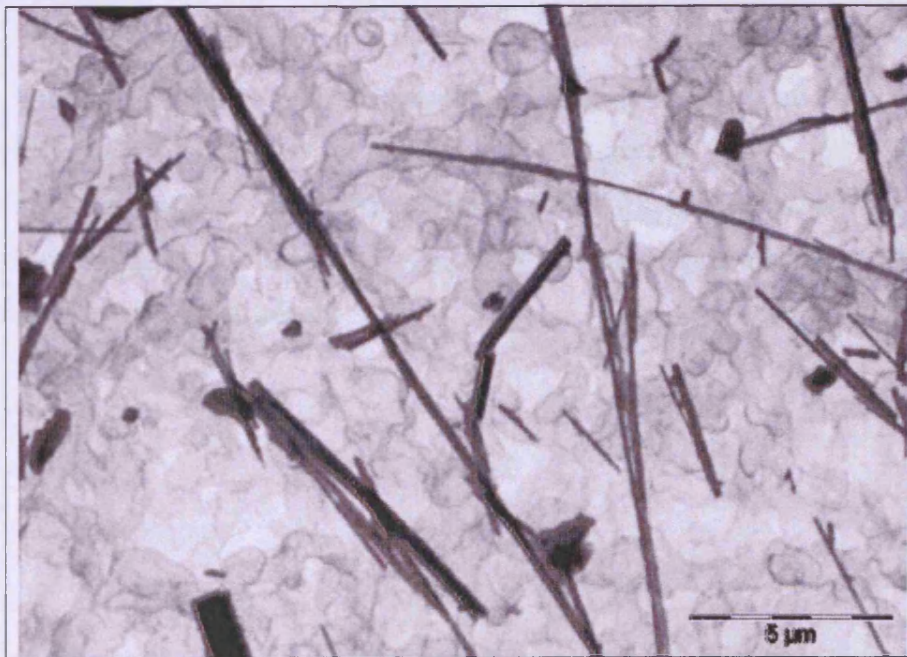


**Figure 6.13 : Filter with Airborne Australian Crocidolite Fibres Preparation at 2,650 X.**



The weight of fibrous dust particles collected of the filter was 0.00003 g or 0.03 mg of material. The concentration of fibres per unit area of filter determined by optical and electron optical techniques were 104 and 715 per 10,000  $\mu\text{m}^2$  of filter area giving a ratio of 7 : 1, TEM to PCOM, therefore 87.5 % of the Australian fibrous dust particles could not be observed with an optical microscope.

A comparison of the length distribution of Australian crocidolite fibres obtained by PCOM and TEM techniques are illustrated by **Figure 6.14**. Over 93.72 % were less than 10  $\mu\text{m}$  by TEM and 83.69 % by PCOM analysis. A comparison of the TEM results per length distribution between the South African and Australian crocidolite fibres are presented in **Figure 6.15** from which it can be seen that the Australian fibres are generally longer than their South African counterparts. When the diameter distributions of the two crocidolite samples are compared it can be seen that on average that fibres in the Australian sample are finer than those from the South African material, although their calculated aerodynamic diameters for each sample have very similar distributions over 95 % of the Australian fibres having calculated aerodynamic diameters less than 1  $\mu\text{m}$  as illustrated by **Figure 6.16** and **6.17**. Comparing the two crocidolite samples, it can be said that they are very similar in terms of size and airborne characteristics.

The Australian crocidolite sample was initially found to have a weight of 0.03 mg with an average fibre concentration of 704 fibres per 10,000  $\mu\text{m}^2$ . As the active filter area onto which fibres were deposited was 20 mm diameter, the total fibre loading of the filter was estimated as  $22.12 \times 10^6$  thus giving a value of  $737.32 \times 10^6$  fibres per mg of dust generated.



**Figure 6.14 : Comparisons of Length Distributions Frequency % of Airborne Australian Crocidolite Fibres Obtained Using PCOM and TEM Analysis Techniques.**

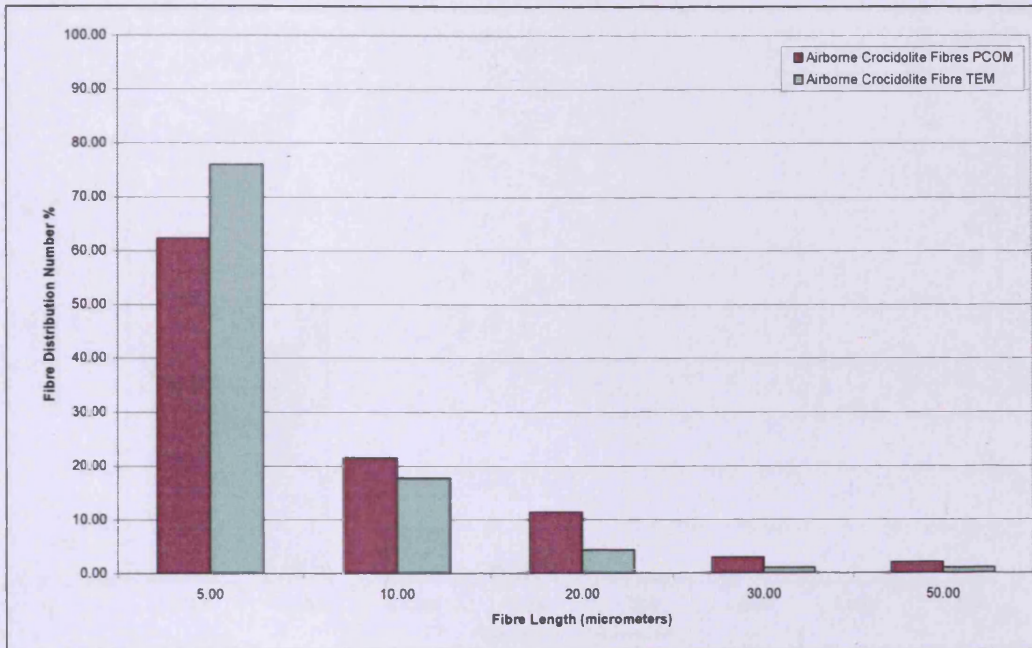


**Figure 6.15 : Comparisons of Length Distributions Frequency % of Airborne Koegas and Airborne Australian Crocidolite Fibres Obtained Using TEM Analysis Techniques.**

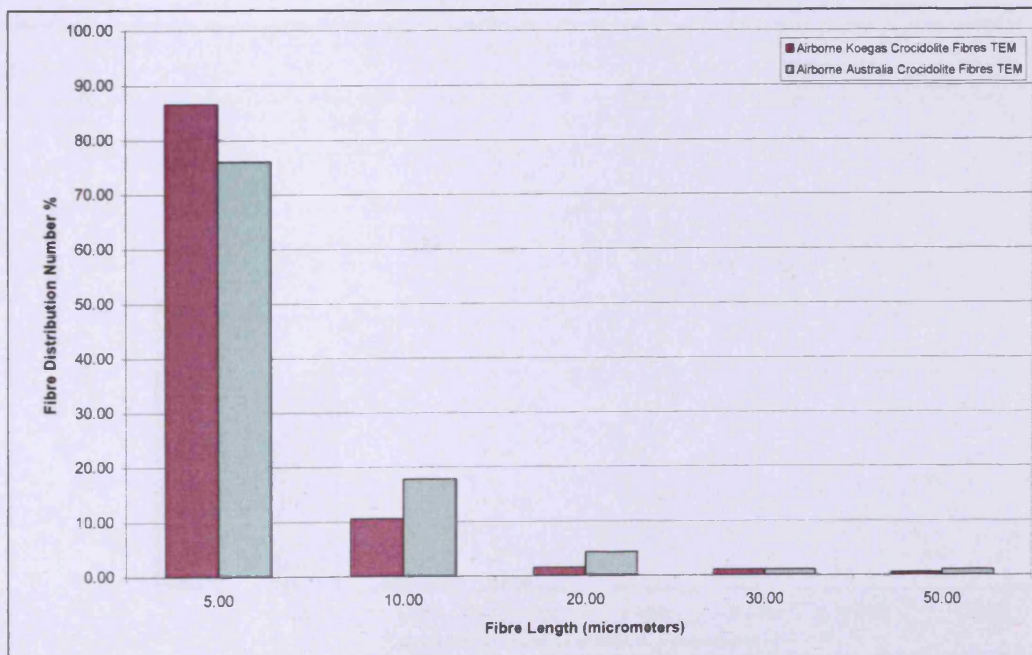


**Figure 6.16 : Comparisons of Diameter Distributions Frequency % of Airborne Koegas and Airborne Australian Crocidolite Fibres Obtained Using TEM Analysis Techniques.**

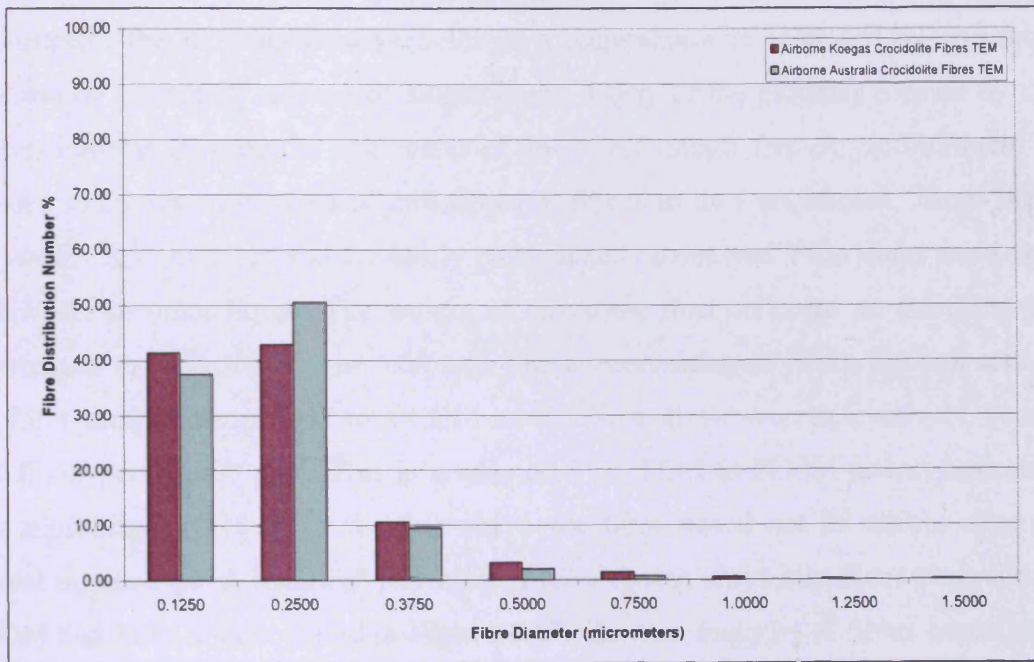
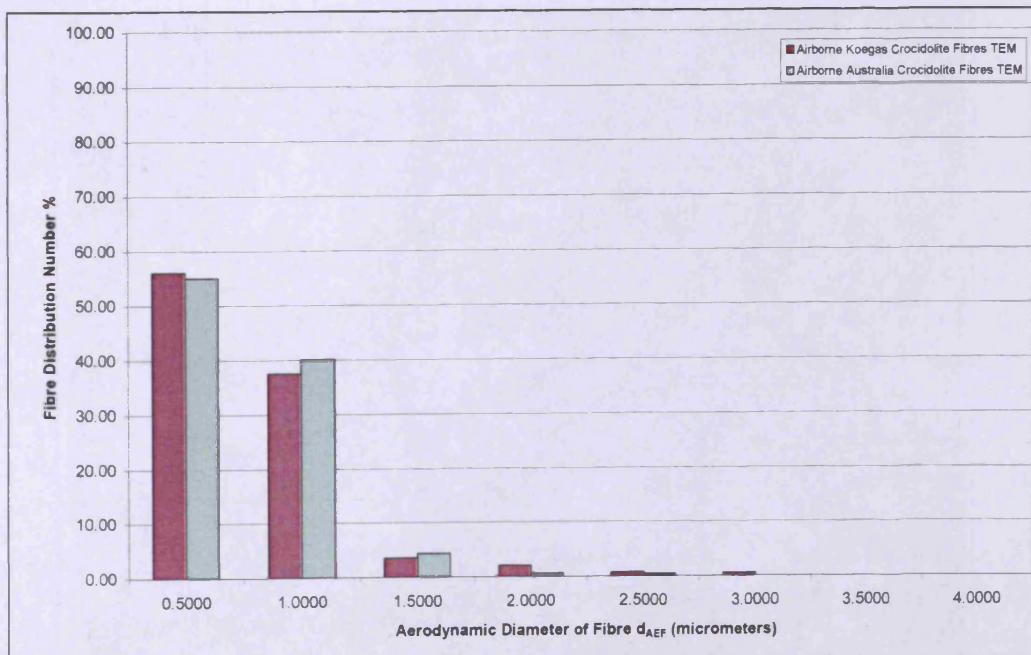


**Figure 6.17 : Comparisons of Aerodynamic Diameter Distributions Frequency % of Airborne Koegas and Airborne Australian Crocidolite Fibres Obtained Using TEM Analysis Techniques.**

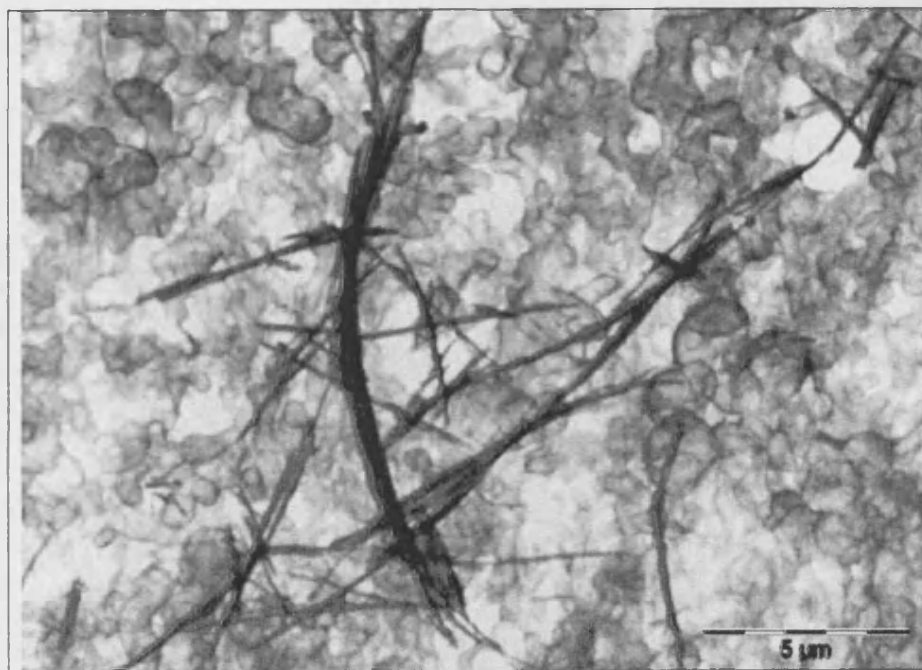




### 6.2.3 Characteristics of Airborne Chrysotile Asbestos Fibres.

The filter preparation of airborne chrysotile dust is illustrated by **Figure 6.18**. It illustrates the fact that dust particles of a respirable size produced by chrysotile asbestos do not totally consist of single fibres. Many of the particles formed by this fibrous mineral are irregular aggregates of fine fibres. Single free chrysotile fibres can be seen to consist of bundles of thin fibres or fibrils as they are known. These fibres are weakly held together and are easily mechanically dispersed if the fibres are wetted with water or other liquid. The weight of chrysotile dust collected on the filter was determined to be 0.00008 g or 0.08 mg. The concentration of fibres per unit area of the filter sample determined by PCOM and TEM analysis were respectively 44 and 178 fibres per 10,000  $\mu\text{m}^2$ . This is a ratio of 4 : 1 TEM to PCOM counts indicating that approximately 75 % of the free chrysotile fibre would not be visible using an optical microscope. A length distribution of the airborne chrysotile fibres observed by PCOM and TEM are compared in **Figure 6.19**. The vast majority of fibres can be seen to be shorter than 10  $\mu\text{m}$  only 1.57 % longer than 10  $\mu\text{m}$  from the PCOM results and 0.1 % from the TEM data. The PCOM results show that 71.13 % by number were shorter than 5  $\mu\text{m}$  and 86 % by TEM analysis.

**Figure 6.18 : Filter with Airborne Chrysotile Fibres Preparation at 2,650 X.**



A comparison of the chrysotile length distribution obtained by TEM analysis with those of the amosite and South African crocidolite is illustrated by **Figure 6.20** from which it can be seen that amosite dust fibres on average are the longest fibres and chrysotile the shortest. **Figure 6.21** illustrates the variation in fibre diameter distribution between the three asbestos mineral dusts. As with the fibre length distribution amosite asbestos forms on average the thickest fibres and chrysotile the finest fibres with the crocidolite distribution between these two mineral type. The comparison of aerodynamic diameter distribution of the three asbestos minerals dusts is illustrated by **Figure 6.22** from which it can be seen that chrysotile produces the finest particles on an aerodynamic basis followed by crocidolite and amosite less so. 61.5 % percent of chrysotile fibres have calculated aerodynamic diameters less than 0.5  $\mu\text{m}$  while the crocidolite fibres have 56.6 % and amosite 24 %. These particles can be classified as nano particles with a size range of 0 – 500 nm in size. The chrysotile dust sample was found to have a weight of 0.08 mg and an average of 178 fibres per 10,000  $\mu\text{m}^2$  of the filter sample. As the active area of the filter onto which the fibres were deposited was 20 mm diameter the total free fibre loading of the filter was estimated as  $5.59 \times 10^6$  thus giving a value of  $69.9 \times 10^6$  fibres per mg of dust.

**Figure 6.19 : Comparisons of Length Distributions Frequency % of Airborne Chrysotile Fibres Obtained Using PCOM and TEM Analysis Techniques.**

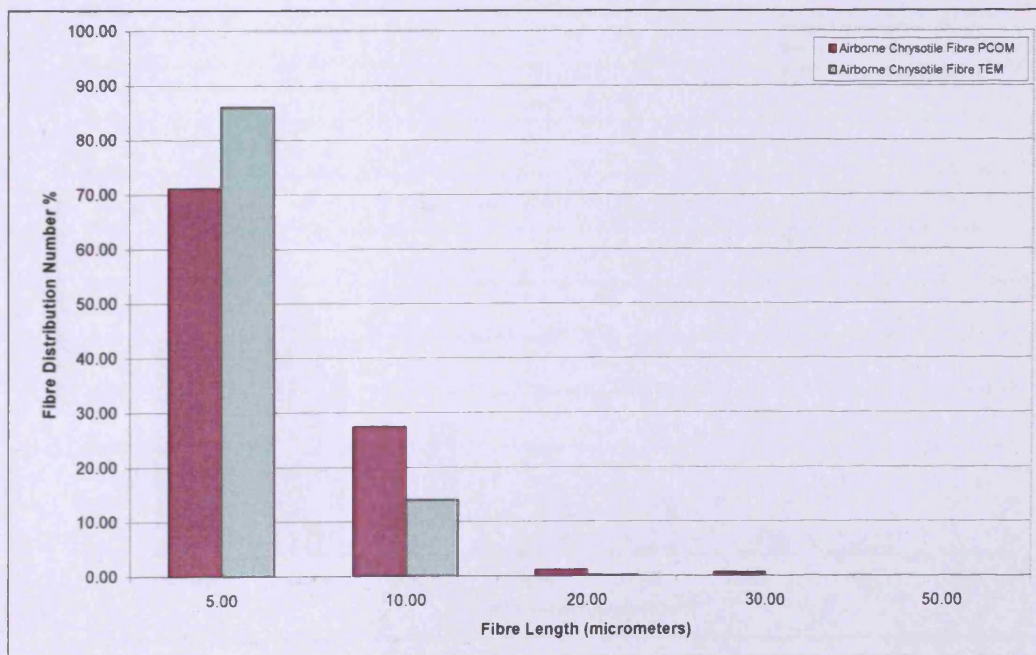




**Figure 6.20 : Comparisons of Length Distributions Frequency % of Airborne Chrysotile Fibre, Airborne Koegas Crocidolite Fibre and Airborne Penge Amosite Fibre Obtained Using TEM Analysis Techniques.**

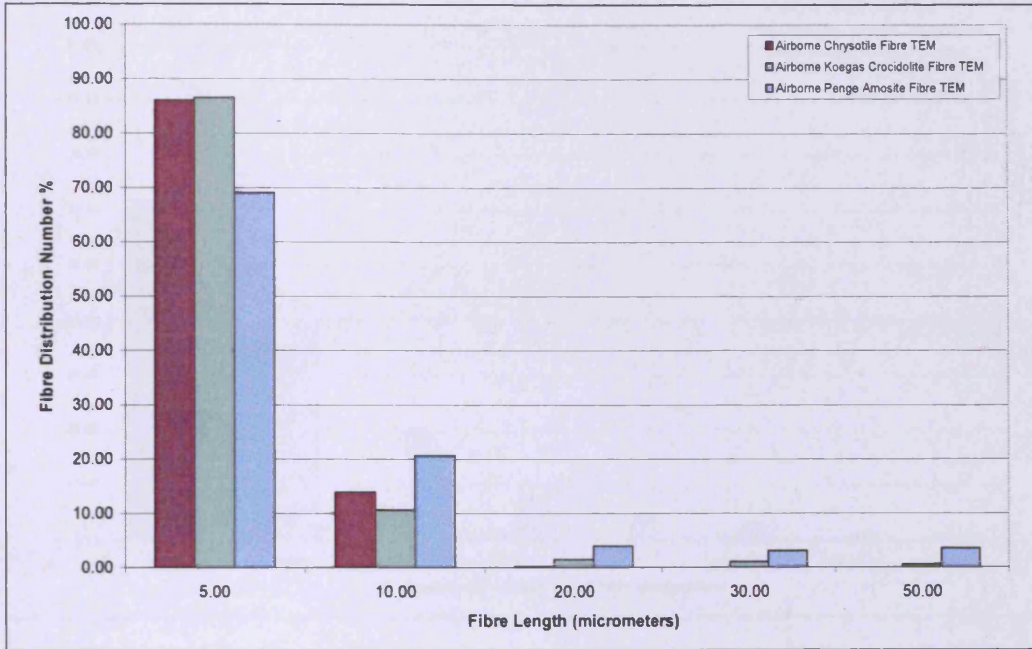


**Figure 6.21 : Comparisons of Diameter Distributions Frequency % of Airborne Chrysotile Fibre, Airborne Koegas Crocidolite Fibre and Airborne Penge Amosite Fibre Obtained Using TEM Analysis Techniques.**

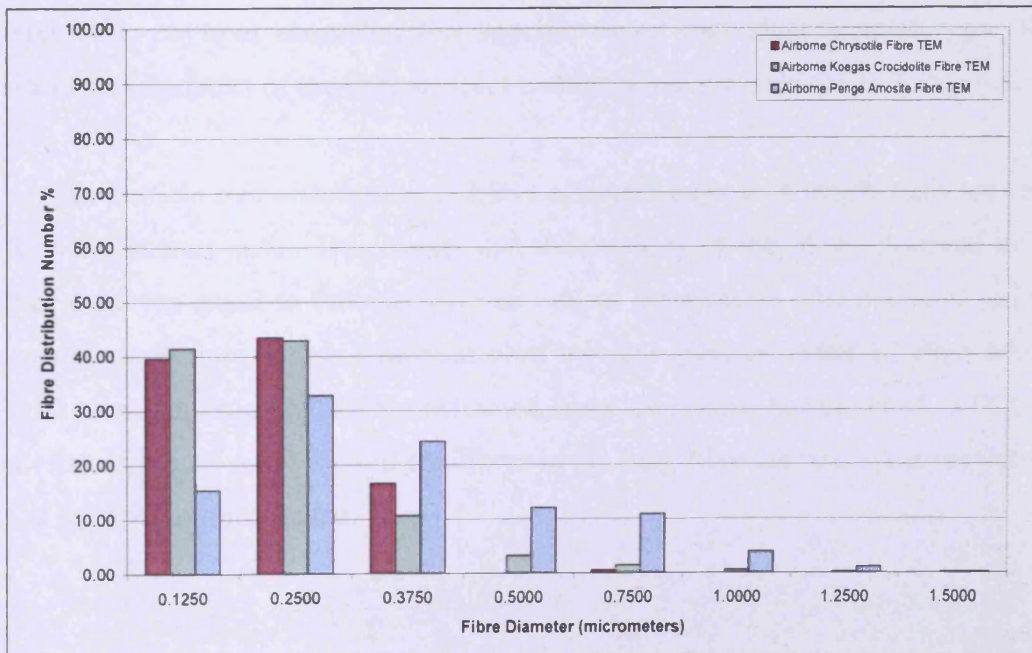
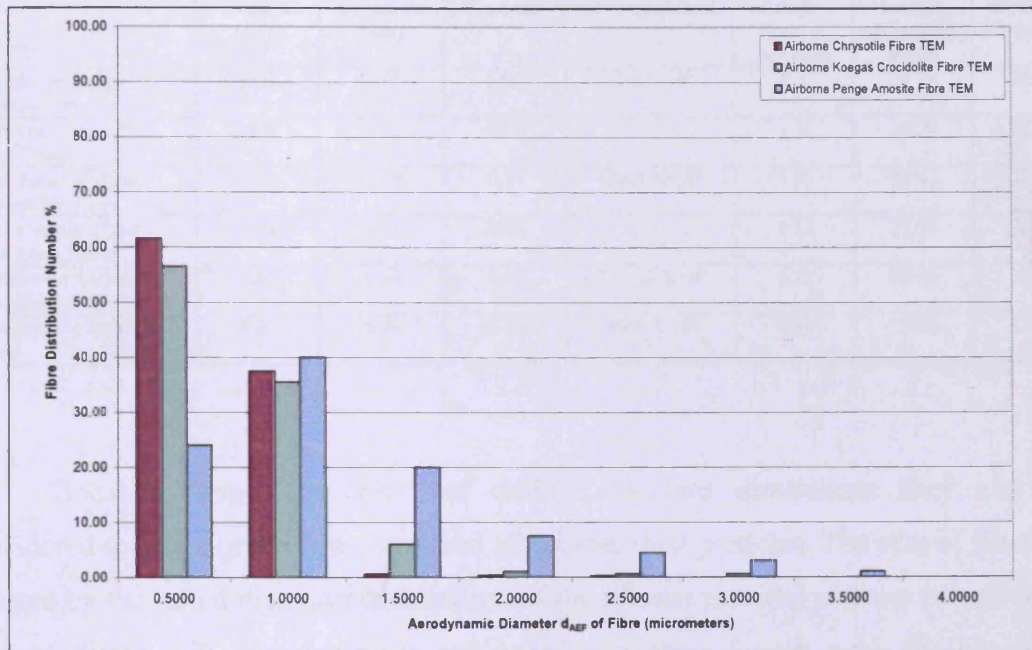


**Figure 6.22 : Comparisons of Aerodynamic Diameter Distributions Frequency % of Airborne Chrysotile Fibre, Airborne Koegas Crocidolite Fibre and Airborne Penge Amosite Fibre Obtained Using TEM Analysis Techniques.**



#### 6.2.4 Physical Characteristics of Airborne Asbestos Fibres.

Examination of dust particles generated from samples of three mineral types which constitute the material known as asbestos has shown that they produce dust particles with physical characteristics specific to an individual mineral type. The physical characteristics of the dust samples examined are summarized in **Table 6.1**.

The particle size distribution of fibres although large on a length basis are very small on a diameter basis. This means that the majority of the fibres observed in all samples were too small to be seen with an optical microscope. The optically visible percentage proportions for each mineral fibre type are given in **Table 6.1** from which it can be seen that crocidolite fibre extracted from lung tissue has on TEM to PCOM count ratio of 9.2 : 1 or 90.2 % of the fibres in the lung fibre are below the resolution limit of the optical microscope.



**Table 6.1 : Summary of Physical Characteristics of Asbestos Fibres from Airborne and Lung Dust Samples.**

Sample	Average Length (µm)	Average Diameter (µm)	Average $d_{AEF}$ (µm)	Concentration per mg of dust	% Longer than 10 microns	Average Length Diameter Ratio	% Optically Visible
1. Airborne Penge Amosite Fibre	6.00	0.31	0.95	226 X 10 <sup>6</sup>	10.42	19.19	20.00
2. Amosite Fibre from Lung Tissue	4.90	0.23	0.68		8.71	21.79	25.61
3. Airborne Koegas Crocidolite Fibre	3.62	0.17	0.51	636.3 X 10 <sup>6</sup>	2.95	21.43	13.33
4. Crocidolite Fibre from Lung Tissue	3.41	0.11	0.33		2.18	31.91	9.80
5. Airborne Australian Crocidolite Fibre	4.52	0.16	0.49	737.32 X 10 <sup>6</sup>	6.28	28.26	14.29
6. Airborne Chrysotile Fibre	3.21	0.16	0.43	69.9 X 10 <sup>6</sup>	0.10	20.05	25.00

Because fibrous particles are defined by two dimensions they can be considered to be unique when compared with other dust particles. The size of fibres is dictated by the initial diameter distribution of the fibrous material and any reduction in size of fibres will occur almost exclusively in their length with the diameter distribution remaining stable. The ability to reduce a fibre in length will also be related to its diameter thicker fibres are less readily broken than thin fibres. This can be observed in the sizing data for the fibres of the asbestos minerals. If the fibres of amosite asbestos are compared with crocidolite fibres, the amosite fibres have a wider range of diameters and also length.

If average lengths of fibre are plotted against average fibre diameter distribution, a relationship between length and diameter for each mineral is obtained. In these graphs the data for airborne amosite fibres and amosite fibres from lung are compared in **Figure 6.24** while similar data for crocidolite fibres are shown in **Figure 6.25**. By comparing the graphs, it can be seen that the average length of fibres retained in the lung are longer on average with change in diameter. This variation from the airborne fibre result is related to the fact that once inhaled shorter fibres are more readily removed from the lung leaving longer fibres to be retained for longer periods. A similar results is demonstrated in **Figure 6.25** for Koegas airborne crocidolite fibre and retained crocidolite fibre from lung. This increase in average fibre length with increase in fibre diameter is a feature of all the fibre types which have been examined

as illustrated by **Figure 6.26** and will hold true for any fibrous material when it is subjected comminution.

**Figure 6.23 : Variation of Average Fibre Length of Airborne Amosite Fibre and Amosite Fibre from Lung Tissue with Diameter of Fibre.**

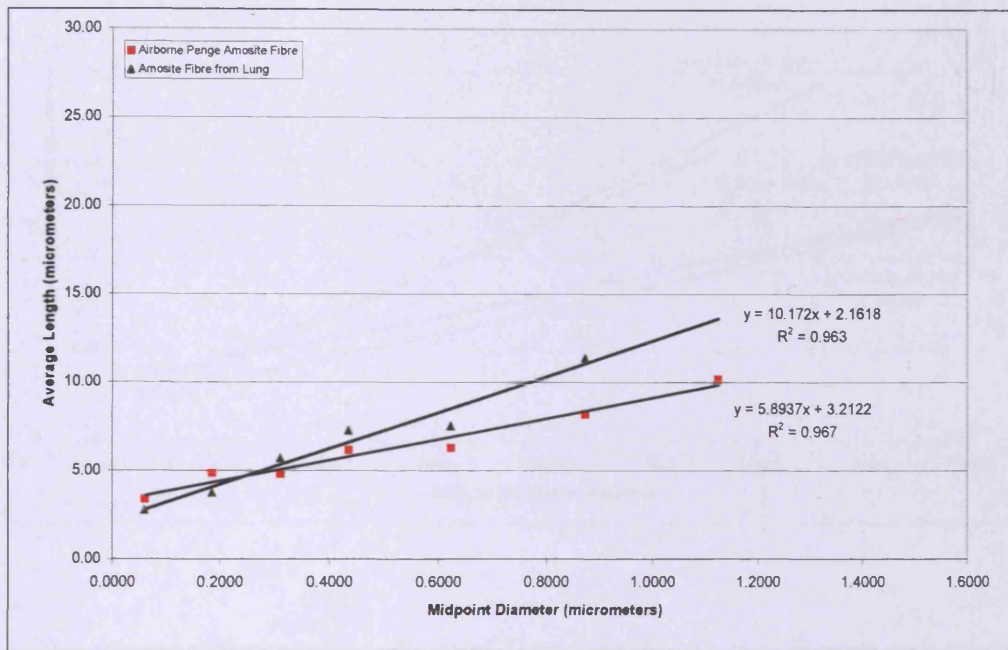


**Figure 6.24 : Variation of Fibre Length For Airborne Crocidolite Fibre and Crocidolite Fibre from Lung with Diameter of Fibre.**

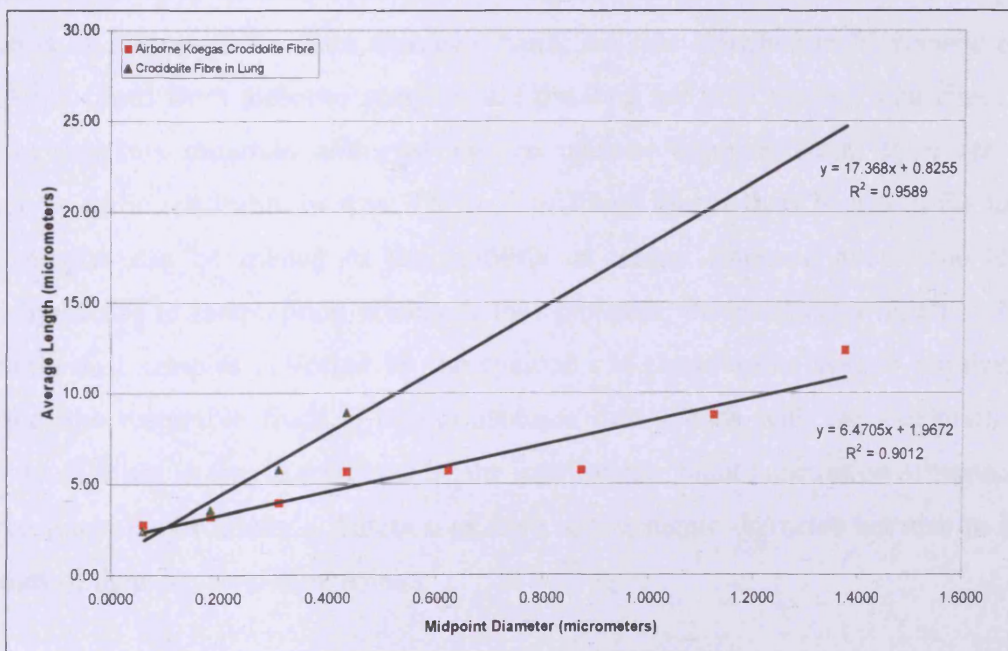
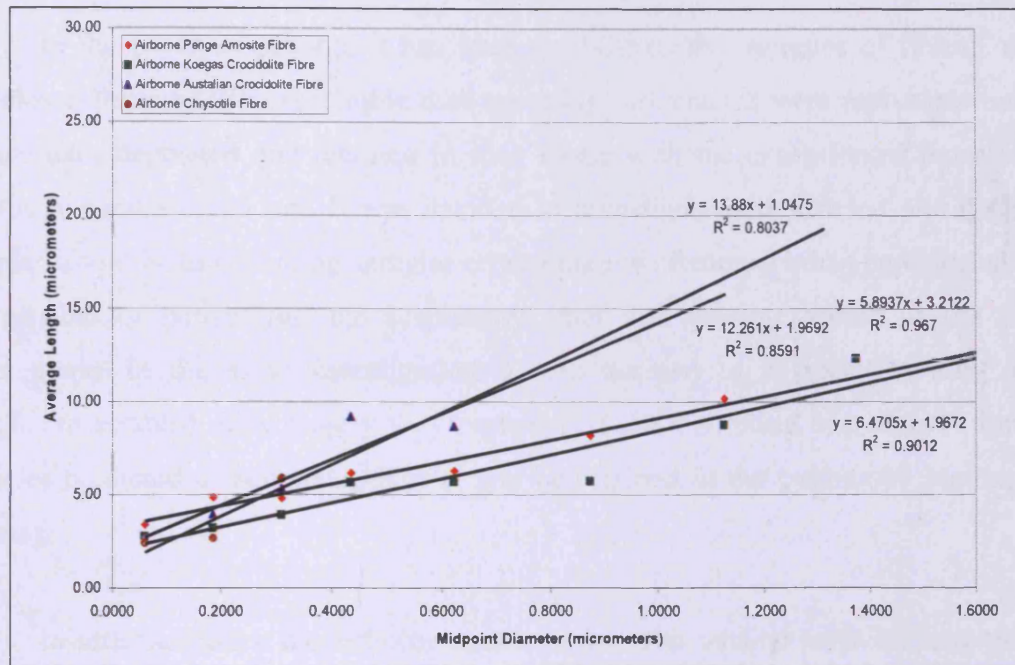




**Figure 6.25 : Variation of Average Fibre Length for Airborne Penge Amosite Fibre, Airborne Koegas Crocidolite Fibre, Airborne Australian Crocidolite Fibre, and Airborne Chrysotile Fibre with Diameter of Fibre.**



The asbestos fibre sample obtained from lung tissue sample represent the true respirable size range of particles that are capable of penetrating into the lung parenchyma. From the data analysis these fibres have length distributions which do not exceed 30  $\mu\text{m}$  for both crocidolite and amosite asbestos dust. The respirable dust collected by the cyclone sampler contained a significant number of fibres with lengths in excess of 30  $\mu\text{m}$ . On a fibre diameter basis, the size distribution of amosite and crocidolite fibres from airborne samples and the lung are very similar. The fibres of the two asbestos minerals collected by the cyclone sampler could therefore be considered to be respirable in size. The lack of fibres longer than 30  $\mu\text{m}$  in the lung fibre samples can be related to the inability of longer fibres to access the lung parenchyma due to interception effects as they penetrate the pulmonary airways. The respirable dust samples collected by the cyclone can therefore be said to physically represent the respirable fraction of the asbestos dust clouds with the exception of fibres over 30  $\mu\text{m}$  in length collected by the instruments. Final penetration of particles into the lungs is not totally a function of their aerodynamic diameter but also to the extremes of their physical dimensions.

### **6.3 Comparison of the Physical Characteristics of Airborne and Inhaled Coal Dust Samples.**

In the previous section, it has been established that samples of fibrous dust particles collected with a respirable dust sampling instruments were representative of the particles deposited and retained in lung tissue with the exception of those with lengths in excess of 30  $\mu\text{m}$ . It was decided to investigate how efficient the cyclone sampler would be in collecting samples representative of compact dust particles which are capable of penetrating the respiratory tract and gaining access to the lung parenchyma. In the same investigation it was decided to characterize lung dust samples to establish how closely they represented the theoretical size distribution of particles predicted to penetrate, deposit and be retained in the pulmonary regions of the lung.

In order to match the airborne dust samples with inhaled particles lung tissue from a case of coal dust exposure was selected. This biological sample had previously been part of extended study of coal workers pneumoconiosis and represented an individual exposed to coal dust at one mining location over many years. The visual appearance of coal dust in this lung sample is illustrated by **Figure 6.26**. This dust was recovered from tissue for examination and characterization and comparison with dust samples collected from coal dust clouds using several dust sampling instruments. These dust samples are illustrated by **Figure 6.27, 6.28, and 6.29**.



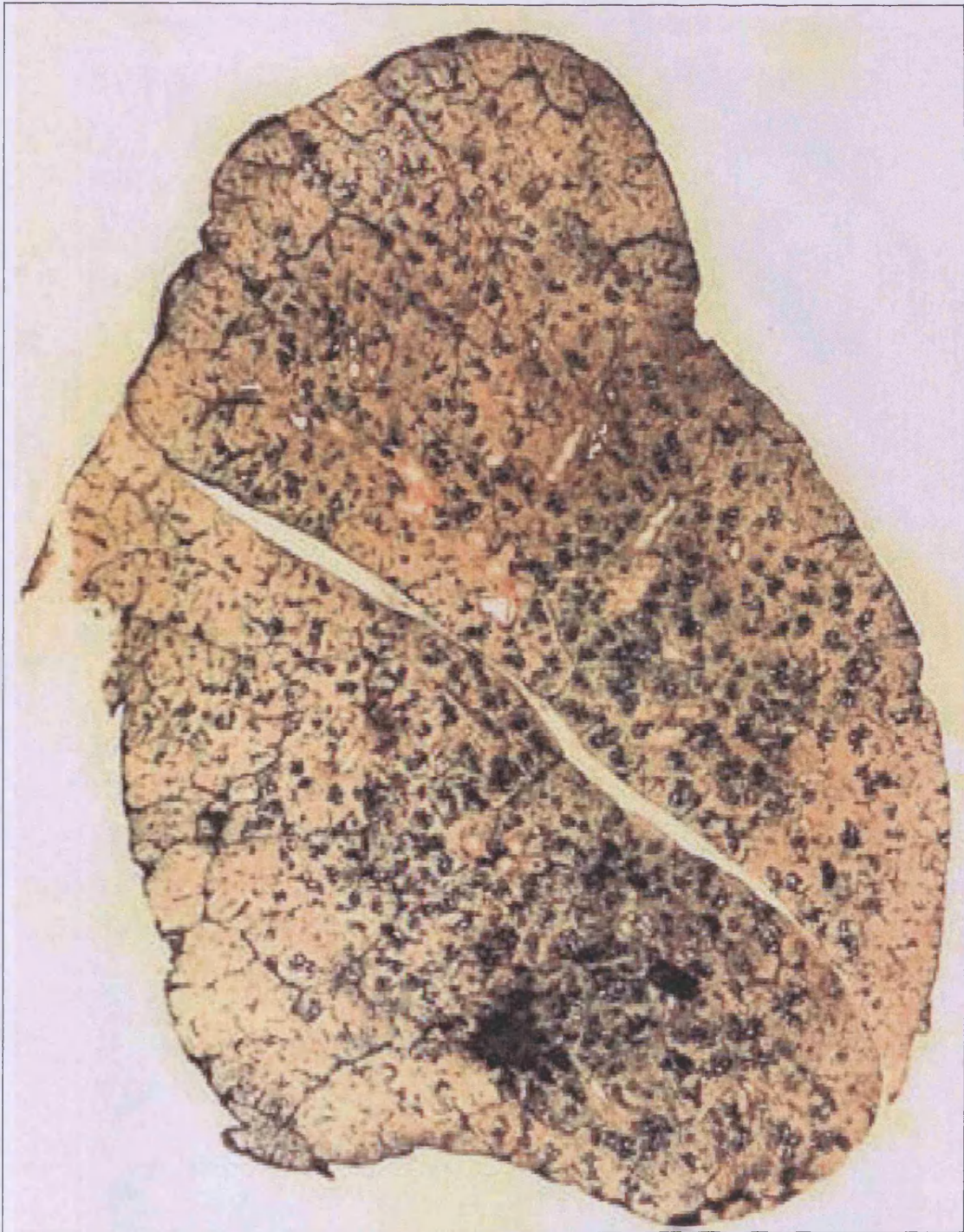


**Figure 6.26 : Thin Section of a Coal Mine Worker Lung.**

**Figure 6.27 : Coal Dust Particles from the Lung Tissue 2,100 X.**

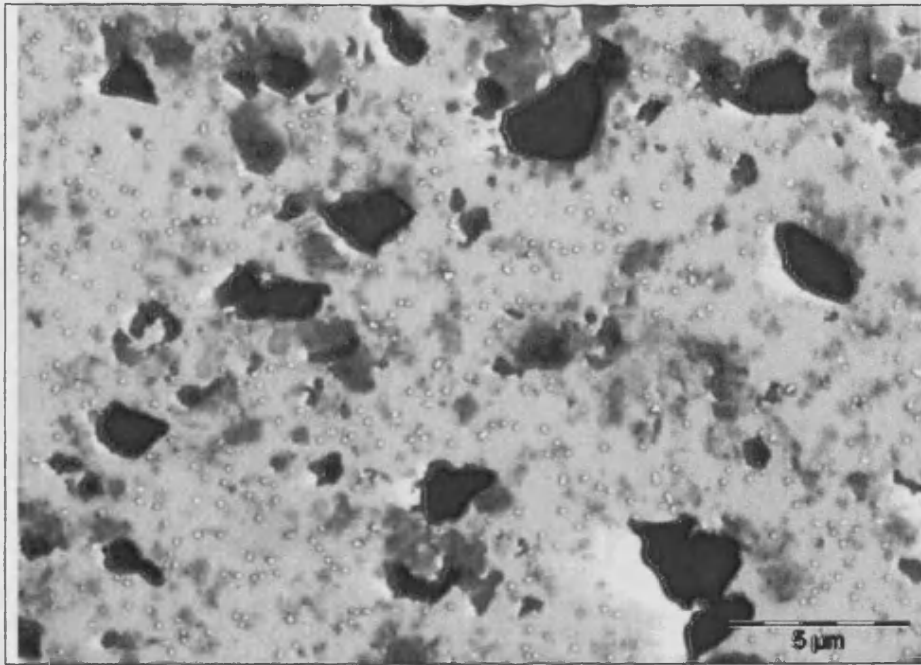


**Figure 6.28 : Coal Dust Particles Sampled Using 7 Hole Sampler 2,100 X.**

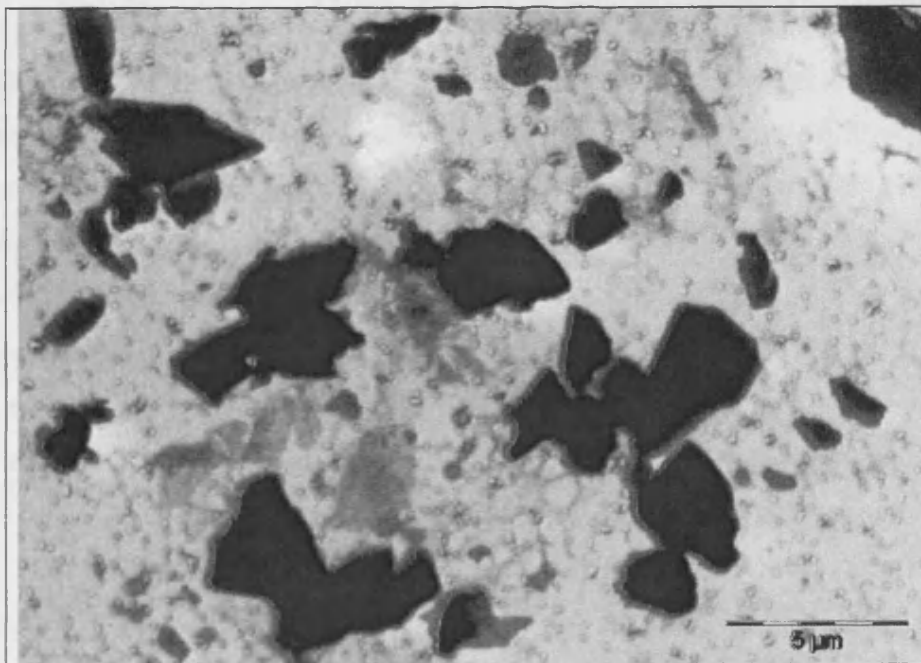
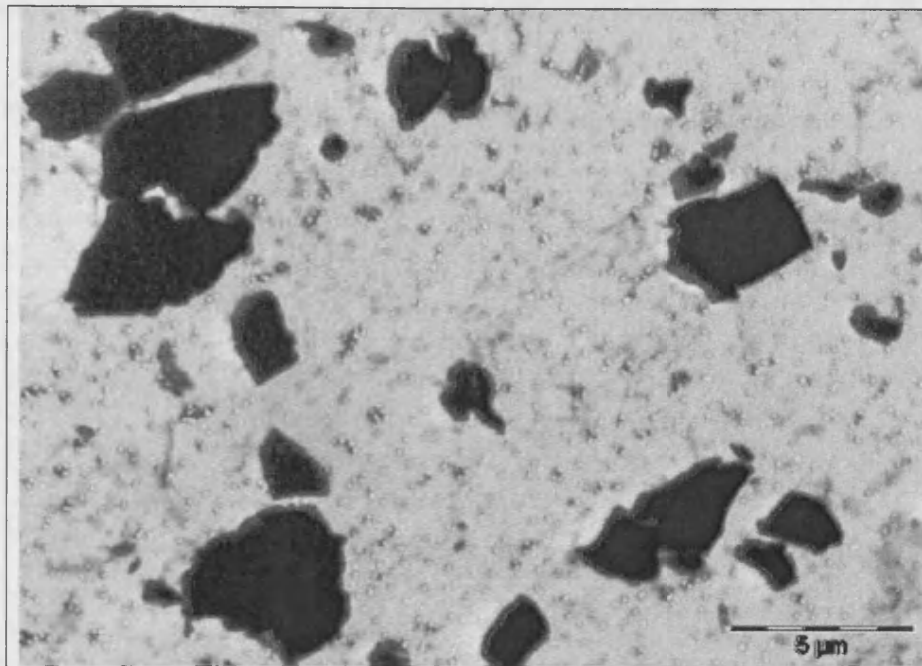




**Figure 6.29 : Coal Dust Particles Sampled Using Cyclone Sampler 2,100 X.**



The type of coal dust to which exposure had occurred was anthracite therefore coal dust clouds were created using a similar type of coal. The samples of airborne coal dusts and the lung dust sample were prepared and sized in the manner described in Chapter 4 to obtain the size distribution of each sample on a particle number basis in terms of equivalent circular diameter (ECD). The ECD value of size relates to the projected area of individual particles once they have deposited on a flat surface. It is well known that particles will mainly orientate themselves in their most stable configuration so that they present their largest surface area for sizing purposes. In order to estimate the volume of individual particles, it was considered necessary to have an estimate of the third dimension or thickness of the individual coal particles. To visualise the third dimension of individual particles, electron microscope samples of the lung dust were coated with aluminium vapour from a point source arranged at an angle of 45 degrees to the surface on which particles has been deposited. Diagrammatically, this is illustrated in **Figure 6.30a** and **6.30b** together with an electron microscope image of the treated samples. This technique is referred to as shadowing as it creates areas around the particles where metal vapour is not deposited which will have dimensions related to the height or thickness of the particle

concerned. These areas can be measured in the direction in which the shadow is thrown to give a direct measurement of particle thickness (T).

**Figure 6.30a : Coal Particle Shadowing Concept.**

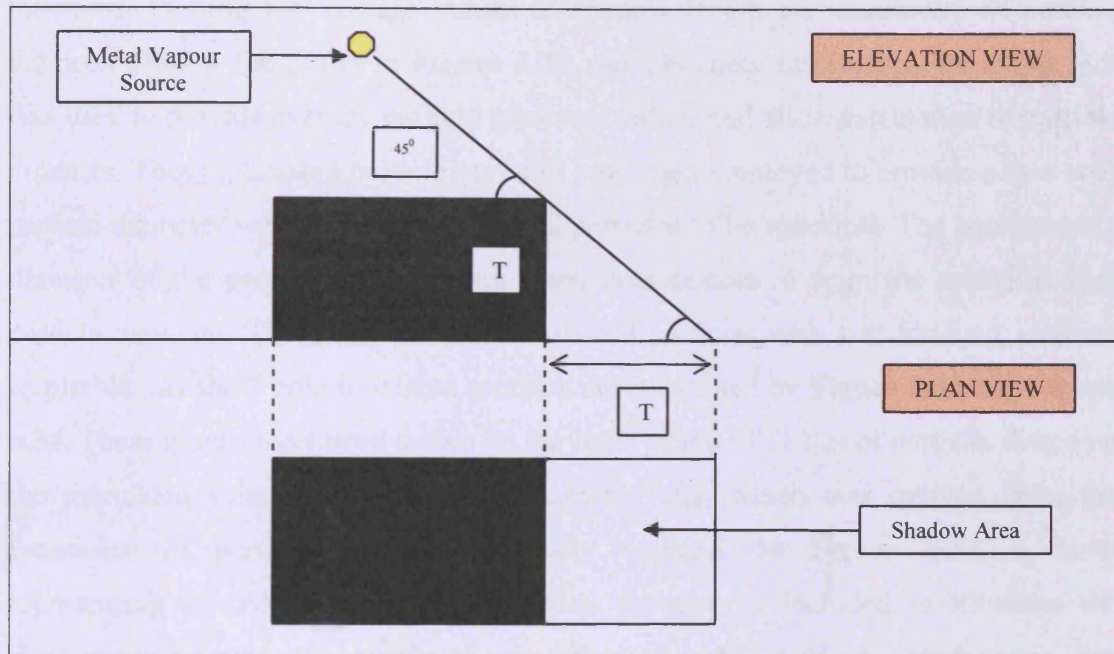
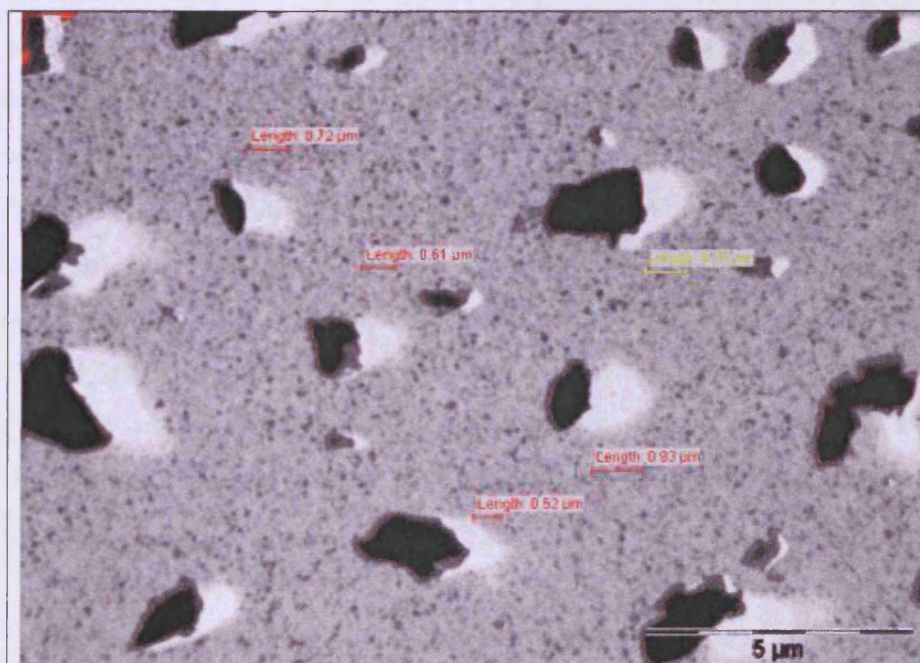


**Figure 6.30b : Coal Dust Particles  $45^\circ$  Shadows at 3,400 X.**



Observation of shadow length and corresponding ECD values for individual particles were collected and analyzed for any mathematical relationship. A plot of the dimensions recorded for each particle in a scatter diagram form is shown in **Figure 6.31** from which it can be seen that a relationship does exist between ECD and thickness. Plotting the average values of shadow length for increments of particle diameter (ECD), the graph in **Figure 6.32** was obtained. Information from this plot was used to provide average particle thickness values and allow calculation of particle volumes. These estimated particle volumes were then employed to provide a new coal particle diameter values assuming the coal particles to be spherical. The aerodynamic diameter of the particulate categories were then calculated from the spherical coal particle diameter. The mass distribution of coal particles with size for lung, cyclone respirable and the 7 hole inhalable samples are illustrated by **Figure 6.33** and **Figure 6.34**. These graphs have been drawn on the basis of the ECD size of particle,  $d$ , and on the calculated value of aerodynamic diameter,  $d_{AE}$ , which was derived from the estimation of particle volume previously outlined. In **Figure 6.33**, a curve representing the BMRC respirable fraction function is included to illustrate the discrepancy between the predicted proportion of particles on an aerodynamic size basis which are respirable and measured values. It can be seen that both the size distributions of the lung dust and respirable dust sampler are similar but are larger than the BMRC predicted values. To investigate this difference further using the 7 hole sampler inhalable dust curve the fraction of the inhalable dust sampled by the cyclone respirable sampler for each size fractions and the proportion of the total dust represented by the lung dust sample for the same size fraction were plotted together with the BMRC respirable function as shown in **Figure 6.35**. It can be seen that the profile of the curves are similar but there are a significant proportion of particles  $> 7 \mu\text{m } d_{AE}$  in both the lung dust and the cyclone respirable dust sample which are not predicted by the theoretical values of the BMRC function. From **Figure 6.33** in which it can be seen that approximately 10 % of the mass of the coal lung and the cyclone coal dust samples are in excess of the respirable mass predicted by the BMRC function.

The cyclone respirable dust sampler has been shown to over estimate the respirable fraction of airborne fibrous particles as it is not capable of reproducing the effect with lung which the length of fibres deposited to  $30 \mu\text{m}$ . When the collection of



respirable compact particles are considered we have demonstrate that the cyclone respirable dust sampler produces a sample with a size diameter which is very comparable to that of dust which has been retained in the lungs, but is not predicted by the BMRC respirable dust mass retention function.

**Figure 6.31 : Particle Size (ECD) vs Thickness (Length) of Coal Dust Particles Shadow.**

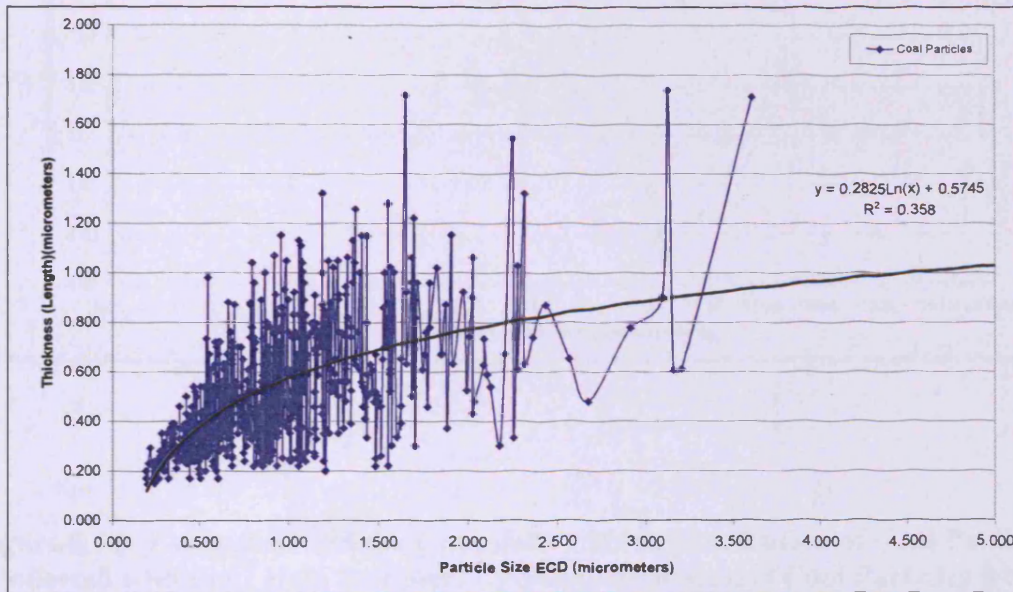


**Figure 6.32 : Average Particle Size (ECD) vs Thickness (Length) of Coal Dust Particles Shadow.**

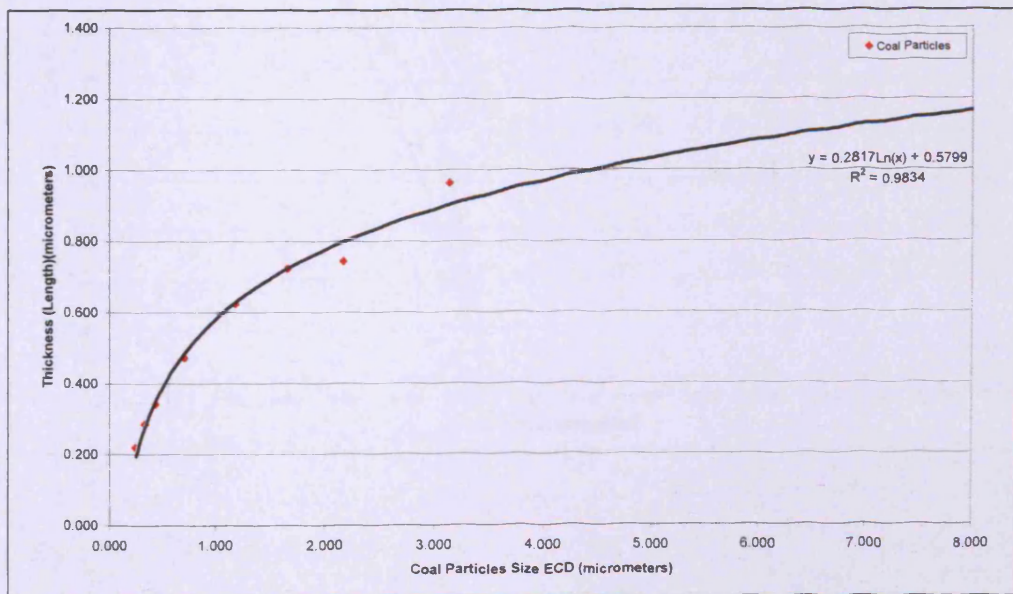




**Figure 6.33 : Comparisons of the Cumulative Mass Distribution of Coal Particles Collected with the 7 Hole Sampler, Cyclone Sampler, and Coal Particles from Lung Tissue on the Basis of Calculated Aerodynamic Diameter Values.**

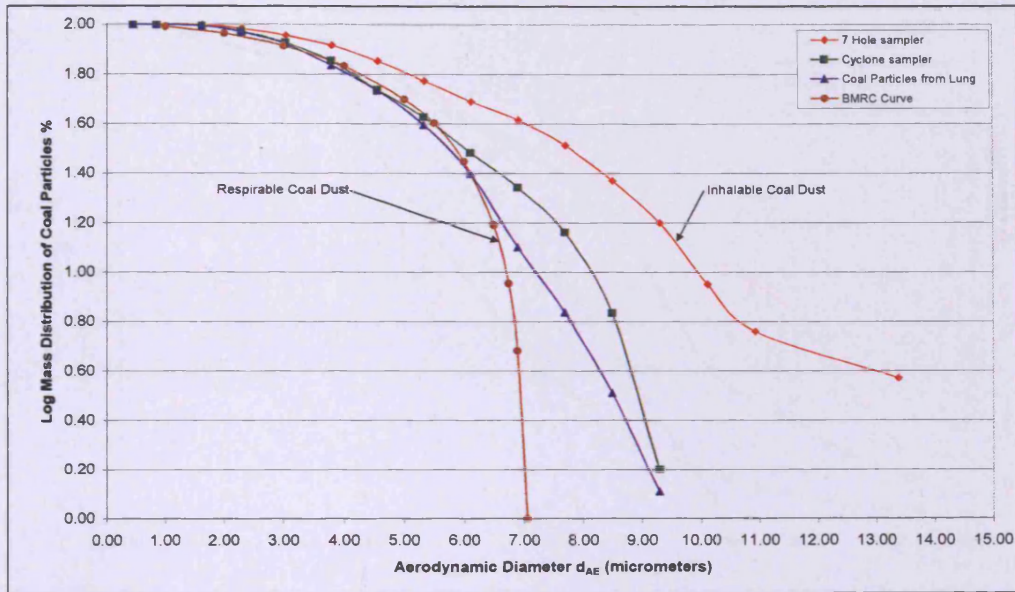


**Figure 6.34 : Comparison of the Cumulative Mass Distribution of Coal Particles Collected with the 7 Hole Sampler, Cyclone Sampler, and Coal Particles from Lung Tissue on the Basis of ECD Diameter Values.**

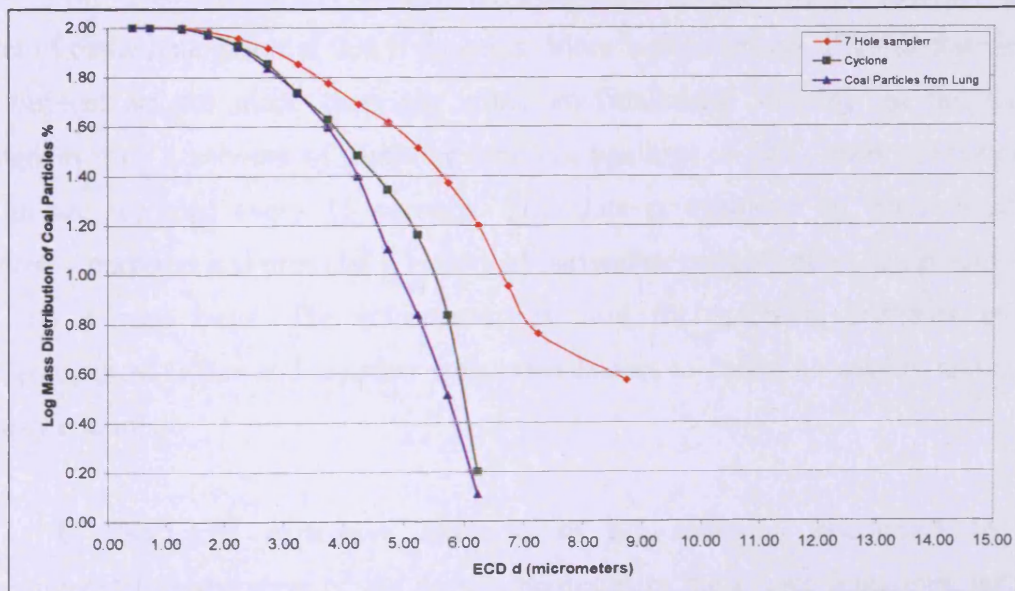
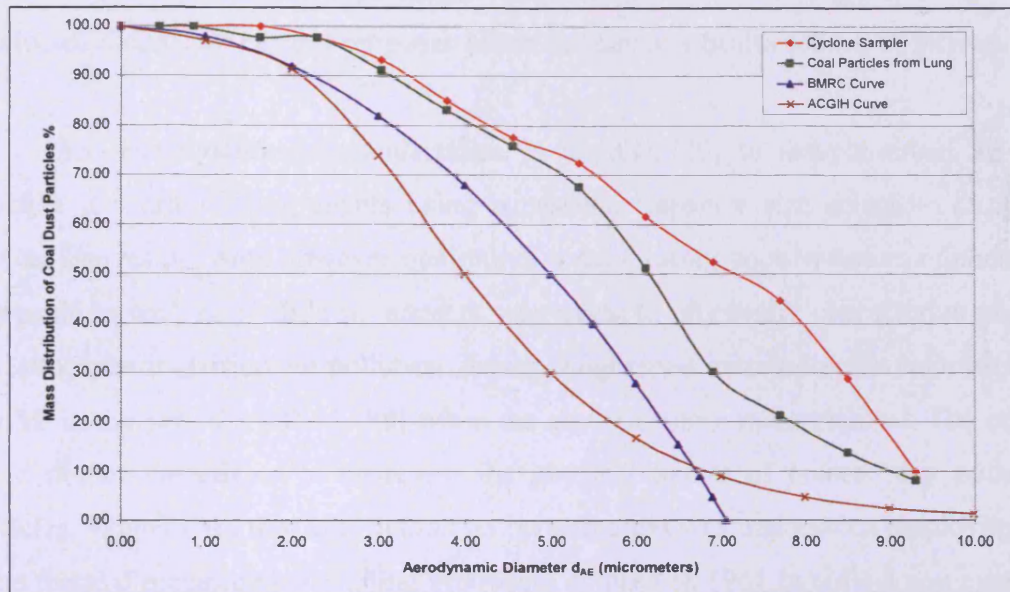




**Figure 6.35 : Cumulative Mass Distributions of Coal Particles which have been Size Selected by a Cyclone Sampler and Retained in Lung Tissue in Comparison with the ACGIH and the BMRC Convention of Predicted Respirable Dust.**



#### 6.4 Physical Characterization of Urban Air Pollution Particulates.

The most extensively studied environmental property of ambient air is the level of particulate material that it contains. More measurements of particulate levels in ambient air are made than any other environmental variable. In the United Kingdom from a network of sampling stations, readings of  $PM_{10}$  mass concentration in air are recorded every 15 seconds. This data is available on the internet for reference purposes and provides a history of particulate concentration levels across the UK on a mass basis. The information is used for modeling purposes by the Meteorological Office and together with other factors to define air quality and assess quality control.

In this very expensive exercise of air sampling conducted by the environmental departments of the county boroughs in the United Kingdom, not one measurement is ever taken to characterize the particulate material, which is automatically collected. Little if any information relating to the size distribution of the suspended particulate material in ambient air is collected although some

measurements of particle number concentrations at selected sites have been conducted. Considering how important the size of particles are from a health point of view it would appear that ambient air monitoring on such a large scale is being conducted mainly for control purposes alone and has few health related objectives.

An investigation was undertaken in Cardiff [79] to sample urban air and describe its various components using a cascade impactor size selective sampling device. The results were however qualitative concentrating upon variation of chemical composition with size while no attempt was made to physically characterize present day atmospheric particulate pollution. Some enlightened measurements were taken in Cardiff in the period 1960-61 [80] when the city was more industrialized. The results could not be considered to represent the physical nature of present day pollution particles. Armed with this information an investigation was undertaken employing the same thermal precipitator sampling procedure as used in 1961 to collect and examine particles with the TEM. It was also possible to take dust samples in roughly the same location as those collected in 1961. Particulate material was sampled directly onto carbon coated electron microscope grids for immediate examination as described in Chapter 4. Images of the particles collected were recorded at a range of magnifications which included 2,100 X, 4,400 X, 11,000 X and 13,000 X magnification and these are illustrated in **Figure 6.36**.

The particles contained in each set of images were sized using the analysis system software to produce comparative size distributions. The distributions obtained from the images recorded at various magnifications are illustrated by **Figure 6.37**. It can be seen that at the lower magnifications fewer fine particles were being detected and more larger particles recorded by the analysis software. The size distribution from the images recorded at the two higher magnifications are however similar and the data collected from those images recorded at a magnification of 13,000 X were chosen to represent the size distribution of the particulate sample. The size distribution of the airborne particulate sample was then compared to similar sample results obtained in 1961. The most dramatic change in the size distribution is the much larger proportion of particles < 60 nm in the size distribution of the air pollution sample from 2006 whereas few particles < 60 nm were observed in the 1961 sample.



**Figure 6.36 : Comparison of 2006 Airborne Particulates at Different Magnifications : a). 2,100 X, b). 4,400 X, c). 11,000 X, and d). 13,000 X.**

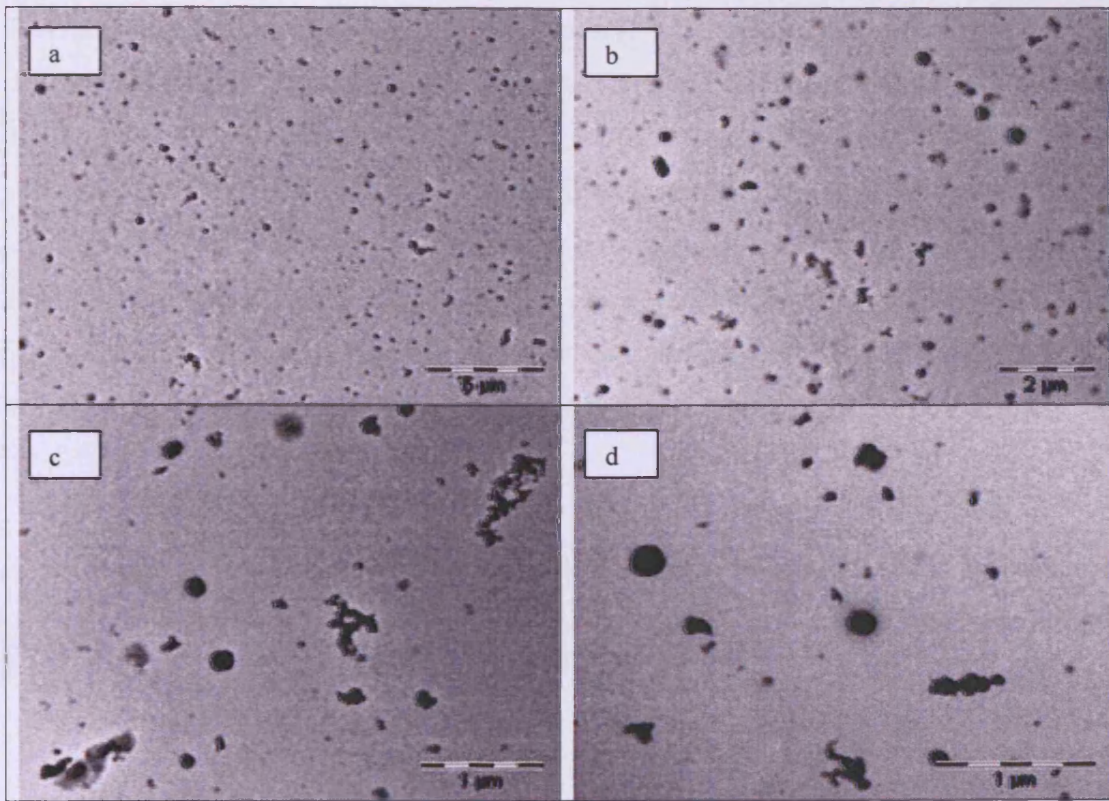
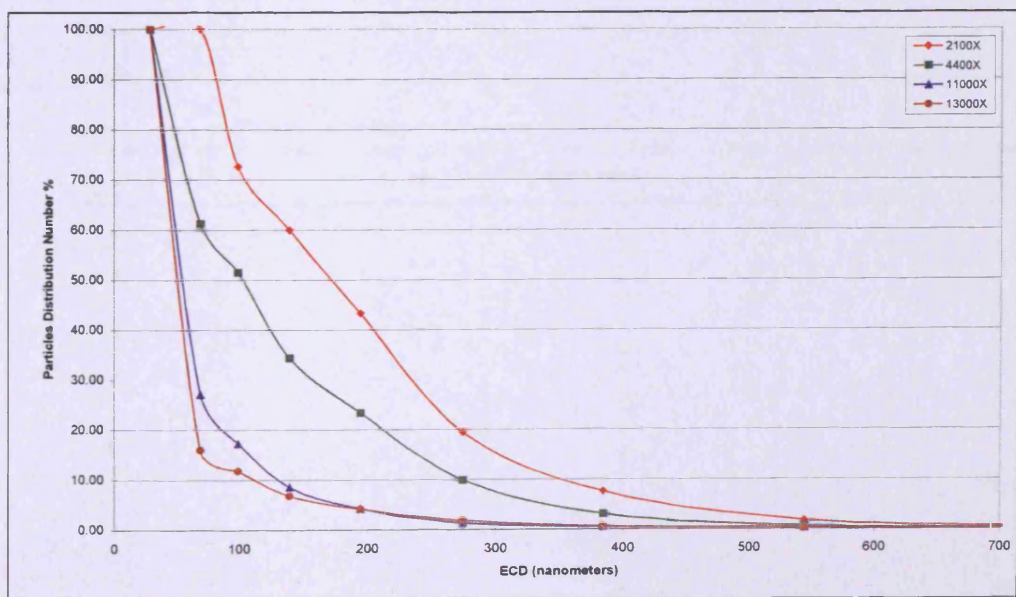


**Figure 6.37 : Comparison of 2006 Airborne Particulates Distribution % at Different Magnification Obtained Using the TEM Analysis Techniques.**





To highlight the difference between the two airborne sample plots on the basis of particle number and mass distribution with size for both ECD and aerodynamic diameters are contained in **Figures 6.38 to 6.41**. On a particle number basis nearly 100 % of 2006 pollution particles have aerodynamic diameters  $< 0.5 \mu\text{m}$  as compared to 80 % of 1961 material. On a mass basis, no 2006 pollution particles have aerodynamic diameters  $> 2 \mu\text{m}$  compared to nearly 30 % of 1961 particles. For comparison purposes, images of the two pollution samples presented at the same magnification are shown in **Figure 6.42** to illustrate the finer nature of 2006 pollution. The changes in the nature of air pollution can be linked to the reduction in heavy industry in Cardiff and also the increase in road traffic especially diesel vehicles.

**Figure 6.38 : Comparison of Particle Distributions Number % of 1961 and 2006 Airborne Particulates on the basis of ECD values.**

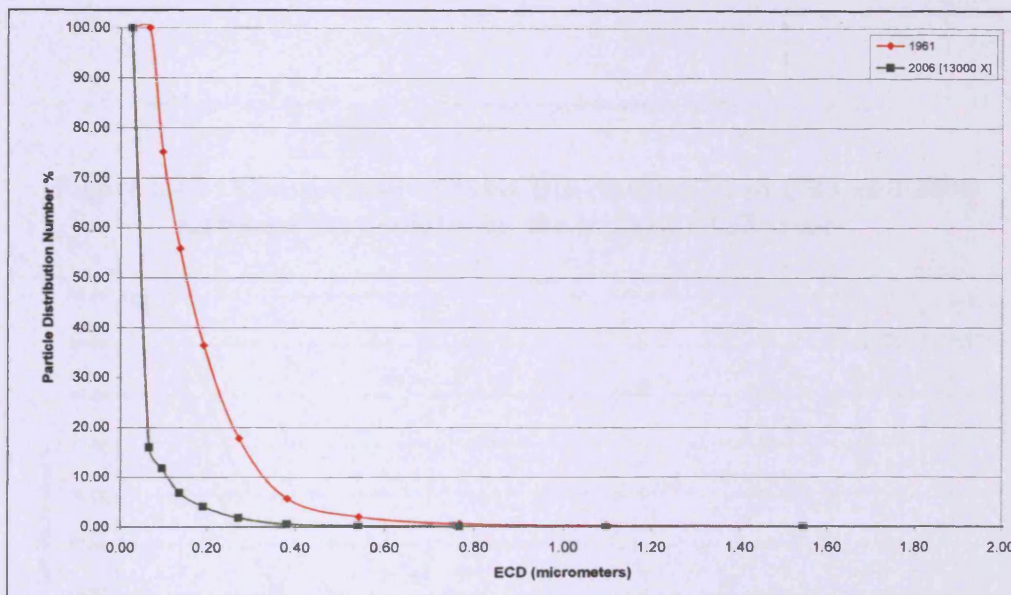


**Figure 6.39 : Comparison of Particle Distributions Number % of 1961 and 2006 Airborne Particulates on the basis of Aerodynamic Diameter values.**

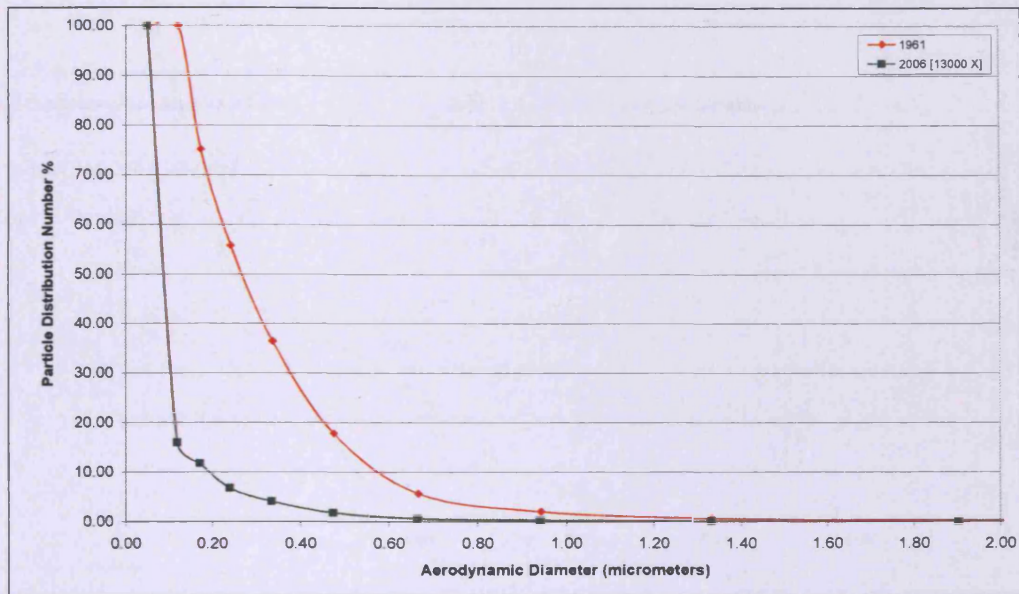


**Figure 6.40 : Comparison of Mass Distribution % of 1961 and 2006 Airborne Particulates on the basis of ECD values.**

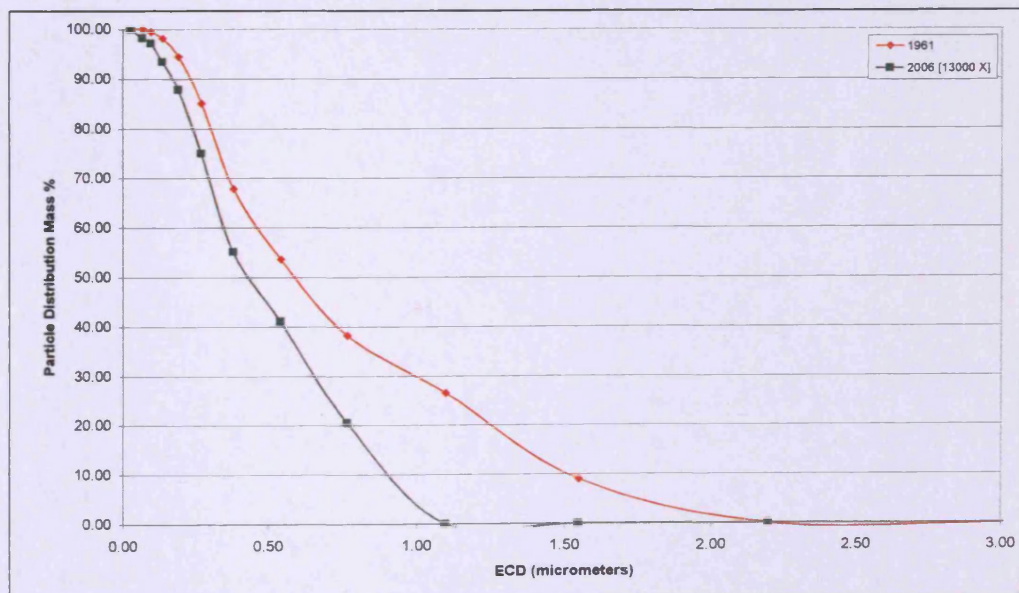




**Figure 6.41 : Comparison of Mass Distribution % of 1961 and 2006 Airborne Particulates on the basis of Aerodynamic Diameter values.**

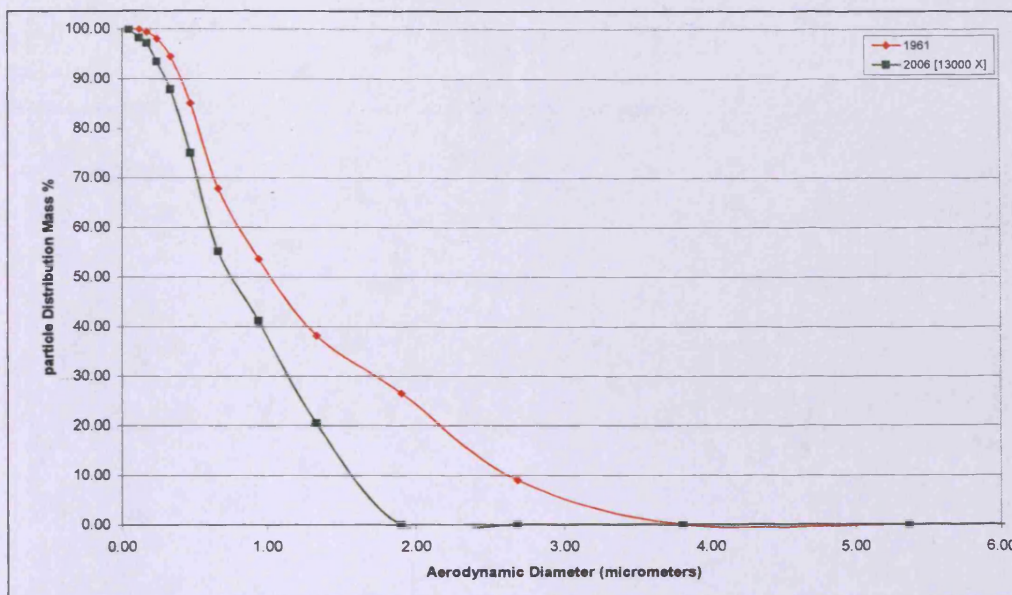
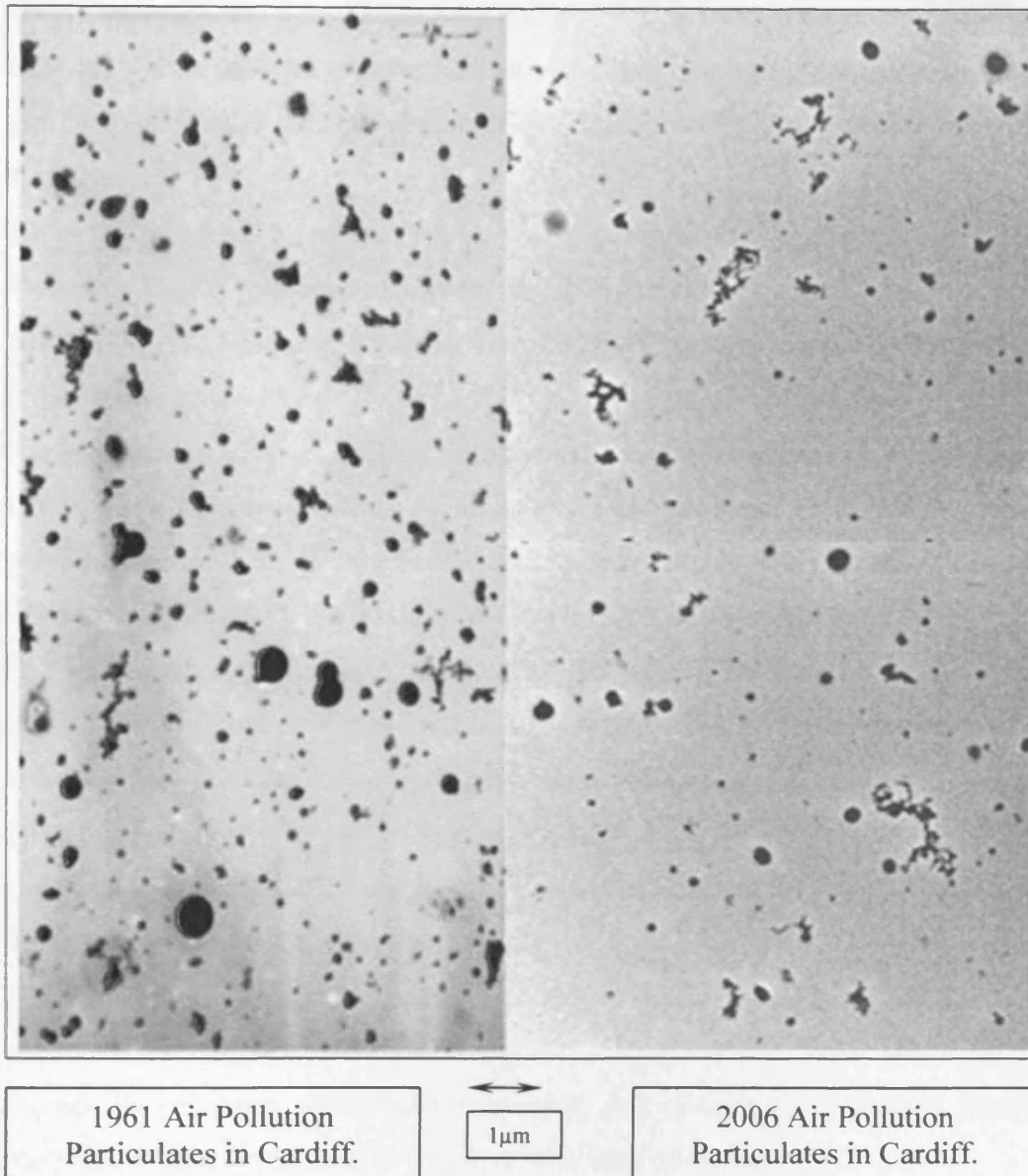


Figure 6.42 : Comparison of 1961 and 2006 Airborne Particulates.



## 6.5 Conclusion

- In characterizing asbestos fibres, TEM has proven to be far better than PCOM for examining fibre lesser than 0.3 μm.
- The length distribution frequency % is similar for airborne amosite fibres and amosite fibres from lung using TEM but not PCOM.

- The respirable fraction of an amosite dust cloud is mainly confined to these fibrous particles less than 30  $\mu\text{m}$  long and less than 0.5  $\mu\text{m}$  diameter.
- TEM results for Koegas crocidolite airborne fibres and lung fibres are remarkably similar to each other and show that Koegas dust cloud is almost totally respirable in nature.
- The respirable fraction of the crocidolite dust clouds was found to be confined to fibres less than 20  $\mu\text{m}$  long and less than 0.375  $\mu\text{m}$  in diameter.
- The airborne Koegas and Australian crocidolite fibres are similar in terms of size and airborne characteristics.
- The comparison of fibre length distribution showed that airborne chrysotile fibre is a finer fibre than crocidolite and amosite fibres. They can be classified as nano particles with 61.5 % of chrysotile fibres having calculated aerodynamic diameter less than 0.5  $\mu\text{m}$  while the crocidolite fibres have 56.6 % and amosite 24 %.
- The size of airborne fibres is dictated by the initial diameter distribution of the fibrous material and any reduction in size of fibres will occur almost exclusively in their length with the diameter distribution remaining stable.
- The average length of fibres retained in the lung are larger on average with change in diameter. Shorter fibres are more readily removed from the lung leaving longer fibres to be retained for longer periods.
- The amosite and crocidolite fibres which are retained in the lung are considered as respirable in size because these fibres have length distributions which do not exceed 30  $\mu\text{m}$  even though the respirable dust collected by cyclone sampler contained a significant number of fibres with lengths in excess of 30  $\mu\text{m}$ .
- On a fibre diameter basis, the size distribution of amosite and crocidolite fibres from airborne samples and the lung are very similar.
- A comparison between a generated Anthracite dust cloud and similar particles inhaled and retained in the lungs has been performed and a marked similarity in the size distributions of both demonstrated.
- It has been shown that a relationship exists between the settled dimensions of coal particles and their thickness.
- A significant proportion of coal dust particles  $> 7 \mu\text{m}$   $d_{AE}$  were estimated in both the lung dust and the cyclone respirable dust sample, which are not predicted by the theoretical values of the BMRC function. 10 % of the mass of the coal lung

and the cyclone coal dust samples were found to be in excess of the respirable mass predicted by the BMRC convention.

- The cyclone respirable dust sampler produces a sample with a size diameter, which is very comparable to that of dust, which has been retained in the lungs, but is not as predicted by the BMRC convention.
- It has been identified that in general environment in Cardiff there are more fine particles < 60 nm in size in air pollution in 2006 than in 1961.
- On a particle number basis, nearly 100 % of 2006 pollution particles have aerodynamic diameters < 0.5  $\mu\text{m}$  as compared to 80 % of 1961 material. On a mass basis, no 2006 pollution particles have aerodynamic diameters > 2  $\mu\text{m}$  compared to nearly 30 % of 1961 particles.

## **CHAPTER 7 :**

### **GENERAL CONCLUSIONS**

From the investigations reported in this thesis, there are a number of general conclusions that can be drawn from the results.

- In an environmental chamber of approximate 0.5 m<sup>3</sup> it is possible to generate a reproducible dust cloud that can be employed to compare the collection efficiencies of low volume dust sampling instruments i.e. < 3 L/min.
- Environmental chambers with such a low volume are not suitable for studying the sampling efficiency of instruments with larger-volume sampling rates e.g.: 25 L/min.
- Dust generation rates and instrumental sampling periods must be adjusted to take into account the rate at which the concentration of dust may increase in the chamber in order that results from individual instruments may be compared.
- A comparison of the results obtained from several inhalable dust samplers showed that they produced similar mass concentration results when operated together in the environmental chamber.
- When respirable dust samplers were operated in the same dust conditions, a variation of results was obtained which can be related to the different size selective principles employed by the various instruments.
- The cyclone respirable dust sampler produced airborne mass concentration results in excess of other instruments, which was linked to the high shear forces generated within the instruments, breaking up particle aggregates and increasing the mass of respirable dust.
- The operating principles of respirable samplers should therefore be taken in account when selecting an instrument to sample dusty atmospheres where particle aggregation in the suspended dust is a feature of its physical characteristics.
- Results obtained using specific respirable dust sampling instruments were consistent although it was necessary to operate at designed sampling rates to ensure accurate readings. The exception to this rule was found to be the

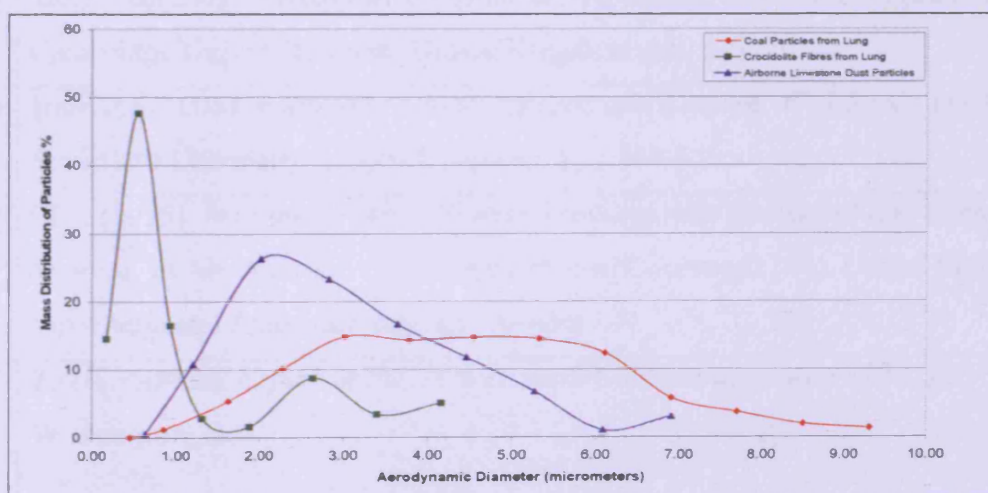


cyclone sampler with which similar results could be obtained with a range of flow rates.

- The inhalable and respirable dust samplers tested were designed for determination of airborne mass concentration only. None of the instruments were capable of sampling airborne dust for particle size characterization.
- The thermal precipitator was found to be the most convenient instrument for sampling individual dust particles and providing samples which could be directly examined by electron microscopy.
- Optical microscopy was found to be an inconvenient method for imaging and sizing particles especially those that were translucent or contained particles which were smaller than the resolution limit of the optical technique.
- Dispersion and resuspension of dust samples in water for sizing purposes is not recommended due to the break down of aggregates and solubility of particles.
- It was found to be possible to predict the respirable mass fraction of an inhalable dust sample employing particle sizing data and material density, and using the BMRC convention for variation of respirable efficiency with aerodynamic size to calculate the proportions of each size fraction which would be theoretically respirable. Theoretical and measured values were found to be similar.
- Fibrous dust clouds sampled with a cyclone respirable dust sampler were examined by both regulatory PCOM and TEM techniques and the PCOM procedure was found to be highly inaccurate for determination of fibrous particle number concentrations in air due to its limited resolution of particles.
- TEM can be stated to be the only technique capable of accurately estimating airborne asbestos fibre concentrations or conversely total airborne particulate matter.
- Comparison of sizing data for fibres sampled from lungs and airborne dust clouds showed that respirable sampling instruments do not collect fibres, which can be considered to be wholly respirable.
- Respirable fibres must be defined on the basis of diameter and length as few fibres with diameters  $> 0.5 \mu\text{m}$  and lengths  $> 30 \mu\text{m}$  can be considered respirable.

- Respirable asbestos fibres were found to have a very small aerodynamic size range, few particles having a  $d_{AEF}$  larger than 1  $\mu\text{m}$ .
- Inhaled and retained coal dust particles from the human lung were found to compare very favourably in terms of calculated aerodynamic size distribution with those particles size selected from a generated coal dust cloud.
- The aerodynamic size range of coal particles from tissue was found to be much larger than that of asbestos fibres from lung. These differences are illustrated by **Figure 7.1**.
- There are extremely large differences in the physical size and therefore aerodynamic properties of dust particles formed by different materials.
- Health and environmental effects of airborne particulate materials are more closely linked to particle size than airborne mass concentration.
- It is apparent that a gap in our knowledge exists regarding the size of dust particles generated by individual materials and their biological effects when inhaled.
- There are few procedures available that can successfully be applied to collect and physically analyze airborne particulate matter and allow a risk assessment to be performed to highlight possible dangers.
- The majority of dust sampling instruments and analytical procedures have been designed for control purposes only and not to investigate possible health effects.

**Figure 7.1 : Comparison of % Mass Distribution of Coal Dust Particle from Lung, Crocidolite Fibres from Lung, and Airborne Limestone Dust Particles on the Basis of Aerodynamic Diameter.**



## REFERENCES

[1]	Nevers, N.D. (1995). <i>Air Pollution Control Engineering</i> . McGraw-Hill, Inc. United States of America. pp.:1-32.
[2]	Bishop, C. A. (1957). <i>EJC Policy Statement on Air Pollution and Its Control</i> . Chemical Engineering Programme, 53(11) :146.
[3]	A.S. Hornby (2005). <i>Oxford Advanced Learner's Dictionary, 7 Edition</i> . Oxford University Press. Oxford. pp.: 32-1167
[4]	Peavy, H.S., Rowe, D.R., & Tchobanoglous, G. (1985). <i>Environmental Engineering, International Edition</i> . McGraw-Hill. Singapore. pp.: 417-572.
[5]	Jackson, A.R.W. and Jackson, J.M.(1996). <i>Environmental Science : The Natural Environment and Human Impact</i> . Longman Group Limited. England. pp.: 75-101.
[6]	Giddings, J. C. (1973). <i>Chemistry, Man, and Environmental Change</i> . Canfield, San Francisco.
[7]	EPA (2004). <i>The Particle Pollution Report : Current Understanding of Air Quality and Emissions through 2003</i> . United States Environmental Protection Agency. North Carolina. pp.: 1-27.
[8]	QUARG (1993). <i>Urban Air Quality in the United Kingdom, 1<sup>st</sup> Report of QUARG</i> . Department of Environment (DOE). UK. pp.: 1-201.
[9]	The Irish Meteorological Service Online (2006). <i>The % Frequency of Winds Direction of Beaufort Force in Ireland</i> . <a href="http://www.met.ie/climate/wind.asp">www.met.ie/climate/wind.asp</a>
[10]	AQEG (2004). <i>Particulate Matter In the United Kingdom</i> . Department of Environment, Food and Rural Affairs (DEFRA). London. Pp.: 1-416.
[11]	Jacobson (2002). <i>Atmospheric Pollution : History, Science, and Regulation</i> . Cambridge University Press. United Kingdom. pp.: 1-377.
[12]	Harrison (2001). <i>Pollution : Cause, Effects, and Control, 4<sup>th</sup> Edition</i> . The Royal Society of Chemistry. United Kingdom. Pp.: 169-351.
[13]	EPA (1975). <i>Institute for Air Pollution Training : Air Pollutants and Their Sources</i> . In Air Pollution Control Orientation Course (422-A). United States Environmental Protection Agency. Atlanta.
[14]	<i>Twelfth Annual Report of the Council on Environment Quality</i> . (1992). Washington, D.C.

[15]	APEG (1999). <i>Source Apportionment of Airborne Particulate Matter in the United Kingdom, Report of the APEG</i> . Department of the Environment, Transport and the Regions. UK. pp.:1-158.
[16]	QUARG (1996). <i>Airborne Particulate Matter in the United Kingdom, 3<sup>rd</sup> Report of QUARG</i> . Department of Environment (DOE). UK. pp.:1-176.
[17]	EPA (1979). <i>Cleaning the Air</i> . Publication No.: 0-294-335. United States Environmental Protection Agency U.S.. Government Printing Office. Washington D.C.
[18]	Pooley, F.D. and Mille, M. (1999). <i>Composition of Air Pollution Particles</i> . In "Air Pollution and Health" By Holgate, S.T., Samet, J.M., Koren, H.S., and Maynard, R.L.. Academic Press. London. pp.:619-634.
[19]	Hutchison, L.M. (1996). <i>Investigation of PM<sub>10</sub><sup>s</sup> Found in the Urban Environment and Human Lungs</i> . M Phil. Thesis. University of Wales, Cardiff.
[20]	Schröder, H.H.E. (1982). <i>The Properties and Effects of Dust</i> . In Environmental Engineering in South Africa Mines, Burrows, J., Hemp, R., Holding, W., and Stroh, R.M. The Mine Ventilation Society of South Africa. Cape & Transvaal Printers Ltd. Cape Town. pp.: 773-790.
[21]	Committee on Air Pollution (1953). <i>Interim Report</i> . London : HMSO.
[22]	Logan, W.P.D. (1953). <i>Mortality in London Fog Incident, 1952</i> . Lancet 1. pp.:336.
[23]	Ministry of Health (1954). <i>Mortality and Morbidity During the London Fog of December 1952</i> . Reports on Public Health and Medical Subjects no.95. London : HMSO.
[24]	Wilkins, E.T. (1954). <i>Air Pollution and London Fog of December, 1952</i> . Journal of Royal Sanitary Institute. vol.74. pp.:1-21.
[25]	Anderson, H.R. (1999). <i>Health Effects of Air Pollution Episodes</i> . Air Pollution and Health. Academic Press. London. pp.:461-486.
[26]	EPA (2003). <i>Particles and Your Health</i> . United States Environmental Protection Agency Office of Air and Radiation. North Carolina. EPA Publication No. 452/F-03-001.
[27]	Pan, X., Day, H.W., Beckett, L.A., and Schenker, M.B. (2005). <i>Residential Proximity to Naturally Occurring Asbestos and Mesothelioma Risk in California</i> . University of California, Davis. American Journal of Respiratory and Critical Care Medicine. vol.172. pp.:1019-1025.

[28]	Hedley, A.J., Mcghee, S.M., Repace, J.L., Wong, L., Yu, M.Y.S., Wong, T., and Lam, T. (2006). <i>Risk for Heart Disease and Lung Cancer from Passive Smoking by Workers in the Catering Industry</i> . Oxford University Press. Toxicological Sciences. vol.:90(2). pp.:539-548.
[29]	Deschamps, F., Barouh, M., Deslee, G., Prevost, A., and Munck, J.N. (2006). <i>Estimates of Work-Related Cancers in Workers Exposed to Carcinogens</i> . Oxford University Press. Occupational Medicine. vol.56. pp.:204-209.
[30]	Morawska, L., Hofmann, W., Hitchins-Loveday, J., Swanson, C., and Mengersen, K. (2005). <i>Experimental Study of the Deposition of Combustion Aerosols in the Human Respiratory Tract</i> . Elsevier. Journal of Aerosol Science vol. 36. pp.:939-957.
[31]	Forastiere. F., D'Ippoliti. D., and Pistelli. R. (2002). <i>Chapter 7 : Airborne Particles are Associated with Increased Mortality and Hospital Admissions for Heart and Lung Disease</i> . ERS Journals Limited. European Respiratory Monograph vol.7 (21). pp.:93-107.
[32]	National Institute of Safety and Health (NIOSH) (2000). <a href="http://www.cdc.gov/niosh/">http://www.cdc.gov/niosh/</a> .
[33]	Luo, S., Liu, X., Tsai, S.P., and Wen, C.P. (2003). <i>Asbestos related Disease from Environmental Exposure to Crocidolite in Da-Yao, China : Review of Exposure and Epidemiological Data</i> . <a href="http://www.occenvmed.com">www.occenvmed.com</a> . Occupational and Environmental Medicine. vol.:60, pp.:35-42.
[34]	Salih, E. and Ahmet, U.D. (2004). <i>Malignant Pleural Mesothelioma in Turkey : Review 2000-2002</i> . Lung Cancer. vol.45. pp.:S17-S20.
[35]	MacNee, W. and Donaldson, K. (1999). <i>Particulate Air Pollution : Injurious and Protective Mechanisms in Lungs</i> . In <i>Air Pollution and Health</i> . Holgate, S.T., Samet, J.M., Koren, H.S., and Maynard R.L., eds. Academic Press. San Diego. pp.:653-672.
[36]	Pope, C.A.III and Dockery D.W. (1999). <i>Epidemiology of Particles Effects</i> . In <i>Air Pollution and Health</i> . Holgate, S.T., Samet, J.M., Koren, H.S., and Maynard R.L., eds. Academic Press. San Diego. pp.:673-705.
[37]	Mackie, A.M. and Davies, C.H. 1981. <i>Environmental Effects of Traffic Changes : TRRL Report LR1015</i> . Transport and Road Research Laboratory. Crowthorne, United Kingdom.



[38]	World Health Organization (WHO) (2000). <a href="http://www.who.int">http://www.who.int</a> .
[39]	Hinds, W.C. (1999). <i>Aerosol Technology : Properties, Behaviour, and Measurement of Airborne Particles (2<sup>nd</sup> Ed.)</i> . John Wiley & Sons Inc. United States of America. pp.:1-14, 150-259.
[40]	Soderholm, S.C. (1989). <i>Proposed International Conventions for Particle Size-Selective Sampling</i> . Pergamon Press Plc. Great Britain. Ann. Occup. Hyg., vol.33, No.3, pp.: 301-320.
[41]	MDHS 14/3 (2000). <i>Methods for the Determination of Hazardous Substances: General Methods for Sampling and Gravimetric Analysis of Respirable and Inhalable Dust</i> . Health and Safety Executive. United Kingdom.
[42]	ISO (1983). <i>Air Quality – Particle Size Fraction Definitions for Health-related Sampling</i> . Tech. Rep. ISO/TR7708-1983. International Organisation for Standards. Geneva.
[43]	ACGIH (1985). <i>Particle Size-selective Sampling in Work Place</i> . Report of ACGIH Technical Committee on Air Sampling Procedures. American Conference of Governmental Industrial Hygienists, Cincinnati, Ohio. This report was also published in <i>ACGIH Transactions –1984</i> , Ann. Am. Conf. Ind. Hyg. Vol.11, pp. 23-100, and parts were summarized in Phalen, R.F., Hinds, W.C., John, W., Liroy, P.J., Lippman, M., McCawley, M.A., Raabe, O.G., Soderholm, S.C. and Stuart, B.O. (1986). <i>Rationale and Recommendations for Particle Size-selective sampling in workplace</i> . Appl. Ind. Hyg. vol.1, pp.:3-14.
[44]	Vincent, J.H. and Armbruster, L. (1981). <i>On the Quantitative Definition of the Inhalability of Airborne Dust</i> . Ann. Occup. Hyg. vol.24, pp.:245-248.
[45]	International Commission on Radiological Protection (1994). <i>Human Respiratory Tract Model for Radiological Protection</i> . Annals of the ICRP. Elsevier Science, Inc.. Tarrytown, NY. Publication 66.
[46]	EPA (1987). <i>U.S. Environmental Protection Agency 40 CFR 53 Subpart D : Procedures for Testing Performance Characteristics of Methods for PM<sub>10</sub></i> . Federal Register. vol. 52. pp.:24, 729 – 24, 735.
[47]	Heyder, J., Gebhart, J., Rudolf, G., Schiller, C.F. and Stahlhofen, W. (1986). <i>Deposition of Particles in the Human Respiratory Tract in the Size Range 0.005-15 µm</i> . Journal of Aerosol Science. vol.17. pp.:811-825. Also Erratum. Journal of Aerosol Science. vol.18. pp.:353 (1987).

[48]	Orenstein, A.J. (1960).(Editor). Recommendation adopted by the Pneumoconiosis Conference. In <i>Proceeding Pneumoconiosis Conference., Johannesburg, 1959.</i> J. and A. Churchill Ltd. London. pp.:610-621.
[49]	ACGIH (1997). <i>Threshold Limit Values and Biological Exposure Indices.</i> ACGIH. Cincinnati, U.S.A.
[50]	Foster, W.M. (1999). <i>Deposition and Clearance of Inhaled Particles, in Air Pollution and Health.</i> Academic Press. Great Britain. pp.:295-324.
[51]	Donaldson.K., Tran, C.L. and MacNee, W. (2002). <i>Chapter 6 : Deposition and Effects of Fine and Ultrafine Particle in the Respiratory Tract.</i> European Respiratory Monogram. ERS Journals Ltd. United Kingdom. Vol. 21. pp.:77-92.
[52]	Collins Dictionary (1986). <i>The Collins, Paperback English Dictionary.</i> William Collins Sons & Co. England. pp.:1-1013.
[53]	Brown. R.C. (1993). <i>Air Filtration : An Integrated Approach to the Theory and Applications of Fibrous Filters.</i> Pergamon. Oxford, U.K.
[54]	Miller, F.J. (2000). <i>Dosimetry of Particles in Laboratory Animals and Human in Relationship to Issues Surrounding Lung Overload and Human Health Risk Assessment : Critical Review.</i> Journal of Inhalation Toxicology. vol. 12. pp.:19-57.
[55]	Kliment, V. (1973). <i>Similarity and Dimensional Analysis, Evaluation of Aerosol Deposition in the Lungs of Laboratory Animals and Man.</i> Journal of Folio Morphology (Praha). Vol. 21. pp.:59-64.
[56]	Stahlhofen, W., Gebhart, J., Heyder, J., Philipson, K., Camner, P. (1981). <i>Intercomparison of Regional Deposition of Aerosol Particles in the Human Respiratory Tract and their Long-term Elimination.</i> Journal of Exp Lung Res. vol. 2. pp.:131-139.
[57]	Kim C.S. and Jaques, P. (2000). <i>Respiratory Dose of Inhaled Ultrafine Particles in Healthy Adults.</i> Philos Trans R Soc Lond. vol.358. pp.:2693-2705.
[58]	Casella London (1958). <i>Instruction Leaflet 3104/AT : Operation and Maintenance for the Gravimetric Dust Sampler Type 113A.</i> C.F. Casella & Co. Ltd. London. pp:1-22.
[59]	SKC (1999). <i>A Step by Step Guide to Air Sampling Featuring an Introduction to the Basics.</i> SKC Ltd. Dorset, UK. pp.:1-12.

[60]	MDHS 14 (1989). <i>General Methods for the Gravimetric Determination of Respirable and Total Inhalable Dust</i> . Health and Safety Executive. United Kingdom.
[61]	Kenny, L., Chung, K., Dilworth, M., Hammond, C., Jones, J.W., Shreeve, Z., and Winton, J. (2001). <i>Applications of Low-Cost, Dual-Fraction Dust Samplers</i> . Pergamon Press. Ann. Occup. Hyg. vol.45. No.45. pp.: 35-42.
[62]	Kenny, L.C., and Stancliffe, J.D. (1997). <i>Characterisation of Porous Foam Size Selectors for Conical Inhalable Sampler</i> . Health and Safety Executive Report : IR/L/A/97/19. <a href="http://bgiusa.com/ih/cisis.htm">http://bgiusa.com/ih/cisis.htm</a> .
[63]	Li, S.N., and Lundgren, D.A. (1999). <i>Weighing Accuracy of Samples Collected by IOM and CIS Inhalable Samplers</i> . American Industrial Hygiene Association Journal. vol. 60. pp.: 235-236.
[64]	Tatum, V., Ray, A.E., and Rixx, D.R. (2002). <i>Performance of the RespiCon Personal Aerosol Sampler in Forest Products Industry Workplace</i> . AIHA Journal. vol.63. pp.: 311-316.
[65]	TSI Manual Model 8522 (2002). <i>Model 8522 RespiCon™ Particle Sampler : Operation and Service Manual</i> . TSI Incorporated. USA. pp.: 1-32.
[66]	Casella London (1959). <i>Thermal Precipitator (Leaflet 804)</i> . C.F.Casella & Co. Ltd. London. pp.: 1-15.
[67]	New Star Series 290 Manual (2006). <i>Instruction Manual : Series 290 Marple Personal Cascade Impactor</i> . New Star Environmental LLC. USA. pp.: 1-29.
[68]	New Star NV Manual (2004). <i>Instruction Manual : 8 Stage Non-Viable Cascade Impactor</i> . New Star Environmental LLC. USA. pp.: 1-22.
[69]	Timbrell, V., Hyett, A.W., and Skidmore, J.W. (1968). <i>A Simple Dispenser for Generation Dust Clouds from Standard Reference Samples of Asbestos</i> . Pergamon Press. Ann. Occup. Hyg. vol.11. pp.: 273-281.
[70]	Lippmann, M. (1991). <i>Industrial and Environment Hygiene : Professional Growth in a Changing Environment</i> . Am. Ind. Hyg. Assoc. Journal. vol.52. pp.: 341-348.
[71]	EN 2402 (2000). <i>Analytical Methods Laboratory Notes, 2000/01</i> . Division of Materials and Minerals, School of Engineering. Cardiff University. Cardiff.
[72]	MDHS 39/3 (1990). <i>Asbestos Fibres in Air : Light Microscope Methods for use with the Control of Asbestos at Work Regulations</i> . Health and Safety Executive. United Kingdom.

[73]	Baron, P.A. (1993). <i>Measurement of Asbestos and Other Fields</i> , in Willeke, K., and Baron, P.A. (Eds), in <i>Aerosol Measurement</i> . Van Nostrand Reinhold. New York.
[74]	Friedrichs, K.H (1986). <i>Measurement and Identification of Single Fibrous Particles in Physical and Chemical Characterization of Individual Airborne Particles</i> edited by Spurny, K.R. (1986). Ellis Horwood Limited. England. pp.:198-211.
[75]	BS ISO 13794 (1999). <i>Ambient Air – Determination of Asbestos Air : Indirect-transfer Transmission Electron Microscopy Method</i> . British Standard. Health and Environment Sector Board, Technical Committee EH/2/3. London. pp.:1-74.
[76]	Spratt, M.R. (2006). <i>Procedure No.5 : Method for the Determination of Asbestos in Lung Tissue using Transmission Electron Microscopy</i> . In SETS UKAS Accredited Procedures Manual Version 1.8. Cardiff University. Cardiff. pp.:21-38.
[77]	IARC (1992). <i>Environmental Carcinogens, Methods of Analysis and Exposure Measurement</i> . IARC Scientific Publications No. 109, International Agency for Research on Cancer. Lyon, France.
[78]	Griffith, W.B., and Vaughn, N.P. (1996). <i>The Aerodynamic Behaviour of Cylindrical and Spherical Particles when Scattering under Gravity</i> . J. Aerosol. Sci. vol.17. pp.:53-65.
[79]	Milagros, Mille (2003). <i>An Investigation of the Collection and Analysis of Airborne Particulate Material</i> . D. Phil. Thesis. University of Wales, Cardiff.
[80]	Golledge, Peter (1962). <i>Underground Studies of Atmospheric Pollution in Coal Mines</i> . D. Phil. Thesis. University of Wales, Cardiff.
[81]	Hastings, C. (1955). <i>Approximations for Digital Computers</i> . Princeton University Press. Princeton, U.S.A.. pp.:186.
[82]	<a href="http://www.classzone.com/books/earth_science/terc/content/investigations/es0103/es0103page08.cfm">http://www.classzone.com/books/earth_science/terc/content/investigations/es0103/es0103page08.cfm</a> . (21 December 2006).
[83]	<a href="http://www.weatheronline.co.uk/feature/wxfacts/aa230902.htm">http://www.weatheronline.co.uk/feature/wxfacts/aa230902.htm</a> . (18 December 2006).

## **Appendix A : A Convenient Algorithm for $F(x)$ .**



**Appendix A-1 : A convenient algorithm for  $F(x)$**

A convenient algorithm for  $F(x)$ , the cumulative probability function of a standardized random variable, is based on one for the error function [81] :

$$F(x) = G(y), \text{ for } x \leq 0,$$

or

$$F(x) = 1 - G(y), \text{ for } x \geq 0,$$

where  $y$  is the absolute value of  $\frac{x}{\sqrt{2}}$  and

$$G(y) = 0.5(1 + 0.14112821y + 0.08864027y^2 + 0.02743349y^3 - 0.00039446y^4 + 0.00328975y^5)^{-8}.$$

The absolute error is less than  $\pm 0.00001$  for  $-4 < y < 4$ .

**Appendix B : Apparatus of Method for the  
Determination of Asbestos using  
Transmission Electron Microscopy.**

**Appendix B-1: Apparatus of method for the determination of asbestos using transmission electron microscopy.**

Centrifuge	Capable of >1000g, for particle sedimentation (Heraeus Varifuge 3.0)
Test tubes	Suitable for centrifuge (e.g. Pyrex, wall thickness 1.8mm, length 125mm, diameter 16mm)
Polycarbonate filters	25mm diameter, 0.2 µm pore size (Nucleleopore)
Buchner funnels	With sintered glass support for polycarbonate filters (Sartorius)
Vacuum carbon-coating unit	For preparation of electron-microscopy specimens (Nonotech)
Electron microscope	Philips 400T fitted with Edax X-Ray energy dispersive analyser also FEI TECHNAI 12 also fitted with Edax X-Ray energy dispersive analyser
Electron-microscope support grids	3.05-mm diameter, 150 or 200 mesh, gold (Polaron)
Heating block	TECAM Dry block DB4

**Appendix C : Mass Concentration and Size  
Distribution of Limestone Dust  
Particles.**

**Appendix C-1a**

**Airborne Particulates Instruments Sampling Performances (5 minutes limestone dust sampling)**

**Title : Comparison of Total Inhalable Samplers**

DGP		2	2	2	2	2	3	3	3	3	3
No.	Instruments	31/01/05 (W67) [5 min]	31/01/05 (W67) [5 min]	01/02/05 (W67) [5 min]	02/02/05 (W67) [5 min]	22/02/05 (W70) [5 min]	02/02/05 (W67) [5 min]	02/02/05 (W67) [5 min]	02/02/05 (W67) [5 min]	04/02/05 (W67) [5 min]	01/03/05 (W71) [5 min]
1	<b>7 Holes Sampler</b>										
	Dust weight (g)	0.00189	0.00148	0.00143	0.00131	0.00233	0.00203	0.00223	0.00201	0.00157	0.00176
	Mass Concentration (mg/m <sup>3</sup> )	189.00	148.00	143.00	131.00	233.00	203.00	223.00	201.00	157.00	176.00
2	<b>Casella (CIS)</b>										
	Dust weight (g)	0.00235	0.00235	0.00225	0.00215	0.00345	0.00343	0.00385	0.00277	0.00279	0.003
	Mass Concentration (mg/m <sup>3</sup> )	134.29	134.29	128.57	122.86	197.14	196.00	220.00	158.29	159.43	171.43
3	<b>IOM</b>										
	Dust weight (g)	0.00171	0.001673	0.001443	0.001393	0.00217	0.00227	0.00249	0.0021	0.00189	0.00229
	Mass Concentration (mg/m <sup>3</sup> )	171.00	167.30	144.30	139.30	217.00	227.00	249.00	210.00	189.00	229.00
DGP		3	3	3	3	3					
No.	Instruments	18/01/06 [I](W117) [5 min]	19/01/06 [I](W117) [5 min]	19/01/06 [II](W117) [5 min]	09/02/06 [I](W120) [5 min]	16/02/06 [I](W121) [5 min]					
4	<b>RespiCon</b>										
	Dust weight (g)	0.00255	0.00394	0.00283	0.00214	0.00194					
	Mass Concentration (mg/m <sup>3</sup> )	163.93	240.44	181.94	137.58	124.72					



**Appendix C-1b**

**Airborne Particulates Instruments Sampling Performances (5 minutes limestone dust sampling)**

**Title : Comparison of Total Inhalable Samplers**

DGP		3	3	3	3	3
No.	Instruments	06/06/2006 (W137) [5 min]	06/08/2006 (W137) [5 min]	06/09/2006 [I](W137) [5 min]	06/09/2006 [II](W137) [5 min]	06/10/2006 (W137) [5 min]
5	<b>Anderson Impactor</b>					
	Dust weight (g)	0.0065	0.00898	0.01075	0.01161	0.01587
	Mass Concentration (mg/m <sup>3</sup> )	46.29	63.46	75.97	82.05	112.16
No.	Instruments	06/12/2006 [I](W137) [5 min]	06/12/2006 [II](W137) [5 min]	06/12/2006 [III](W137) [5 min]	13/6/2006 [I](W137) [5 min]	13/6/2006 [II](W137) [5 min]
6	<b>Marple Impactor</b>					
	Dust weight (g)	0.00174	0.00214	0.00179	0.00233	0.00213
	Mass Concentration (mg/m <sup>3</sup> )	174.00	214.00	179.00	233.00	213.00

## Appendix C-2a

### Airborne Particulates Instruments Sampling Performances (10 minutes limestone dust sampling)

Title : Comparison of Total Inhalable Samplers

DGP		2	2	2	2	2	3	3	3	3	3
No.	Instruments	04/02/05 (W67) [10 min]	07/02/05 (W68) [10 min]	14/03/05 (W73) [10 min]	15/03/05 (W73) [10 min]	02/03/05 (W71) [10 min]	08/02/05 (W68) [10 min]	08/02/05 (W68) [10 min]	12/02/05 (W68) [10 min]	03/03/05 (W71) [10 min]	03/03/05 (W71) [10 min]
1	<b>7 Holes Sampler</b>										
	Dust weight (g)	0.00375	0.00406	0.00371	0.00338	0.00339	0.00347	0.00433	0.00488	0.00402	0.00351
	Mass Concentration (mg/m <sup>3</sup> )	187.50	203.00	185.50	169.00	169.50	173.50	216.50	244.00	201.00	175.00
2	<b>Casella (CIS)</b>										
	Dust weight (g)	0.00688	0.00674	0.00676	0.00581	0.00582	0.00533	0.00655	0.00784	0.00711	0.0063
	Mass Concentration (mg/m <sup>3</sup> )	196.57	192.57	193.14	166.00	166.29	152.29	187.14	224.00	203.14	180.00
3	<b>IOM</b>										
	Dust weight (g)	0.00488	0.00439	0.00422	0.003527	0.001833	0.003793	0.004517	0.00492	0.004707	0.004137
	Mass Concentration (mg/m <sup>3</sup> )	244.00	219.50	211.00	176.35	91.65	189.65	225.85	246.00	235.35	206.85
DGP		3	3	3	3	3					
No.	Instruments	18/01/06 [I](W117) [10 min]	23/01/06 [I](W118) [10 min]	23/01/06 [II](W118) [10 min]	24/01/06 [I](W118) [10 min]	16/02/06 [I](W121) [10 min]					
4	<b>RespiCon</b>										
	Dust weight (g)	0.00982	0.00525	0.00451	0.00694	0.00552					
	Mass Concentration (mg/m <sup>3</sup> )	315.65	168.76	144.97	223.08	177.44					

**Appendix C-2b**

**Airborne Particulates Instruments Sampling Performances (10 minutes limestone dust sampling)**

**Title : Comparison of Total Inhalable Samplers**

DGP		3	3	3	3	3
No.	Instruments	06/07/2006 [I](W137) [10 min]	06/07/2006 [I](W137) [10 min]	06/09/2006 [I](W137) [10 min]	06/09/2006 [II](W137) [10 min]	06/09/2006 [III](W137) [10 min]
5	<b>Anderson Impactor</b>					
	Dust weight (g)	0.01388	0.01609	0.01113	0.02543	0.02868
	Mass Concentration (mg/m <sup>3</sup> )	49.05	56.86	39.33	89.86	101.34
No.	Instruments	13/6/2006 [III](W137) [10 min]	13/6/2006 [IV](W137) [10 min]	13/6/2006 [V](W137) [10 min]	14/6/2006 (W137) [10 min]	15/6/2006 (W137) [10 min]
6	<b>Marple Impactor</b>					
	Dust weight (g)	0.00436	0.00434	0.00398	0.00363	0.0049
	Mass Concentration (mg/m <sup>3</sup> )	218.00	217.00	199.00	181.50	245.00

### Appendix C-3

#### Airborne Particulates Instruments Sampling Performances (5 minutes limestone dust sampling)

Title : Comparison of Respirable sampler

DGP		2	2	2	2	2	3	3	3	3	
No.	Instruments	31/01/05 (W67) [5 min]	31/01/05 (W67) [5 min]	01/02/05 (W67) [5 min]	02/02/05 (W67) [5 min]	22/02/05 (W70) [5 min]	02/02/05 (W67) [5 min]	02/02/05 (W67) [5 min]	02/02/05 (W67) [5 min]	04/02/05 (W67) [5 min]	01/03/05 (W71) [5 min]
1	<b>Cyclone Head</b>										
	Dust weight (g)	0.00112	0.00111	0.0011	0.00107	0.00151	0.00177	0.00191	0.00161	0.0013	0.00143
	Mass Concentration (mg/m <sup>3</sup> )	101.82	100.91	100.00	97.27	137.27	160.91	191.00	146.36	118.18	130.00
2	<b>Casella (MRE)</b>										
	Dust weight (g)	0.0012	0.001	0.00091	0.00062	0.00138	0.00128	0.00134	0.00115	0.00096	0.001
	Mass Concentration (mg/m <sup>3</sup> )	96.00	80.00	72.80	49.60	100.40	102.40	107.20	92.00	76.80	80.00
3	<b>IOM</b>										
	Dust weight (g)	0.00092	0.00095	0.000867	0.00086	0.001143	0.00106	0.00128	0.001293	0.001043	0.00119
	Mass Concentration (mg/m <sup>3</sup> )	92.00	95.00	86.70	86.00	114.30	106.00	128.00	129.30	104.30	119.00
DGP		3	3	3	3	3					
No.	Instruments	18/01/06 [I](W117) [5 min]	19/01/06 [I](W117) [5 min]	19/01/06 [II](W117) [5 min]	09/02/06 [I](W120) [5 min]	16/02/06 [I](W121) [5 min]					
4	<b>RespiCon</b>										
	Dust weight (g)	1.3700	1.5200	1.3000	1.1100	0.9600					
	Mass Concentration (mg/m <sup>3</sup> )	102.75	114.00	97.50	83.25	72.00					
No.	Instruments	31/01/06 [I](W119) [5 min]	31/01/06 [II](W119) [5 min]	02/01/06 [I](W119) [5 min]	15/02/06 [I](W121) [5 min]	15/02/06 [II](W121) [5 min]					
5	<b>Casella (CIS)</b>										
	Dust weight (g)	0.00179	0.00151	0.00120	0.00177	0.00208					
	Mass Concentration (mg/m <sup>3</sup> )	83.62	58.86	68.76	101.14	118.86					

## Appendix C-4

### Airborne Particulates Instruments Sampling Performances (10 minutes limestone dust sampling)

Topic : Comparison of Respirable sampler

DGP		2	2	2	2	2	3	3	3	3	3
No.	Instruments	04/02/05 (W67) [10 min]	07/02/05 (W68) [10 min]	14/03/05 (W73) [10 min]	15/03/05 (W73) [10 min]	02/03/05 (W71) [10 min]	08/02/05 (W68) [10 min]	08/02/05 (W68) [10 min]	12/02/05 (W68) [10 min]	03/03/05 (W71) [10 min]	03/03/05 (W71) [10 min]
1	<b>Cyclone Head</b>										
	Dust weight (g)	0.00305	0.00334	0.00298	0.00265	0.00282	0.00294	0.00314	0.00397	0.00313	0.00279
	Mass Concentration (mg/m <sup>3</sup> )	138.64	151.82	135.45	120.45	128.18	133.64	142.73	180.45	142.17	126.82
2	<b>Casella (MRE)</b>										
	Dust weight (g)	0.0018	0.00176	0.00206	0.00222	0.00177	0.00182	0.00213	0.00225	0.00171	0.00200
	Mass Concentration (mg/m <sup>3</sup> )	72.00	70.40	82.40	88.80	70.80	72.80	85.20	90.00	68.40	80.00
3	<b>IOM</b>										
	Dust weight (g)	0.002363	0.002317	0.002143	0.00187	0.000983	0.002193	0.002123	0.00267	0.002263	0.002213
	Mass Concentration (mg/m <sup>3</sup> )	118.15	115.85	107.15	93.50	49.15	109.65	106.15	133.50	113.15	110.65
DGP		3	3	3	3	3					
No.	Instruments	18/01/06 [I](W117) [10 min]	23/01/06 [I](W118) [10 min]	23/01/06 [II](W118) [10 min]	24/01/06 [I](W118) [10 min]	16/02/06 [I](W121) [10 min]					
4	<b>RespiCon</b>										
	Dust weight (g)	5.0400	2.8300	2.4400	4.0800	3.0400					
	Mass Concentration (mg/m <sup>3</sup> )	189.01	106.13	91.50	153.00	114.00					
No.	Instruments	10/02/06 [I](W120) [10 min]	10/02/06 [II](W120) [10 min]	10/02/06 [III](W120) [10 min]	13/02/06 [I](W121) [10 min]	13/02/06 [II](W121) [10 min]					
5	<b>Casella (CIS)</b>										
	Dust weight (g)	0.00281	0.00306	0.00302	0.00346	0.00324					
	Mass Concentration (mg/m <sup>3</sup> )	80.38	87.33	86.29	98.95	92.67					



## Appendix C-5

### Airborne Particulates Instruments Sampling Performances (5 minutes limestone dust sampling)

Topic : Comparison of cyclone sampler at different flow rates 1.6 to 2.4 LPM.

DGP		3	3	3	3	3
No.	Instruments	02/02/05 (W67) [5 min]	02/02/05 (W67) [5 min]	02/02/05 (W67) [5 min]	04/02/05 (W67) [5 min]	01/03/05 (W71) [5 min]
1	<b>Cyclone Head (1.6 LPM)</b> Dust weight (g) Mass Concentration (mg/m <sup>3</sup> )	0.00127 158.75	0.00102 127.50	0.00107 133.75	0.0013 162.50	0.00116 145.00
2	<b>Cyclone Head (1.8 LPM)</b> Dust weight (g) Mass Concentration (mg/m <sup>3</sup> )	0.00124 137.78	0.00117 130.00	0.00131 145.56	0.00150 166.67	0.00114 126.67
3	<b>Cyclone Head (2.0 LPM)</b> Dust weight (g) Mass Concentration (mg/m <sup>3</sup> )	0.00165 165.00	0.00169 169.00	0.00135 135.00	0.0013 130.00	0.00136 136.00
4	<b>Cyclone Head (2.2 LPM)</b> Dust weight (g) Mass Concentration (mg/m <sup>3</sup> )	0.00177 160.91	0.00191 191.00	0.00161 146.36	0.0013 118.18	0.00143 130.00
5	<b>Cyclone Head (2.4 LPM)</b> Dust weight (g) Mass Concentration (mg/m <sup>3</sup> )	0.00151 125.83	0.00157 130.83	0.00139 115.83	0.00125 104.17	0.00133 110.30

## Appendix C-6

### Raw Data : Latex Standard

ID Class	From um	To um	d	Rate	Rate %
1	0.80-0.85	0.85	0.825	8	1.26
2	0.85-0.90	0.90	0.875	29	4.58
3	0.90-.095	0.95	0.925	297	46.92
4	0.95-1.00	1.00	0.975	255	40.28
5	1.00-1.05	1.05	1.025	26	4.11
6	1.05-1.10	1.10	1.075	10	1.58
7	1.10-1.15	1.15	1.125	8	1.26
TOTAL				633	100.00

**Appendix C-7a**

**Title : Comparison of number of frequency limestone dust particles obtained using TEM for 7 Hole, CIS, RespiCon sampler with Thermal Precipitator.**

ECD (micrometers)	7 Hole sampler		CIS sampler		RespiCon sampler		Thermal Precipitator	
	Particle Number	Particle Number %	Particle Number	Particle Number %	Particle Number	Particle Number %	Particle Number	Particle Number %
0.30-0.50	1425	16.29	5096	16.29	1442	16.29	455	16.29
0.50-1.00	989	62.61	2849	66.11	1058	55.76	1307	46.80
1.00-1.50	221	13.99	477	11.07	306	16.13	691	24.74
1.50-2.00	64	4.05	166	3.86	127	6.69	223	7.98
2.00-2.50	27	1.71	60	1.39	54	2.85	75	2.69
2.50-3.00	14	0.89	31	0.73	23	1.22	29	1.04
3.00-3.50	1	0.07	14	0.32	11	0.58	10	0.36
3.50-4.00	2	0.12	8	0.18	4	0.21	1	0.04
4.00-4.50	3	0.19	2	0.04	6	0.32	2	0.07
4.50-5.00	1	0.07	1	0.02	1	0.05	0	0.00
5.00-5.50	0	0.00	0	0.00	2	0.11	0	0.00
5.50-6.00	0	0.00	0	0.00	1	0.05	0	0.00
6.00-6.50	0	0.00	0	0.00	0	0.00	0	0.00
6.50-7.00	0	0.00	1	0.02	1	0.05	0	0.00
7.00-7.50	0	0.00	0	0.00	0	0.00	0	0.00
7.50-8.00	0	0.00	0	0.00	0	0.00	0	0.00
8.00-8.50	0	0.07	0	0.00	0	0.00	0	0.00
8.50-9.00	0	0.07	0	0.00	0	0.00	0	0.00
9.00-9.50	0	0.00	0	0.00	0	0.00	0	0.00
9.50-10.00	0	0.00	0	0.00	0	0.00	0	0.00
<b>TOTAL</b>	<b>2747</b>		<b>8705</b>		<b>3036</b>		<b>2793</b>	

**Appendix C-7b**

**Title : Comparison of limestone dust particles size distribution obtained using TEM for 7 Hole, CIS, RespiCon sampler with Thermal Precipitator.**

ECD, d (micrometers)	d <sub>AE</sub> (micrometers)	Log d <sub>AE</sub> (micrometers)	7 Hole sampler	CIS sampler	RespiCon sampler	Thermal Precipitator
			Particle Number Cum %	Particle Number Cum %	Particle Number Cum %	Particle Number Cum %
0.30	0.488	-0.311255808	100.00	100.00	100.00	100.00
0.50	0.814	-0.089407059	83.71	83.71	83.71	83.71
1.00	1.628	0.211622937	21.10	17.60	27.95	36.91
1.50	2.442	0.387714196	7.11	6.53	11.82	12.17
2.00	3.256	0.512652933	3.06	2.67	5.13	4.19
2.50	4.070	0.609562946	1.35	1.28	2.28	1.50
3.00	4.884	0.688744192	0.46	0.55	1.06	0.47
3.50	5.698	0.755690981	0.39	0.23	0.48	0.11
4.00	6.512	0.813682928	0.27	0.05	0.27	0.07
4.50	7.325	0.864835451	0.08	0.01	-0.05	0.00
5.00	8.139	0.910592941	0.01	-0.01	-0.10	0.00
5.50	8.953	0.951985626	0.01	-0.01	-0.21	0.00
6.00	9.767	0.989774187	0.01	-0.01	-0.26	0.00
6.50	10.581	1.024536294	0.01	-0.01	-0.26	0.00
7.00	11.395	1.056720977	0.01	-0.03	-0.31	0.00
7.50	12.209	1.0866842	0.01	-0.03	-0.31	0.00
8.00	13.023	1.114712924	0.01	-0.03	-0.31	0.00
8.50	13.837	1.141041863	-0.06	-0.03	-0.31	0.00
9.00	14.651	1.165865446	-0.13	-0.03	-0.31	0.00
9.50	15.465	1.189346542	-0.13	-0.03	-0.31	0.00
10.00	16.279	1.211622937	-0.13	-0.03	-0.31	0.00

**Appendix C-7c**

**Title : Comparison of limestone dust particles mass distribution obtained using TEM for 7 Hole, CIS, RespCon sampler with Thermal Precipitator.**

			7 Hole sampler	CIS sampler	RespCon sampler	Thermal Precipitator
ECD, d (micrometers)	d <sub>AE</sub> (micrometers)	Log d <sub>AE</sub> (micrometers)	Particle Mass Cum %	Particle Mass Cum %	Particle Mass Cum %	Particle Mass Cum %
0.30	0.488	-0.311255808	100.00	100.00	100.00	100.00
0.50	0.814	-0.089407059	99.52	99.48	99.72	99.62
1.00	1.628	0.211622937	81.30	78.63	90.35	88.86
1.50	2.442	0.387714196	62.44	62.46	77.81	62.51
2.00	3.256	0.512652933	47.47	46.99	63.53	39.18
2.50	4.070	0.609562946	34.03	35.16	50.60	22.50
3.00	4.884	0.688744192	21.26	23.81	40.50	10.73
3.50	5.698	0.755690981	19.60	15.59	32.57	4.03
4.00	6.512	0.813682928	15.24	8.50	28.16	3.00
4.50	7.325	0.864835451	5.18	6.20	18.38	0.00
5.00	8.139	0.910592941	0.00	4.60	16.25	0.00
5.50	8.953	0.951985626	0.00	4.60	9.91	0.00
6.00	9.767	0.989774187	0.00	4.60	6.12	0.00
6.50	10.581	1.024536294	0.00	4.60	6.12	0.00
7.00	11.395	1.056720977	0.00	0.00	0.00	0.00
7.50	12.209	1.0866842	0.00	0.00	0.00	0.00
8.00	13.023	1.114712924	0.00	0.00	0.00	0.00
8.50	13.837	1.141041863	0.00	0.00	0.00	0.00
9.00	14.651	1.165865446	0.00	0.00	0.00	0.00
9.50	15.465	1.189346542	0.00	0.00	0.00	0.00
10.00	16.279	1.211622937	0.00	0.00	0.00	0.00



**Appendix C-8a**

**Title : Comparison of number of frequency limestone dust particles obtained using TEM for Cyclone 2.2, MRE, RespiCon and IOM sampler.**

ECD (micrometers)	Cyclone2.2 sampler		MRE sampler		RespiCon sampler		IOM sampler	
	Particle Number	Particle Number %	Particle Number	Particle Number %	Particle Number	Particle Number %	Particle Number	Particle Number %
0.30-0.50	298	16.29	994	16.29	867	16.29	424	16.29
0.50-1.00	438	50.47	953	60.43	613	58.08	609	53.40
1.00-1.50	205	23.62	256	16.23	175	16.58	234	20.52
1.50-2.00	60	6.91	65	4.12	60	5.68	63	5.53
2.00-2.50	13	1.50	28	1.78	24	2.27	33	2.89
2.50-3.00	3	0.34	17	1.07	8	0.76	13	1.14
3.00-3.50	3	0.34	1	0.06	2	0.18	2	0.17
3.50-4.00	4	0.46	2	0.13	1	0.10	2	0.17
4.00-4.50	0	0.00	2	0.13	1	0.10	0	0.00
4.50-5.00	0	0.00	0	0.00	0	0.00	0	0.00
5.00-5.50	0	0.00	0	0.00	1	0.10	0	0.00
5.50-6.00	0	0.00	0	0.00	0	0.00	0	0.00
6.00-6.50	0	0.00	0	0.00	0	0.00	0	0.00
6.50-7.00	0	0.00	0	0.00	0	0.00	0	0.00
7.00-7.50	0	0.00	0	0.00	0	0.00	0	0.00
7.50-8.00	0	0.00	0	0.00	0	0.00	0	0.00
8.00-8.50	0	0.00	0	0.00	0	0.00	0	0.00
8.50-9.00	0	0.00	0	0.00	0	0.00	0	0.00
9.00-9.50	0	0.00	0	0.00	0	0.00	0	0.00
9.50-10.00	0	0.00	0	0.00	0	0.00	0	0.00
<b>TOTAL</b>	<b>1024</b>		<b>2318</b>		<b>1752</b>		<b>1380</b>	

**Appendix C-8b**

**Title : Comparison of limestone dust particles size distribution obtained using TEM for Cyclone 2.2, MRE, RespiCon and IOM sampler.**

ECD, d (micrometers)	d <sub>AE</sub> (micrometers)	Log d <sub>AE</sub> (micrometers)	Cyclone2.2 sampler	MRE sampler	RespiCon sampler	IOM sampler
			Particle Number Cum %	Particle Number Cum %	Particle Number Cum %	Particle Number Cum %
0.30	0.488	-0.311255808	100.00	100.00	100.00	100.00
0.50	0.814	-0.089407059	83.71	83.71	83.71	83.71
1.00	1.628	0.211622937	33.24	23.28	25.63	30.31
1.50	2.442	0.387714196	9.62	7.05	9.05	9.79
2.00	3.256	0.512652933	2.71	2.93	3.37	4.26
2.50	4.070	0.609562946	1.21	1.15	1.10	1.37
3.00	4.884	0.688744192	0.87	0.08	0.34	0.23
3.50	5.698	0.755690981	0.53	0.02	0.16	0.06
4.00	6.512	0.813682928	0.07	-0.11	0.06	-0.11
4.50	7.325	0.864835451	0.07	-0.24	-0.04	-0.11
5.00	8.139	0.910592941	0.07	-0.24	-0.04	-0.11
5.50	8.953	0.951985626	0.07	-0.24	-0.14	-0.11
6.00	9.767	0.989774187	0.07	-0.24	-0.14	-0.11
6.50	10.581	1.024536294	0.07	-0.24	-0.14	-0.11
7.00	11.395	1.056720977	0.07	-0.24	-0.14	-0.11
7.50	12.209	1.0866842	0.07	-0.24	-0.14	-0.11
8.00	13.023	1.114712924	0.07	-0.24	-0.14	-0.11
8.50	13.837	1.141041863	0.07	-0.24	-0.14	-0.11
9.00	14.651	1.165865446	0.07	-0.24	-0.14	-0.11
9.50	15.465	1.189346542	0.07	-0.24	-0.14	-0.11
10.00	16.279	1.211622937	0.07	-0.24	-0.14	-0.11

**Appendix C-8c**

**Title : Comparison of limestone dust particles mass distribution obtained using TEM for Cyclone 2.2, MRE, RespIcon and IOM sampler.**

ECD, d (micrometers)	d <sub>AE</sub> (micrometers)	Log d <sub>AE</sub> (micrometers)	Cyclone2.2 sampler	MRE sampler	RespIcon sampler	IOM sampler
			Particle Mass Cum %	Particle Mass Cum %	Particle Mass Cum %	Particle Mass Cum %
0.30	0.488	-0.311255808	100.00	100.00	100.00	100.00
0.50	0.814	-0.089407059	99.58	99.51	99.57	99.58
1.00	1.628	0.211622937	86.69	81.48	84.57	85.87
1.50	2.442	0.387714196	58.77	59.06	64.73	61.49
2.00	3.256	0.512652933	36.36	43.44	46.09	43.46
2.50	4.070	0.609562946	26.02	29.10	30.26	23.43
3.00	4.884	0.688744192	21.74	13.36	20.58	9.00
3.50	5.698	0.755690981	14.68	11.91	16.79	5.45
4.00	6.512	0.813682928	0.00	7.06	13.56	0.00
4.50	7.325	0.864835451	0.00	0.00	8.86	0.00
5.00	8.139	0.910592941	0.00	0.00	8.86	0.00
5.50	8.953	0.951985626	0.00	0.00	0.00	0.00
6.00	9.767	0.989774187	0.00	0.00	0.00	0.00
6.50	10.581	1.024536294	0.00	0.00	0.00	0.00
7.00	11.395	1.056720977	0.00	0.00	0.00	0.00
7.50	12.209	1.0866842	0.00	0.00	0.00	0.00
8.00	13.023	1.114712924	0.00	0.00	0.00	0.00
8.50	13.837	1.141041863	0.00	0.00	0.00	0.00
9.00	14.651	1.165865446	0.00	0.00	0.00	0.00
9.50	15.465	1.189346542	0.00	0.00	0.00	0.00
10.00	16.279	1.211622937	0.00	0.00	0.00	0.00

**Appendix D : Size Distribution of Asbestos Fibres,  
Coal Dust Particles, and Urban  
Airborne Pollution.**

## Appendix D-1a

**Sample : Penge Amosite Set No.1**

**Title : Particle Number Cumulative % of Amosite Respirable Fibres using Optical Microscope (OM)**

<b>Length, ECD (micrometers)</b>	<b>Log ECD (micrometers)</b>	<b>Rate</b>	<b>OM %</b>	<b>Cumulative % OM</b>
0.00	#NUM!	259	31.74	100.00
5.00	0.699	209	25.61	68.26
10.00	1.000	183	22.43	42.65
20.00	1.301	165	20.22	20.22
<b>TOTAL</b>		<b>816</b>	<b>100.00</b>	

**Sample : Penge Amosite Set No.2**

**Title : Particle Number Frequency of Amosite Respirable Fibres using Optical Microscope (OM)**

<b>Length, ECD (micrometers)</b>	<b>Log ECD (micrometers)</b>	<b>Rate</b>	<b>OM %</b>	<b>Cumulative % OM</b>
0.00	#NUM!	341	31.81	100.00
5.00	0.699	274	25.56	68.19
10.00	1.000	209	19.50	42.63
20.00	1.301	248	23.13	23.13
<b>TOTAL</b>		<b>1072</b>	<b>100.00</b>	



## Appendix D-1b

**Sample** : *Amosite Fibres from Lung (10%)*

**Title** : Particle Number Frequency of Amosite Fibres from Lung (10%) using Optical Microscope (OM)

<b>Length, ECD (micrometers)</b>	<b>Log ECD (micrometers)</b>	<b>Rate</b>	<b>OM %</b>	<b>Cumulative % OM</b>
0.00	#NUM!	260	71.23	100.00
5.00	0.699	40	10.96	28.77
10.00	1.000	35	9.59	17.81
20.00	1.301	30	8.22	8.22
<b>TOTAL</b>		<b>365</b>	<b>100.00</b>	

**Sample** : *Crocidolite Fibres from Lung (20%).*

**Title** : Particle Number Frequency of Crocidolite Fibres from Lung (20%) Respirable Fibres using Optical Microscope (OM)

<b>Length, ECD (micrometers)</b>	<b>Log ECD (micrometers)</b>	<b>Rate</b>	<b>OM %</b>	<b>Cumulative % OM</b>
0.00	#NUM!	290	83.33	100.00
5.00	0.699	46	13.22	16.67
10.00	1.000	5	1.44	3.45
20.00	1.301	7	2.01	2.01
<b>TOTAL</b>		<b>348</b>	<b>100.00</b>	

## Appendix D-1c

**Sample** : *Koegas Crocidolite very light (2).*

**Title** : Particle Number Frequency of Koegas Crocidolite Respirable Fibres using Optical Microscope (OM)

<b>Length, ECD (micrometers)</b>	<b>Log ECD (micrometers)</b>	<b>Rate</b>	<b>OM %</b>	<b>Cumulative % OM</b>
0.00	#NUM!	369	72.78	100.00
5.00	0.699	85	16.77	27.22
10.00	1.000	33	6.51	10.45
20.00	1.301	20	3.94	3.94
<b>TOTAL</b>		<b>507</b>	<b>100.00</b>	

**Sample** : *Australia Crocidolite very light.*

**Title** : Particle Number Frequency of Australia Crocidolite Respirable Fibres using Optical Microscope (OM)

<b>Length, ECD (micrometers)</b>	<b>Log ECD (micrometers)</b>	<b>Rate</b>	<b>OM %</b>	<b>Cumulative % OM</b>
0.00	#NUM!	668	62.26	100.00
5.00	0.699	230	21.44	37.74
10.00	1.000	122	11.37	16.31
20.00	1.301	53	4.94	4.94
<b>TOTAL</b>		<b>1073</b>	<b>100.00</b>	

**Appendix D-1d**

**Sample : Airborne Chrysotile Fibres**

**Title : Particle Number Frequency of Airborne Chrysotile Fibres using Optical Microscope (OM)**

<b>Length, ECD (micrometers)</b>	<b>Log ECD (micrometers)</b>	<b>Rate</b>	<b>OM %</b>	<b>Cumulative % OM</b>
0.00	#NUM!	271	71.13	100.00
5.00	0.699	104	27.30	28.87
10.00	1.000	4	1.05	1.57
20.00	1.301	2	0.52	0.52
				0.00
<b>TOTAL</b>		<b>381</b>	<b>100.00</b>	

## Appendix D-2a

### Comparison of Amosite Fibres Length and Diameter Distribution TEM Results

- i. Airborne Penge Amosite Fibres
- ii. Amosite Fibres from Lung Tissue

<b>Length (micrometers)</b>	<b>Airborne Cumulative %</b>	<b>Lung Cumulative %</b>
0.00	100.00	100.00
1.00	92.15	89.56
2.00	71.51	70.98
3.00	49.85	52.50
4.00	38.96	38.14
5.00	31.00	29.00
6.00	24.45	21.80
8.00	15.65	13.18
10.00	10.42	8.71
20.00	6.50	3.00
30.00	3.50	0.00
50.00	0.00	0.00

<b>Diameter (micrometers)</b>	<b>d<sub>AEF</sub> (micrometers)</b>	<b>Airborne Cumulative %</b>	<b>Lung Cumulative %</b>
0.0000	0.0000	100.00	100.00
0.1250	0.3795	84.62	69.37
0.2500	0.7589	51.88	30.03
0.3750	1.1384	27.67	13.96
0.5000	1.5179	15.71	8.10
0.7500	2.2768	4.97	1.53
1.0000	3.0358	1.11	0.55
1.2500	3.7947	0.12	0.12
1.5000	4.5537	0.00	0.00

## Appendix D-2b

### Comparison of Crocidolite Fibres Length and Diameter TEM Results

- i. Airborne Koegas Crocidolite Fibres
- ii. Airborne Australian Crocidolite Fibres
- iii. Crocidolite Fibres from Lung Tissue

Length (micrometers)	Koegas	Australian	Lung Cumulative %
	Airborne Cumulative %	Airborne Cumulative %	
0.00	100.00	100.00	100.00
1.00	80.66	83.30	86.25
2.00	49.20	60.09	57.30
3.00	29.91	38.57	34.70
4.00	19.80	31.17	19.86
5.00	13.50	24.00	13.00
6.00	9.69	18.39	8.90
8.00	5.22	9.53	4.20
10.00	2.95	6.28	2.18
20.00	1.50	2.00	1.00
30.00	0.50	1.00	0.00
50.00	0.00	0.00	0.00

Diameter (micrometers)	d <sub>AEF</sub> (micrometers)	Koegas	Australian	Lung Cumulative %
		Airborne Cumulative %	Airborne Cumulative %	
0.0000	0.0000	100.00	100.00	100.00
0.1250	0.3795	58.63	62.56	29.54
0.2500	0.7589	15.80	12.11	3.86
0.3750	1.1384	5.24	2.69	0.67
0.5000	1.5179	2.10	0.67	0.39
0.7500	2.2768	0.72	0.00	0.32
1.0000	3.0358	0.27	0.00	0.10
1.2500	3.7947	0.13	0.00	0.05
1.5000	4.5537	0.00	0.00	0.00



## Appendix D-2c

### Comparison of Chrysotile Fibres Length and Diameter TEM Results

#### i. Airborne Chrysotile Fibres

<b>Length (micrometers)</b>	<b>Airborne TEM</b>
0.00	100.00
1.00	89.80
2.00	57.90
3.00	32.80
4.00	20.90
5.00	14.00
6.00	8.20
8.00	0.90
10.00	0.10
20.00	0.00
30.00	0.00
50.00	0.00

<b>Diameter (micrometers)</b>	<b>d<sub>AEF</sub> (micrometers)</b>	<b>Airborne Cumulative %</b>
0.0000	0.0000	100.00
0.1250	0.3347	60.40
0.2500	0.6693	17.00
0.3750	1.0040	0.50
0.5000	1.3387	0.50
0.7500	2.0080	0.10
1.0000	2.6773	0.10
1.2500	3.3466	0.10
1.5000	4.0160	0.10

**Appendix D-3a**

**Title : Comparison of number of frequency coal dust particles obtained using EM for 7 hole sampler, cyclone sampler, and from lung tissue.**

ECD (micrometers)	Ratio	d <sub>coal</sub> (micrometers)	d <sub>AE</sub> (micrometers)	7 Hole sampler		Cyclone sampler		Lung Tissue	
				Particle Number	Particle Number %	Particle Number	Particle Number %	Particle Number	Particle Number %
0.45	0.35	0.37	0.46	239	6.01	295	8.71	302	8.68
0.75	0.50	0.68	0.86	1106	27.80	1118	33.03	1157	33.27
1.30	0.65	1.29	1.63	961	24.15	753	22.25	774	22.25
1.75	0.74	1.81	2.29	647	16.26	515	15.21	532	15.30
2.25	0.81	2.40	3.03	371	9.32	310	9.16	336	9.66
2.75	0.86	3.00	3.79	264	6.63	202	5.97	166	4.77
3.25	0.91	3.60	4.56	164	4.12	84	2.48	98	2.82
3.75	0.95	4.22	5.33	88	2.21	52	1.54	60	1.73
4.25	0.99	4.84	6.12	44	1.11	24	0.71	34	0.98
4.75	1.02	5.46	6.91	34	0.85	15	0.44	11	0.32
5.25	1.05	6.09	7.71	26	0.65	11	0.32	5	0.14
5.75	1.07	6.72	8.51	16	0.40	2	0.06	2	0.06
6.25	1.10	7.36	9.31	11	0.28	4	0.12	1	0.03
6.75	1.12	8.00	10.12	4	0.10	0	0.00	0	0.00
7.25	1.14	8.65	10.94	2	0.05	0	0.00	0	0.00
8.75	1.19	10.59	13.40	2	0.05	0	0.00	0	0.00
10.00	1.23	12.23	15.47	0	0.00	0	0.00	0	0.00
<b>TOTAL</b>				3979	100.00	3385	100.00	3478	100.00

### Appendix D-3b

Title : Comparison of coal dust particles size distribution obtained using EM for 7 hole sampler, cyclone sampler, and from lung tissue.

ECD (micrometers)	Ratio	d <sub>coal</sub> (micrometers)	d <sub>AE</sub> (micrometers)	7 Hole sampler	Cyclone sampler	Lung Tissue
				Particle Number Cum %	Particle Number Cum %	Particle Number Cum %
0.45	0.35	0.37	0.46	100.00	100.00	100.00
0.75	0.50	0.68	0.86	93.99	91.29	91.32
1.30	0.65	1.29	1.63	66.20	58.26	58.05
1.75	0.74	1.81	2.29	42.05	36.01	35.80
2.25	0.81	2.40	3.03	25.79	20.80	20.50
2.75	0.86	3.00	3.79	16.46	11.64	10.84
3.25	0.91	3.60	4.56	9.83	5.67	6.07
3.75	0.95	4.22	5.33	5.70	3.19	3.25
4.25	0.99	4.84	6.12	3.49	1.65	1.52
4.75	1.02	5.46	6.91	2.39	0.95	0.55
5.25	1.05	6.09	7.71	1.53	0.50	0.23
5.75	1.07	6.72	8.51	0.88	0.18	0.09
6.25	1.10	7.36	9.31	0.48	0.12	0.03
6.75	1.12	8.00	10.12	0.20	0.00	0.00
7.25	1.14	8.65	10.94	0.10	0.00	0.00
8.75	1.19	10.59	13.40	0.05	0.00	0.00
10.00	1.23	12.23	15.47	0.00	0.00	0.00

### Appendix D-3c

**Title : Comparison of coal dust particles mass distribution using EM for 7 hole sampler, cyclone sampler, and from lung tissue.**

ECD (micrometers)	Ratio	d <sub>coal</sub> (micrometers)	d <sub>AE</sub> (micrometers)	7 Hole sampler	Cyclone sampler	Lung Tissue
				Particle Mass Cum %	Particle Mass Cum %	Particle Mass Cum %
0.45	0.35	0.37	0.46	100.00	100.00	100.00
0.75	0.50	0.68	0.86	99.95	99.89	99.88
1.30	0.65	1.29	1.63	98.93	97.96	97.84
1.75	0.74	1.81	2.29	94.82	91.96	91.49
2.25	0.81	2.40	3.03	87.23	80.69	79.52
2.75	0.86	3.00	3.79	77.97	66.26	63.46
3.25	0.91	3.60	4.56	65.95	49.11	48.97
3.75	0.95	4.22	5.33	53.62	37.33	34.84
4.25	0.99	4.84	6.12	43.46	26.13	21.56
4.75	1.02	5.46	6.91	36.06	18.61	10.61
5.25	1.05	6.09	7.71	28.08	12.04	5.66
5.75	1.07	6.72	8.51	19.84	5.54	2.62
6.25	1.10	7.36	9.31	13.18	3.99	1.02
6.75	1.12	8.00	10.12	7.30	0.00	0.00
7.25	1.14	8.65	10.94	4.60	0.00	0.00
8.75	1.19	10.59	13.40	2.93	0.00	0.00
10.00	1.23	12.23	15.47	0.00	0.00	0.00

**Appendix D-3d**

**Title : Coal Particles Shadowing 45° Length.**

<b>Particle Size ECD (micrometers)</b>	<b>Mean Shadow Length (micrometers)</b>	<b>Standard Deviation Deviation (SD)</b>
0.255	0.220	0.048156
0.347	0.286	0.063683
0.448	0.342	0.087630
0.719	0.472	0.186475
1.194	0.624	0.243633
1.672	0.723	0.289986
2.183	0.744	0.319447
3.151	0.964	0.534146



**Appendix D-4a**

**Title : Comparison of sizing data obtained using TEM at different magnification of 2006 airborne dust sample.**

ECD (micrometers)	2006 [2100 X]		2006 [4400 X]		2006 [11000 X]		2006 [13000 X]	
	Particle Number	Particle Number %	Particle Number	Particle Number %	Particle Number	Particle Number %	Particle Number	Particle Number %
0.00-0.06	0	0.00	4915	38.76	2610	72.97	8469	84.03
0.06-0.08	5897	27.41	1237	9.76	350	9.78	422	4.19
0.08-0.12	2726	12.67	2172	17.13	312	8.72	502	4.98
0.12-0.16	3588	16.68	1399	11.03	156	4.36	270	2.68
0.16-0.23	5130	23.85	1702	13.42	105	2.94	232	2.30
0.23-0.32	2551	11.86	874	6.89	30	0.84	127	1.26
0.32-0.45	1240	5.76	306	2.41	7	0.20	33	0.33
0.45-0.64	304	1.41	54	0.43	6	0.17	17	0.17
0.64-0.90	51	0.24	14	0.11	1	0.03	6	0.06
0.90-1.30	15	0.07	6	0.05	0	0.00	0	0.00
1.30-1.80	6	0.03	0	0.00	0	0.00	0	0.00
1.80-2.60	2	0.01	0	0.00	0	0.00	0	0.00
2.60-3.60	1	0.00	0	0.00	0	0.00	0	0.00
3.60-5.10	0	0.00	0	0.00	0	0.00	0	0.00
> 5.10								
<b>TOTAL</b>	<b>21511</b>	<b>100.00</b>	<b>12679</b>	<b>100.00</b>	<b>3577</b>	<b>100.00</b>	<b>10078</b>	<b>100.00</b>

## Appendix D-4b

**Title : Comparison of particle size distribution using TEM at different magnification between 1961 and 2006 airborne dust sample.**

ECD (micrometers)	d (nanometers)	d <sub>AE</sub> (nanometers)	ECD, d (micrometers)	d <sub>AE</sub> (micrometers)	1961	2006 [13000X]
					Particle Number Cum %	Particle Number Cum %
0.00-0.06	30.000	51.962	0.03	0.05	100.00	100.00
0.06-0.08	70.000	121.244	0.07	0.12	100.00	15.97
0.08-0.12	100.000	173.205	0.10	0.17	75.17	11.78
0.12-0.16	140.000	242.487	0.14	0.24	55.81	6.80
0.16-0.23	195.000	337.750	0.20	0.34	36.41	4.12
0.23-0.32	275.000	476.314	0.28	0.48	17.74	1.82
0.32-0.45	385.000	666.840	0.39	0.67	5.66	0.56
0.45-0.64	545.000	943.968	0.55	0.94	2.00	0.23
0.64-0.90	770.000	1333.679	0.77	1.33	0.60	0.06
0.90-1.30	1100.000	1905.256	1.10	1.91	0.23	0.00
1.30-1.80	1550.000	2684.679	1.55	2.68	0.04	0.00
1.80-2.60	2200.000	3810.512	2.20	3.81	0.00	0.00
2.60-3.60	3100.000	5369.358	3.10	5.37	0.00	0.00
3.60-5.10	4350.000	7534.421	4.35	7.53	0.00	0.00
> 5.10	5100.000	8833.459	5.10	8.83	0.00	0.00

## Appendix D-4c

**Title : Comparison of particle mass distribution using TEM at different magnification between 1961 and 2006 airborne dust sample.**

					1961	2006 [13000X]
ECD (micrometers)	d (nanometers)	d <sub>AE</sub> (nanometers)	ECD, d (micrometers)	d <sub>AE</sub> (micrometers)	Particle Mass Cum %	Particle Mass Cum %
0.00-0.06	30.000	51.962	0.03	0.05	100.00	100.00
0.06-0.08	70.000	121.244	0.07	0.12	100.00	98.29
0.08-0.12	100.000	173.205	0.10	0.17	99.42	97.20
0.12-0.16	140.000	242.487	0.14	0.24	98.10	93.44
0.16-0.23	195.000	337.750	0.20	0.34	94.46	87.89
0.23-0.32	275.000	476.314	0.28	0.48	85.02	75.01
0.32-0.45	385.000	666.840	0.39	0.67	67.87	55.23
0.45-0.64	545.000	943.968	0.55	0.94	53.63	41.13
0.64-0.90	770.000	1333.679	0.77	1.33	38.16	20.52
0.90-1.30	1100.000	1905.256	1.10	1.91	26.52	0.00
1.30-1.80	1550.000	2684.679	1.55	2.68	8.94	0.00
1.80-2.60	2200.000	3810.512	2.20	3.81	0.00	0.00
2.60-3.60	3100.000	5369.358	3.10	5.37	0.00	0.00
3.60-5.10	4350.000	7534.421	4.35	7.53	0.00	0.00
> 5.10	5100.000	8833.459	5.10	8.83	0.00	0.00

